AN EXPERIMENTAL INVESTIGATION OF FIRE PERFORMANCE OF EARTHQUAKE DAMAGED STRUCTURES

Ph.D. THESIS

by

ASIF HUSSAIN SHAH

DEPARTMENT OF CIVIL ENGINEERING
INDIAN INSTITUTE OF TECHNOLOGY ROORKEE
ROORKEE-247667, UTTARAKHAND, INDIA

SEPTEMBER, 2015

AN EXPERIMENTAL INVESTIGATION OF FIRE PERFORMANCE OF EARTHQUAKE DAMAGED STRUCTURES

A THESIS

Submitted in partial fulfilment of the requirements for the award of the degree

of

DOCTOR OF PHILOSOPHY

in

CIVIL ENGINEERING

by

ASIF HUSSAIN SHAH

DEPARTMENT OF CIVIL ENGINEERING
INDIAN INSTITUTE OF TECHNOLOGY ROORKEE
ROORKEE-247667, UTTARAKHAND, INDIA

SEPTEMBER, 2015

INDIAN INSTITUTE OF TECHNOLOGY ROORKEE
ROORKEE

CANDIDATE'S DECLARATION

I hereby certify that the work which is being presented in the thesis entitled **"AN EXPERIMENTAL INVESTIGATION OF FIRE PERFORMANCE OF EARTHQUAKE DAMAGED STRUCTURES"** in partial fulfillment of the requirements for the award of the degree of Doctor of Philosophy and submitted in the Department of Civil Engineering of the Indian Institute of Technology Roorkee, Roorkee, is an authentic record of my own work carried out during the period from January, 2013 to September, 2015 under the supervision of Dr. Umesh Kumar Sharma, Associate Professor, Department of Civil Engineering, Indian Institute of Technology Roorkee, Roorkee.

The matter presented in this thesis has not been submitted by me for the award of any other degree of this or any other institute.

(ASIF HUSSAIN SHAH)

This is to certify that the above statement made by the candidate is correct to the best of my knowledge.

Date: September, 2015 (Umesh Kumar Sharma)

Supervisor

The Ph.D. Viva-Voce Examination of Asif Hussain Shah, Research Scholar, has been held on…….

Chairman, SRC **External Examiner**

This is to certify that the student has made all the corrections in the thesis.

Supervisor **Head of the Department**

Dated: _____

ABSTRACT

Fire is possibly the most severe environmental hazard to which the built infrastructure might be subjected to. The risk of fires in the aftermath of earthquakes is a credible extreme load in seismic regions around the world and such events are considered a major threat to life and property. A very important aspect of the research on the concrete structures exposed to elevated temperatures is the study of impact of fires on the structures pre-damaged by earthquakes. Over the past centuries fire has emerged as an integral part of emergency response strategies which are focused on life safety as well as the infrastructure safety of any nation. However no current regulations consider the fire and earthquake hazard in a sequential manner. The overall behaviour of reinforced concrete structures, during the time it is exposed to fire and even after, is still a hot issue in civil engineering. As far as the behaviour during fire is concerned, the human safety and the structural resistance of the structures are two important associated interests involved while as the behaviour of the structure after fire is related to the residual bearing capacity of the structure. In spite of the fact that the structural materials undergo mechanical decay after a thermal accident, it is generally necessary to ascertain and quantify the residual capacity of a structure and compare it with the safety levels.

A critical literature review reveals that a number of studies have been carried out on the different aspects of concrete structures at elevated temperatures. However no significant research attempt has been made in the past for assessment of structures under fire following earthquake. A critical literature review mandates consideration of such loading conditions under performance based design techniques. Since fire following earthquake falls out of scope of practising professionals in earthquake and fire service fields, it has stimulated the interest amongst various groups of researchers in the structural engineering community to carry out a rigorous investigation in this regard. Another important observation from the literature review suggests that the past studies have been mostly carried on the ductile detailed concrete structures. This has led to a information gap with regards to the behaviour of non-ductile concrete structures, built before 1980's, which are still more in number than the ductile ones.

Most of the design codes specify the fire rating, i.e. the time to failure of a structural member exposed to fire, as the measure of the building elements to resist fire. However the biggest drawback of these codes is the approach of relating the size and the cover to reinforcement as the only parameters to determine the fire endurance of the structural elements. The effect of the

concrete strength, the tie configuration and the percentage confining reinforcement is completely neglected in determining the fire ratings in reinforced concrete columns. The effect of confining reinforcement on the fire resistance of RC columns is not well documented. No design tools are available in the literature which takes into consideration the effect of confinement on the fire ratings of RC columns

Thus the research efforts needed to fill the gaps in the state of art may be put at three different levels: structural, elemental and material. Structural level represents the holistic behaviour of a framed structure consisting of beams, columns, slabs and joints. Elemental level represents the behaviour of full scale individual structural elements like columns, beams etc whereas, material level constitutes the studies on the behaviour of constituent materials such as steel and concrete.

The principal objective of the current research was to experimentally obtain the behaviour of a full scale RC frame with non ductile detailing with and without infill. At elemental level, a study was carried out to study the effect of degree of confinement and concrete strength on fire resistance of reinforced concrete columns.

In order to evaluate the behaviour of a reinforced concrete (RC) frame in post earthquake fire, a full-scale RC frame assemblage was constructed without following the ductile detailing guidelines of the Indian standards. A three phase test procedure was adopted in testing the RC frame. The frame was first subjected to a cyclic lateral load to simulate the seismic effects which was then followed by a one hour compartment fire. After fire the frame was subjected to a residual cyclic load test. The cyclic lateral load was applied on the RC frame using two double acting hydraulic actuators acting in tandem with each other against a strong reaction wall. The main aim of the mechanical loading was to induce a damage corresponding to the collapse prevention performance level (S5) as prescribed by FEMA 356:2000. Following the lateral seismic load test, the RC frame was subjected to a full scale fire test wherein a designed compartment fire was developed using kerosene as the fire source. After exposing the RC frame to compartment fire, the RC frame was again tested under lateral seismic load for measuring the residual lateral load capacity of the frame. Numerous sensors, namely thermocouples, strain gauges and linear variable differential transducers were embedded at key locations of the frame to capture important information during the tests. The results show a marked influence of reinforcement detailing on the post-earthquake fire performance of the concrete structures. The simulated earthquake loading caused wider cracks and more severe concrete spalling in the frame without ductile detailing compared to the frame with ductile detailing. Spalling of

concrete and buckling of reinforcement was observed in top beams. The present study reveals the conservativeness of the damage levels specified in Table C1-2 of FEMA 356 (2000) vis-à-vis both the RC frames (ductile and non-ductile). The overall damage in the test frame was not severe as anticipated in the Table C1-2. However, the damage caused in the non-ductile detailed frame was in line with the expected damage specified by C1-3 of FEMA 356. Present study also reveals overestimation of permanent drifts given in FEMA 356. However, the permanent drift in non-ductile detailed RC frames is higher than in ductile detailed frames. The investigation validates the time-temperature curve designed according to the fire design equation of Thomas and Heseldon (1972). The tests reveal the vulnerability of thin elements like slabs and shells of non-ductile RC frames to spalling in post-earthquake fire events. While drawing the attention towards addressing the issues of fire following earthquakes, the melting of reinforcement after spalling of thin elements like slab and shells needs to be considered in design codes. The test reflects the better performance of the RC frames with ductile detailing. Thus, the recommendations generally used in the seismic resistant design may also be helpful in enhancing the fire resistance of the RCC structures.

The next component of the dissertation was carried out to study the effect of the masonry infill on the response of an in-filled RC framed building in post-earthquake fire. Same testing procedure, as in earlier component, was followed in this study also. The results reveal a better performance of the frame in the cyclic load test with higher load carrying capacity at S5 level than the bare frame. Cracks were developed on the in-plane infill walls, though the masonry walls remained intact after the cyclic load test. The plinth beams, along the loading direction, however got damaged with a hinge formation and buckling of reinforcement. This study indicates that for a frame that is properly designed for seismic loads, infill panels will most likely have a beneficial influence on its performance. The study reveals that infill panels can be used to improve the performance of existing non-ductile frames. The masonry infill helps in delaying the flashover. The time taken to reach the maximum temperature is higher in masonry in-filled frames. The brick infill walls provided insulation to the RC structural elements and slowed the transmission of heat to these elements. This beneficial effect of masonry walls should be considered while designing the columns and beams, which are integrated in the masonry walls.

Finally, towards the end, the effect of the degree of confinement, tie configuration and concrete strength on the fire resistance of the RC columns was studied. A total of eight full scale columns of dimensions 2800×300×300 mm were cast with different confinement levels

achieved by changing the spacing of the traverse steel reinforcement. A full scale column fire furnace was designed and built to test the columns under a standard fire curve of ISO 834:1975. A standard testing procedure was followed where in the columns were axially loaded to the 40% of the ultimate load carrying capacity, 60 minutes before exposing them to the fire. The fire was continued till the columns failed to take load. The results show that the degree of the confinement has a marked role to play in the fire rating of the reinforced concrete columns. With the increase in the confining reinforcement factor, the fire resistance of the RC columns gets enhanced. The effect of the confining reinforcement is more pronounced in NSC columns than in HSC columns. Higher confinement also prevents the spalling of the higher strength concrete. A design equation has also been developed to measure the fire resistance of RC columns which also takes confinement parameters into account. The design equation can be integrated in the design standards to facilitate the fire design of columns.

ACKNOWLEDGEMENT

All praise is due to Allah, the Lord of the Worlds. The Beneficent, the Merciful, Master of the Day of Judgment. It is incumbent upon me to express my thanks and gratitude to Him, that He has bestowed on me His endless bounties and favors and blessed me with His guidance to the right path. I am greatly indebted to my parents who raised me with a love of science and supported me in all my pursuits and instilled a sense of purpose during the course of this study.

I would like to acknowledge my deepest regards, sincere appreciation and heartfelt thanks to my supervisor and mentor Dr. Umesh Kumar Sharma, Associate Professor, Department of Civil Engineering, Indian Institute of Technology Roorkee. Scientific acumen, pedagogic methodology, abiding physical insight, conceptual thinking and heuristic approach by my supervisor made my research proceeded in a systematic manner and helped me to understand the fundamental concepts of the subject. It is a rare delight for me, to work under such a nice person who inspired and encouraged me from my very first day till today. Sir, you have been a tremendous mentor for me. I would like to thank you for encouraging my research and for allowing me to grow as a research scientist. Your advice on both research as well as on my career have been priceless.

Further, I would like to thank Dr. Pradeep Bhargava, Professor, Department of Civil Engineering, IIT Roorkee for his enlightening and unparalleled support that he has rendered me in throughout my research work. I would like to acknowledge Prof. Vipul Prakash, Chairman SRC, for providing me with the valuable suggestions during this course. I would like to thank my Ph.D. committee members: Dr. Bhupinder Singh, Associate Professor, Department of Civil Engineering, IIT Roorkee and Dr. Yogendra Singh, Professor, Department of Earthquake Engineering, IIT Roorkee, for their time and invaluable guidance.

I must thank Dr. Javed Ahmad Naqash, my mentor at NIT Srinagar for introducing me to a wonderful guide, Dr. Umesh Sharma.

This investigation involved enormous concrete construction which would not have been possible without the help and support of staff of Structural Engineering Group, Civil Engineering Department, IIT Roorkee. I am grateful to the head of the department and faculties in the Structural Engineering Group, Civil Engineering Department, IIT Roorkee, for making the state-of-the-art laboratory facilities available to me. I am thankful to the staff members particularly Mr. Anil Sharma and Mr. Chetan Chand of the concrete laboratory and structural engineering laboratory for their timely support and co-operation. I must acknowledge the

support extended by Mr. Anil Sharma whenever I used to call him on weekends for my experimental work. I extend my thanks to the laboratory technicians and helpers for assisting me in carrying out the experimental work. The help and support rendered by Shahnawaaz, Sitaram, Subash was exceptional.

I would also like to thank the construction division of IIT Roorkee and UPRNN for providing timely support in developing the necessary test facilities for this investigation.

Eagerness and vitality to continue interest in research has been provided by my colleagues and friends through frequent discussions. In particular, the support received from Dr. Praveen Kamath, Dr. Danie Roy and Dr. Heaven Singh are sincerely acknowledged.

My time at IIT Roorkee was made enjoyable in large part due to the many friends and groups that became a part of my life. The support and encouragement from Dr Faisal Hassan, Md. Irfanul Haque Sidiqi, Tabish Alam, Md.Yawar Ali Khan, Mohammad Aamir, Syed Naved Ali and Mohammad Kashif is highly acknowledged.

I gratefully acknowledge the funding sources that made my Ph.D. work possible. I was funded by the Board of Research in Nuclear Sciences, Department of Atomic Energy, Govt. of India, Mumbai.

Lastly, I would like to thank my family for all their love and encouragement. For my parents who raised me with a love of science and supported me in all my pursuits. For my siblings whose encouragement and patience made me achieve this feat. Thank you.

(Asif Hussain Shah)
IIT ROORKEE
SEPTEMEBER 2015

Dedicated To

My Grandmothers: Ateeqah Shah, Raja Begum
My Parents : Tanveera Jahan , Dr. Gias Ud Din Shah
My Siblings : Gouseya Shahnaaz and Aarif Shah

CONTENTS

LIST OF FIGURES

LIST OF TABLES

CHAPTER – 1
INTRODUCTION AND LITERATURE REVIEW

1.1 INTRODUCTION

Fire remains one of the serious potential risks to which the buildings and structures can be exposed to. Famous for its ubiquitous influence, concrete is most widely used material in the construction arena thereby making the research on fire resistance more and more important. The overall behaviour of Reinforced concrete structures, during the time it is exposed to fire and even after, is still a hot issue in Civil Engineering. As far as the behaviour during fire is concerned, the human safety and the structural resistance of the structures are two important associated interests involved while as the behaviour of the structure after fire is related to the residual bearing capacity of the structure. In spite of the fact that the structural materials undergo mechanical decay, it is generally necessary to ascertain and quantify the residual capacity of a structure and compare it with the safety levels.

Concerns related to material integrity of concrete exposed to elevated temperatures have always been there, in spite of concrete being an incombustible material. The thermal properties and the behaviour of concrete exposed to elevated temperatures have received considerable experimental and analytical attention in the past. However, the behavior of concrete subjected to fire is understood to a lesser extent as compared to that of steel. It is important to scrutinize the behavior of concrete structures exposed to elevated temperatures with an aggressive fire or heat source. Recently concern has been shown about the behavior of reinforced concrete structures during fires following earthquakes (FFE). In the recent past, FFE scenarios have been increasingly recognized as a credible extreme loading case, though not much work, analytical or experimental has been reported on the behaviour of structures exposed to fire following earthquake events.

In this chapter a critical review of the literature related to the material behaviour of steel and concrete subjected to elevated temperatures as well as the behaviour of a RCC structural assemblage exposed to fire has been carried out. Particular attention has been paid to the published literature on the material and structural behaviour of RCC during FFE. On the basis of the literature review, gaps in our current understanding of structural behaviour, particularly during FFE scenarios, have been identified and the need for the present investigation justified.

1.2 BEHAVIOUR OF CONCRETE EXPOSED TO ELEVATED TEMPERATURES

Concrete is a non-homogeneous two phase material at the macroscopic level, consisting of hardened cement paste and aggregate. The heterogeneous nature of porous medium of concrete is very sensitive to unwanted fire or high temperatures conditions. Due to the composition of concrete and the acute thermal conditions that exist in a fire, concrete and fire have a multifarious interaction. Each of the constituents of concrete reacts differently to thermal exposures and the behavior in fire of the composite system is not easy to describe or model (Khoury 2000). Lea (1920), and Lea and Strandling (1922) pioneered investigations on the influence of high temperature on the behaviour of concrete in RC structures. In the early stages, researchers gave consideration to the physical and chemical changes within the concrete composition due to exposure to elevated temperatures (Malhotra 1956, Saemann and Washa 1957, Zoldners 1960, Purkiss and Dougill 1973). They have shown that when concrete is exposed to elevated temperatures, its chemical composition and physical properties change significantly which occur primarily in the hardened cement paste and simultaneously it may also occur in aggregates. A number of chemical and physical changes occurring in concrete due to exposure to elevated temperature have been discussed by Khoury (2000), Bazant and Kaplan (1996), Schneider and Herbst (2002) and Carvel (2005). They have noticed that depending on the temperature attained, some of these changes get reversed upon cooling, while others are non-reversible and may deteriorate concrete significantly after a fire.

Table 1.1 (Schneider and Herbst 2002) and the schematic illustration in Fig. 1.1 (Khoury 2000), give an overview of the most important chemical processes occurring in concrete at elevated temperature. These changes take place primarily in the hardened cement paste and to a little extent in aggregates also. Between 30 to 120ºC, the evaporable water gets released from the saturated concrete. The chemically bound water is expelled as the temperature is increased to 300ºC. At temperatures up to 500ºC, removal of water from both gel pores and capillary leads to a radical increase in the average pore volume and alterations in the pores system from isolated closed to interconnected network. The changes produced by high temperatures are more pronounced when the temperature exceeds 500ºC. As temperature exceeds 500ºC, calcium silicates hydrates and calcium hydroxide in the cement paste start decomposing, until silicates collapse at 900ºC. It is reported that siliceous aggregates, especially quartzite, experience phase transformation at approximately T = 570°C from α-quartz to β-quartz. Above 1200ºC, aggregate fusion or melting occurs, which results in the collapse of concrete. The subsequent chemical decomposition and physical changes of major constituents

of concrete leads to cracking, spalling and decline in mechanical properties of concrete. Finally, severe micro-structural changes are induced and concrete loses its durability and strength. Figure 1.1 shows the physical and chemical deterioration of plain concrete as a function of temperature.

Table 1.1: Decomposition of cement paste at various temperatures ranges (Schneider and Herbst 2002)

Temperature range (°C)	Transformation or decomposition reaction
30-120	Evaporation of physically adsorbed water
30-300	Gel destruction, first stage of dehydration
120-600	Release of chemically adsorbed water
450-550	Decomposition of portlandite Ca(OH)2
570	Transformation of quartz α to β SiO2
600-700	Decomposition of C-S-H phases, formation of β-C2S
1100-1200	Melting of concrete, formation of glassy materials

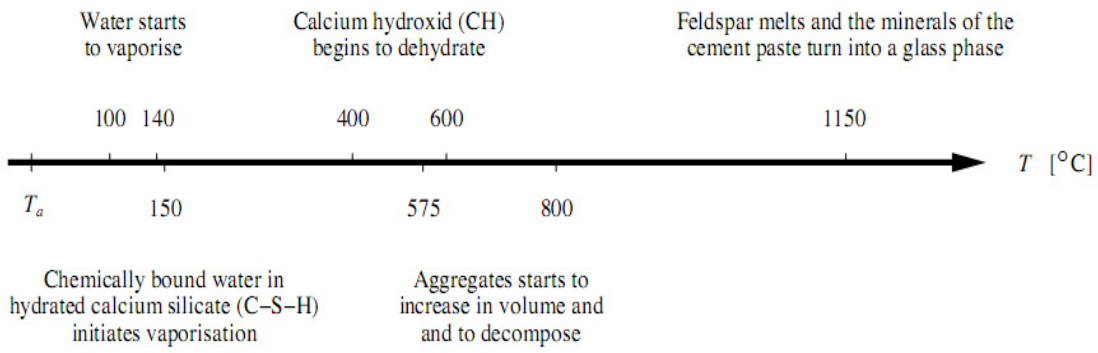

Fig. 1.1 Schematic view of physical and chemical deterioration of plain concrete as a function of temperature (Hertz 2005)

It is always possible that physical modifications may also occur in the aggregates at elevated temperatures. On a standalone basis, the thermal response of aggregate or cement paste may be simple but the overall combined response of the concrete and cement matrix can be much more complex. Fletcher et al. (2007) reported that the volume of quartz-based (siliceous) aggregates increases owing to a mineral transformation at about 575 °C, whereas decomposition of limestone aggregates begins at about 800 °C. Hence, this differential expansion between the cement and the aggregate matrix may cause spalling and cracking.

When combined, these chemical and physical changes in concrete will have the effect of reducing the compressive strength of the material. In fact, Fletcher et al. (2007) has indicted that the critical temperature for considerable strength reduction of the concrete depend necessarily on the type of aggregate used, approximate values being: sand light-weight aggregate (650 °C), carbonate aggregate (660 °C) and siliceous aggregate (430 °C). Even at lower exposure temperatures, the strength reduction of concrete was found to be unpredictable being dependent on composition and environmental factors (Khoury 2000). As sharp temperature gradients exist within the depth of concrete in a RCC structure, therefore a typical local temperature reading in the concrete may provide only an indirect indication of the fire performance of concrete structures. Fletcher et al. (2007) has reported that significant loss of strength of steel reinforcing bars due to elevated temperatures in fires may result in failure of a RCC structure.

The major damage mechanisms accountable for deterioration of properties of concrete exposed to elevated temperatures may be categorized into four sections: (i) phase transformations occurring in cement paste (Malhotra 1956, Khoury 2000), (ii) phase transformation occurring in aggregate (Fletcher et al. 2007), (iii) thermal incompatibility between the aggregate and cement paste (Fletcher et al. 2007), and (iv) spalling of concrete (Khoury and Anderberg 2000).

The influence of various material and environmental factors on the fire performance of concrete was reported by many investigators. A lot of experimental data has been generated and numerical models were developed in the last century to study the degradation in mechanical properties of concrete exposed to elevated temperatures. Many researchers have investigated the mechanical properties of concrete exposed to elevated temperatures (Lea and Straddling 1922, Malhotra 1956, 1982, Lankard et al. 1971, Abrams 1971, 1978, Mohamedbhai et al.1986, Schneider 1985, Diederichs et al. 1988, Kumar and Bhattacharjee 1995, Hammer 1995, Saad et al. 1996, Terro 1998, Kodur and Sultan 1998, Chakrabarti and Jain 1999, Khoury et al. 2002, Suresh 2002, 2006, Baruah and Talukdar 2007, Xiao and Konig 2004, Metin 2006, Xiangjun et al. 2008, Topcu and Ikdag 2008). The material factors included the types of aggregates, mix design, the types of mineral admixtures and saturation level of the concrete. The service and environmental factors included rate of heating, maximum temperature attained, duration of exposure at the maximum temperature, method of cooling, type of end restraints and level of applied load. Data from various studies show that the

degradation of mechanical properties of concrete exposed to elevated temperature are affected by the following factors:

(i) Effect of compressive strength of concrete: Many studies been done to investigate the effect of concrete strength on the degradation of mechanical properties and explosive spalling during exposure to elevated temperature (Diederichs et.al. 1988, Phan 1996, Chan et.al. 1999, Peng 2000, Poon et.al. 2004, Cheng et al. 2004, Lau and Anson 2006, Xiao et al. 2006, Raju et al. 2007, Demirel and Kelestemur 2010). The above literature indicates that the strength of concrete plays a major role in its behaviour at elevated temperature. The loss of strength of concrete at high temperature increases with the increase in strength of the concrete. The phenomenon of spalling is attributed to decrease in permeability of the concrete with increase in strength. Therefore, a greater degradation of various mechanical properties has been observed with an increase in concrete strength due to spalling. It has been reasoned that understanding the various factors influencing fire performance will help in developing appropriate solutions for mitigating spalling and enhancing fire resistance of high strength concrete (HSC) members (Kodur and Phan 2007). Tests reveal that addition of polypropylene fibers decreased the strength and probability of explosive spalling (Tao et al. 2010). The exposure to high temperature also decreased the modulus of elasticity of concrete regardless of the preloading condition as well as the strength of concrete (Castillo and Durrani 1990). Felicetti and Gambarova (1998) have reported that while the toughness of high-strength concretes (f'_c > 60 MPa) increases after exposure to high temperature, there is a dramatic decrease strength and stiffness, and the recovery of strength with time is either zero or negligible. Furthermore, they have reported that the stress-strain curves show a rather prominent softening branch which has implications while assessing concrete toughness in compression. Ghan et al. (1999) has reported that HSC lost its mechanical strength in a manner similar to that of normal strength concrete (NSC). They have indicated that the temperature range between 400 and 800 °C was critical to strength loss. A coarsening effect on the microstructure of both HSC and NSC was observed. It was observed from these tests that HSC and NSC suffered damage to almost the same degree, although HSC appeared to suffer a greater loss of permeability-related durability.

(ii) Effect of aggregate type: Aggregate is a major fraction of a concrete mix and thereby its behaviour at elevated temperature has a significant effect on the mechanical properties

of concrete (Malhotra 1956, Abrahm 1971, Kodur et al. 2003, Cheng et al. 2004, Hertz 2005, Yan et al. 2007). Survey of the literature indicates that siliceous aggregate expands more than other types of aggregate and hence is responsible for the largest damage at elevated temperature. Lightweight aggregate like expanded clay undergo little thermal expansion and therefore only slight damage to concrete is caused. Calcareous aggregate (predominantly limestone) has more fire endurance compared to siliceous aggregate (predominantly quartz). Ahmed et al. (1992) has indicated that exposure of limestone aggregate concrete to high temperatures may result in a noticeable reduction in its strength, especially in the temperature range of 400-600 °C. Kodur and Sultan (2003) have reported that there is a significant influence of the type of aggregate on thermal properties of HSC, while the influence of presence of steel fiber reinforcement is very little.

(iii) Effects of moisture content: Moisture is an integral part of a concrete mix. The role of moisture content at elevated temperature has been reported by several researchers (Sanjayan & Stocks 1993, Chan et al. 2000, Luccioni et al. 2003, Zhang 2011). These studies concluded that the explosive spalling of concrete depends on moisture content in addition to concrete strength. Moisture content has a dominant influence on spalling. The effect of moisture content and concrete strength on spalling confirms the vapour pressure build-up hypothesis as the principle mechanism of spalling. The higher moisture content at the time of compressive testing is probably responsible for greater loss of strength at elevated temperatures in saturated than in dry concrete test specimens.

(iv) Effect of heating & cooling regimes: Heating and cooling are the two phases during exposure to temperature cycles and these regimes affect the behaviour of concrete at elevated temperatures (Malhotra 1956, Abrahms 1971, Mohamedbhai 1986, Khoury 1992, Bazant & Kaplan 1996, Terro & Hamoush 1997, Wetzig 2001, Phan and Carino 2002, Ali et al. 2004, Benmarce and Guenfound 2005, Franssen 2005, Hertz 2005, Peng et al. 2006, 2008). The above literature cites the importance of variations in maximum exposure temperature, rate of heating and cooling and duration of exposure. The major loss of strength of concrete has been seen to occur during the first hour of exposure though the loss of strength also depends on the maximum temperature reached. Cooling with water results in greater loss of strength than cooling in air. But rates of heating and cooling have no effect on the residual strength of concrete heated above 600 °C.

(v) Effect of steel reinforcement: Steel reinforcement is embedded in concrete matrix to cater to tensile stress but it has several other effects at elevated temperatures, as reported by many researchers (Morley and Royles 1979/80, Diederichs and Schneider 1981, Hertz 2004, Kodur et al. 2006, Haddad et al. 2008, Phani et al. 2009). The overall behaviour of reinforced concrete depends on various aspects of reinforcing bars like yield strength, bond strength, concrete cover, strength of concrete mix, diameter, configuration, manufacturing process, constituent materials, application of load, spacing, etc. of the steel reinforcing bars. The bond characteristics between steel reinforcement and concrete are important when modelling global behaviour and predicting reinforcement fracture at ultimate failure (Giroldo and Bailey 2008). A detailed account on the effects of elevated temperature on steel reinforcement is given in Sec. 1.3.

(vi) Effect of test methods: Phan (1996) discussed three types of tests methods, namely stressed test, unstressed test, and unstressed residual strength tests to investigate the effect of high temperature on the mechanical properties of concrete under uni-axial compression. A schematic view of these three test methods is shown in Fig. 1.2 which explains the state of mechanical pre-loading and thermal loading during the testing process of the concrete specimens under uni-axial compression. Phan (1996) has mentioned that the test results of the above mentioned methods may correspond to the following scenarios: (i) fire performance of concrete in a column or in the compression zone of beams and slabs – stressed test (ii) the performance of concrete elements with low stress levels under service conditions and loaded under high temperatures– unstressed test and (iii) assessing the post fire (or residual) properties of concrete – unstressed residual tests.

The test methods mentioned by Phan (1996) may be used to determine the compressive strength (the maximum stress), the modulus of elasticity and the strain at the maximum stress as function of temperatures. The test results of Abrams (1971) indicate that compressive strengths of specimens with preload (stressed tests) were generally 5 percent to 25 percent higher than those without preload (unstressed tests), with the reasoning that the preload helps to close existing cracks in concrete. Abrams (1971) has also reported that the unstressed residual specimens had the lowest strength compared to the stressed and unstressed specimens tested after exposure to elevated temperature. This is because the cooling of concrete actually generates very significant damage in

concrete as shown recently by Lee et al. (2008). Figs. 1.3 and 1.4 compare test data on NSC and HSC tested under hot conditions with the predictions of Eurocode EC 2 (ENV 1992-1-2 1995) for siliceous and carbonate concretes whereas, there is no degradation of the compressive strength up to 100 °C in the case of normal strength concrete. Fig. 1.4 shows an early reduction of compressive strength to 75 % when high strength concrete was tested at 100 °C. Morita et al. (1992) showed that high strength concrete has higher rate of reduction in residual compressive strength.

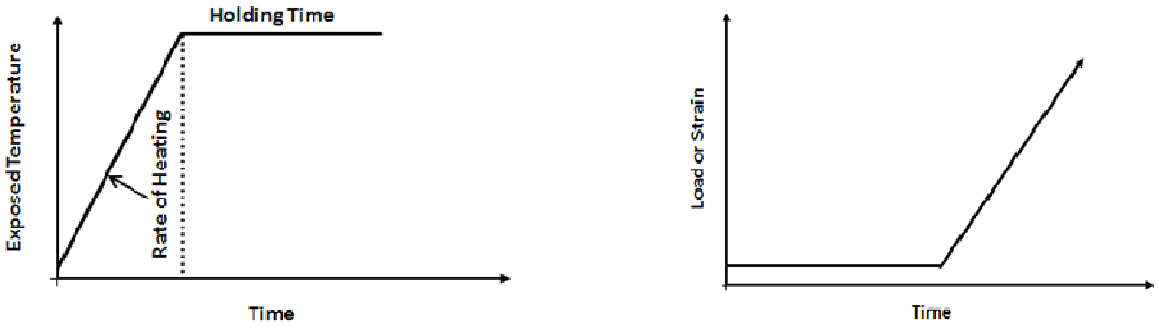

(a) Stressed Test Method

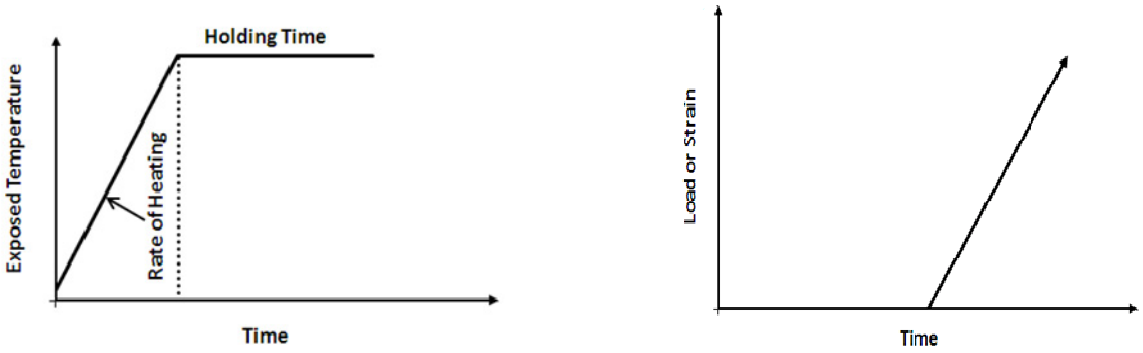

(b) Unstressed Test Method

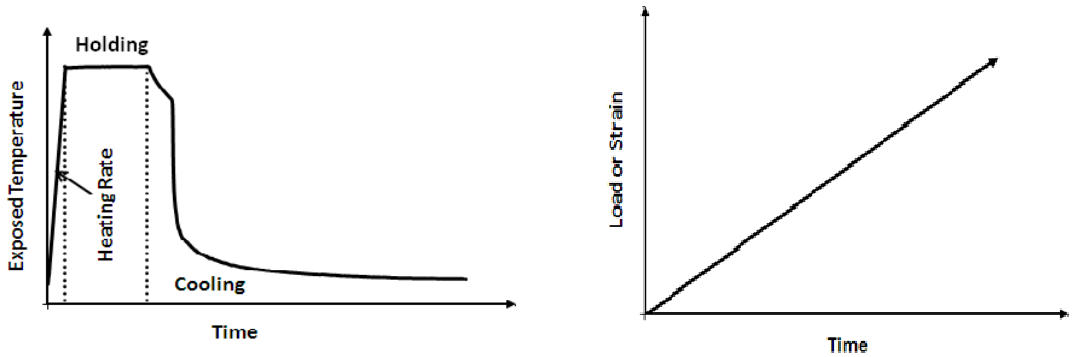

(c) Unstressed Residual Test Method

Fig. 1.2 - Schematic of temperature and loading histories for the test methods in uni-axial compression (Phan 1996)

The effect of elevated temperatures on concrete strength and load-deformation behaviour of high strength concrete (HSC) and normal strength concrete (NSC) has also been investigated by many other researchers (Castillo and Durani 1990, Furumura et al. 1995, Noumowe et al. 1996, Freskakis 1979, Kodur et al. 2008). Castillo and Durani (1990) have plotted load-deformation relationships for HSC and NSC some of which are shown in Fig. 1.5 (a)-(b). Fig. 1.5 (a)-(b) shows that NSC specimens exhibited ductile failure except for an exposure temperature of 200 °C whereas for exposure temperatures between 300 °C and 800 °C. The NSC specimens were able to undergo large post-peak strains while the decrease in strength was more gradual. On other hand, HSC showed brittle failure up to 300 °C, and with further increase of temperature, the HSC specimens began to exhibit a more ductile failure. Khoury (2002) showed that there is an enhancement of the residual compressive strength and elastic modulus with 20 % preloading during heating as illustrated in Fig. 1.6 (a)-(b).

Several models for prediction of residual stress-strain curves of concrete exposed to high temperatures were developed mainly for numerical analysis of the thermal response of concrete structures (Nielsen et al. 2004). Similar to compressive strength of concrete, stiffness of concrete also decreases with increasing temperature (Castillo and Durani 1990). Morita et al. (1992) observed that the rate of reduction in modulus of elasticity is higher in high strength concrete than in normal strength concrete after being exposed to temperature of up to 500 ºC, as shown in Fig 1.7. Furumura et al. (1995) observed the modulus of elasticity, in general, decreased gradually with increase of temperature. The degradation of the temperature dependent modulus of elasticity under unloaded condition has been described with the help of a parabolic expression by Nielsen et al. (2004). Most recently, Lee et al. (2009a) developed a multi-scale model for predicting the stiffness of concrete under high temperatures. The peak stress (the strength) and the initial slope (the stiffness) of the stress-strain curves when fast cooling method was adopted were lower than those obtained for normal cooling (Lee et al. 2008). They have concluded that rate of cooling following heating of concrete has an adverse effect on both strength and stiffness of concrete.

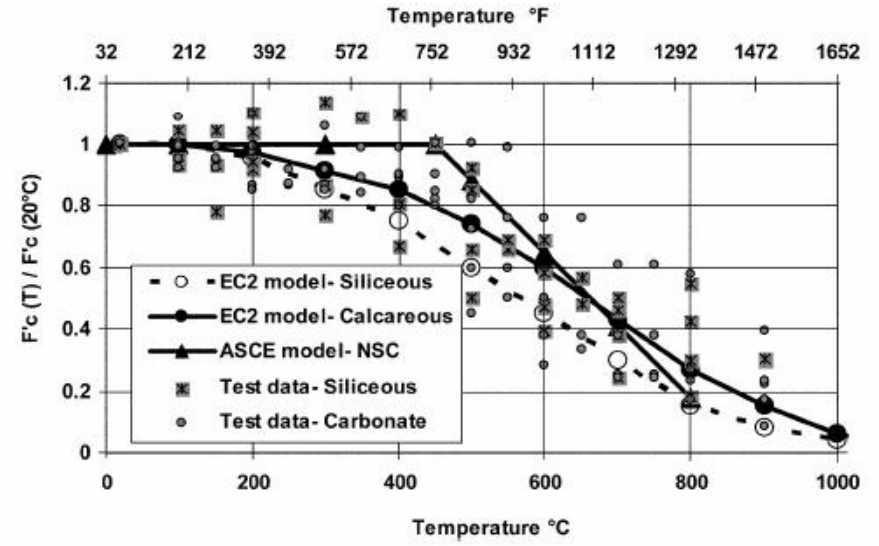

Fig. 1.3 - High temperature models for NSC concrete (Kodur et al. 2008)

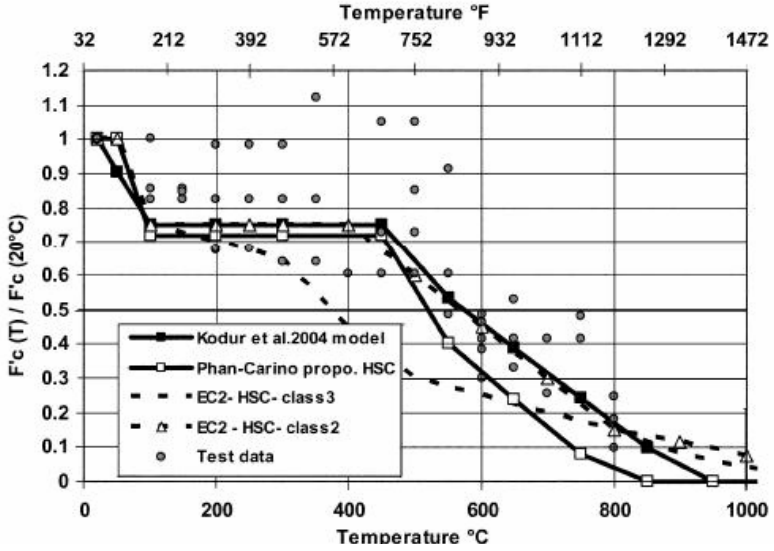

Fig. 1.4 - High temperature models for HSC concrete (Kodur et al. 2008)

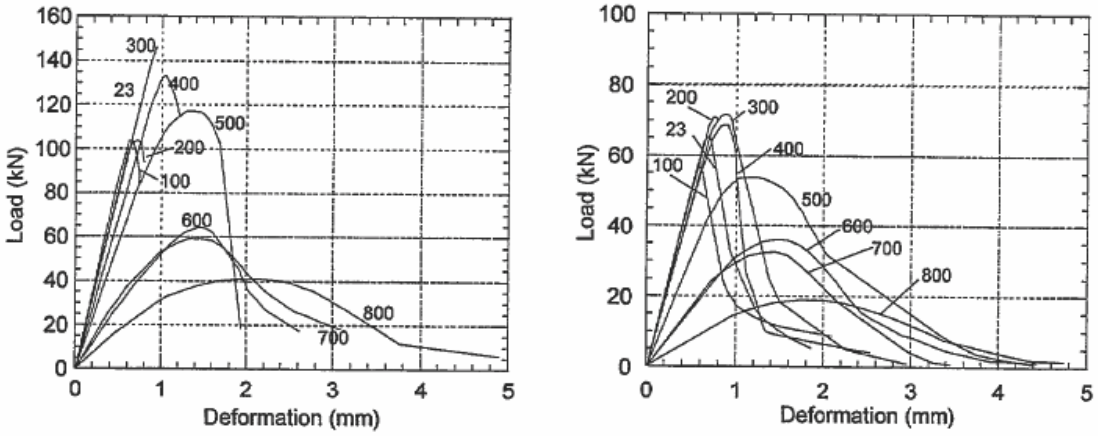

(a) Load-deformation of HSC (b) Load-deformation of NSC

Fig. 1.5 (a)-(b) - Hot isothermal test results (Castillo and Durani 1990)

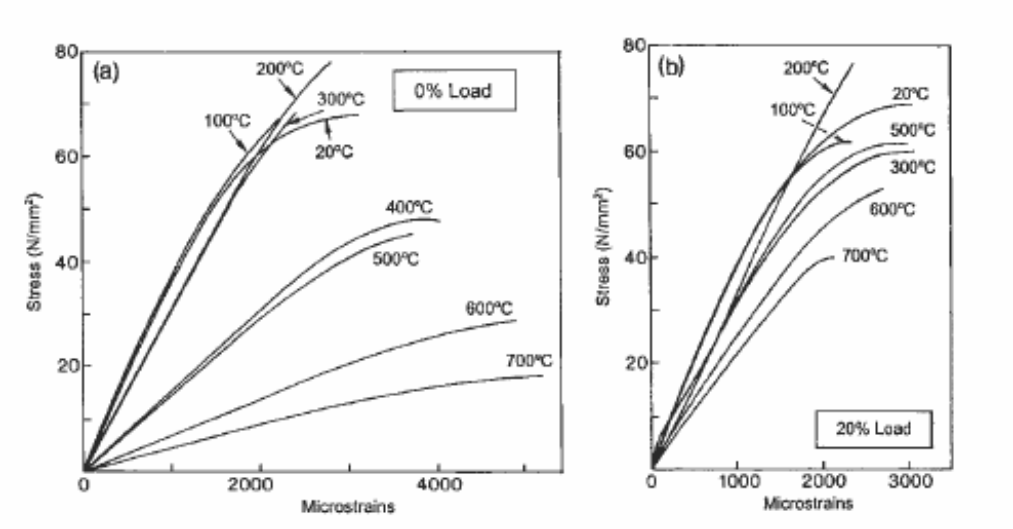

(a) For 0% load (b) For 20% load

Fig. 1.6 (a)-(b) - The effects of loading and temperature on uni-axial compression behaviour of unsealed concrete specimens (Khoury et al. 2002)

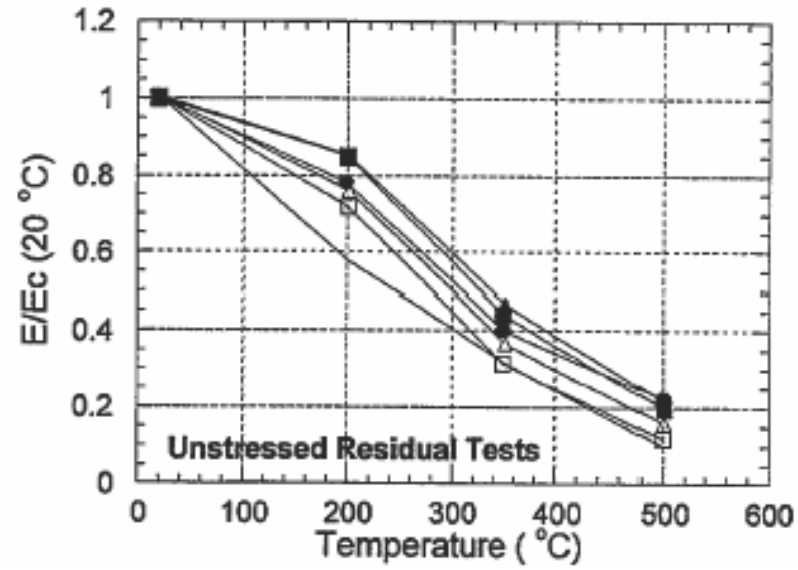

Fig. 1.7 - Hot isothermal test results for residual normalized elastic modulus (Morita et al.1992)

Gary (1916) recognized four categories of spalling: (a) aggregate spalling (popping sound) (b) surface spalling (violent-cracking sound) (c) explosive spalling (violent-loud bang) and (d) corner spalling (non-violent). The first three occur during the first 20-30 minutes of a fire while the corner spalling occurs after 30 minutes. Spalling is defined as the 'violent or non-violent breaking off of layers or pieces of concrete from the surface of a structural element when it is exposed to high and rapidly rising temperatures as experienced in fires'. Some findings related to causes, prediction and prevention of spalling of concrete have been given by

several researchers (Sanjayan and Stocks 1993, Both et al. 1999, Khoury 2000, Kalifa et al. 2001, Canisius et al. 2003, Hertz 2003, 2005, Ali et al. 2004, Tenchev. & Purnell 2005, Georgali & Tsakiridis 2005, Noumowé et al. 2006, Han et al. 2005, 2008, Schneider & Lebeda 2007, Bamonte et al. 2008, Ko et al. 2011). BS 8110: Part 2 (1985) states that 'rapid rates of heating, large compressive stresses or high moisture contents (over 5 % by volume or 2 % to 3 % by mass of dense concrete) can lead to spalling of concrete cover at elevated temperatures, particularly for thicknesses exceeding 40 mm to 50 mm. In fact, many more factors have been identified in the literature cited above which influence explosive spalling in concrete. Their summary is as follows: heating profile, heating rate, section shape, section size, pore pressure, moisture content, permeability, age of concrete, strength of concrete, compressive stress and restraint, aggregate size, type of aggregate, reinforcement, cover to reinforcement, cracking, fibre types, etc. One of the most intricate and hence scantily understood behavioural characteristics of concrete in fires is the phenomenon of 'explosive spalling' (Khoury 2000, Tenchev & Purnell 2005). Two forms of explosive spalling, both influenced by external loading have been identified as pore pressure spalling and thermal stress spalling. Although explosive spalling is frequently assumed to occur only at elevated temperatures, yet it has also been reported in the initial stages of a fire (Canisius et al. 2003) and at temperatures as low as 200 °C (Both et al. 1999). Researchers have reported the effects of wrapping a concrete member in a variety of fabrics so as to evaluate any enhancement of spalling resistance (Bisby et al. 2005). Polypropylene fibres melt at about 160 °C thus making channels for vapour to escape and thus releasing the pore pressures (Han et al. 2005). Steel fiber decreases spalling by provision of lateral confinement pressure to the concrete member which is more than the internal vapour pressure which causes spalling. Wu et al. (2010) has conducted experiments to examine the creep behaviour of high-strength concrete (HSC) containing polypropylene (PP) fibers exposed to elevated temperature. Literature review indicates that polypropylene fibers, when uniformly distributed within concrete, play an active role in improving spalling resistance of concrete at elevated temperature (Bayasi and Dhaheri 2002, Zaidi 2011). Behnooda & Ghandehari (2009) have concluded that the addition of 2 kg/m^3 of polypropylene fibers can significantly promote the residual mechanical properties of HSC during heating.

In reality, a typical fire loading scenario in concrete structures is accompanied by drying as well as heating. Under conditions of fire, drying and heating are coupled together and their separate study is very difficult. Khoury et al. (1985) has suggested that under elevated temperature conditions the total deformation of concrete is because of the actions of all three

variables simultaneously, viz. heating, drying and loading and has been called as the Load Induced-Thermal Strain (LITS). No systematic research on the coupling effects under high temperature are reported in the literature. It is important to note that load-induced thermal strain (LITS) is not the elastic strain due to sustained load, and moreover it increases drastically with increasing temperature. Khoury et al. (1985) has reported that under simultaneous loading and heating, there may be significant reduction in the thermal expansion of concrete by LITS.

It has been reported that at elevated temperatures multi-axial behaviour of concrete specimens gives better indication of performance than testing under uni-axial conditions (Linse et al. 1976, Aschl and Moosecker 1979, Ehm et al. 1985, 1986). A few studies have also been reported on the effect of external fabric or sheet confining material on the fire endurance of concrete columns (Han et al. 2005, 2009). These studies indicated that such external confinement can be helpful in enhancing the thermal stability and fire resistance of concrete columns. It has been demonstrated that appropriately designed fiber-reinforced polymers (FRP)-wrapped reinforced concrete columns are capable of achieving the required fire endurances (Bisby et al. 2005).

It is well documented that mechanical properties of unconfined concrete deteriorate very rapidly with rise in temperature under uni-axial testing conditions (Phan and Carino 1998, Li et al. 2004, Cheng et al. 2004, Li and Purkiss 2005, Fu et al. 2005, Chang et al 2006, Youssef and Moftah et al. 2007, Kim et al. 2009, Sideris et al. 2009, Chen et al. 2009, Knaack et al. 2010, Ghandehari et al. 2010, Bastami and Aslani 2010, Aslani and Bastami 2011, Knaack et al. 2011, Sharma et al. 2012). Therefore, the concept of confinement has been utilized by several researchers to improve the strength and ductility of the concrete specimen at elevated temperature under uni-axial compression testing. Wu et al. (2002) conducted an experimental study to investigate the residual mechanical properties of unconfined and confined high strength concrete on small scale prisms exposed to temperatures of up to 900 °C. The main parameters of the study were exposure temperature and spacing of ties. It was shown that though the stress-strain properties of confined concrete deteriorated with the increase in temperatures, the thermally induced damage was less pronounced in confined concrete than in unconfined concrete. Wu et al. (2002) proposed an empirical stress-strain model to estimate the residual compressive curve of confined concrete. Kodur and McGrath (2006) reported that the provision of cross-ties and reduced tie spacing are beneficial in minimizing spalling in HSC and in increasing fire resistance of HSC columns. Terro and Hamoush (1997) have reported an improvement in the residual compressive strength of up to about 30 percent and in the ductility

of concrete at elevated temperatures due to the effect of tie confinement. Zaidi et al. (2012) has shown elaborately the advantage of confined concrete specimens vis-a-vis unconfined concrete with respect to strength and ductility in the temperature range of ambient to 800 °C. Zaidi et al. (2012) however did not investigate the effect of pre-damage on the residual mechanical properties of concrete exposed to elevated temperatures.

1.3 BEHAVIOUR OF REINFORCING STEEL BARS AT ELEVATED TEMPERATURE

Uni-axial tensile tests are the standard tests to determine the characteristics of reinforcing bar. On the basis of tensile testing, the qualifying parameters for reinforcing bars have been fixed. For example as per IS 1786 (BIS 2008), two parameters are mentioned i.e. minimum guaranteed yield strength and total elongation for the reinforcing bars used in the building structures. The typical stress - strain curves of reinforcing bars exhibit an initial elastic portion up to yield strain (elastic range), a yield plateau i.e. a yield point beyond which the strain increases with little or no increase in stress called plastic range, a strain hardening range in which the stress again increases with strain (strain-hardening range) and finally a range in which the stress drops off until fracture occurs (necking range). Ramberg and Osgood (1943) presented the first model to study the stress - strain behaviour of reinforcing bars at ambient temperature by defining three parameters namely Young's modulus and two secant yield strengths. With the passage of time, several studies have been undertaken for mechanical properties of the reinforcing bars at room temperature (Menegotto and Pinto 1973, Papia et al. 1988, Monti and Nuti 1992, Hoehler and Stanton 2006, Kunnath et al. 2009).

The effects of high temperature on the mechanical properties of pristine steel rebars have been investigated by many researchers (Holmes et al. 1982, Schneider 1985, Krampf and Haksever 1986, Gustaferro and Martin 1988, Schneider 1989, Dotreppe 1997, Phan and Carino 1998, Felicetti and Gambarova 1998, Zilli and Fattorini 2002, Eurocode-2 2004). Under elevated temperatures, both stiffness and strength of steel deteriorate in a fashion approximately similar to concrete (Freskakis 1980). Typical stress-strain response at elevated temperatures is characterized by a drastic reduction of the proportion limit under increasing temperatures accompanied by an increase in the ultimate yield strength up to 300 °C with reduced ductility as given in Fig. 1.8. Freskakis (1980) also reported that beyond this temperature limit, the ultimate strength and the yield strength decreases rapidly with temperature while the ductility increases.

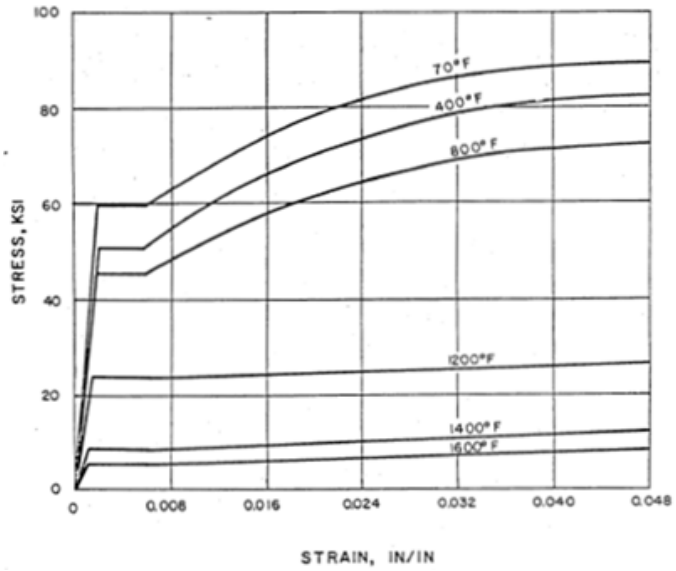

Fig. 1.8 - Stress-strain relationships for steel at different temperatures (Freskakis 1980)

A large amount of data is available in the literature on steady state and transient tests on steel reinforcing bars at high temperature (Harmathy and Stanzak 1970, Holmes et al. 1982, Lie 1992, Hertz 2004, Elghazouli et al. 2009). Elghazouli et al. (2009) has carried out an experimental investigation of the influence of elevated temperatures on the mechanical properties of hot-rolled and cold-worked steel reinforcement of diameters 6, 8 and 10 mm. This study included tests carried out at ambient temperature as well as under steady-state and transient elevated temperature conditions. A residual steady-state tensile test series was also discussed in this investigation to assess the residual post-cooling properties of reinforcing bars. For the hot-rolled bars in this experiment, ultimate strains increased by a factor of over two at 600 °C. On the other hand, the enhancement of ultimate strains in cold-worked bars was in excess of three times the ambient values at 600 °C and increased more rapidly at higher temperatures. Results from this tests showed that the post-cooling residual properties of both hot-rolled and cold-worked reinforcement bars remain largely unchanged up to 400 °C. However, after being exposed to higher temperature levels, a reduction in strength is observed reaching 10-15 % in the case of cold-worked bars at exposure temperature of 600 °C. More importantly, the enhancement in the residual ultimate mechanical strain at 600 °C was shown to be about 50 % in hot rolled specimens and about 150 % in the case of cold-worked bars. Elghazouli et al. (2009) has reported that the findings related to ultimate mechanical strain at elevated temperature and after cooling, are critical for dependable evaluation of the performance of structural members in fire as well as for post-fire rehabilitation. The mechanical

properties of steel rebars deteriorate when they are heated, and conventional steel at 600 °C has a yield strength less than 1/3 the specified yield strength at room temperature (Ünlüoğlu. et al. 2007). It has been reported that the degradation in stiffness is more pronounced than that in strength of steel reinforcement due to the effect of heating. Further, the reduction in strength and stiffness of steel reinforcement with increase in temperature depends on the process of manufacturing of the reinforcing bars (Anderberg 1978, Buchanan 2001, Eurocode-2 2004).

Relatively little data is available on the residual properties of steel reinforcement after a complete cycle of heating and cooling (Neves et al. 1996, Topcu and Karakurt 2008, Elghazouli et al. 2009, Felicetti et al. 2009). Neves et al. (1996) has reported results of experimental studies on steel rebars subjected to a complete cycle of heating and cooling. The results obtained from their tests showed no major alterations in mechanical properties for temperatures of up to 600 °C, whereas for temperatures above 700 °C, significant changes in the steel properties was observed. Felicetti et al. (2009) has studied the residual mechanical properties of steel bars subjected to temperatures up to 850 ºC, with reference to a number of steel and bar types (viz. quenched and self-tempered bars, carbon and stainless steel, smooth and deformed bars, hot-rolled and cold-worked bars). The test results showed that quenched and self-tempered bars (QST), are more sensitive to temperatures above 600 ºC compared to carbon-steel bars. Further, the best response was exhibited by the stainless-steel bars, provided that they were hot rolled and strength loss was sizeable in the case of cold-worked bars. Finally, it was suggested on the basis of this investigation that design codes should give more consideration to reinforcement residual properties relevant to the fire design of reinforced concrete sections.

Topcu and Karakurt (2008) have indicated that the reduction of modulus of elasticity and yield strength of steel rebars is considered as the primary element which affects the performance of RC structures in fires. They have recommended that the protective cover thickness should be more for enhancing the fire safety of reinforced concrete members. Chen and Young (2006) have presented the mechanical properties of stainless steel at higher temperatures. They conducted both transient and steady tensile coupon tests at different temperatures ranging from nearly ambient to 1000 °C to obtain the material properties of stainless steel. In this investigation, the yield strength obtained at different strain levels, elastic modulus, thermal elongation, ultimate strength and ultimate strain were evaluated as functions of temperature. Cooke (1988) has presented data on mechanical properties of hot rolled structural steel used in buildings and has discussed properties like stress-strain relationships, thermal expansion and phase transformation, Poisson's ratio and elastic modulus. Chen et al.

(2009) has reported an experimental research on the influence of fire exposure time on the post-fire behaviour of reinforced concrete columns. The results obtained from this test showed that as the fire exposure time increases, the residual load-bearing capacity decreases. They have also reported that reduction in strength resulting from an increase in fire exposure time can be decelerated by strength reclamation of hot rolled reinforcing bars after cooling. Zaidi (2011) has reported the results of an experimental investigation carried out to evaluate the residual mechanical properties of reinforcing bars exposed to elevated temperatures in the range of ambient to 800 °C followed by air cooling.

Bingo and Gul (2009) has investigated the effects of cooling regimes and elevated temperatures on the residual bond strength between reinforcing steel bars and concrete. The test results of this investigation showed an increase in bond strength for temperatures up to 150 °C, though there was a decrease for temperatures in the range of 150 to 700 ºC. In this experiment, the effect of cooling conditions was observed to be less pronounced for the concrete-rebar bond strength. They have concluded that concrete-rebar bond strength increases with compressive strength of concrete and embedment length of the rebar. Giroldo and Bailey (2008) have presented the bond characteristics between steel reinforcement and concrete at ambient and elevated temperatures for modeling global behaviour and predicting reinforcement fracture at ultimate failure. Haddad et al. (2008) has investigated the bond behaviour between fiber reinforced concrete and 20 mm diameter reinforcing steel rebars exposed to elevated temperatures. The results of this investigation presented noticeable reductions in residual compressive, splitting and steel–concrete bond under elevated temperatures with sudden changes in bond stress–free-end slip behaviour.

1.4 BEHAVIOUR OF RC STRUCTURES IN FIRES

A structural element (slab, beam or column) is generally evaluated for fire resistance rating using standard fire test without any provision for interaction effects of these elements with the rest of the structure. A standard heating curve ISO 834 (ISO 1975), developed in a fire resistance test furnace is normally used to assess the performance of an individual concrete element (Drysdale 1999, Buchanan 2001). A temperature-time curve can be used to define this heating regime, which is a representative of the development of a fire in a standard room and expressed in essentially identical form in a number of standards viz. ISO 834 and ASTM E-119 (ISO 1975, ASTM E 2001). Analytically, fire resistance can be determined based on modeling and analysis of the structural assembly or element using available software tools.

1.4.1 Slabs

Several experimental and analytical studies considering the effect of key parameters have been reported on the behaviour of isolated RCC slabs in fires. No measurable difference in performance of high-strength concretes and conventional strength concretes slab in fires were reported (Shirley et al. 1988). The influence of varying type of concrete, slab thickness, soffit protection, imposed load and nature of fire exposure on the axial movements of the slab ends and mid-span flexural deflection were reported on the basis of testing of simply supported precast reinforced concrete floor slab panels exposed to two standardized heating regimes (Cooke 2001). Kodur et al. (2005) has carried out experimental studies to examine the thermal performance of concrete slabs reinforced with carbon and glass fiber-reinforced polymer (FRP) bars taking the test parameters as aggregate type, reinforcement type, concrete cover thickness, slab thickness and effectiveness of supplemental fire insulation. The type of reinforcement and the thickness of the concrete cover to the reinforcement were found to be the key parameters in this study. The results obtained from this parametric study revealed that FRP-reinforced concrete slabs have lesser fire resistance than slabs reinforced with conventional reinforcing steel. A series of simple design charts have been presented based on this parametric study that can be used to evaluate the fire endurance of FRP-reinforced concrete slabs. The complex features of structural behaviour of reinforced concrete slabs in fire conditions, such as thermal expansion, reinforcement type, boundary conditions, spalling, cracking or crushing, aggregate type and change of material properties with temperature have also been analytically investigated (Hurst and Ahmed 1998, Huang et al. 1999, 2003, 2004, Lim et al. 2004, Elghazouli and Izzuddin 2004, Kodur and Bisby 2005, Bailey and Toh 2007, Yu et al. 2008, Huang 2010, Dong 2010, Abu et al 2011, Abu et al 2013)

1.4.2 Beams

The behaviour of reinforced concrete (RC) beams exposed to fire depends on the internal temperatures experienced by the beam, the load levels during the fire event, the cooling method, the rate of cooling, the strength recovery time following the cooling period and support conditions, axial restraints and concrete cover (Khan and Royles 1986, Shi et al. 2004, Izzuddin and Elghazouli 2004, Kodur et al. 2010, Panda et al. 2011, Kodur and Dwaikat 2012). Desai (1998) has reported a method for estimating the residual flexural and shear capacities of a reinforced concrete beam for various exposure durations. Residual strength tests on model reinforced concrete beams and columns after exposure to temperatures of up to 1000 ºC along

one face have been investigated (Mohamedbhai 1982). A three-dimensional finite element (FE) model for prediction of response of reinforced concrete (RC) beams reinforced with either steel or fiber-reinforced polymer (FRP) bars under an elevated temperature regime was presented by Rafi et al. (2008). The fire resistance of high strength concrete beams can be lower than that of normal strength concrete beams due to fire induced spalling resulting from low permeability in high strength concrete (Kodur and Dwaikat 2008). Kodur and Dwaikat (2008) applied a macroscopic finite element model to study the effect of six parameters, namely load level, fire scenario, aggregate type, concrete cover thickness, span length and failures criteria on the fire response of RC beams. Dwaikat and Kodur (2009) have presented that higher levels of spalling is exhibited by HSC beams which is mainly influenced by load level, permeability of concrete, type of fire exposure and restraint conditions. Similarly, load level, axial restraint and the types of fire scenario have significant influence on the overall fire resistance of RC beams (Dwaikat and Kodur 2009). Fitiany and Youssef (2009) have proposed a simple method for prediction of the flexural and axial behaviour of RC sections during exposure to high temperatures.

1.4.3 Columns

The provision of suitable fire safety measures for reinforced concrete columns is one of the fundamental safety requirements in building design, since they are the principal load transferring components of a building structural frame. The origin for this requirement can be recognized by the fact that, when other features for containing a fire fail, structural integrity is the last line of defense. A review of literature indicates that there have been a number of experimental and numerical studies in recent years on the performance of RC columns in fires (Book et al. 1990, Dotreppe et al. 1996, Sidibe et al. 2000, Ali et al. 2004, Benmarce and Guenfoud 2005, Yu et al. 2007, Jau and Huang 2008, Yao and Tan 2009, Bisby et al 2011). These studies investigated the effect of various key parameters, such as concrete strength, cross-section size, presence of fibres, load intensity, etc. on the fire response of columns. Kodur et al. (2006) has reported a comparison of the fire resistance of full-scale FRP-strengthened RC columns and conventional unstrengthened RC columns. Several full-scale reinforced concrete (RC) columns with different shapes viz. T-shaped cross-sections, L-shaped cross-sections, square cross-section and plus (+)-shaped cross-sections were studied experimentally for fire resistance by Xua and Wub (2009). The test results obtained from these experiments explain the effects of fire exposure condition and axial load ratio on axial deformation, failure mode and fire resistance of the columns. A simple and rational method to predict the fire resistance of RC

columns subjected to four-face heating was developed by Tan and Yao (2003). This method can be extended to 1, 2 and 3 face heated columns with some modifications. The development of mathematical models for the calculation of fire resistance of different types of columns of various sizes and shapes has been reported by many researchers (Lie and Celikko 1991, Lie and Irwin 1993, Lie and Chabot 1993, Dotreppe et al. 1999, Kodur et al. 2004, Tan and Tang 2004, Bisby et al. 2005, Wang et al. 2009).

Lie and Woolerton (1988) tested 41 RC columns made with normal strength concrete (NSC) under standard fire conditions. The main aim of the study was to generate the experimental data on fire resistance of RC columns and to develop the calculation methods for predicting the fire resistance of concrete columns and walls. The different parameters which were studied included the shape of cross section, cover thickness, reinforcement, aggregate type, load, and load eccentricity on the fire resistance of RC columns. The study concluded the better fire performance with carbonaceous aggregate.

Aldea et al. (1997) tested six RC columns under ISO 834 standard fire exposure. The main aim of testing was to examine the influence of the reinforcement diameter and number on the spalling of concrete. It was observed that the HSC columns showed corner spalling at an early stage of fire exposure which caused the premature heating of steel rebars. Spalling in NSC columns was not witnessed which concluded the more significant influence of material behaviour on the fire resistance of the columns.

Franssen and Dotreppe (2003) performed tests on four circular RC columns to examine the effect of circular shape on the fire behaviour of concrete columns. It was aimed to examine whether the circular sections are less susceptible to spalling owing to the fact the circular cross sections are devoid of the corners. No effect of circular shape was seen in mitigating the spalling of the columns. The experimental research led to the development of a simple calculation method.

Kodur (2003) carried out an experimental study on large number of full-scale RC columns and it was aimed to develop the fire resistance guidelines for HSC columns. The columns were cast using NSC as well as HSC with strength varying from 34 to 110 MPa and were subjected to ASTM E119 standard fire exposure. A large number of variables were taken and their effect on the fire ratings of RC columns was studied which included the type of aggregate, the tie configuration, the fiber reinforcement, type of fiber, applied load and the

eccentricity of the load. The test results revealed that the columns made with HSC are more susceptible to spalling and result in decreased fire ratings. Concrete with strength more than 70 MPa was found to be prone to higher spalling due to its lower permeability. The columns which had the 135° bent ties and closer ties showed higher fire resistance. It was also seen in this study that addition of polypropylene fibers by about 0.1-0.15 % by volume minimises the phenomenon of spalling. Same effect was observed vis-à-vis steel fibers. Kodur et al. (2003) carried out fire experiments on 15 RC columns. The columns were divided into five sets of three columns each. Four sets of columns were made of HSC while one set was made with NSC. Steel and polypropylene fiber reinforcement was added to two sets. Four sets were made with siliceous aggregate and set 3 was made with carbonate aggregate. Columns were tested under concentric loads with fixed end conditions and exposed to ASTM E119 fire exposure. The variables considered in these tests included concrete strength (NSC and HSC), aggregate type (siliceous and carbonate aggregate), and fiber reinforcement (steel and polypropylene fibers). It was seen that the temperatures in NSC column were lower than the corresponding temperatures in the HSC columns due to the variation in the thermal properties of the two concretes. The HSC columns showed significant corner spalling just before the failure while as the NSC column didn't underwent any spalling. Spalling was also shown to be more prominent in the columns made with siliceous aggregate.

Kodur and McGrath (2003) conducted fire resistance tests on six square RC columns, of length 3810 mm, to study the factors influencing the thermal and structural behaviour of HSC columns under standard fire conditions. The columns were tested under concentric loads varying from 54% to 123% of the service load. The tie configuration was found to play a role in the performance of the columns. The rebars yielded before the failure occurred. The ties with 135° bend did not open up, while the 90° bent ties opened up. The fire resistance of HSC columns increases with decreasing load, and carbonate aggregate concrete columns provides about 10% higher fire resistance than column made with siliceous aggregate concrete.

Ali et al. (2004) tested 99 short columns aimed at investigating the effect of load ratio, the degree of axial restraint and the heating rates on the fire performance of HSC and NSC columns. It was observed that the load levels up to 60% of the design strength have no effect on the spalling whatsoever is the heating regime. It was seen that spalling can be a major cause for the failure of the columns due to the loss of major portion of the concrete section causing the reduction of carrying capacity of the columns and ultimately the failure. Higher heating rates

led to explosive spalling. The study revealed that higher tensile strength in HSC balances or overcomes the low permeability effect to some extent. Therefore, NSC could show more susceptibility for spalling due to its low tensile strength (which is approximately half the tensile strength of HSC). This observation is in contradiction to many other studies in the literature, which reported that HSC is more susceptive to explosive spalling.

Benmarce and Guenfoud [2005] studied the fire behavior of HSC columns by conducting fire tests on twelve HSC columns. Three load ratios, 20%, 40 and 60% were applied to the columns at two restraining ratios of 0.1 and 0.2. From these fire tests, it was concluded that fire resistance of HSC columns reduced with the increase in load ratio. The large load ratios reduced the steel and concrete temperatures at which the failure occurred in the columns. The drop in failure temperatures was as anticipated, since less restraint force was required for the failure load to be reached. Imposing a restraint against axial expansion (of column) leads to lesser forces generated in the column.

Raut and Kodur (2011) have carried out an experimental investigation on HSC columns and have presented a comparative performance of HSC and normal-strength concrete (NSC) columns under design fire conditions. The results obtained from their fire experiments showed that lower fire resistance is exhibited by HSC columns compared to NSC columns.

Inelastic deformability of reinforced concrete elements is essential for the overall stability of structures in order to sustain various natural and man-made hazards. The desired deformability of reinforced concrete structural components is generally achieved through proper confinement of the core concrete **(**Sheikh and Uzumeri, 1980, Mander et al., 1988, Saatcioglu, and Razvi, 1992). The effects of various key parameters of confinement on the strength and ductility of confined concrete at ambient temperatures are well documented now (Sargin, 1971, Park and Sampson, 1972, Sheikh and Uzumeri, 1980, Mander et al., 1988, Saatcioglu and Razvi, 1992, Sheikh and Toklucu, 1993, Sharma et al., 2005). The design and detailing of critical hinge regions of concrete columns has been of great concern to engineers and designers in the recent past with respect to their performance during earthquakes only. On the contrary, little research has been undertaken to investigate the significance of confined end regions of reinforced concrete columns during fire. Therefore, there is a need to account for the confinement provided by ties in the procedures for fire resistant design of reinforced concrete columns. In order to achieve that, it becomes important to evaluate the effectiveness of

confinement reinforcement in confining core concrete after exposure to elevated temperatures. It also remains to be seen that how the various parameters of confinement would affect the behavior of concrete after exposure to elevated temperatures.

1.4.4 Frames

Structural fire testing is undergoing rejuvenation with full scale tests being performed on various structural systems. The conventional, and widely used, method for fire testing, where in single structural elements are subjected to a standard fire test (ISO, 1975) and thereby obtaining a fire resistance rating which is mainly in the form of a time to failure, has of late been noticed to have a number of drawbacks (Drysdale, 1999) though the method is still widely used. The perception that the concrete structures behave well in fire has led to overly simplified design guidelines, in the form of concrete cover. However the behavior of structural systems in fire is proved to be quite complex due to interaction effects between different structural elements of the structural system. This simplification in design procedure was a result of standard fire tests of simple building elements or isolated structural assemblies in testing furnaces which subject the loaded elements to a standard temperature-time curve. The issues of the inherent problems, which are associated with using simplified single element based laboratory tests subjected to standard temperature-time curves, are being solved by performing large scale non standard fire tests using real fires. This shift in testing philosophy from prescriptive standard fire testing to large scale non standard fire testing using real fires has been aimed at understanding the global behaviour of structures in fire which has received relatively little attention in the past. The significance of performing the large scale tests is reflected by the lack of experimental data on the performance of complete concrete structure in fire.

The response of individual structural elements exposed to standard fires is fairly well understood and documented but the behaviour of a structural assemblage may vary extensively from element response because of interaction effects. The extension of analytical or experimental results to a comprehensive modeling or testing of a structure as a whole was a significant advancement in fire engineering. In an experimental study by Vecchio and Sato (1990), three large-scale reinforced concrete portal frame models were subjected to combinations of thermal and mechanical loads under different test conditions viz. unrestrained thermal deformation, restrained deformation under shock thermal loads, and loading to ultimate capacity. In this investigation, the different aspects of response were monitored in terms of resulting restraint forces, deflections, strains, cracking, and leakage. The results obtained from

these tests indicated that thermal loads can result in significant stressing of a structure and can lead to concentrated damage in local regions. Mutairi and Shaleh (1997) on the basis of their inspection of fire-damaged Kuwaiti structures reported that these structures showed damage in the form of buckling, distortion and collapse of structural steel frames, yielding of steel reinforcements within concrete (causing large deflections), disintegration of reinforced concrete, and buckling of structural elements, as well as damage to a variety of interior elements. Flint et al. (2007) has reported an investigation of the effects of fire on long span truss floor systems in a tall building environment with a phenomenon of progressive collapse. Irfanoglu and Hoffmann (2008) have done a simulation study of the performance of the North Tower WTC-I of the World Trade Center complex during the impact of American Airlines Flight 11 on September 11, 2001 and finally estimated that a core collapse mechanism could be initiated if the tower core column temperatures were elevated to about 700 °C. Xiao et al. (2008) has presented an extensive experimental study on the fire response of frame structures constructed with high-performance concrete (HPC) as well as the post-fire seismic performance. They have concluded that under a fire attack, an indeterminate structure may fail prematurely due to the additional stress from internal force distribution whereas after a fire attack, the difference in stiffness degradation between beam and column can possibly transform a strong-column-weak-beam frame into a strong-beam-weak-column one that performs poorly under cyclic loadings.

Some testing programmes on full-scale multi-storey composite as well as steel buildings were conducted to study the structural response of a building to fire (Wang 2000, Elghazouli and Izzuddin 2001, Usmani et al. 2001, Lennon and Moore 2003, Foster et al. 2007, Vassart et al. 2012, Phan et al. 2015, Johnston et al. 2015). Under full-scale testing, the behavioural aspects such as the complex structural interactions that occur under fire conditions and influence of restraint to thermal expansion were investigated. Sanad et al. (2000) reported that the response of highly redundant structures is dominated by thermal expansion under local fires, and that large deflections and local yielding can be beneficial in reducing damage to the complete structure. Cioni et al. (2001) has illustrated fire damage to reinforced-concrete buildings with some thermal history and irreversible thermo-chemical reactions. Folic et al. (2002) have investigated the effect of fire which spread over the top six floors of the 54 m tall building of the Open University in Novi Sad. The fire caused severe damage to the steel facade structure and the load-bearing reinforced concrete structure. Lamont et al. (2004) has described the results of a finite element analyses on small generic composite steel and lightweight

concrete frames during two different single floor compartment fires. Franssen et al (2007) has developed a concept of zoning for analyzing fire behaviour of a structure. Dong and Prasad (2009) has conducted a furnace test on two full-scale composite steel frames. On comparison, the data obtained from the two tests reveals that the composite beam has a significantly better fire resistance than a steel column. Fire resistance rating of frames constructed with slim floor slabs is found to be at least as good as that of frames with conventional floor slab construction (Dong and Prasad 2009). Hopkin et al. (2011) has conducted full-scale fire tests on engineered floor joist assemblies and gypsum lined structural insulated panel (SIP) and finally recognized a number of system redundancies and alternative load paths, because of which the total collapse of any of the test buildings subjected to natural fire scenarios was prevented.

Vecchio (1987) has derived a simple analytical procedure for accurate prediction of the response of reinforced concrete plane frames to thermal and mechanical loads. The influencing factors such as nonlinear material stress-strain response, tension stiffening effects, membrane action, thermal creep, load and time history, nonlinear thermal gradients, and material properties at elevated temperatures were taken into account using appropriate models (Vecchio 1987).

A computerized thermal and strength simulation system was newly developed for concrete structures in fires by Kuwahara and Koh (1995). Huang and Platten (1997) have described a nonlinear finite element procedure for predicting the structural behaviour of planar-reinforced concrete members subjected to fire. They have considered the complex features of structural behaviour in fire conditions, such as shrinkage, thermal expansion, cracking, or crushing, creep and change of material properties with temperature, excluding the spalling of concrete. Terro (1998) has developed finite element thermal and structural computer programs to predict the behaviour of three-dimensional reinforced concrete structures in fire. The results obtained from this program highlight the important role that transient thermal creep plays, particularly in columns. Sanad et al. (2000) has modeled the full-scale Fire Tests at Cardington in an effort to develop a new understanding of the behaviour of structures under fire conditions. Wong (2001) has presented a plastic analysis method for the calculation of critical temperature distribution in structures at collapse under fire conditions. Aiello et al. (2001) have carried out the analysis of fiber-reinforced polymer (FRP) reinforced concrete elements under thermal loads. Huang et al. (2009) has developed a robust nonlinear finite-element procedure for three-dimensional modeling of reinforced concrete beam-column structures in fire conditions, where both geometric and material nonlinearities were taken into account in the formulation. In this

procedure, the more complicated aspects of structural behaviour in fire conditions, such as transient state strains in the concrete, thermal expansion, yielding of steel, cracking or crushing of concrete, and change in material properties with temperature were modeled. From this research, it can be concluded that the effect of transient state strains of concrete on the deflection of structures can be very significant. They have also emphasized that the impact of concrete spalling on both structural and thermal behaviour of reinforced concrete members is very significant. Jeffers and Sotelino (2009) have introduced a new type of heat transfer finite element which can be used to model the three-dimensional thermal response of structural beams and columns subjected to high temperatures and this tool can be used for modeling the behaviour of framed structures in fire. Yu et al. (2010) has developed and presented a three-dimensional eight-noded brick element capable of representing the performance of composite structures subjected to 3D stress conditions at ambient and elevated temperatures.

Building Research Establishment (BRE) laboratories in Cardington, UK has conducted two major fire tests on full-scale multi-story and multi-bay structures exposed to fires. The first fire test program consisting of a set of six tests during 1995-1996 was conducted on a full-scale multi-storey composite building constructed at BRE, Cardington (Newman et al. 2000). Bailey (2002) has reported experimentally on a full-scale seven-storey in-situ reinforced concrete building constructed at the BRE laboratories in Cardington and the fire test was carried out on this structure on 26th September 2001 using a fire load provided by wood cribs in an open compartment on the ground floor, surrounding a high-strength concrete column. The tested building was constructed of normal and high-strength concretes and was designed for 60 minutes fire resistance, using the UK design Code. The completed building comprised 3 × 4 bays, each of 7.5 m. Each floor slab had a nominal thickness of 250 mm and was made of normal-weight concrete and designed as a flat slab supported by internal columns 400 mm square and external columns 400 mm by 250 mm. Spalling in fire was reduced by adding 2.7 kg/m^3 of polypropylene fibres to the concrete mix. This test presented that the floor slab underwent extensive spalling and exposed the bottom steel reinforcement as shown in Fig.1.9. The explosive nature of the spalling observed during the test and inspection of the area of spalling suggests that there were high compressive forces induced in the slab because of restraint to thermal expansion of the concrete slab due to the presence of cold surrounding areas in the structure. These compressive stresses were probably favorable for the survival of the floor slab due to compressive membrane action. The nature of spalling around the service holes (Fig. 1.10) also suggests that spalling was predominantly due to high compressive stresses,

since no spalling occurred where the compressive stresses got reduced along the edges of the hole. Although concrete spalling considerably reduced the flexural strength of the slab, collapse did not take place. This could be attributed to the behavior of slab in compressive membrane action. This test also presented significant lateral displacement of external columns because of thermal expansion of the heated slab as illustrated in Fig. 1.11. The results obtained in this Cardington test were used to provide input data for a finite element model which made large number of assumptions regarding the performance of concrete in fire (viz. the effects of spalling were neglected) (Canisius et al. 2003). Further study of the effects of fire on full-scale buildings is highly desirable and will yield valuable data which can be used for the calibration of numerical models.

Fig. 1.9 - Picture showing extent of spalling of roof slab (Bailey 2002)

Fig. 1.10 - Picture showing spalling around service hole (Bailey 2002)

Fig. 1.11 - Picture showing lateral displacement of external columns (Bailey 2002)

The performance of a whole building in fire may be judged from observed behaviour in a real fire incident. This recorded data on real fires in buildings may be an additional source of information for current research work, as for example, the Windsor Tower fire in Madrid (February 2005) (Capote et al. 2006), core collapse of Sao Paulo Power company (CESP) 21-story office building-2 (Fig. 1.12) in a fire on May 21, 1987 (Berto and Tomina 1988) and fire in the 8-story Katrantzos building (Fig. 1.13) in Athens on December 19, 1980 (Papaioannou and Kyriakos 1986). The prime objective is the reproduction of the fire scenarios which might have existed in real fire for which use of advanced modelling tools can be of great support together with scientific interpretation of various forms of records and observations related to a fire, e.g. video evidence etc.

Fig. 1.12 - CESP 2 core collapse in Sao Paulo, Brazil (Beitel and Iwankiw 2002)

Fig. 1.13: Katrantzos department building in Athens after the 1980 fire **(**Beitel and Iwankiw 2002)

Review of the literature shows that application of performance based assessment and analysis necessitates modeling and analysis of the entire structures taking into account the boundary conditions, restraints and large deformation effects viz. P-Δ effects (Bailey 2004, Iwankiw et al. 2008, Dwaikat and Kodur 2008). Brief review on past building collapses due to fire show the reality that performance and behaviour of structures in fires is significantly dependent on three-dimensional effects and the overall properties of structures including thermal expansion mechanism (Beitel and Iwankiw 2002, NIST 2008, Usmani 2001). Further, structural thermal expansion mechanism is the main induced effect during fire in building structures, for which very limited data and information is available. An illustration of thermal expansion effects on structural performance in fire is given in Fig. 1.14, during a massive fire at the US Military Personnel Records Centre Building (Beitel and Iwankiw 2002). Lateral deformations of columns due to floor thermal expansion have also been observed in full-scale fire tests as shown in Fig. 1.11 (Bailey 2002). Typically the larger the floor size is, larger are the thermal expansion and lateral deformations (Beitel and Iwankiw 2002, Bailey 2002). Thermal expansion of members exposed to heating may lead to forces being exerted upon the cooler members because of differential expansion, with compression forces inside the heated members due to restrictive forces provided by the rest of the structure as shown in Fig. 1.11 (Bailey 2002). Although thermal expansion may not be a main design concern at ambient temperature for building structures, but when it comes to structural performance under fire exposure, studies on past building damages and collapses under the effect of fire have showed

that thermal expansion plays a key role in the behavior and response of buildings (Sunder 2008). A survey of the past collapse of buildings on fire (Beitel and Iwankiw 2002) has shown that thermal expansion can induce large deformations on the structural systems which may result in partial or total collapse of structures. Presently, there is a lack of knowledge and design methodology to evaluate and mitigate the thermal expansion effects on the performance of structures in fire.

The problem of thermal expansion of concrete structures is compounded by the lack of experimental studies on sub-assemblages or whole structural systems. Only a limited amount of experimental data is available on the behaviour of full–scale frames because of difficulties and high cost associated with the test set up and experimental facilities.

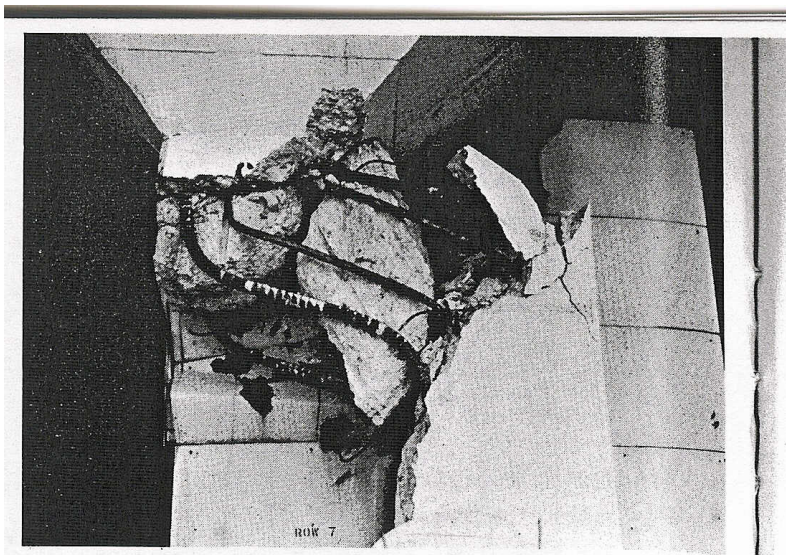

Fig. 1.14: Shear failure of a column due to the floor thermal expansion in fire (Beitel and Iwankiw 2002)

1.5 BEHAVIOUR OF RC FRAMES IN FIRE-FOLLOWING-EARTHQUAKE SCENARIO

Fire is the most severe environmental hazard to which built infrastructure is subjected to and the situation is further exacerbated by other hazards such as earthquake, impact and blast. In the past centuries, several post-earthquake fires have resulted in the failure of buildings reinforced concrete structures and subsequent collapse of whole structural systems. Some studies on post-earthquake fire have been reported in the past (Chung et al. 1995, Taylor 2003, Della Corte et al. 2003, Eidinger 2004, Scawthorn et al. 2005, Scawthorn et al. 2006, Pintea et al. 2008, Mousavi et al. 2008, Rini & Lamont 2008, Wikipedia 1906 San Francisco Earthquake 2009, Wikipedia 1923 Great Kanto earthquake 2009, Wikipedia 1995 Great Hanshin (Kobe)

Earthquake 2009, Ghoreishi et al. 2009, Tesfamariam 2010). In the first of its kind, Sharma et al (2012) tested an earthquake damaged reinforced concrete frame in fire. A Reinforced Concrete (RC) 3D vertically-loaded frame, consisting of four columns, four plinth beams, four roof beams and a slab, was first subjected to cyclic loading representing an earthquake and subsequently to a compartment fire. Massive spalling in different members of the assembly was observed. Even though the lateral strength of the frame was greatly reduced after the fire, no structural failure was observed. The test provided data in terms of temperatures, strains, displacements as recorded for the beams, columns and the roof slab. Kamath (2014) also tested a reinforced concrete frame with higher level of seismic damage and subsequently exposed the same to one hour compartment fire. These studies have investigated the in-situ performance of members as well as the response of whole structures to fires following earthquake events.

Studies on post-earthquake fires, such as fires-following April 18, 1906 San Francisco earthquake and the September 1, 1923 Tokyo earthquake the largest peacetime urban fire in history, indicate that 80% of building damages (28,000 buildings destroyed in San Francisco alone) were due to the post-earthquake fire rather than earthquake-induced ground shaking (Scawthorn et al. 2006).

Beitel et al. (2002) has reported some historical records of recent post earthquake fires viz. October 17, 1989 Loma Prieta Earthquake, January 17, 1994 Northridge, CA Earthquake and January 17, 1995 Kobe Earthquake, which didn't evidently indicate any specific multi-story building failures because of post-earthquake fires. Nevertheless, there is a severe risk to all types of construction in their potentially damaged post-earthquake state due to such fires, both in terms of their decreased structural and fire resistance. While there is not any direct evidence of such occurrences in multi-story buildings from past experience, the probability for this combined extreme hazard from both earthquake and fire exposures does exist.

The need for ductile behaviour of various structural components during any major earthquake has been acutely felt and demonstrated amply during several seismic events. Although it is preferable to dissipate seismic energy by post-elastic deformations in beams, column hinging cannot be avoided entirely in most buildings during severe earthquakes. To achieve sufficient ductility in columns, their potential plastic hinge regions should be reinforced with appropriately designed and detailed longitudinal and lateral confining steel. Reinforced concrete (RC) frame structures constructed before the mid-1970s lack important features of good seismic design, such as strong columns and ductile detailing of reinforcement, making them potentially vulnerable to earthquake-induced collapse. These non-ductile RC frame

structures have incurred significant earthquake damage in the 1971 San Fernando, 1979 Imperial Valley, 1987 Whittier Narrows, and 1994 Northridge earthquakes in California, and many other earthquakes worldwide (Liel et al, 2011). Building code requirements for seismic design and detailing of reinforced concrete have changed significantly since the mid- 1970s, in response to observed earthquake damage and an increased understanding of the importance of ductile detailing of reinforcement. However much of the building stock, especially built before 1970's in developed countries and before 1990's in developing countries like India, has been designed as non-ductile frames and therefore are vulnerable to multi hazard damage also. In developing countries like India, most of the concrete structures have been built without ductile detailing of the reinforcement. Although a number of studies have been carried out on the effect of reinforcement detailing in earthquake resistance (Arlekar et al. 1997, Murty et al. 2003, Mondal 2013), no study is available on the effect of detailing on post-earthquake performance. A systematic study of behaviour of these structures in post earthquake fire is thus very important. To the best of the author's knowledge, no such study has been carried out till date.

As discussed above reinforced concrete structures usually get exposed to fire after an earthquake event while at the same time they continue to resist gravity loads. Certainly, new research effort is required to properly address the challenge posed by fire following earthquake scenarios. Currently, there is a serious lack of experimental data to understand the performance of structural members subjected to earthquake-induced fires and loads. Therefore, there is a need of a comprehensive research program to develop appropriate techniques and design solutions for the evaluation of post-earthquake fire performance of reinforced concrete structures.

1.6 RESEARCH GAPS AND SIGNIFICANCE

Fires following earthquake events are recognized to be a major possibility with catastrophic consequences especially in densely populated urban settlements and more so in the developing world where response systems to such events are inadequate at best or simply non-existent at the worst. Relatively, little information is available in the literature on the residual strength and behaviour of RCC framed structures exposed to such events and this becomes an important issue in the context of India with its rapidly urbanizing population taking increasing shelter in RCC buildings in the metros and in the emerging cities in the hinterland. Similarly the effect of FFE events on the RC structures with non-ductile detailing (as is the case with the structures built till late 1990's in India) is still unknown. The research reported in the thesis is targeted at addressing this gap in the literature and is a combination of experimental

investigations on full scale structures and structural components with the aim to aid prediction of fire resistance of RCC structures in FFE events. At the component level fire resistance of RC columns with varying confinement levels has been studied and empirical equation for the fire ratings of RC columns has been proposed. The strength and behaviour of frame sub-assemblages has been experimentally investigated under simulated FFE events.

It is the fervent hope of the author that his effort will incrementally add to the state-of-the-art in the field of structures in fire.

1.7 OBJECTIVES OF THE INVESTIGATION

Following are the objectives of this research:

1. To investigate the behavior of a Non-Ductile RC framed structure in post earthquake fire and thereby to study the influence of ductile detailing on the fire performance of earthquake damaged RC structures.
2. To investigate the behavior of an RC framed structure with masonry infill in post earthquake fire and thus to study the influence of infill walls on the fire performance of earthquake damaged RC structures.
3. To investigate the effect of degree of confinement and concrete strength on the fire resistance of reinforced concrete columns.
4. To establish a design equation for estimating the fire resistance of RC columns.

1.8 ORGANIZATION OF THE THESIS

The thesis is broadly divided into five chapters. The **Chapter 1** presents a literature review in the areas relevant to the present research. A brief survey of the existing literature on the behaviour of concrete subjected to elevated temperatures has been given. A brief review of the literature on the behaviour of RC frames subjected to earthquake loading has been included. The behaviour of RC frames exposed to fires has been critically reviewed. Finally the behaviour of the RC frame exposed to fires following earthquake events has been briefly reviewed and the need for the present investigation has been identified.

Chapter 2 presents the experimental investigation carried out to study the behaviour of the non-ductile reinforced concrete (RC) frame subjected to post-earthquake fires. The construction details of the frame are thoroughly discussed. The material details and construction features of the RC frame sub-assemblage and the set up for mechanical loading, instrumentation and simulated lateral cyclic loading are presented. Successful implementation of the compartment fire to the pre-damaged RC frame with detailed instrumentation for temperature, strain and

displacement are also discussed. A comparison of the behavior of the test frame with some past tests on ductile detailed frames has also been presented.

Chapter 3 focuses on the structural response of a full-scale brick in-filled reinforced concrete frame subjected to post-earthquake fire. The chapter deals with the results of an extensive test programme comprising of three test phases; the initial simulated earthquake loading, the fire test and the residual test.

Chapter 4 presents an experimental study on the effect of confining reinforcement on the fire resistance of RC columns. A brief literature review on the behavior of RC columns in fire is presented. A detailed report on the development of a novel test setup for the fire test of full scale RC columns has been provided. Towards the end a design equation has been developed for calculation of fire resistance of the RC columns.

Chapter 5 deals with the main conclusions of this study and identifies scope for further research.

The last part of this thesis consists of references and the list of publications.

CHAPTER – 2

BEHAVIOUR OF A NON-DUCTILE RC FRAME UNDER POST-EARTHQUAKE FIRE

2.1 INTRODUCTION

A very important aspect of the research on the concrete structures exposed to elevated temperatures is the study of impact of fires on the structures damaged by earthquakes. Over the past centuries fire has emerged as an integral part of emergency response strategies which are focussed on life safety as well as the infrastructure safety of any nation. However no current regulations consider the fire and earthquake hazard in a sequential manner (Usmani, 2008). The occurrence of fires in many past earthquakes has led to widespread devastations which resulted in damage, greater in extent and magnitude than the original earthquake. This has made it necessary to consider the effect of seismic and fire loading on the structures not on a separate basis but in a sequential manner. Even though the strategy of taking both the extreme loads together in a sequential manner sometimes may not be desirable and feasible, but in highly important structures where economics and technology are no barriers, it will be sensible to provide such resistance.

Fires following earthquakes have resulted in damage more pronounced than caused by the original shaking. Earthquakes more often are regarded as low probability but high consequence events and are difficult to plan for. Fire conflagrations can develop from situations other than earthquake, although both local and international experience confirm that earthquake is a major initiator of large-scale urban fires. The threat posed by fire following earthquake has been highlighted by a number of overseas earthquakes, notably San Francisco (1906), Northridge, Los Angeles USA (1994), and Kobe, Japan (1995). Devastating fires which broke out as the aftermath of an earthquake and lasted for several days completely destroyed 80% of San Francisco, leaving more than 3000 people dead and the property damage was estimated at $500,000,000 in 1906 dollars (Hansen, 2015). Similar case was found in the deadly earthquake in Tokyo (1923) where in the earthquake together with the fire following it, claimed more than 140000 lives. Most of the major earthquakes which have struck Californian belt have been followed by varying number of ignitions, the famous being the 1971 San Fernando and 1994 Northridge earthquakes, which were followed by more than 100 ignitions. Recent earthquakes including 1989 Loma Prieta earthquake in California, 1995 Hanshin (Kobe) earthquake in Japan, 1999 Marmara earthquake in Turkey were all followed by major incidents of fire, the

intensity of which has been reported to have varied from few hours to three days (Chen and Scawthorn, 2003). Scenario studies of future large-scale earthquakes in San Francisco and Tokyo indicate that Fire Following Earthquake will be a major factor in subsequent property damage and lives lost (Wellington Lifeline Group, 2002).

The engineers and the associated researchers in the seismically vulnerable belts of the world would be able to ensure much of the structural safety in the event of an earthquake with the available design tools and technologies. However, in case of a fire following earthquake the ultimate performance of the structure is still not being evaluated and the analysis and design exercise is often being culminated at the cost of some residual damage in the structure. It is high time that one needs to consider the occurrence of a fire significantly more risky under post earthquake conditions than under normal conditions and in such a case it needs to be acknowledged that the current state of affairs, where in the post earthquake fires are altogether ignored in seismic design, is indeed a strange oddity (Usmani, 2008).

Structural fire testing is undergoing rejuvenation with full scale tests being performed on various structural systems. The conventional, and widely used, method for fire testing is the standard fire test where in single structural elements are subjected to a standard fire (ISO, 1975). The results of the standard fire test are fire resistance ratings which are mainly in the form of a time to failure. Although the method is still widely used, however it has of late been noticed to have a number of drawbacks (Drysdale, 1999). The perception that the concrete structures behave well in fire has led to overly simplified design guidelines in the form of concrete cover. However the behaviour of structural systems in fire is proved to be quite complex due to interaction effects between different structural elements of the structural system. This simplification in design procedure was a result of standard fire tests of simple building elements or isolated structural assemblies in testing furnaces which subject the loaded elements to a standard temperature-time curve. The issues of the inherent problems, which are associated with using simplified single element based laboratory tests subjected to standard temperature-time curves, are being solved by performing large scale non standard fire tests using real fires. This shift in testing philosophy from prescriptive standard fire testing to large scale non standard fire testing using real fires has been aimed at understanding the global behaviour of structures in fire, which had received relatively little attention in the past. The significance of performing the large scale tests is also reflected by the lack of experimental data on the performance of complete concrete structures in fire.

Fire tests on full scale concrete structures are very rare and very few tests have been carried on complete structural systems. In their experimental testing, Vecchio and Sato (1990) subjected three large-scale reinforced concrete portal frame models to combinations of thermal and mechanical loads under different test conditions and the results indicated that the thermal loads can result in significant stressing of a structure and can lead to concentrated damage in local regions. Full scale test on a reinforced concrete frame conducted at Cardington, UK (Bailey 2002) provided an insight into the structural behaviour of a heated concrete structure. Although this test suffered from premature instrumentation failure, rendering the dataset incomplete, a number of observations were derived from these tests. This test showed that the spalling of the floor slab was extensive and exposed the bottom steel reinforcement. Although concrete spalling considerably reduced the flexural strength of the slab, collapse did not occur which could be attributed to slab behaving in compressive membrane action. In the first of its kind, Sharma et al (2012) tested a damaged reinforced concrete frame in fire. A Reinforced Concrete (RC) frame assemblage was first subjected to simulated earthquake loading which was followed by subjecting the damaged frame to a compartment fire. Massive spalling in different elements of the assemblage was observed. Even though the strength of the frame got reduced after the fire, the frame assemblage escaped the complete structural failure. The test provided data in terms of temperatures, strains, displacements as recorded for the beams, columns and the roof slab. Kamath (2014) also tested a reinforced concrete frame with higher level of seismic damage and exposed the same to one hour compartment fire.

The need for ductile behaviour of various structural components during any major earthquake has been acutely felt and demonstrated amply during several seismic events. Although it is preferable to dissipate seismic energy by post-elastic deformations in beams, column hinging cannot be avoided entirely in most buildings during severe earthquakes. To achieve sufficient ductility in columns, their potential plastic hinge regions should be reinforced with appropriately designed and detailed longitudinal and lateral confining steel. Reinforced concrete (RC) frame structures constructed before the mid-1970s lack important features of good seismic design, such as strong columns and ductile detailing of reinforcement, making them potentially vulnerable to earthquake-induced collapse. Such non-ductile RC frame structures experienced significant earthquake damage in the 1971 San Fernando, 1979 Imperial Valley, 1987 Whittier Narrows, and 1994 Northridge earthquakes in California, and many other earthquakes worldwide (Liel et al, 2011). Building code requirements for seismic design and detailing of reinforced concrete have changed significantly since the mid- 1970s, in response to observed earthquake damage and an increased understanding of the importance of ductile

detailing of reinforcement. However much of the building stock, especially built before 1970's in developed countries and before 1990's in developing countries like India, has been designed as non-ductile frames and therefore are vulnerable to multi hazard damage. In developing countries like India, most of the concrete structures have been built without ductile detailing of the reinforcement. A systematic study of behaviour of these structures in post earthquake fire is thus very important. To the best of the author's knowledge, no such study has been carried out till date.

The main aim of the present investigation was to study the influence of ductility on the behaviour of RC Frames in Post earthquake fire. In this study, a comparison, vis-à-vis ductility, will also be drawn between the behaviours of two full-scale RC Framed structures subjected to Post Earthquake fire. It is hoped that the results presented here provide the means to reduce the uncertainties associated with the behaviour of concrete structures in fire.

2.2 TEST ARRANGEMENT

In order to evaluate the behaviour of a Reinforced Concrete (RC) frame in post earthquake fire, a full scale RC frame assemblage was constructed before subjecting to predetermined earthquake damage and then exposing it to a compartment fire of one hour duration.

2.2.1 Design and Construction Details of the RC frame

To perform the experimental studies a three storey framed structure (G+3) with 4 bays in East-West direction and 3 bays in North- South direction was designed in accordance with the relevant Indian standard codes. The G+3 structure was modelled and designed, out of which a frame sub assemblage was constructed, as it was not feasible to construct the complete G+3 structure due to the paucity of space and the economics associated. The sub frame assemblage was first tested against the simulated seismic loading and then the fire loading. The plan and the elevation of the structure are shown in Fig. 2.1. The hatched area in the figure represents the actual constructed RC frame sub assemblage. The test frame consisted of four columns *(300 mm × 300 mm)*, four plinth beams *(230 mm × 230 mm)*, four roof beams *(230 mm × 230 mm)* and a roof slab *(120 mm thick)*. All the elements of the test frame were cast monolithically and the column fixity at the base was provided by the termination of all the four columns into a 900 mm thick RC raft foundation of plan size 6900 x 8700 mm. The RC frame was designed as per the guidelines of Indian standard code of practise IS 456:2000 (BIS, 2000) without providing the ductile detailing, however the minimum shear reinforcement was provided as per the recommendations prescribed in IS 456: 2000. This was done so as to test the frame as a non

ductile structure and evaluate its behaviour and hence compare the same with that of the ductile RC frame as tested and reported by (Kamath, 2014). Equivalent gravity load, the wall load and the live load on the roof slab were imposed as per the recommendations of the Indian seismic design code, IS 1893 (Part-1):2002 (BIS, 2007). An M30 concrete was designed, and utilized for the construction of the RC frames. The frame was designed using the reinforcement bars of grade Fe500 having the yield strength of 500 MPa. Figures 2.2-2.4 show the typical reinforcement details in the different elements of the test frame.

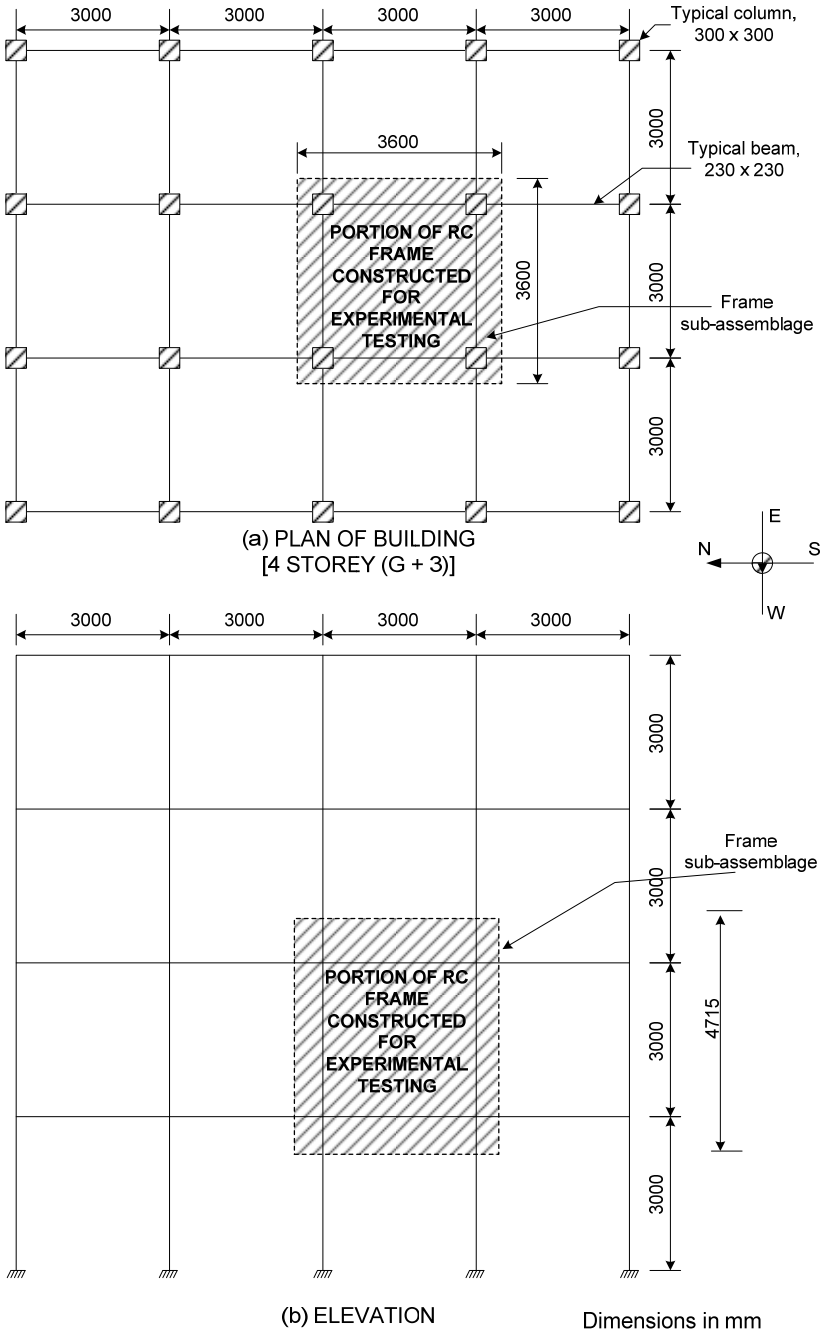

Fig. 2.1 G+3 RC Frame Structure (a) In plan (b) In Elevation.

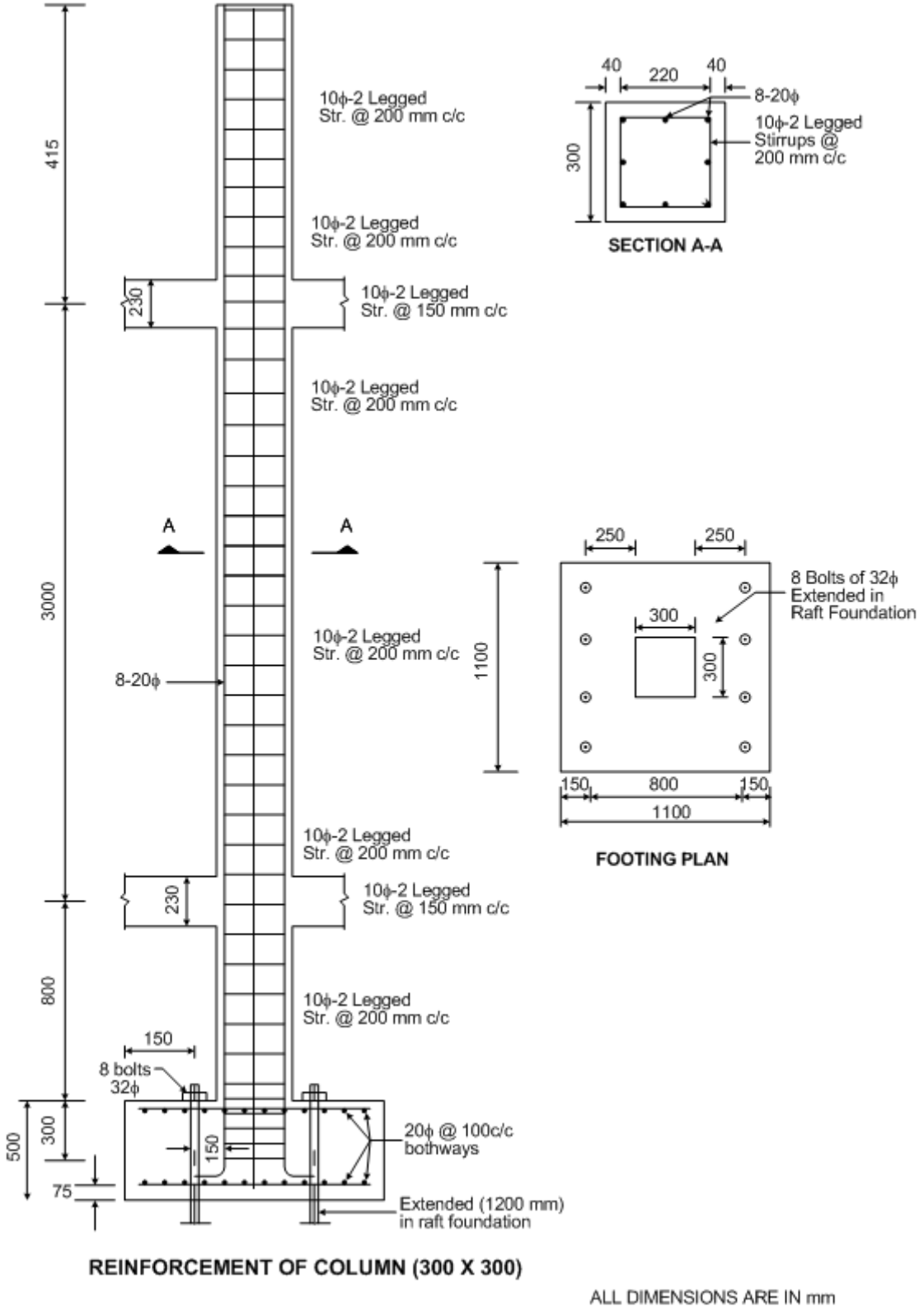

Fig 2.2 Detailing of Column Reinforcement

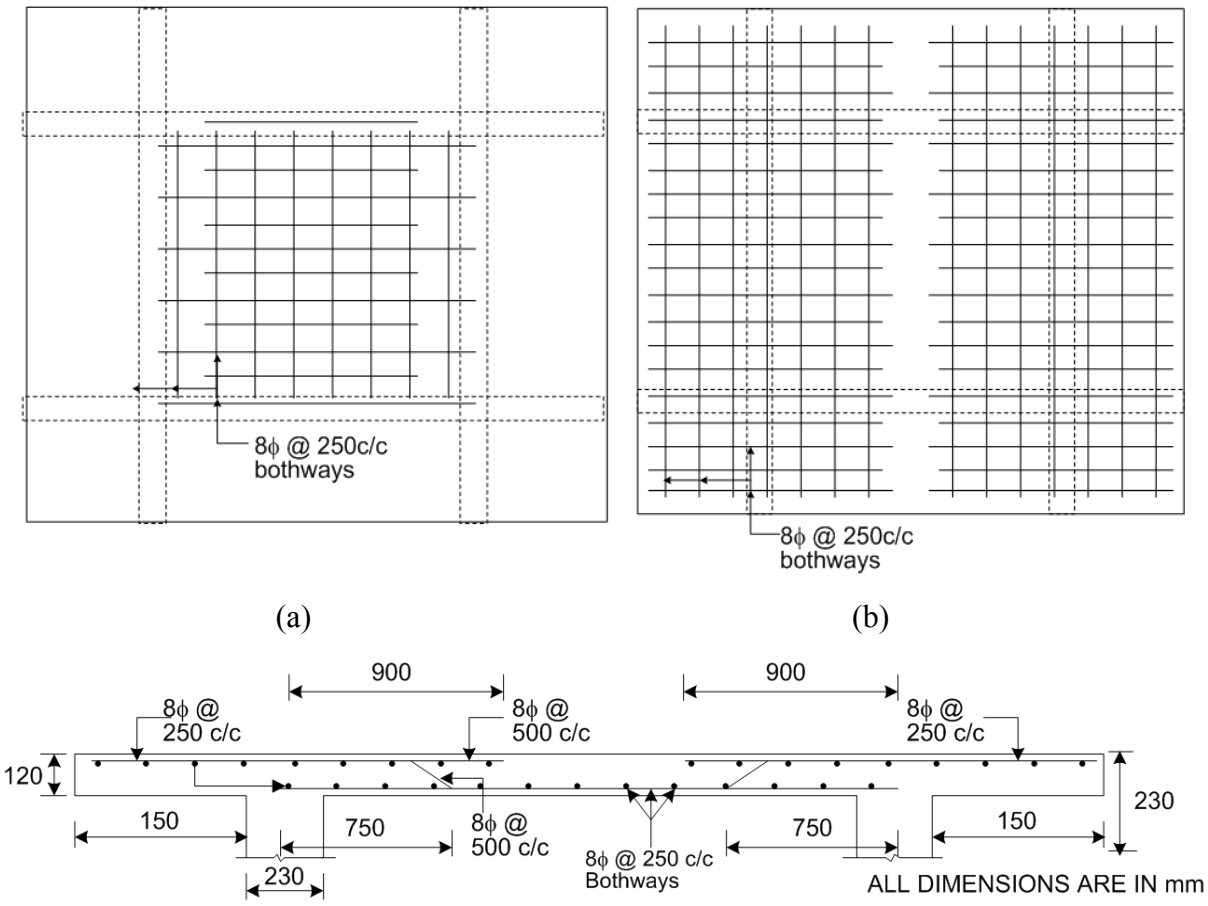

Fig 2.3 Detailing of Slab (a) Plan showing bottom reinforcement. (b) Plan showing top reinforcement. (c) A section through the slab

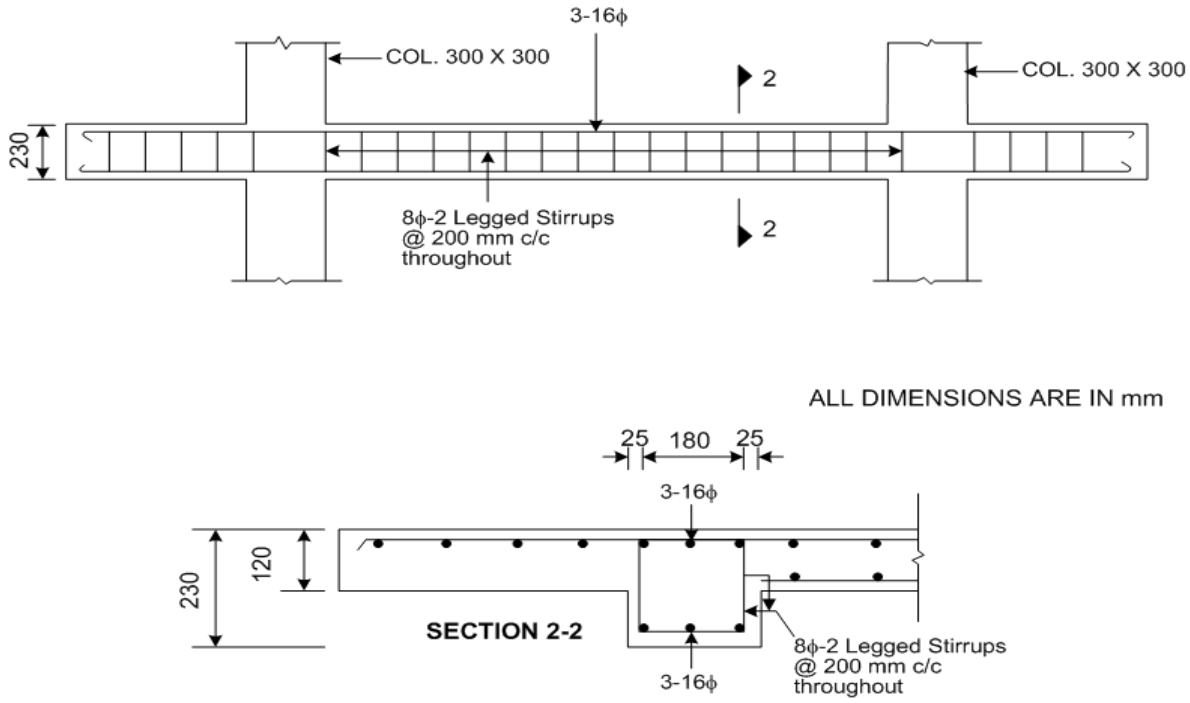

Fig 2.4 Detailing of beam reinforcement

2.2.1.1 Material Properties

The frame was constructed using normal strength concrete with 28 day strength of 30MPa. The concrete was designed using ordinary Portland cement of 43-grade, fine aggregate, coarse aggregate and tap water making the use of guidelines as recommended by IS: 10262 (BIS 2009). The detailed characteristics of the materials are presented below:

2.2.1.1.1 Steel Reinforcing bars

The steel reinforcement consisted of different diameter bars in different elements of the RC frame as shown in Figs. 2.2-2.4. The different mechanical properties of the steel bars of different diameters are given in Table 2.1.

Table 2.1: Mechanical properties of the steel reinforcement bars

Dia of steel rebar	Yield stress (MPa)	Ultimate stress (MPa)	Yield strain (mm/mm)	Ultimate strain (mm/mm)	Elongation (%)	Young's Modulus ($x10^5$ MPa)
8 mm	550.69	642.97	0.0047	0.2070	20.7	2.14
10 mm	446.57	538.21	0.0042	0.1960	19.6	2.13
16 mm	420.05	541.18	0.0023	0.1689	16.89	2.03
20 mm	448.55	567.50	0.0021	0.1458	14.58	2.10

2.2.1.1.2 Cement

Ordinary Portland cement of 43-grade (OPC) was used for construction of the RC frame sub assemblage. Cement samples were tested in the laboratory for various properties to determine their feasibility per the relevant Indian Standards, IS: 4031 (BIS 2005) and IS: 4032 (BIS 2005). The different properties of the cement are listed in Table 2.2 and Table 2.3

2.2.1.1.3 Aggregate

Fine aggregate used in the construction was locally available river sand which as per IS 383 (BIS 2002) conformed to Zone II type. The particle size distribution and other relevant physical properties of the fine aggregate are given in Tables 2.4 and 2.5 respectively.

Table 2.2: Physical properties of OPC 43 – grade cement

Characteristics	Units	Obtained results	Recommended values per IS 8112:1989 (BIS 1989)
Blaine's fineness	m^2/kg	275	225 (minimum)
Specific gravity	-	3.13	-
Soundness (Le-Chatelier test)	mm %	2 0.08	10 (maximum) 0.8 (maximum)
Normal consistency (Percent of cement by weight)	%	29	30
Setting time (i) Initial (ii) Final	 Minutes Minutes	 90 175	 30 (minimum) 600 (maximum)
Compressive strength (i) 3-days (ii) 7-days (iii) 28-days	 MPa MPa MPa	 30.10 38.34 46.02	 23.0 33.0 43.0

Table 2.3: Chemical composition of OPC 43 - grade cement

Characteristics	Test results (%)	Limiting (%) values specified as per IS 8112:1989 (BIS 1989)
Silica (SiO_2)	21.30	19-24
Alumina (Al_2O_3)	5.10	3-6
Ferric Oxide (Fe_2O_3)	3.70	1-4
Sodium Oxide (Na_2O)	0.25	≤0.6
Potassium Oxide (K_2O)	0.28	-
Calcium Oxide (CaO)	63.22	59-64
Magnesium Oxide (MgO)	2.20	≤6
Sulphuric Anhydrite	1.30	≤3
Insoluble residue	1.10	≤2
Loss on ignition	0.75	≤5

Table 2.4: Sieve analysis of fine aggregate

IS Sieve designation	Weight retained (g)	Percentage of weight retained (%)	Cumulative percentage of weight retained (%)	Cumulative percentage of weight passing (%)	Range specified in percentage passing for grading Zone-II of IS 383:1970 (%)
10 mm	0	0	0	100	100
4.75 mm	10	1.0	1.0	99	90-100
2.36 mm	86	8.6	9.6	90.4	75-100
1.18 mm	195	19.5	29.1	70.9	55-90
600 mm	247	24.7	53.8	46.2	35-59
300 mm	340	34.0	87.8	12.2	8-30
150 mm	110	11.0	98.8	1.2	0-10
Residue	12	1.2	-	-	-
Total	1000	100	280.1		

Table 2.5: Physical properties of fine aggregate

Characteristics	Requirements per IS 383: 1970	Obtained results
Grading	-	Conforming to grading Zone – II
Fineness modulus	2.0 to 3.5	2.80
Specific gravity	2.6 to 2.7	2.57
Density (loose) (kN/m^3)	-	13.8
Water absorption (%)	-	1.1
Moisture content (%)	-	0.33

2.2.1.1.4 Coarse aggregate

Coarse aggregate used was locally available crushed stone aggregates with nominal sizes of 20 mm and 10 mm. The final aggregate used in the construction of the frame was made

by mixing the aggregate fractions (20 mm and 10 mm) in the ratio of 40% and 60%. Sieve analysis of the coarse aggregate used is provided in Table 2.6.

Table 2.6: Sieve analysis of coarse aggregate

IS Sieve Designation	Weight retained (g)	Percentage of weight retained (%)	Cumulative percentage of weight retained (%)	Percentage of weight passing (%)	Range specified for 12.5 mm downgraded coarse aggregate per IS 383:1970
20 mm	0	0	0	100	100
16 mm	0	0	0	100	-
12.5 mm	300	6	6	94	90-100
10 mm	755	15.1	21.1	78.9	40-85
4.75 mm	3930	78.6	99.7	0.3	0-10
2.36 mm	15	0.3	100	0.0	-
Residue	-	-	-	-	-
Total	5000	100.0	226.8	-	-

2.2.1.1.5 Concrete Mix proportions

As mentioned earlier the concrete mix was designed and proportioned on the basis of the guidelines laid down in IS: 10262 (BIS 2009).The details of the designed mix proportions along with the 28-days cube compressive strengths are given in Table 2.7.

Table 2.7: Concrete mix proportions

Mix Type	**Cement (kg/m^3)**	**Water (kg/m^3)**	**Coarse aggregates (kg/m^3)**	**Sand (kg/m^3)**	**Cube compressive strength at 28 days, f_{ck} (MPa)**
Normal Strength Concrete (NSC)	438	193	1183	539	33.6

2.2.1.2 Construction of RC Test Frame

The RC frame sub assemblage was constructed on a strong floor in an outdoor testing facility in the department of Civil Engineering, IIT Roorkee. The strong floor testing facility had already been utilised for two similar tests in the past. The construction of the test frame was carried out in a number of stages starting with the footings. The test frame was founded on four isolated footings, 500 mm in depth. Each footing was constructed in a manner that eight 1200

mm long protruding bolts extended in raft foundation passed through it. This was done to avoid any uplift of the footings later during the seismic testing by holding the footings down. The construction of footings was followed by casting of 800 mm height of columns, the top of which formed the base of plinth beams. Next stage of the construction involved the plinth beams. The columns were constructed in two stages of 1500 mm each. The construction culminated with the casting of the roof beams, slab and the top 400 mm extensions of the columns. Extensive efforts were made to avoid formation of cold joints and to ensure quality control during the construction stages. During each stage of construction, sufficient number of cubes were collected as per the guidelines provided in IS 456 2000 to monitor the strength of concrete. The different stages of the RC frame construction are shown in Fig.2.5.

(a)

(b)

Fig.2.5 Construction stages of the frame (a) Protruding bolts from the strong floor and the reinforcement cage for footing. (b) Casting of footing. (c) View of the completed footings and the first lift of columns. (d) The final lift of the columns. (e) & (f) Casting of floor beams and slab. (Contd.)

(e)

(f)

Fig.2.5 Construction stages of the frame (a) Protruding bolts from the strong floor and the reinforcement cage for footing. (b) Casting of footing. (c) View of the completed footings and the first lift of columns. (d) The final lift of the columns. (e) & (f) Casting of floor beams and slab.

2.2.2 Instrumentation

Extensive instrumentation was planned for the test frame and a number of sensors were installed to record the data. Figures 2.6 to 2.9 provide the details about the instrumentation used in the testing. Data which was planned to be recorded during all the phases of the tests for the structural aspects consisted of temperatures within the roof slab, columns, beams, and the compartment ; strains on the rebars embedded in all the structural elements of the RC frames and deflections of the roof slab at different points both vertical as well as horizontal.

The temperature measurement was taken by means of thermocouples embedded in concrete at a number of points and at different levels. The temperature build up inside the concrete of various structural elements of the RC frame was recorded using 0.5 mm dia K-type thermocouples embedded along the depth and width of the elements. Thermocouples were installed at five different sections in the various members i.e. near the end supports, at the midspan and at the section between these two locations. Each section in case of columns and top beams consisted of five thermocouples with three thermocouples along the depth of the cross section and two along the width of the cross section. In case of plinth beams the thermocouples were embedded only along the depth and in case of slab the three thermocouples were placed along the depth at nine sections.

To record the build up of the gas temperature inside the frame compartment thermocouple trees were placed at five different plan locations, one each at the four corners (near four columns, TMIC1, TMIC2, TMIC3, TMIC4) and one near the centre (TMIC). Each thermocouple tree consisted of five 6 mm diameter metal insulated (MI) thermocouples positioned at different heights, of 0.20 m, 0.90 m, 1.60 m, 2.30 m and 2.90 m from the floor

level of the compartment, to obtain the thermal profiles inside the compartment. A total of 312 thermocouples, which included 287 K- type and 25 MI type thermocouples, were utilized for the measurement of the temperatures. Figure 2.6 – Fig 2.7 shows the position of the thermocouples in different elements of the frame.

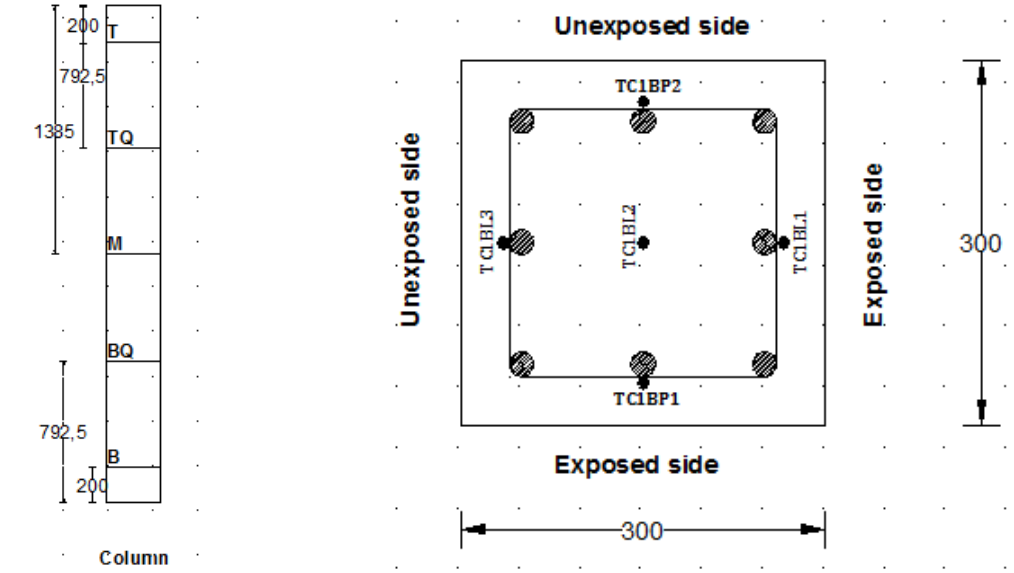

(a)

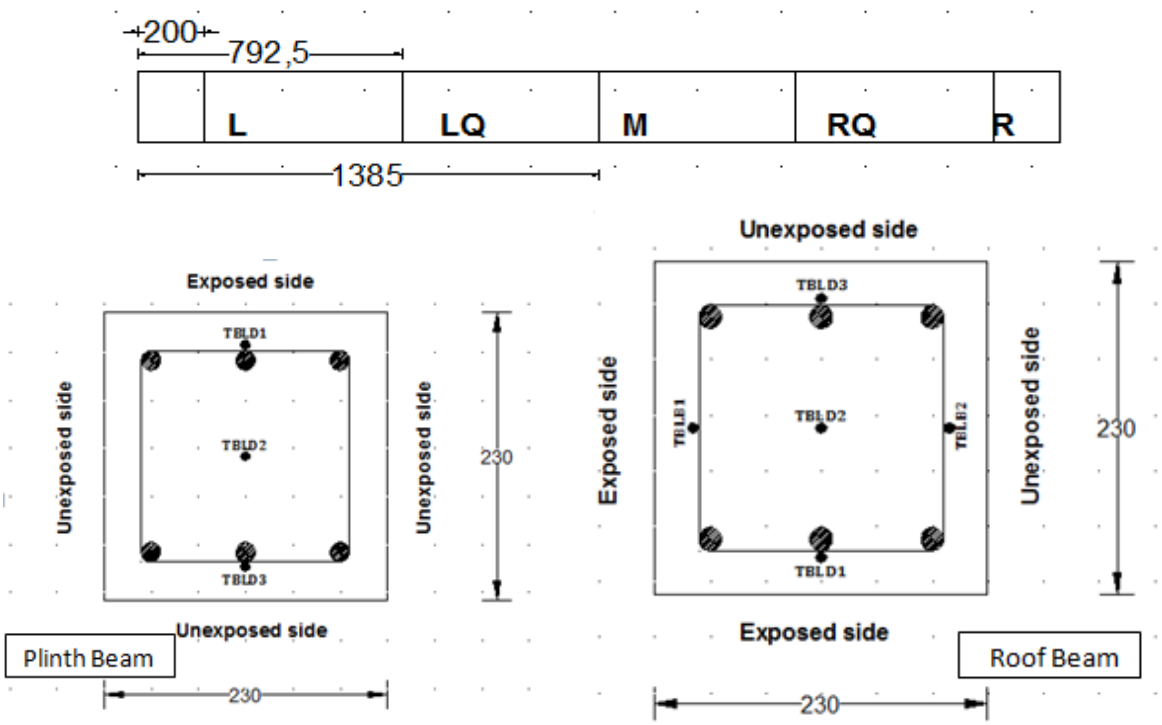

(b)

(Dimensions in mm)

Fig.2.6 Position of thermocouples in (a) Columns (b) beams and (c) slab (Contd.)

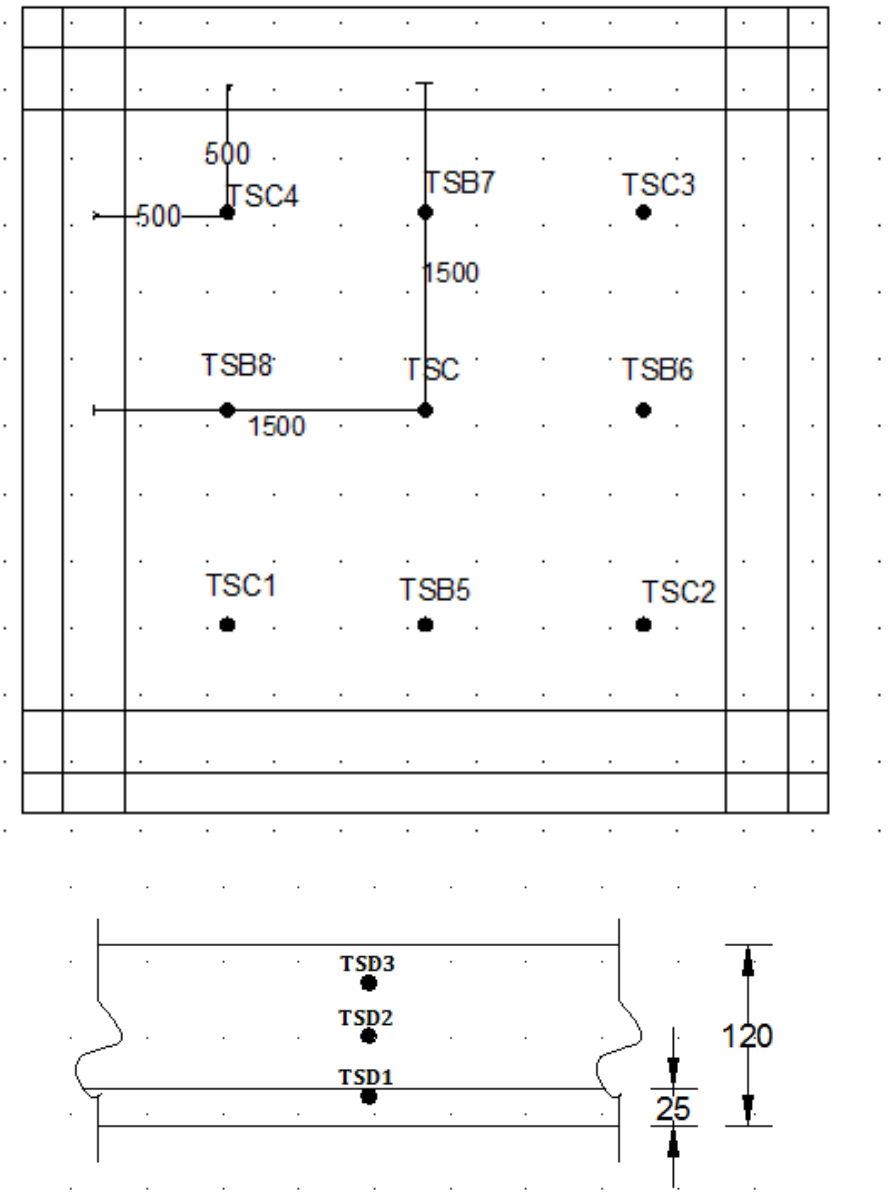

(c)

(Dimensions in mm)

Fig.2.6 Position of thermocouples in (a) Columns (b) beams and (c) slab

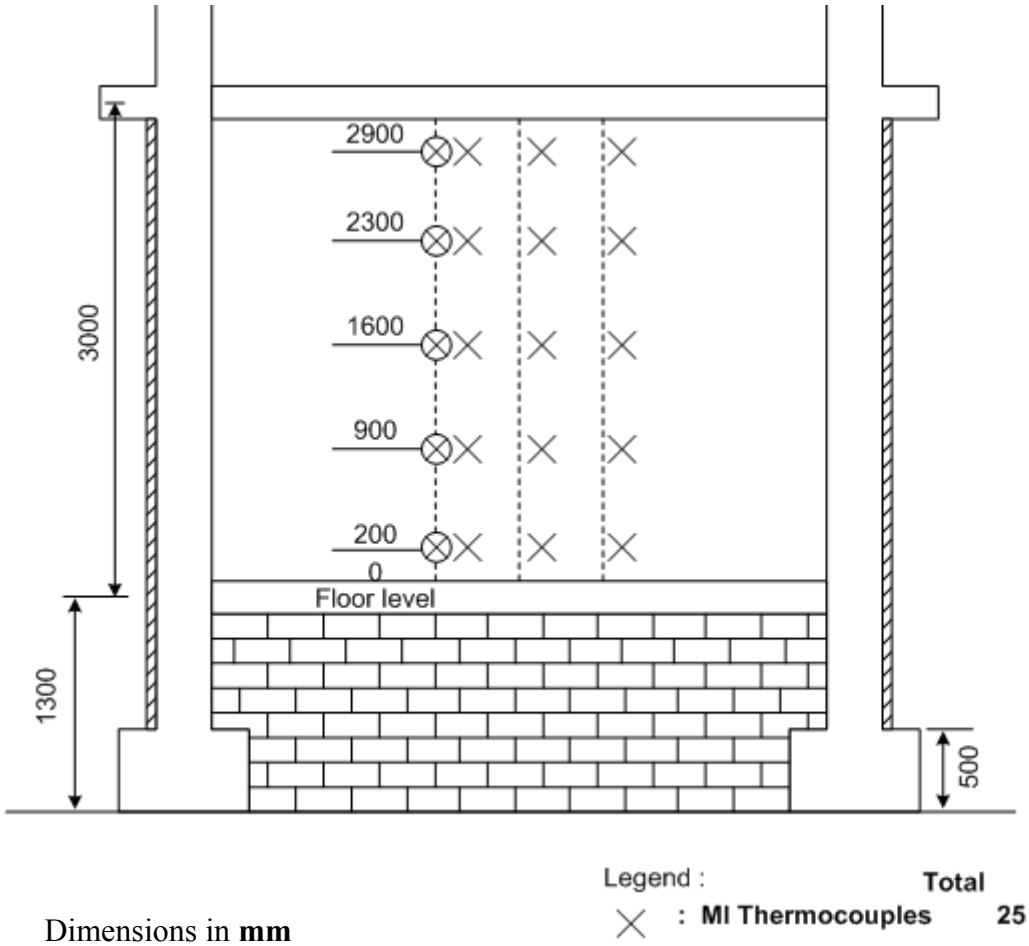

Fig.2.7 Position of thermocouples in fire compartment

The strains were recorded by pasting strain gauges on the steel rebars at different locations in the RC frames. Electrical resistance-type surface mounted strain gauges were mounted on rebars at three sections of plinth beams, columns and top beams. Each location had two strain gauges, one on the exposed rebar and the other on the opposite unexposed rebar. Similarly steel rebars at four key locations in plan of the roof slab were instrumented with strain gauges. Before mounting the strain gauges on the rebars, the rebar surface was prepared by grinding at the chosen locations and treated with acetone before finally fixing the strain gauges. The strain gauges were coated with high temperature and water resistant coatings. For the measurement of strains during the different phases of the experimental testing, eighty strain gauges were pasted at different locations of the frame on the steel rebars which included twenty four strain gauges each in plinth beams, columns and top beams and eight strain gauges in slab. Figure 2.8 shows the position of the strain gauges in the different elements of the test frame.

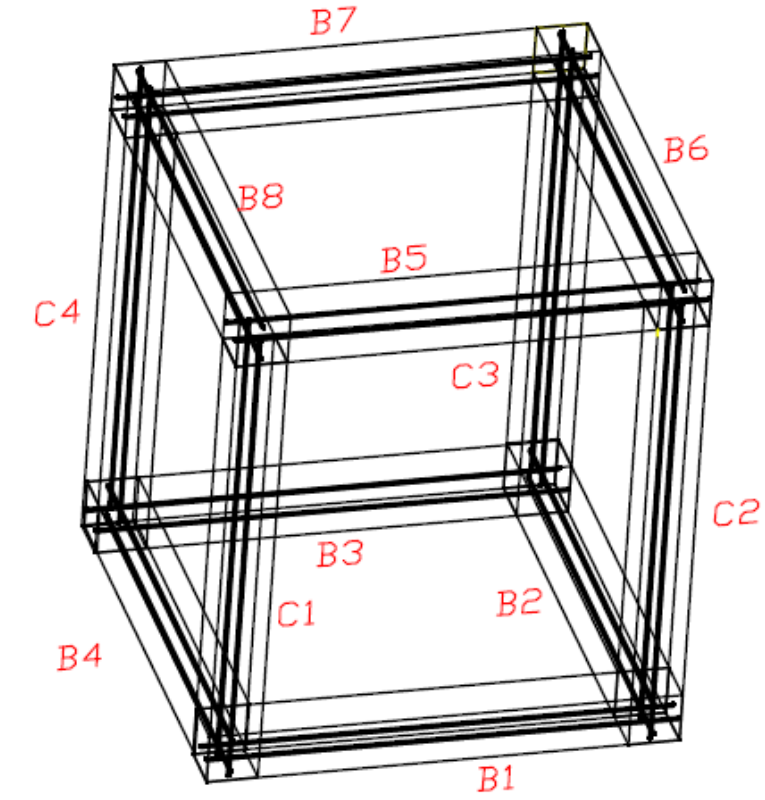

(a)

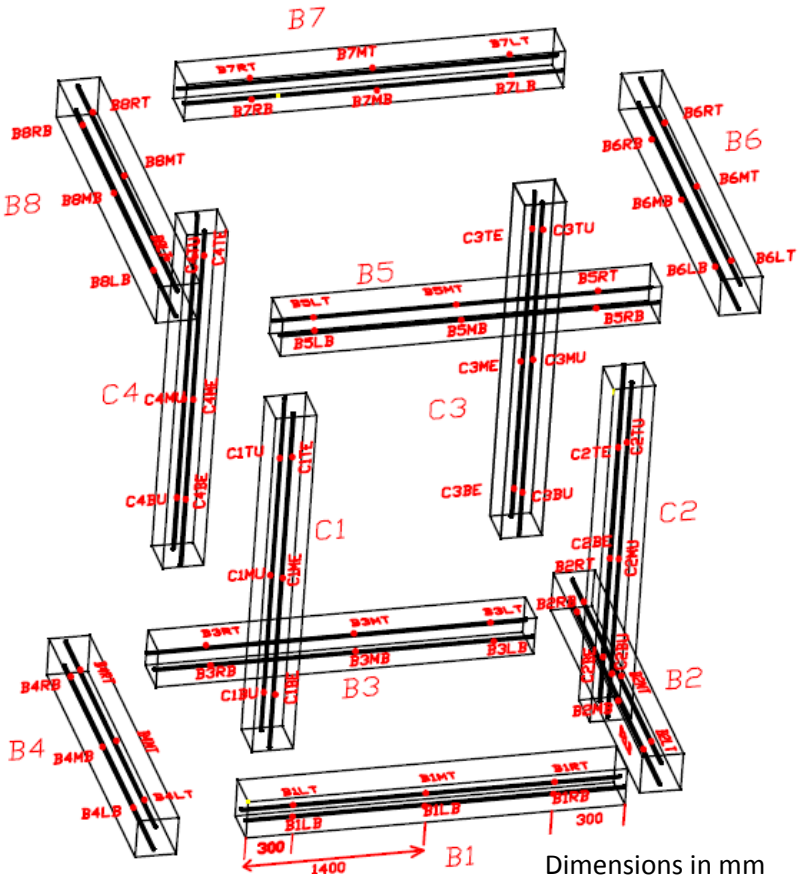

Dimensions in mm (b)

Fig.2.8 (a) Nomenclature for different elements (b) Position of strain gauges in columns and beams

(a)

(b)

(c)

(d)

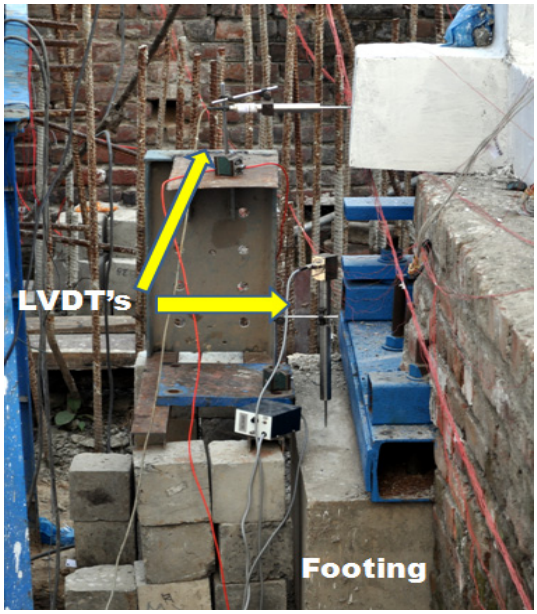

(e)

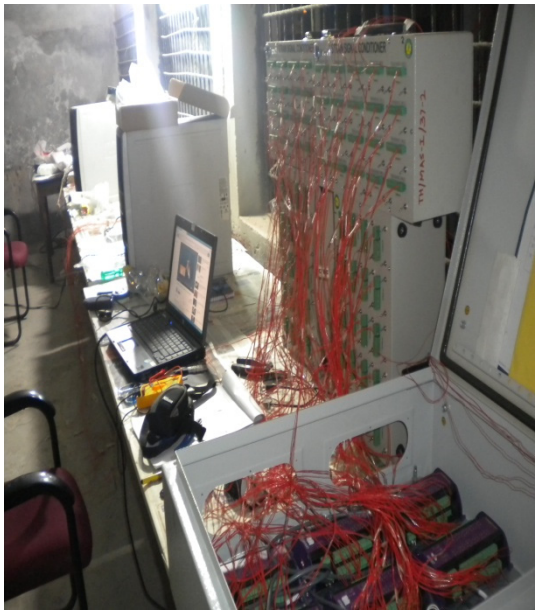

(f)

Fig. 2.9. (a) Reinforcement after surface preparation for strain gauge pasting. (b) Strain gauge attached to the reinforcement. (c) water proof coatings to the strain gauges. (d) thermocouples paced in the concrete reinforcement cage before casting (e) LVDT's mounted on footings to measure uplift, if any. (f) a view of data logging arrangement

Number of linearly varying displacement transducers (LVDT's) of different ranges and stroke lengths were used in order to measure displacements of the different structural elements during all the test phases. During the first phase of test i.e. the simulated seismic loading, seven LVDT's were mounted to measure the horizontal displacements at roof level in different directions while four LVDT's were used to measure horizontal displacements along different directions at plinth level. In order to check the unlikely possibility of footings of the RC test frame undergoing any uplift during the seismic loading, each footing was instrumented with LVDT's to measure any vertical displacement. An array of nine displacement transducers was used to record the deflections of roof slab during the fire loading. The horizontal displacement of the beams and the roof slab was also recorded using the displacement transducers. All these displacement transducers were mounted on a secondary steel frame which was independent of the RC test frame. To monitor the output from the sensors three data acquisition systems were connected to three workstations kept in a specially designed control room. Unique identifications (ID) were given to each of the sensors to enable programming of the channels of data acquisition systems. Data from all the sensors was recorded at a frequency of 20 Seconds through all the test phases. An uninterrupted power supply was assured throughout the control room by connecting the power to a power-supply backup.

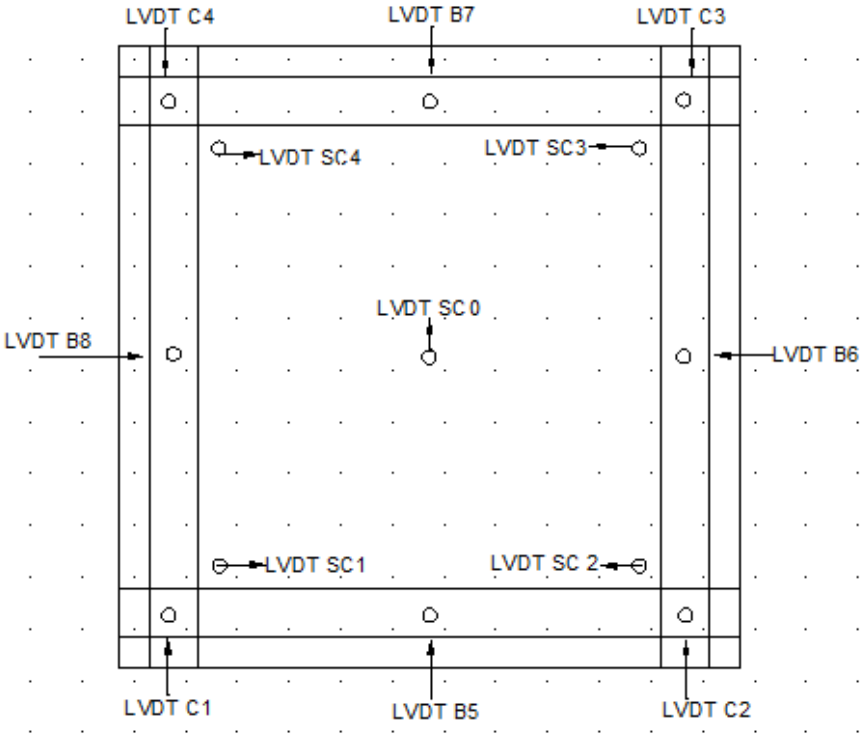

Fig.2.10 Position of vertical LVDT's on slab during fire

2.2.3 Simulation of gravity and live loads on the Test Setup

The test setup was a part of a G+3 building, which was designed as per the guidelines of the relevant Indian building codes.

2.2.3.1 Gravity loads

The gravity loads applied on the frame were based on the Indian standards for general loading, IS: 875 (Part 1 & part 2): 1987 (BIS, 2003) and the Indian seismic design code, IS 1893 (Part-1):2002. The gravity load and the imposed load applied were 1kN/m^2 and 2kN/m^2 respectively. The design loads applied for earthquake forces was however 0.5kN/m^2 (25% of 2kN/m^2) as per the guidelines of IS 1893 (Part-1):2002. In order to simulate gravity loads of the upper floors of the G+3 structure on the columns of the test frame a self equilibrating loading arrangement was developed as shown in the Figure 2.11.

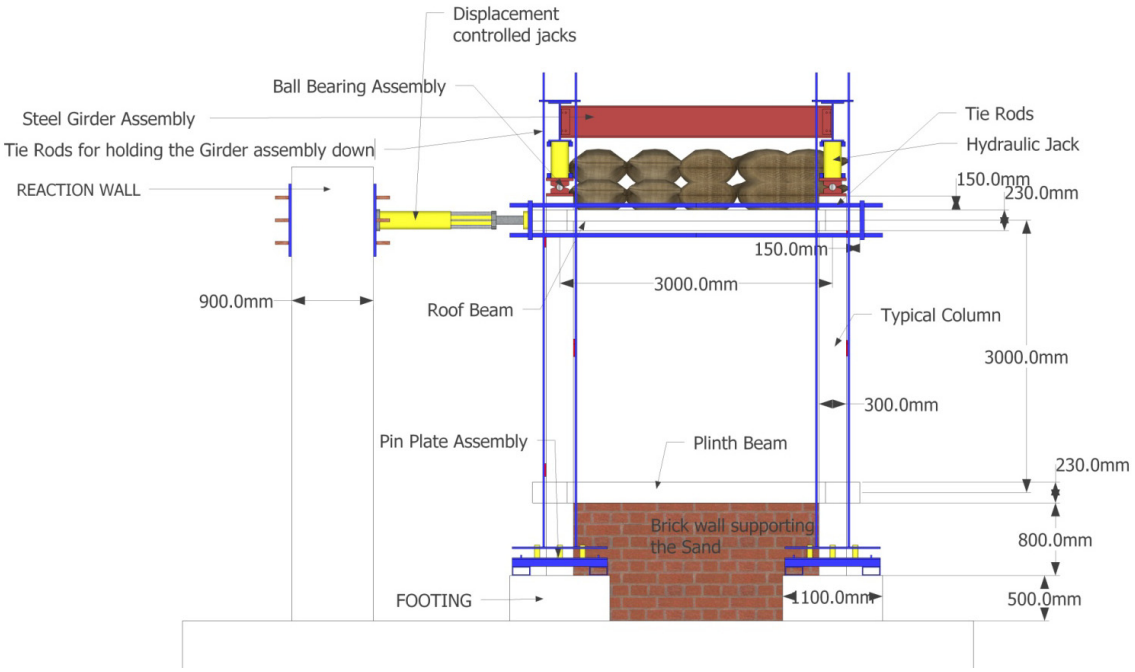

Fig.2.11: A schematic of the test arrangement (Elevation).

The vertical loading from the top stories was simulated by applying the calculated equivalent load using four hydraulic jacks positioned centrally on each column. These jacks were made to rest on a specially designed ball bearing assembly to keep the verticality of the jacks maintained during the simulated seismic load. This was done so that the actual simulation of the applied top loads is achieved. The final setup showing final arrangement of simulating the gravity loads is shown in Fig.2.12. Two steel girders were placed on these hydraulic jacks in East- West directions parallel to the reaction wall with each girder positioned on the columns opposite to each other.

Fig.2.12: Test Arrangement for the seismic loading as seen from the top

Cross girders were connected to these girders, which held them together causing a rigid diaphragm action during the loading and also avoided the overturning of the jacks during the seismic loading. A total of eight tie rods were used to hold the top girder assembly down with two tie rods at each column connected with MS plate resting on the top flange of the protruding portion of steel girder and the bottom ends with a specially designed pin plate assembly at the footing. The arrangement ensured lateral movement of the frame while maintaining the verticality of the applied gravity loads throughout the test cycles. The superimposed gravity loads equal to the gravity loads of all the top floors above were applied through these hydraulic jacks and maintained throughout all the three test phases. The live load on the slab of the test frame was calculated and simulated by putting the equivalent load using the sand bags placed uniformly throughout the area of the slab. Similarly the wall load on the top beams coming from the walls of the immediate top floor was calculated and simulated by putting the sand bags along the four top beams. The sand bags were put in four layers and their stability during the load tests was ensured by putting a steel mesh all around the sand bags.

2.2.3.2 Seismic loading

The RC frame, a part of which was constructed for testing, was designed to resist the seismic loading and the seismic loads were taken during the design process as per the clauses of Indian standard, IS 1893(Part-1):2002. The test frame being constructed in Roorkee, India, a zone factor (Z) 0.24 corresponding to the seismic zone IV was taken during the design process. Table 2.8 shows the different seismic parameters involved in the design of the test frame

Table 2.8 Seismic parameters considered for the design of G+3 Structure

Factor	Value considered for the design
Seismic Zone	IV (IS: 1893 (Part-1):2002)
Seismic Zone Factor (Z)	0.24 (IS: 1893 (Part-1):2002)
Importance Factor of Building (I)	1 (IS: 1893 (Part-1):2002)
Type of Soil	Medium Soil (IS: 1893 (Part-1):2002)
Response Reduction Factor (R)	5 (for Special moment resistant frame (IS: 1893 (Part-1):2002)
Seismic response coefficient (Sa/g)	Sa/g = 1+15T; 0.00< T<0.10 = 2.50; 0.10< T<0.550 = 1.36/T; 0.55< T<4.0 (IS: 1893 (Part-1):2002)
Damping	5% (IS: 1893 (Part-1):2002)
Fundamental Natural Period	$T_s = \frac{0.09}{\sqrt{d}}$ h, Where, d = base dimension in the considered direction. h = height of the building (IS: 1893 (Part-1):2002)
Load Combinations	(i) 1.5(D.L. + I.L.) (ii) 1.2(D.L.+I.L.+E.L.) (iii) 1.5(D.L.+E.L.) (IS: 1893 (Part-1):2002)

2.3 THE TEST PROCEDURE AND TEST RESULTS

A three phase test procedure was adopted and followed in testing the RC frame. The test procedure consisted of subjecting the frame to a simulated cyclic lateral load in a quasi-static fashion followed by a one hour compartment fire and after which the frame was subjected to a residual load test. The simulated cyclic lateral load was applied on the RC frame using two displacement controlled double acting hydraulic actuators acting in tandem with each other against a strong reaction wall. A schematic showing the three phase test procedure is shown in Fig.2.13

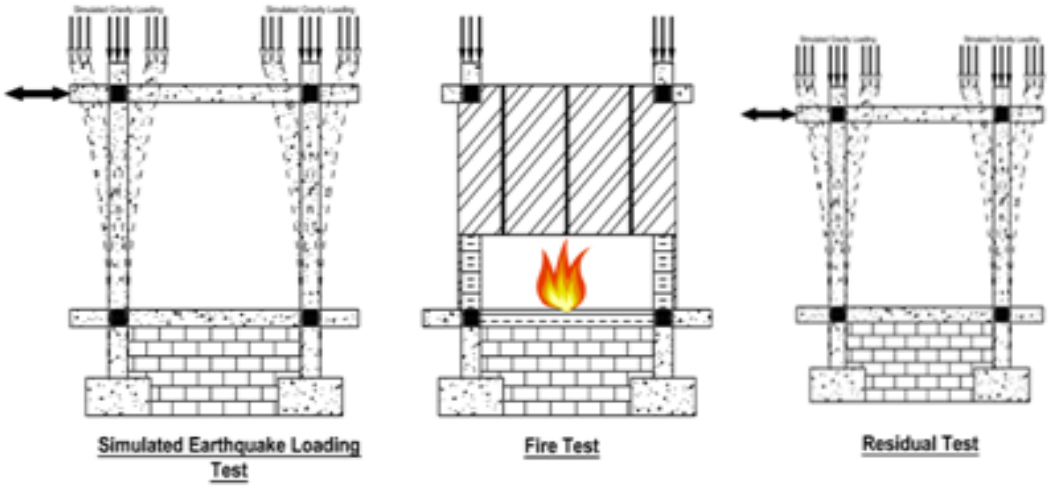

Fig. 2.13 Frame test procedure

2.3.1 Test Phase I: Simulated Seismic Load Test

The RC frame sub assemblage was subjected to a predefined seismic damage by subjecting the test setup to a simulated cyclic lateral load in a quasi-static manner with the help of two displacement controlled double acting hydraulic actuators. The jacks had a capacity of producing the displacement of 300 mm in either direction. The initial seismic damage was achieved by inducing a pre-planned lateral displacement through applying lateral cyclic load corresponding to the collapse prevention structural performance level (S-5) of FEMA 356:2000 (FEMA 2000). The code describes the structural performance level of any structure in terms of four structural performance levels and two intermediate structural performance ranges, with each performance level correlating to a codified structural performance level. The structural performance levels include, Immediate Occupancy (S-1), Life Safety (S-3), Collapse Prevention (S-5), and Not Considered (S-6) while as the intermediate structural ranges are, the Damage Control Range (S-2), and the Limited Safety Range (S-4). The pre-damage given to the RC frame tested by Sharma et al (2012) corresponded to the life safety level (S-3) of the code. The maximum targeted roof level lateral displacement of the test frame was 76 mm which corresponds to a roof drift ratio of 2 %. The predamage to which Kamath (2014) subjected the RC test frame corresponded to the collapse prevention (S-5) level. The frame was subjected to 152 mm displacement corresponding to a roof drift ratio of 4% (FEMA, 2000).

In the present study the seismic damage corresponding to the Collapse Prevention structural performance level (S-5) was considered and as per the code FEMA 356 a lateral drift of 4% which amounts to a displacement of 150 mm was imparted to the frame. The pre-damage was considered in order to have a comparative study with the RC frame as tested by Kamath

(2014) and hence study the influence of ductile detailing on the post earthquake fire behaviour of RC frames.

As per the code (FEMA, 2000) concrete frames when subjected to the collapse prevention structural performance level undergo extensive cracking and hinge formation takes place in ductile elements while as limited cracking with splice failure takes place in non ductile columns. At this drift, extensive spalling takes place in columns and beams and some joints get severely damaged with reinforcement getting buckled. Generally the buildings undergo severe damage at this level with little residual stiffness and strength though the load bearing columns and walls function. The structure retains large permanent drifts with some infills and parapets failed or at incipient failure. Though the structure doesn't fall but anticipates collapse at this level.

Same damage level was selected for the test frame RC assemblage and as per the code a 4% lateral drift, corresponding to a displacement of 150 mm was imparted to the frame in increments. The test frame was subjected to 15 push pull cycles starting with 10 mm cycle and then each successive cycle was increased with an increment of 10 mm till the 150 mm push pull cycle. After completion of the 150 mm displacement cycle corresponding to 4% drift, the frame was subjected to a push of 160 mm at which the hydraulic jacks were turned off, the tie rods were removed and plungers of jacks were powered to return to their zero position without pulling the frame. This was done so as to measure the any amount of residual deformation that would set in the frame.

2.3.1.1 Mechanical behaviour

Fig. 2.14 shows the load time history of the test frame while Fig. 2.15 shows the displacement time history. After achieving the target displacement in each cycle, the load was maintained and the distress mapping was carried out by marking the crack orientation, crack growth and the crack widths on the different elements of the test frame.

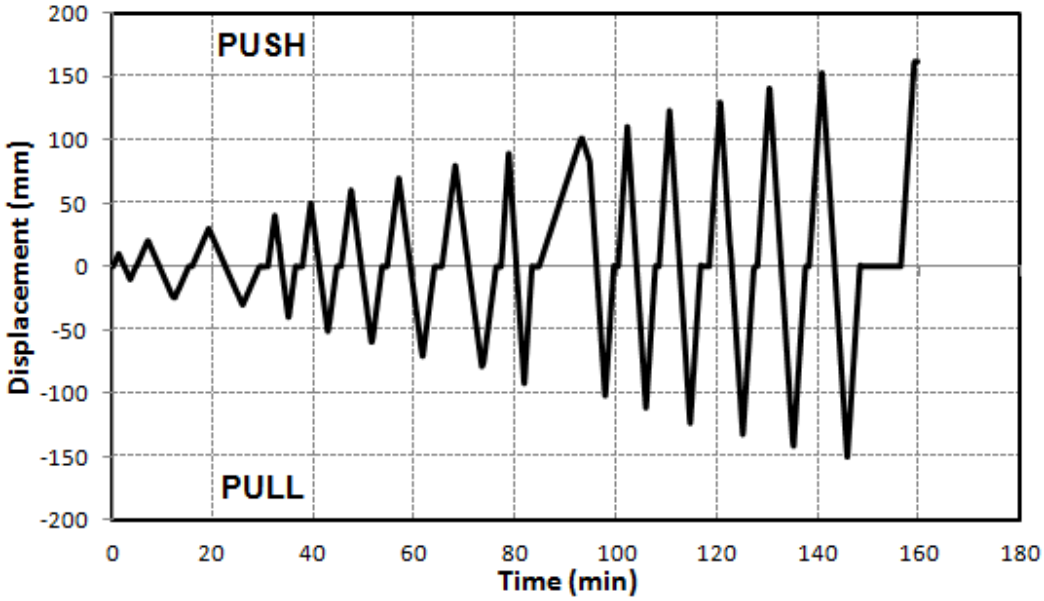

Fig.2.14: Displacement- time history of the frame

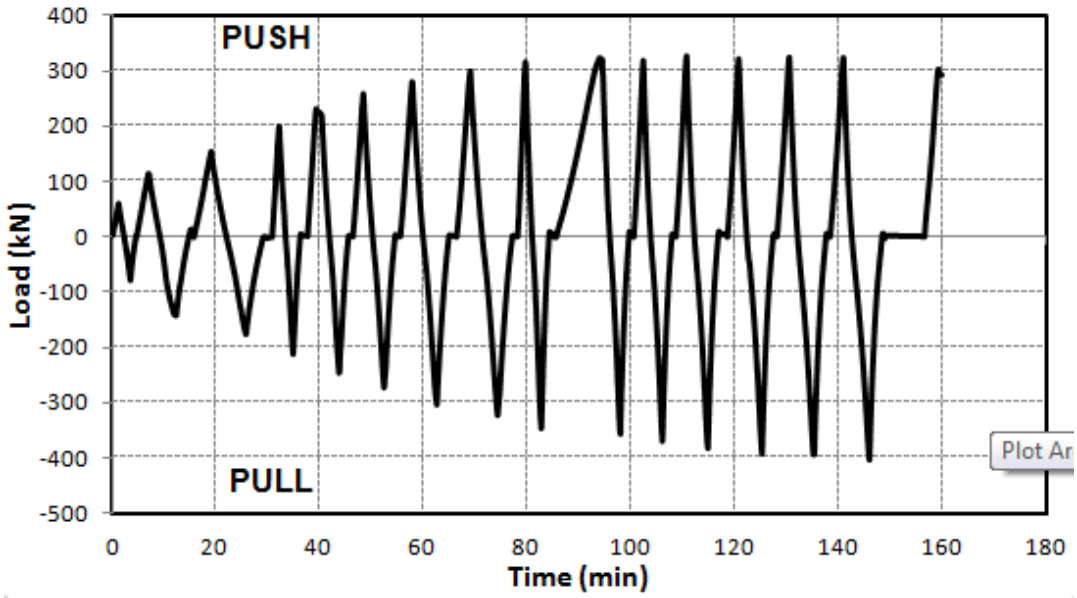

Fig.2.15: Load- time history of the frame

2.3.1.1.1 Observations during the test

At the displacement of 10 mm in the first cycle some fine cracks were seen at the ends of beams B1 and B3, which closed at the end of the first cycle. With each subsequent cycle the number of cracks increased with the crack widths also getting increased. After the 20 mm cycle the cracks started growing at the ends of beams B1 and B3. At the displacement of 30 mm (push) cracks with a width of 0.1 mm started appearing at the top of columns C1, C2 and C3, which disappeared at the displacement of 30 mm (pull) and the cracks started appearing at the bottom of columns C1, C2 and C3. At the end of 30 mm displacement cycle 0.08 mm cracks

started getting developed at the end of beam B7 and the inspection of the slab revealed a 0.06 mm crack near beam B8 running parallel to beam B8. With the 40 mm displacement (push) the cracks at the top ends of columns C1, C2, C3, C4 started getting manifested with widths of 0.14 mm. At the end this cycle cracks with a width of .08 mm appeared on the slab running parallel to the beam B6.

With the 50 mm displacement cycle the width of the cracks started increasing and the crack widths of about 0.5 mm were observed on the critical locations of the beam column joints. Cracks were mostly localized with wider cracks at the ends of the beam column joints. At the end of the 50 mm displacement cycle, cracks as wide as 0.4 mm were observed on the columns. After 80 mm displacement cycle a number of diagonal shear cracks started forming at the ends of plinth and top beams, with these shear cracks running into the slab offsets. With 100 mm (push) displacement cycle the cracking noise was quite audible with wide diagonal shear cracks getting developed at the ends of the beams B1, B3, B5, and B7 and these shear cracks progressed in the slab also, symptomatic of the composite action between the RC slab of the test frame and the roof beams. Cover spalling at the beam column joints started to occur with each progressive cycle. The diagonal shear crack at the end of beam B7 near column C3 started from the top section and progressed to the half of the beam depth. 0.9 mm wide cracks were observed at the beam ends.

After the 100 mm displacement cycle, the cracks started widening at a faster rate and started growing up, with the shear cracks at the end of beam B3 at column C4 moving into the full cross section of the beam at the end of the 120 mm displacement cycle. The shear cracks at the ends of beams B5, B7 widened and the width of 1.7 mm was measured at the end of 130 mm displacement cycle. As the frame was subjected to 140 mm displacement cycle, the beam B5 started getting damaged significantly with initiation of concrete spalling at its end near column C1. The end of the beam B7 at the column C3 spalled extensively leaving the cover concrete totally damaged and exposing the bottom reinforcement of the beam B7. All the shear cracks in beams B5 and B7 at this stage extended in the slab area with some of the cracks from beam B5 extending into the slab soffit and meeting the shear cracks of beam B7. With the frame subjected to the targeted displacement cycle of 150 mm the spalling continued to occur at the beam column joints rendering the reinforcing bars exposed at the beam column joints. The frame was subjected to a total of 15 push pull displacement cycles and target displacement of 150 mm. A maximum load of 323 kN was observed at a displacement of 120 mm. A load of 320 kN was measured at the lateral displacement of 150 mm. At the end of the simulated

seismic loading the frame was actually subjected to a push of 160 mm and left to take its own position and thus a plastic residual displacement of 41 mm was registered after unloading. Figure 2.16 shows the recorded load-displacement hysteresis.

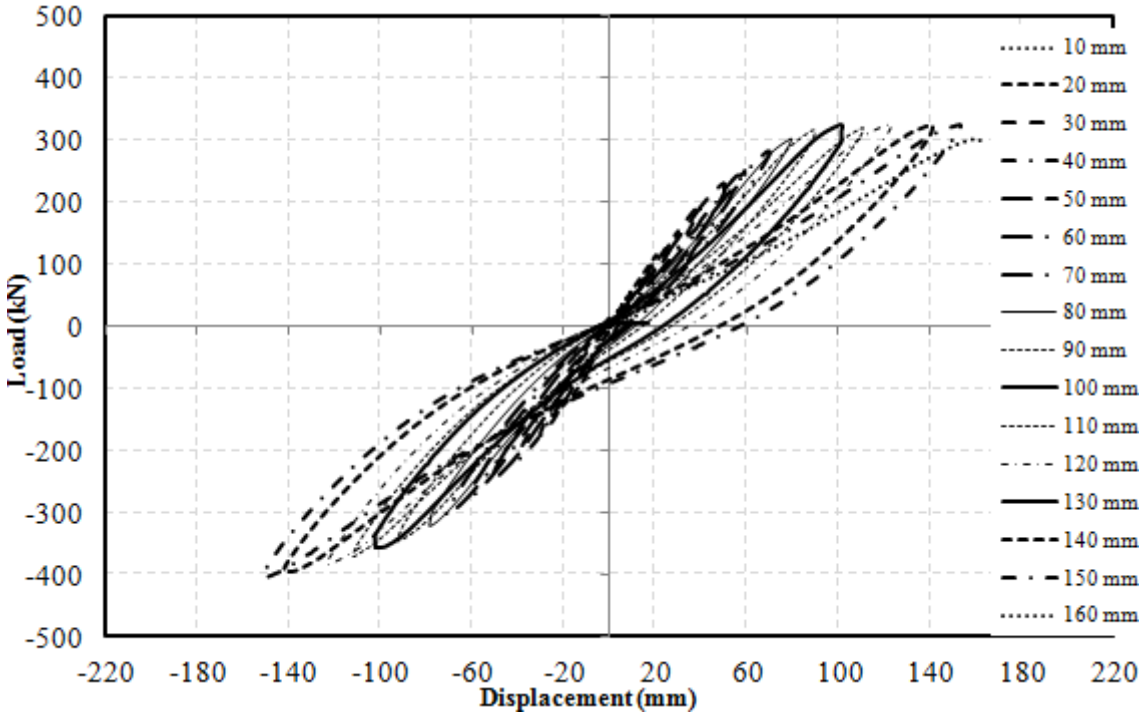

Fig.2.16: Load displacement hysteresis curve of the test frame.

2.3.1.1.2 Distress mapping after the test

After the seismic loading a detailed distress mapping was carried in all the structural elements of the RC test frame assemblage. Figure 2.17 shows the damage induced in the members of the frame. It was observed that the beams, (plinth as well as the roof) B2, B4, B6 and B8, perpendicular to the loading were not damaged as expected. However, the columns, slab and the beams parallel to the seismic loading direction were observed to have undergone extensive damage in terms of cracks and the concrete cover spalling. The roof beam B5 near column C1 had undergone extensive spalling with a spalled chunk of 230 mm × 60 mm × 16 mm being registered resulting in the exposure of the underlying reinforcing rebars (Figure 2.17 a). A 3 mm wide crack was measured throughout the cross section of the beam at 160 mm from the face of the column C1, which made its influence into the slab span also. A shear crack was observed with a width of 3.6-4 mm which traversed through the span of the slab at a distance of 60 mm from the face of beam B8 and converged with the shear cracks of the beam B7 which was symmetrically opposite to the beam B8. Another crack 1.5 mm wide was measured which started as an offshoot of shear crack of beam B5 and traversed the span of the slab at a distance of 300 mm from the face of beam B8 and terminated by joining the shear crack of the beam B7.

(a)

(b)

(c)

(d)

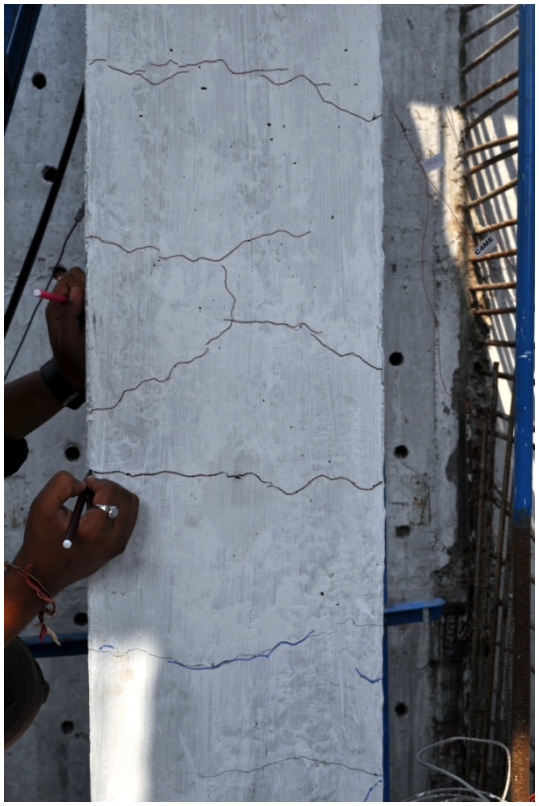

(e)

(f)

Fig.2.17: Damage induced in different elements of the test frame. (a) Beam B5 (b) Beam B7 (c) Slab (d) Beam B3 (e) Column C4 (f) Slab at Column C2

Another crack with a width of 0.1 mm traversed throughout the slab span at a distance of 420 mm from the beam B8. Some fine cracks with a width of 0.04 mm were measured on the beam B5 towards the centre of the beam. However the number of fine cracks was very less and a number of wider cracks were observed towards the beam ends. The crack widths showed a decreasing trend as we go towards the centre of the beam.

Delamination of concrete cover was found on the beam B5 near column C2 and very loose concrete was observed near the beam column joint. The shear crack with a width of 2 mm protruding into the beam depth and extending into the slab offsets was registered near the beam column joint. Spalling was also registered in the beam B7 near column C3 with a spall volume of 210 mm × 230 mm × 35 mm (Fig. 2.17 b) which rendered all the three main reinforcement rebars and the shear reinforcement exposed. The exposed reinforcing bars had buckled between the shear stirrups at this beam column joint. The concrete adjacent to the spalled portion had undergone delamination and was quite loose. A number of cracks were registered on the beam B7 near column C4 with little spalling at the corners of the beam column joint. A number of shear cracks developed at this end which joined the shear cracks of the beam B5 by traversing through the slab span. The roof beams B6 and B8 suffered very less damage as they were perpendicular to the direction of loading. However, the beam column joints of these beams also suffered some damage due to the moment transfer mechanisms.

A 3 mm wide shear crack was also measured in beam B3 near the beam column joint at column C3 (Fig.2.17 d), which originated at the bottom corner of the beam and propagated through the cross section meeting the top surface of the beam at 180 mm from the face of the column. Delaminated concrete was noticed in this beam with delamination starting from the mid section of the beam at 180 mm from the face of the column C3, moving up to 680 mm with a delaminating width of 2mm. The other plinth beams perpendicular to the direction of the loading did not have any substantial damage. The roof slab of the RC test frame got damaged with a number of shear cracks from the beams B5 and B7 running into the slab span from one end to another (Fig. 2.17 c). These cracks ran parallel to beams B8 and B6 with some of the cracks protruding into the entire slab depth appearing at the top of the roof slab also. A crack with a width of 6-7.5 mm (Fig. 2.17 f) was measured on the top of the slab, which originated as a shear crack in the beam B5 near column C2 and protruded into the slab depth, running through the slab extensions and on the top of the slab traversing through the slab top along the edge of the beam B6. This crack is believed to be due to the torsion of beam B6 due to the

loading perpendicular to it. This crack converged with the shear crack originated from the beam B7. Similar crack was observed on the opposite end near the beam B8.

A number of cracks of widths ranging 0.5-3 mm were recorded along the span of the slab, parallel to the beams B6 and B8, either as independent formations or as the extensions of the shear cracks of the beams B5 and B7. These cracks got formed in the slab in a symmetric fashion spread over a distance of about 700 mm from both B6 and B8 beams. The crack pattern demonstrated the uniform behaviour of the composite slab- beam system in both the push as well as the pull events of the pseudo static seismic loading. These flexural cracks on the either ends of the slab in one particular direction also indicate that an RC roof slab will not always behave as a rigid diaphragm under the in plane loading.

Similarly a number of cracks were measured in the columns of the test frame assemblage which were also localised in nature with most of them being formed at the beam column joints. Cracks with widths ranging from 0.06 mm to 1.7 mm were found mostly in the end regions of the all the columns. The degradation of the RC test frame assemblage due to these cracks, spalling and delamination is also manifested by the load displacement history as shown in Fig. 2.16 where in a clear decrease in stiffness and pinching of the hysteresis loops can be seen. The pinching effect is the direct manifestation of the deviation of the steel reinforcement direction from the coordinate of the principal stresses. This was caused in the structural elements of the RC test frame assemblage due to the extensive cracking of the various structural elements of the frame. The pinching effect can also be attributed to the rapid increase in the shear strains which is evident from the wide shear cracks formed in the roof beams B5, B7 and plinth beams B1, B3 (Mansour and Hsu, 2002). During the loading a large number of shear cracks got formed in different elements of the frame, which indicates build up of large vertical strains. From compatibility, the large vertical strain produce a large increase of strains in steel bars, which has been captured by the strain gauges on the steel rebars as shown in Figs 2.18-2.29. From equilibrium, the large stresses in the steel bars and in the vertical concrete produce large shear stresses causing the pinched shape of the hysteretic loops.

2.3.1.2 Strain data

As mentioned earlier in the section on “instrumentation of the test frame assemblage”, eighty strain gauges were positioned at a number of points in the different structural elements of the frame. Although some of the strain gauges malfunctioned during the test, however a good amount of strain data could be captured.

2.3.1.2.1 Strains in Columns

Figure 2.18 represents the strains as measured by the strain gauges pasted on the rebars of the column C1. Three strain gauges were positioned at different places on each of the opposite faces; one towards the inner side which was later exposed to fire and the other on the opposite face, which remained directly unexposed during the fire test. Figure 2.18 (b) represents the strain development profile at mid height towards the unexposed face (C1MU). The numbers of peaks in the strain profile correspond almost to the number of peaks in the load-time history of the frame. A maximum strain of 2400μ strain i.e. 0.0024 was registered during the loading excursion which indicates the occurrence of the initial yielding. The strain profile shows a residual permanent set which increased with time indicating the development of plasticity in the columns, which was also reflected by the damage caused to the columns. Figure 2.18(a) represents the strain profile at bottom joint towards the unexposed face (C1BU). Strains increased with each cycle following a well definite trend with the peaks approximately coinciding on the time scale with the peaks in load displacement history. The peaks were higher in tensile region indicating a strain of 0.0046 at 80 minutes of loading corresponding to a load of 314 kN. The strain reached a value of 0.0052 at 88 minutes thereafter remaining almost constant up to 110 minutes at which the tensile strains changed into compressive strains. At the load of 126 kN (pull) the first rebar slip was captured in the strain profile which was also manifested in the load- displacement hysteresis as pinching. After this point a number of rebar slips were captured till the strains reached a maximum tensile strain value of 0.0080.

Figure 2.18 (c) represents the time- strain plot at the top beam column joint in column C2 towards the unexposed face (C2TU). Again the strain is observed to rise with each displacement cycle with most of the strains tensile in nature. The strains peaked synchronously with the peaks of the load time history. The maximum measured stain was 0.0061. Figure 2.18 (d) shows the strain variations in column C2 at top section on exposed face (C2TE). As expected the strains were mostly compressive in nature with the maximum tensile micro strain of 181.44 and the maximum compressive micro strain of 300. Figure 2.19 (a) shows the development of strains in column C2 at mid section on exposed face (C2ME). The strain plot shows the initiation of the permanent set in the steel rebar at time 7 minutes with the set intercept increasing with the time. A maximum compressive strain of .0012 and a maximum tensile strain of .0021 were registered at this section. A look at the strain plot figure 2.19 (b), which is the strain development at midsection on unexposed face (C2MU), reveals the similarity of the strain profiles. The peaks of both the opposite faces almost synchronise with

each other with respect to the time scale however the strains at C2MU are much higher than those at C2ME with the maximum strain of .0076 at C2MU. Figure 2.19 (c) represents the strain- time plot at bottom section on exposed face (C2BE). The plot matched with the strain plot at C1BU except that the value of strains was lower than those in column C1. Strains increased with each cycle following a well definite trend with the peaks approximately coinciding on the time scale with the peaks in load displacement history. The peaks were higher in tensile region measuring a strain of 0.0024 at 80 minutes of loading corresponding to a load of 314 kN. The strains reach a value of 0.0026 at 88 minutes thereafter remaining almost constant up to 117 minutes at which the tensile strains change into compressive strains. The strains registered are almost half of the strains at the same position in column C1.

Figure 2.19 (d) represents the strains captured in column C3 at the top section on the exposed face (C3TE). Both tensile as well as the compressive strains have been captured. At this point also the strain – time plot is well synchronised with the load time history of the frame with the strain values increasing with the increase in the load applied. The strain plot is also similar to the strain plot C1BU with higher tensile strains, however with a phase difference of 180°. A compressive strain of 0.0013 was measured at 80 minutes of loading. At time 83 minutes, the strains were tensile in nature with a value of 0.0024. A maximum strain value of 0.0029 was captured at this position. Fig. 2.20 (a) represents the time- strain plot as captured by the strain gauge at mid section of the column C3 on the unexposed face (C3MU). The strain plot shows the setting of permanent set from the initiation of the loading which may caused due to the local crushing of the concrete at the strain gauge point. The value of the permanent set increased with time and a maximum strain of 0.0012 was captured at this point which infers the setting of initial yield in the rebars. Figure 2.19 (c) represents the strain profile at bottom section of the column C3 on the exposed face (C3BE). The strain profile was almost similar to that of the profile at C2BE which was subjected to the same conditions. The strains peaked at the same time and the variation of the peaks was almost similar reflecting the similar structural behaviour of the columns in the seismic loading phase. The plot also matched with the strain plot at C1BU having a symmetric location with C3BE and C2BE except that the value of strains is lower than those in column C1. Strains increased with each cycle following a well defined trend with the peaks approximately coinciding on the time scale with the peaks in load displacement history. At 147 minutes, corresponding to a load of 126 kN (pull), the strain value reached 0.0006 and the first rebar slip was captured in the strain profile, similar to what was seen in C2BE. After this a number of rebar slips were captured till the strains reached a maximum tensile strain value of 0.0038.

Figure 2.20 (c) represents the strain development plot in column C4, top section on the unexposed face (C4TU). It can be observed that the strains are higher in magnitude which was also manifested by the higher level of damage caused at this location. A maximum compressive strain of 0.015 was registered at this location. C4TE (fig 2.20 d) shows a trend similar to C3BE, C2BE. Figures 2.21 (a,b,c) represent the time-strain plots in column C4 at mid section (exposed, unexposed) and bottom section (unexposed) respectively. A perusal of the time-strain plots of the columns reveals development of large strains at the joints (top and bottom sections) and relatively lower strains at the midsections which was also manifested by the distress mapping which revealed major damage at the joints.

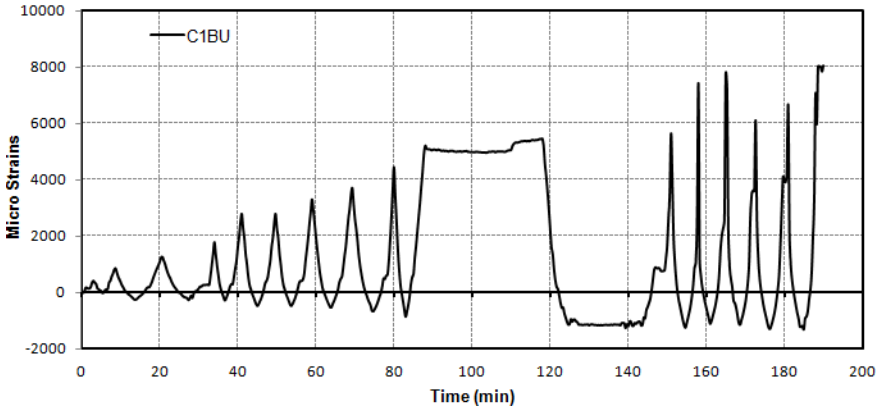

(a)

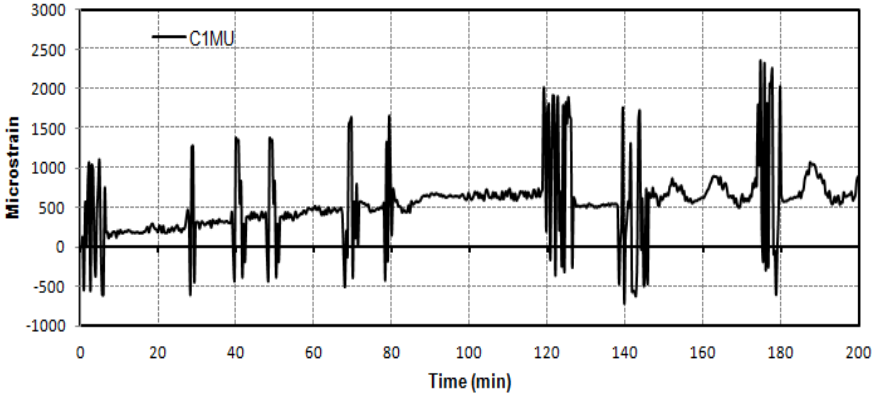

(b)

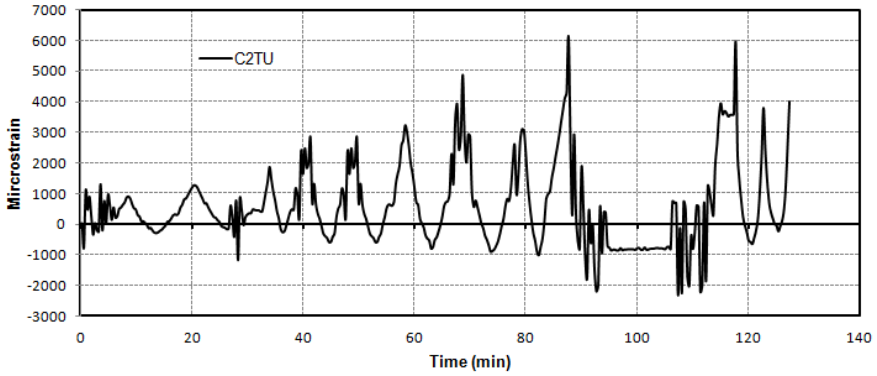

(c)

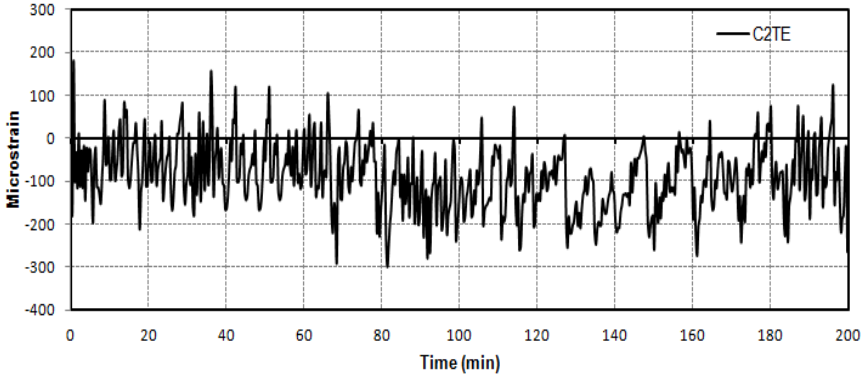

(d)

Fig.2.18: Time- Strain plots for Column C1 and C2.

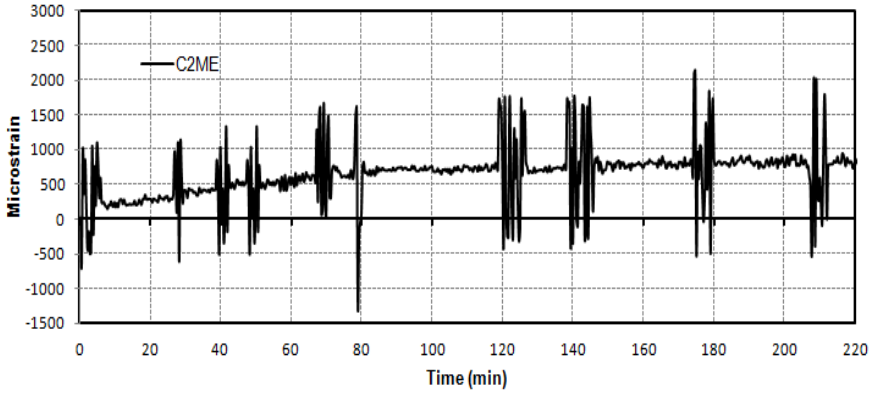

(a)

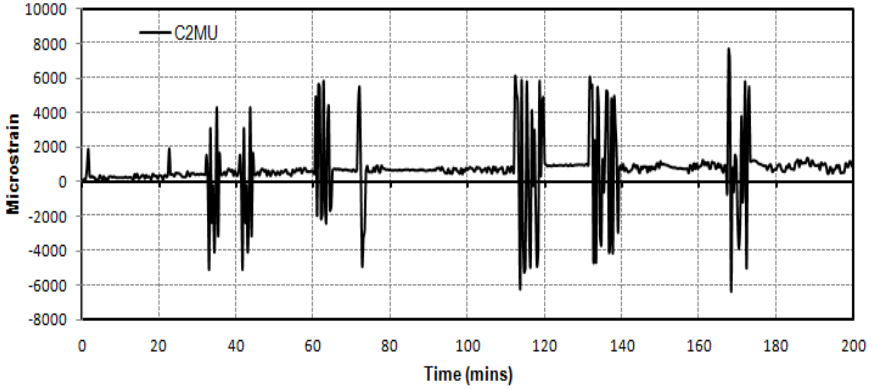

(b)

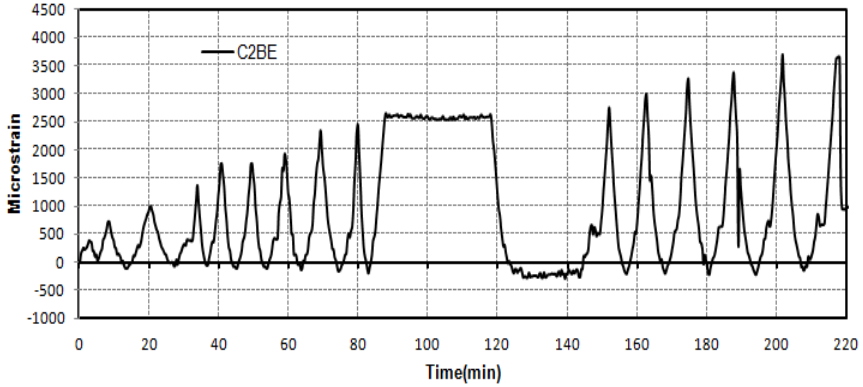

(c)

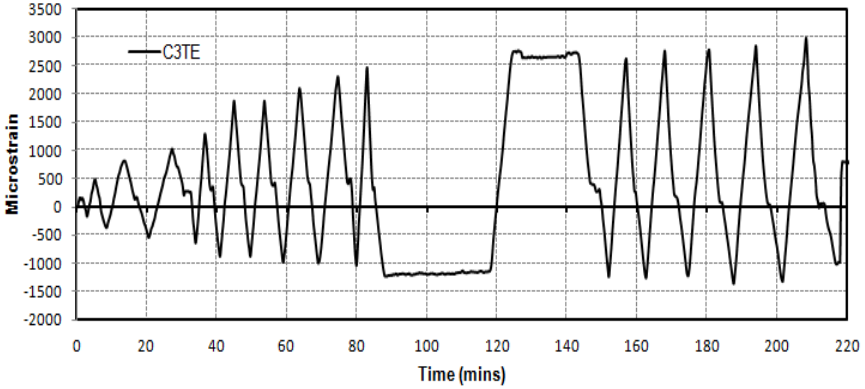

(d)

Fig. 2.19: Time- Strain plots for Column C2 and C3.

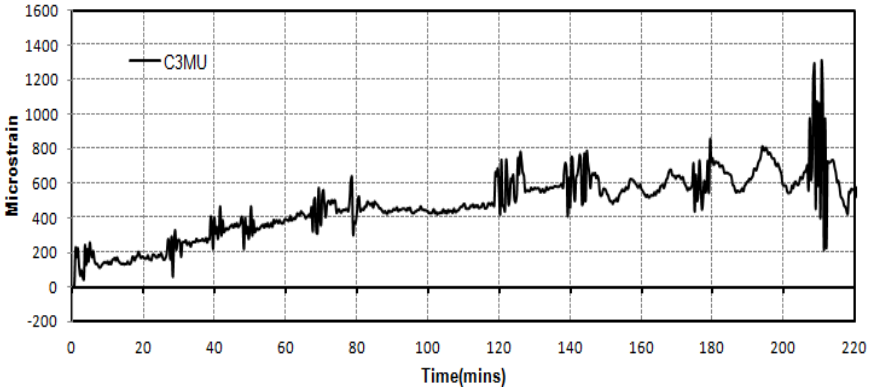

(a)

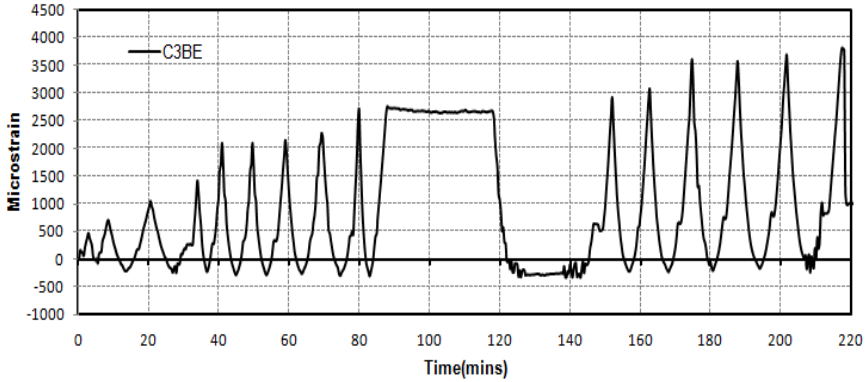

(b)

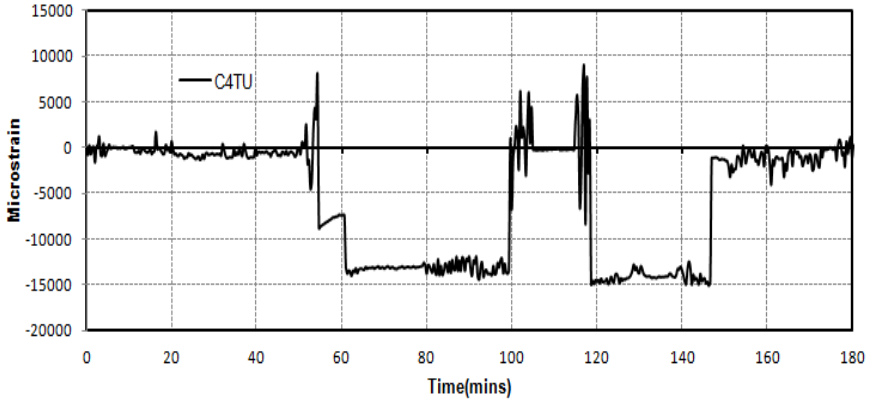

(c)

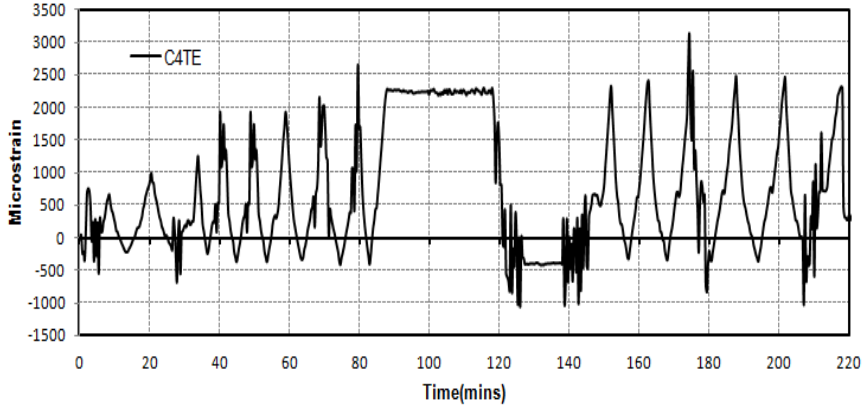

(d)

Fig. 2.20: Time- Strain plots for Column C3 and C4.

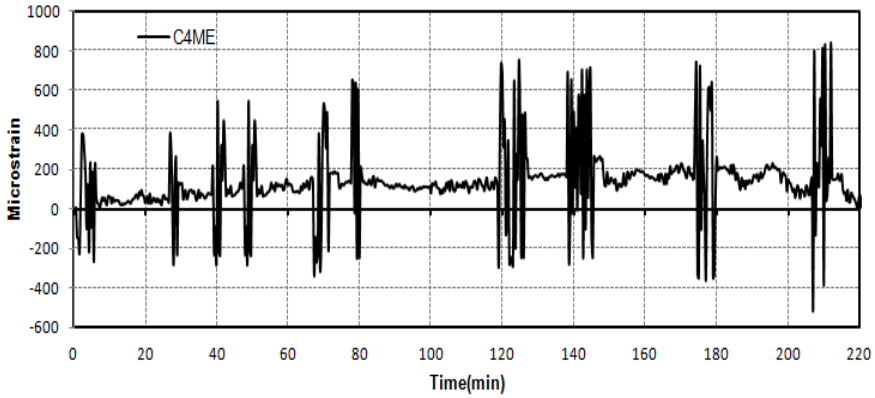

(a)

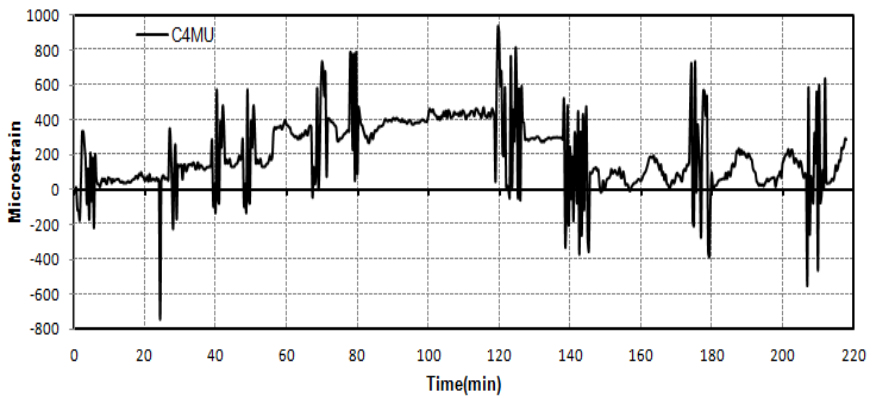

(b)

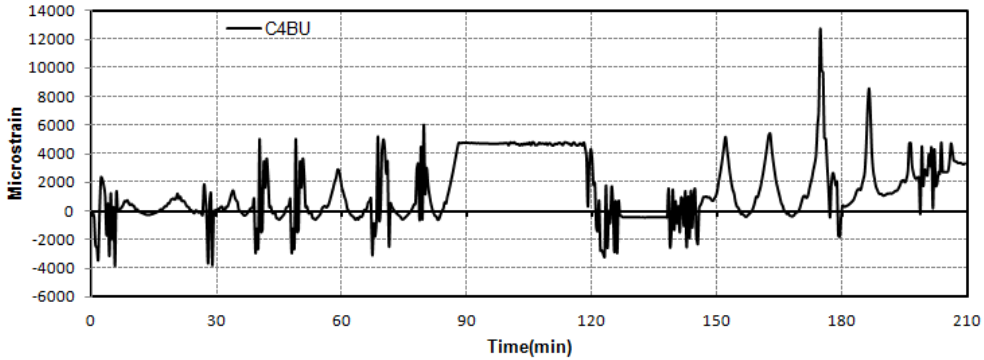

(c)

Fig. 2.21: Time- Strain plots for Column C4.

2.3.1.2.2 Strains in Beams

Fig 2.22 (a) represents the strain – time plot for lower rebar in beam B1 at left section (B1LB). The strains increased with the increase in the target displacement. The strains followed a trend similar to those in columns at the joints, however the strains were higher in beams than those in columns at any given time. The peaks are in agreement with the peaks in load – time history and the displacement- time history. A strain value of 0.0013 was registered at the end of 20 minutes time. The strains peaked to a value of 0.0042 at 88 minutes after which the strain variation followed a wide crust till 117 minutes with the strain value of 0.0031. The strains took a dip at this point and followed a wide trough from 120 minutes till 147 minutes and the strains varied from 0.0009 to 0.0006. This wide behaviour of crust and trough during this period was also present in C4BU, C4TE, C3BE, C2BE, and C1BU. The strains increased with each loading cycle until the highest strain value of 0.015 was achieved. The higher strains at this location are expected being the part of the beam column joint and the frame was designed as per the strong column and weak beam design philosophy making the beams vulnerable to the more damage.

Fig 2.22 (b) represents the strain – time plot for top rebar in beam B1 at left section (B1LT). The time-strain variation at this location was out of phase by 180^{o} from that of B1LB. However the crusts of B1LB and troughs of B1LT were synchronous with each other on the time axis which was expected as the strains gauges were pasted on the opposite rebars at the same location. The maximum strain measured at this location is 0.010. Fig 2.22 (c) shows the time- strain plot for the bottom rebar at the mid-section of the beam B1 (B1MB). The values of the strains were quite low as compared to the strains at the beam ends with the maximum value of 0.0008 being measured in the final stages of the loading. This is due to the fact that under the simulated loading the prominent bending occurs at the beam ends and the mid span remains less stressed. Figures 2.22 (d) and 2.23 (a) respectively show the time-strain plots for the bottom (B1RB) and top (B1RT) rebars at the right hand section in beam B1. It is observed from the plots that the strain variations were out of phase from each other by 180^{o} as expected and also the B1RT was having same strain variation as that of B1LB and B1RB was having same variation as that of B1LT. This is due to the outward bending of the bottom and the top rebars at the beam ends which renders the top face at the left section and the bottom face at the right section of the beam into same mode of bending in push and pull events and likewise the bottom face at the left section and the top face at the right section into same mode of bending in the

simulated loading events. While as the maximum strain of 0.0056 was measured in B1RB, a maximum strain of 0.012 was measured in B1RT.

Figures 2.23 (b-d) and 2.24 (a-b) represent the time – strain plots for the bottom and the top rebars of the beam B2 at different sections. Being positioned perpendicular to the direction of the simulated seismic loading; the damage in this beam was lower than the beams parallel to the loading direction which is also reflected by the comparatively lower strains in this beam as registered by the strain gauges positioned at different locations. The maximum strains registered in the beam B2 were as; 0.0011 in B2LB, .0008 in B2LT, 0.0010 in B2MB, 0.0013 in B2RB and 0.0027 in B2RT.

Figure 2.24 (c) represents the time strain plot for the bottom rebar of the beam B3 at left section (B3LB). The variation of strains is similar to that in B1RB being at the similar position with respect to the loading direction. A maximum strain was measured to be 0.0035. Large strains were registered in the top rebar of the beam B3 at the left section (B3LT) with a maximum strain 0.011 being measured at this point as shown in the figure 2.24(d). These large strains were also manifested by wide shear cracks at this section as shown in Fig. 2.16 (d). Figs 2.25 (a) and (b) respectively represent the strain variation with time for the top (B3MT) and bottom (B3MB) rebars at the mid section of the beam respectively. The variations in both the strain gauges was almost similar and was characterised by lower strains on the bottom rebar and relatively higher strain on the top rebar, however the strains were relatively lower than those at the left and the right sections of the beam. Figs 2.25 (c) and (d) show the time strain plots for the bottom (B3RB) and top (B3RT) rebars at the right section in beam B3. It is observed from the plots that the strain variations are out of phase from each other by 180^{o} and also the B3RT had almost same variation as that of B3LB. While as the maximum strain of 0.0055 was measured in B3RB, a maximum strain of 0.002 was measured in B3RT.

Beam B4 registered lower values of strains (fig. 2.26 a–c) as in beam B2, being perpendicular to the direction of the loading. The maximum strains measured at the different locations were: 0.0005 at B4LB, 0.0007 at B4LT, 0.0006 at B4MB, 0.0015 at B4MT, 0.0014 at B4RB and 0.0012 at B4RT.

The roof beams registered higher value of the strains which was also corroborated by the damage caused to these beams during the simulated seismic loading. Fig 2.27 (a) represents the time strain plot in the bottom rebar for the beam B5 at the left section (B5LB). The crusts and the troughs are seen in the plot and the strains remain lower than 0.005 till almost the end of the loading until the strains reached a very large value of 0.03 which means the stress in the

steel rebar at this point had reached its plastic yield value. This large value of strain in the steel rebar was also manifested by a number of wider cracks at this location and the spalling of the concrete rendering the steel reinforcement entirely exposed as shown in Fig 2.17. Fig 2.27 (b) shows the time- strain plot in the bottom rebar of the beam at the right section (B5RB). The strain variation was similar to that in B1RB in the plinth beam B1, which was just at a similar position with respect to the loading, up to the 120^{th} minute after which the strains in B5RB were entirely tensile in nature; however the value of strains in B5RB is higher than those in B1RB. A maximum strain of 0.0087 was measured at this location.

In beam B6, being perpendicular to the direction of the seismic loading, the strains measured were of low magnitude with a maximum measured strain of 0.0028 as shown in the Fig. 2.27 (c) and (d)

Beam B7 registered high strains at the joints especially at the joint with column C3 where in the maximum strains of 0.035 (B7LB) were registered as shown in Fig. 2.28 (a). The large strains are also accompanied by the buckling of the reinforcement at this location as shown in the Fig 2.17. Among all the beams, the beam B7 was the worst damaged with highest amount of spalled concrete with the buckling of bottom reinforcement at the beam column joint. The strain variation at the mid section (B7MB) and the right section (B7RB) of the beam are shown in Fig. 2.28 (b) and (c) respectively. The mid section of the beam had registered lower strains values than the end sections.

Strains were also measured on the rebars in the slab. Figs. 2.28 (d) and 2.29 (a) – (d) represent the time- strain plots as recorded by the strain gauges at different key locations in the slab.

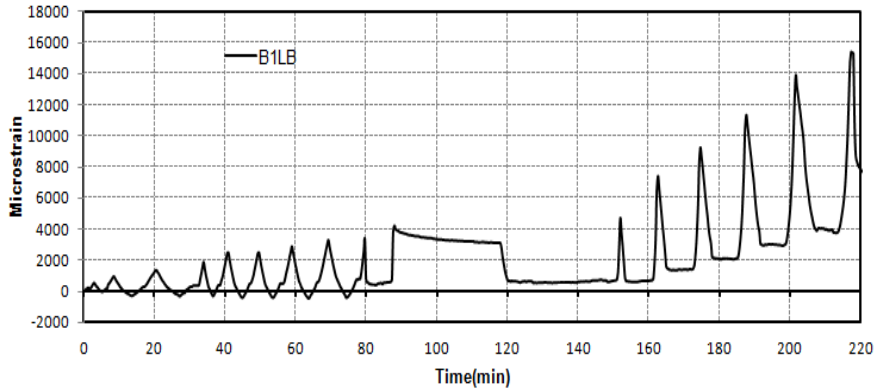

(a)

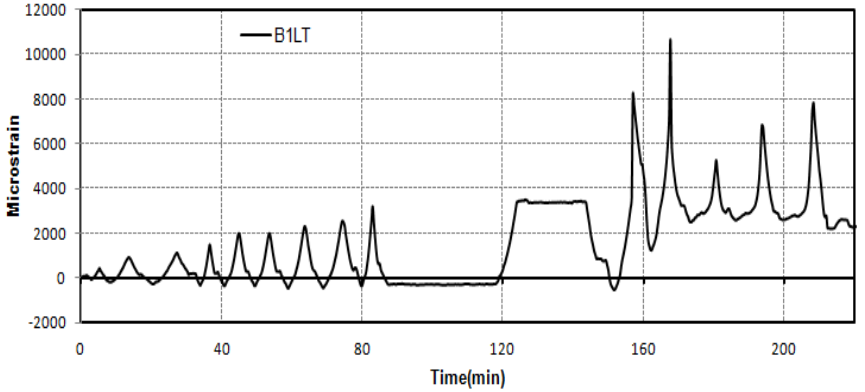

(b)

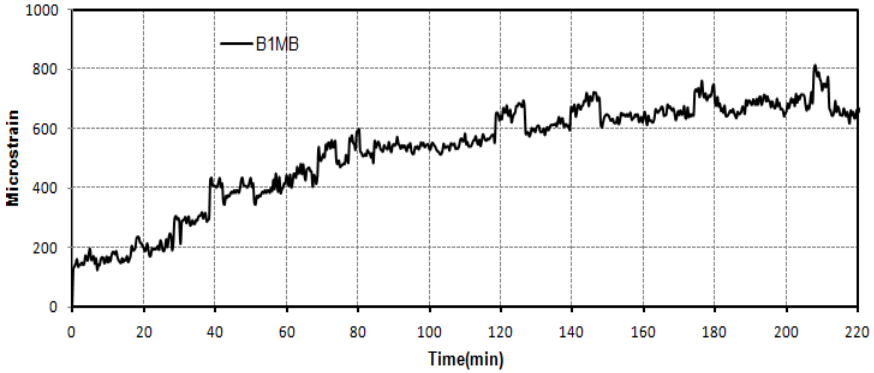

(c)

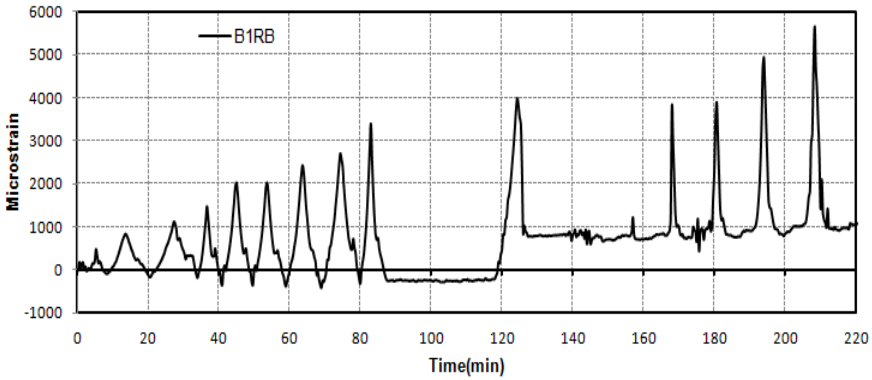

(d)

Fig. 2.22: Time- Strain plots for Beam B1

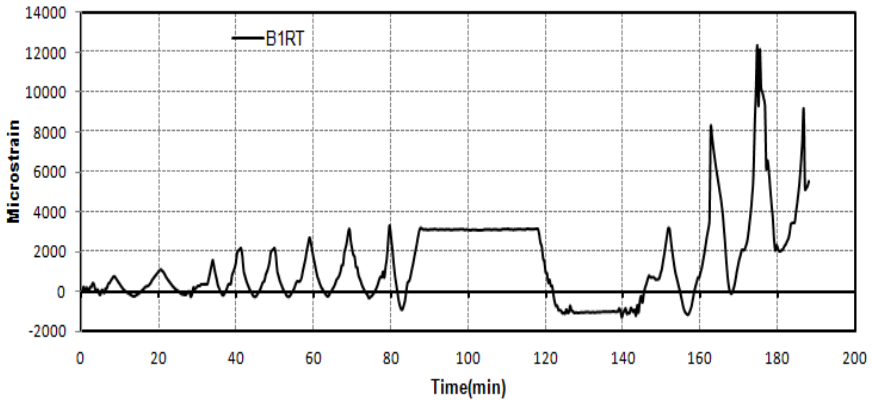

(a)

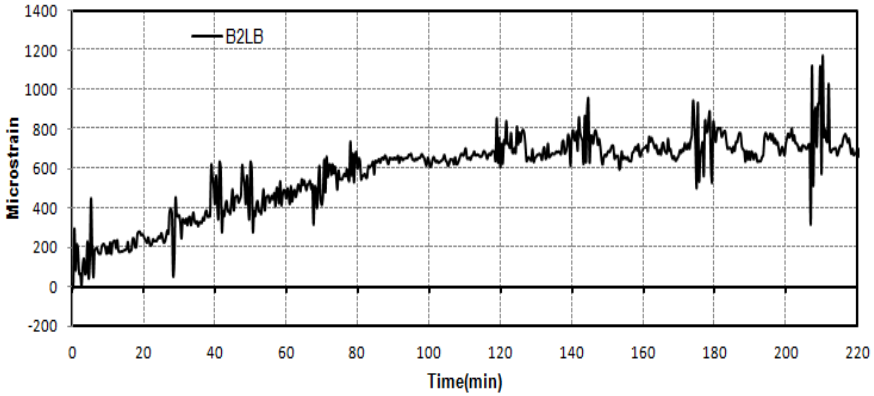

(b)

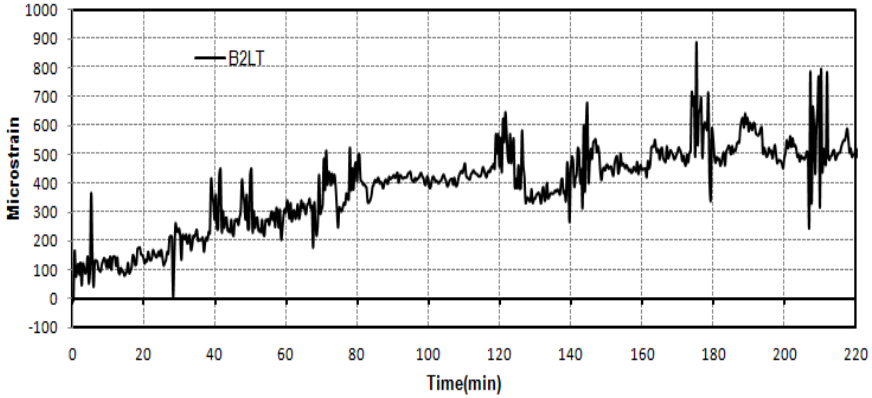

(c)

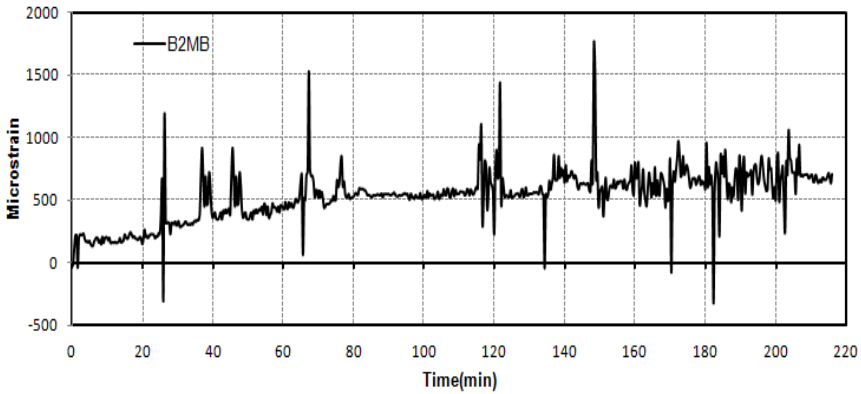

(d)

Fig. 2.23: Time- Strain plots for Beams B1 & B2

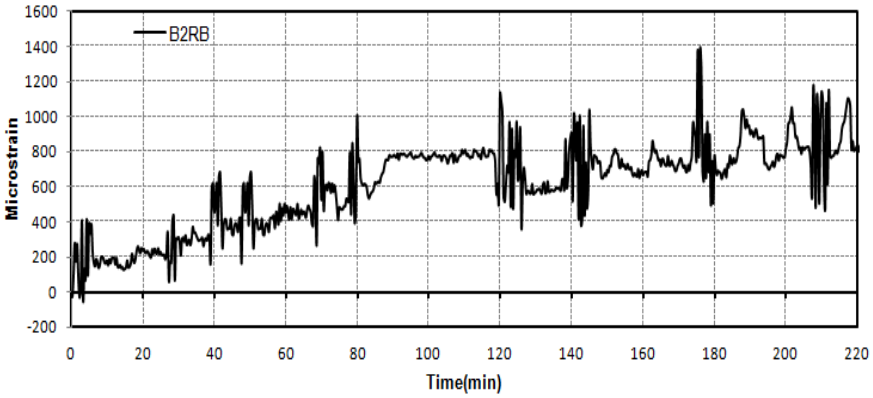

(a)

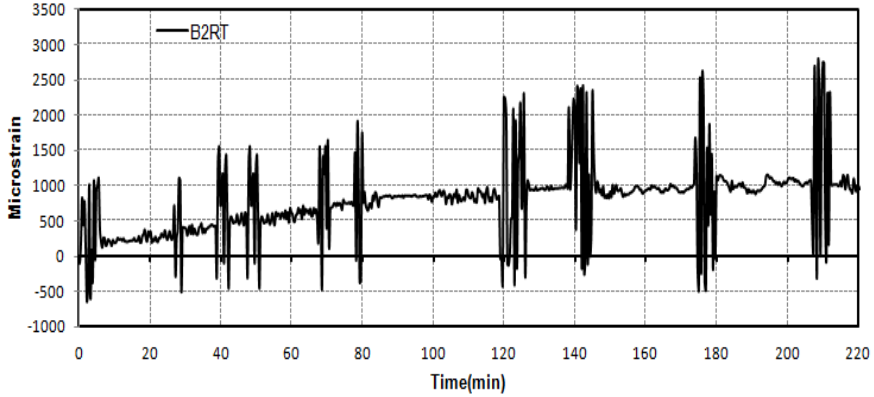

(b)

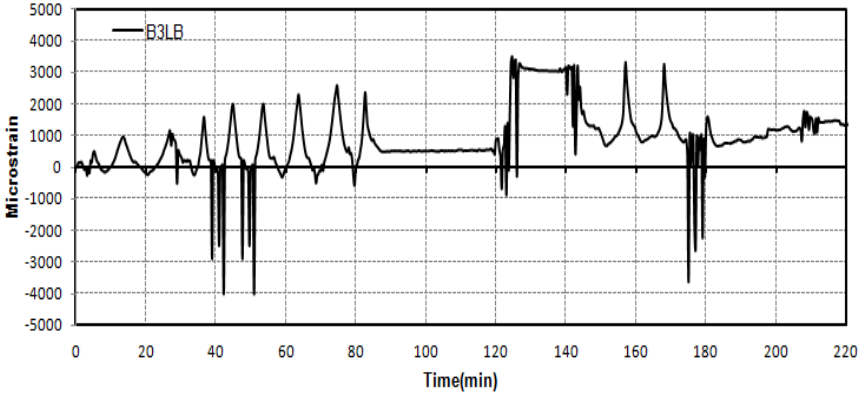

(c)

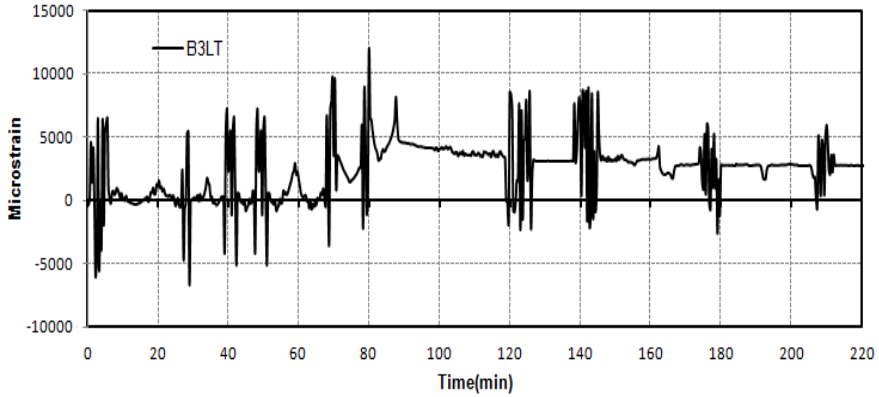

(d)

Fig. 2.24: Time- Strain plots for Beams B2 & B3

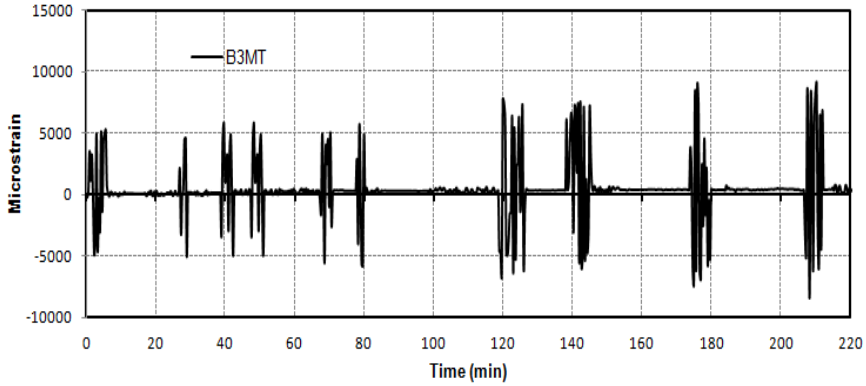

(a)

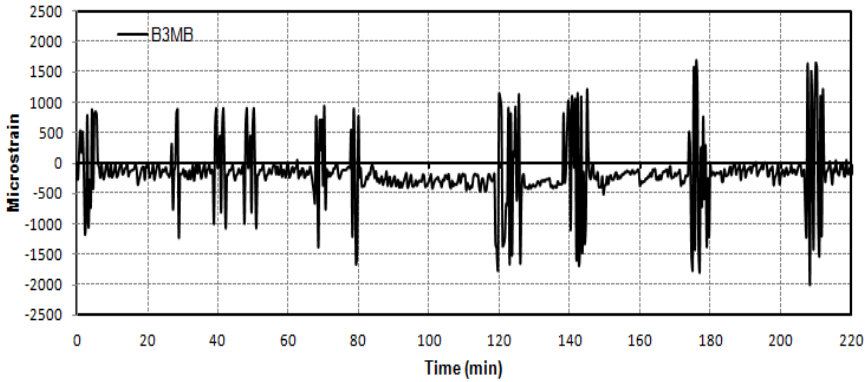

(b)

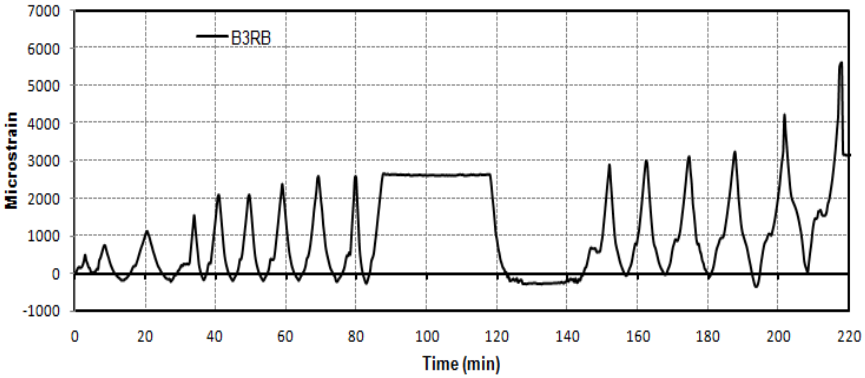

(c)

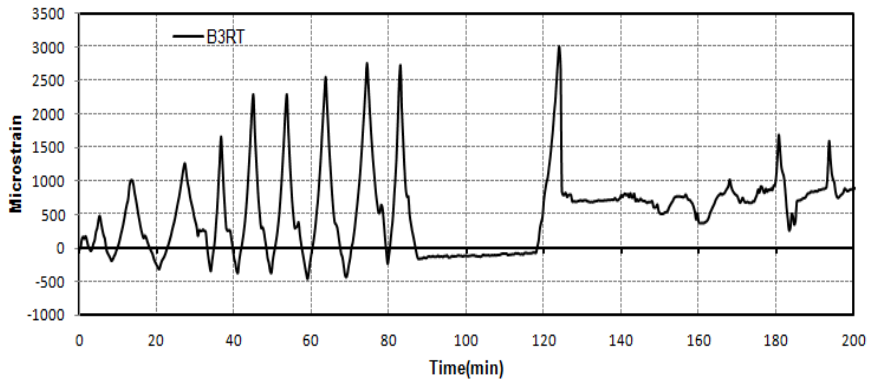

(d)

Fig. 2.25: Time- Strain plots for Beam B3

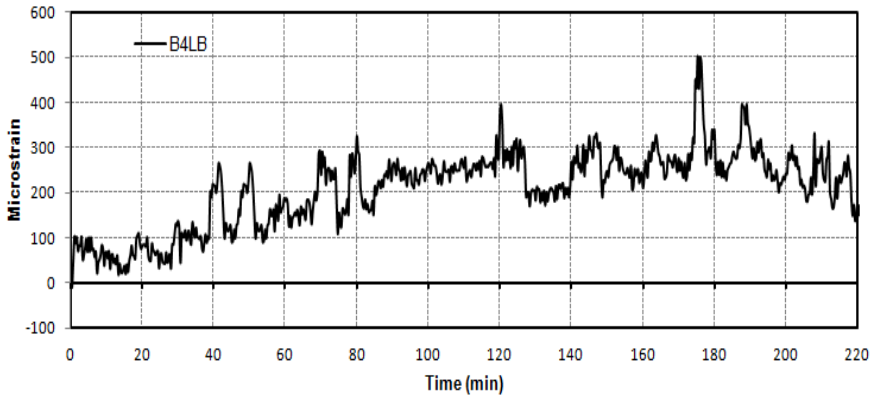

(a)

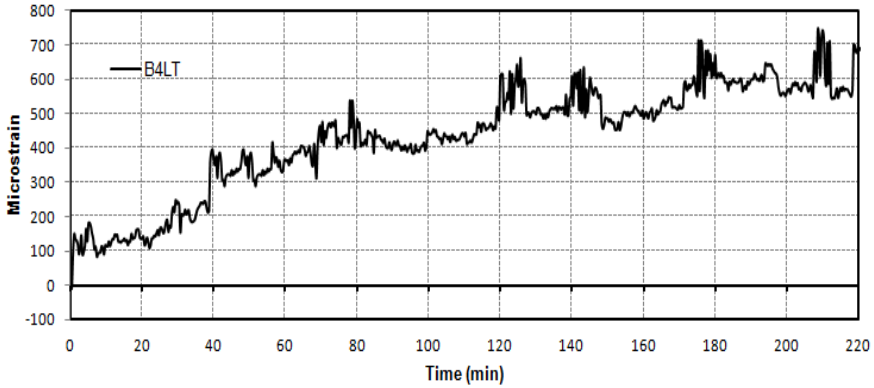

(b)

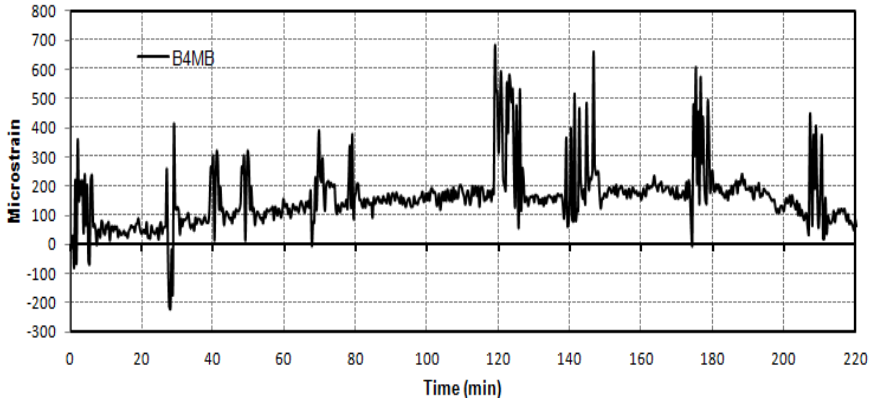

(c)

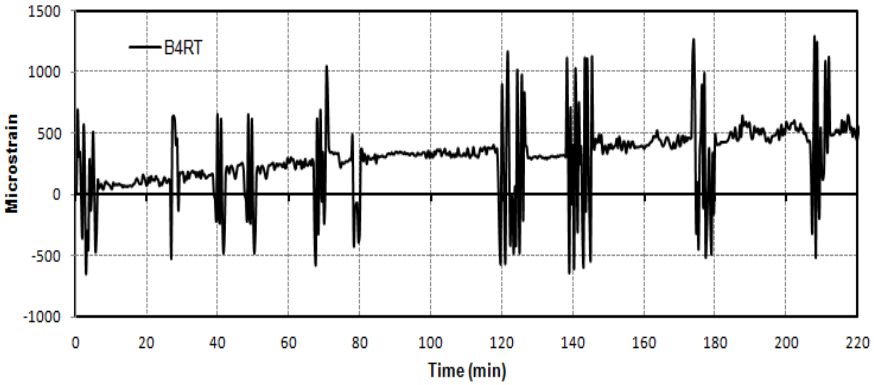

(d)

Fig. 2.26: Time- Strain plots for Beam B4

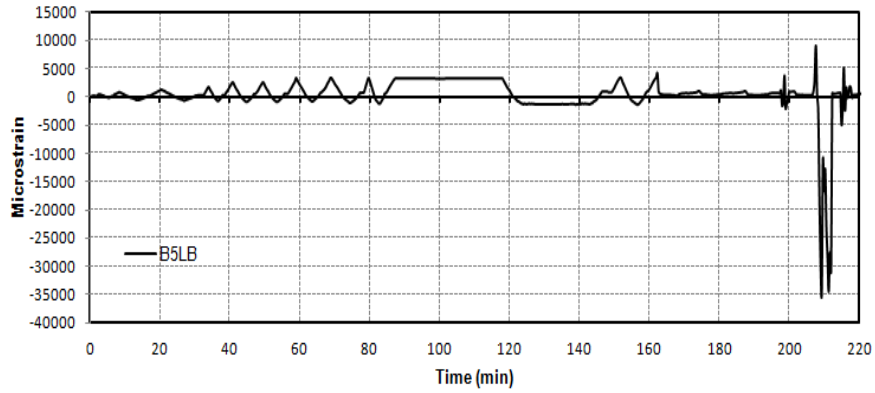

(a)

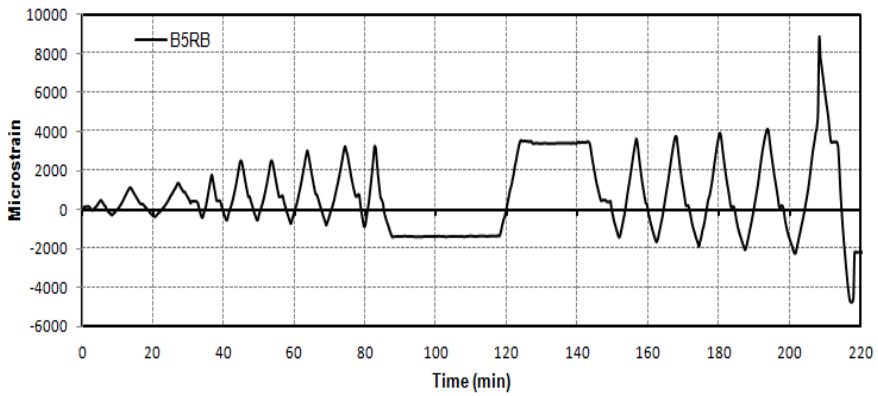

(b)

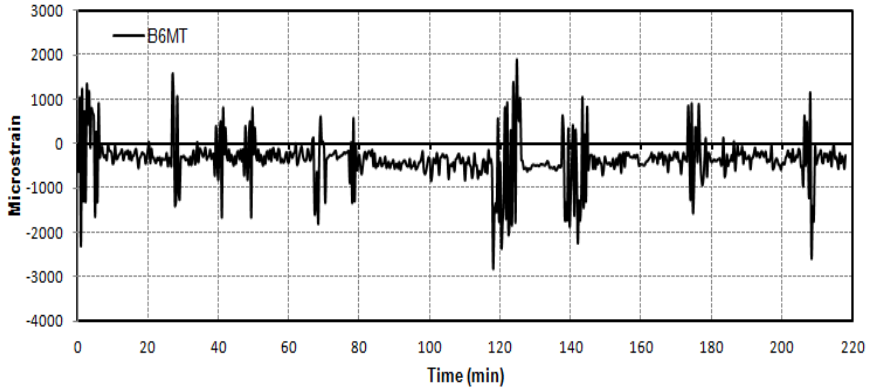

(c)

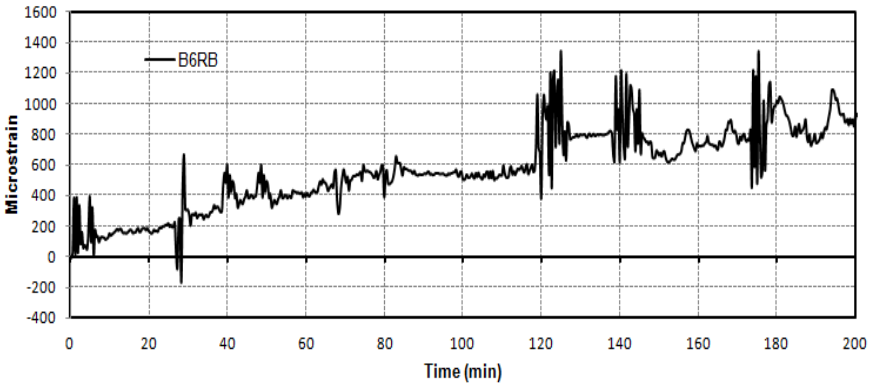

(d)

Fig. 2.27: Time- Strain plots for Beams B5 & B6

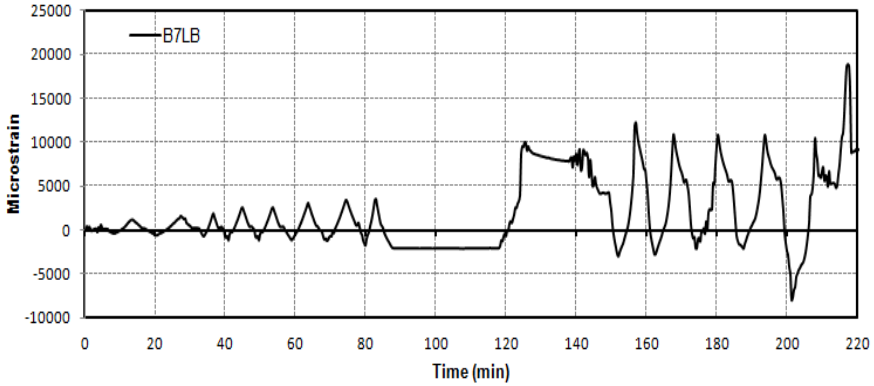

(a)

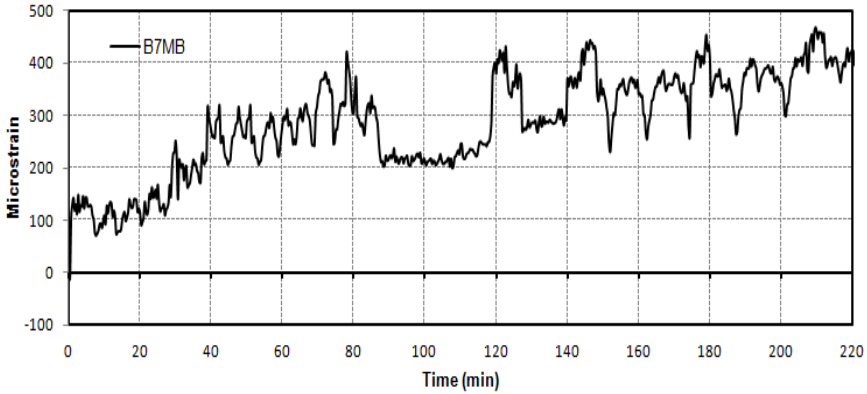

(b)

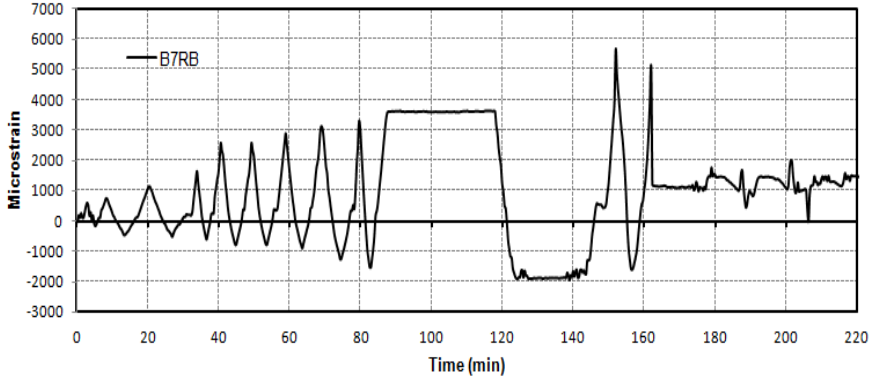

(c)

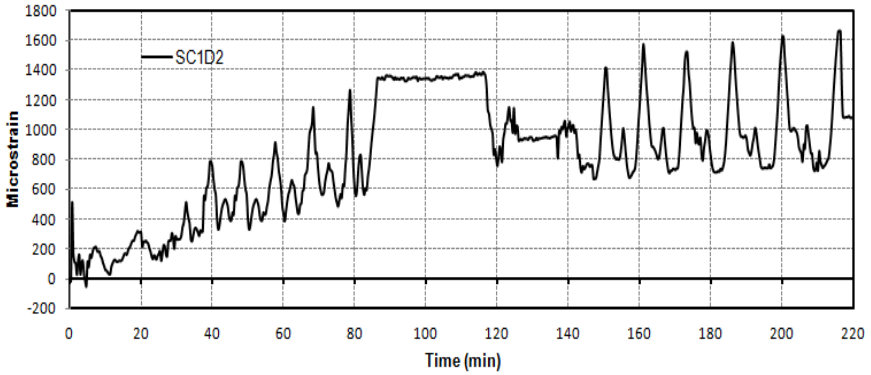

(d)

Fig. 2.28: Time- Strain plots for Beam B7 & Slab

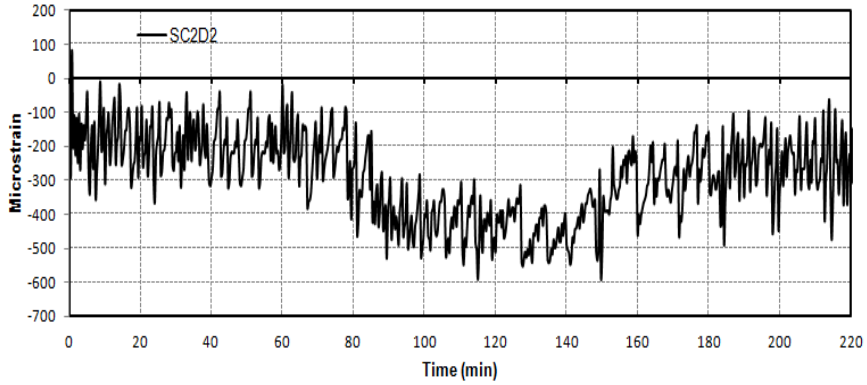

(a)

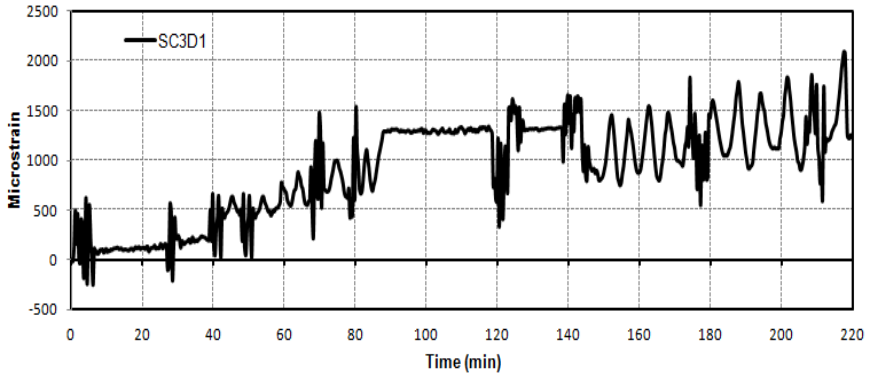

(b)

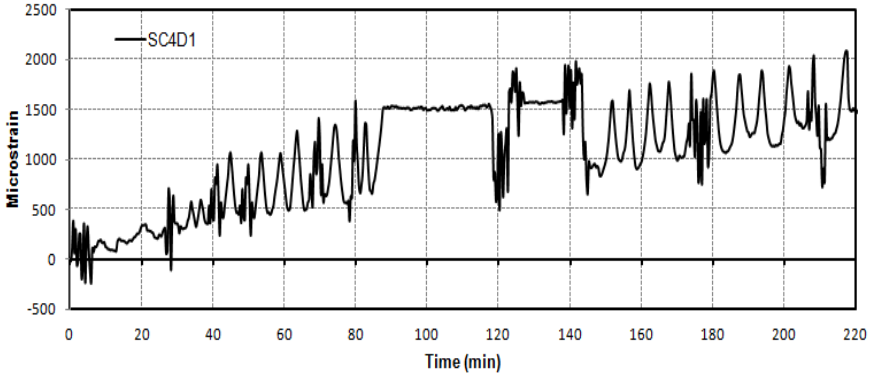

(c)

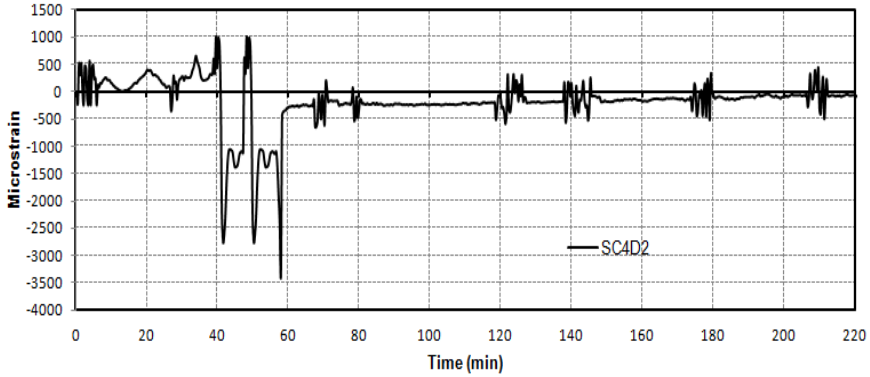

(d)

Fig. 2.29: Time- Strain plots for Slab

2.3.2 Test phase II: Fire Test

After pre-damaging the frame by inducing a defined level of damage, the frame was subjected to a one hour designed compartment fire to assess its structural behaviour in a simulated fire following earthquake event. The test was planned carefully keeping all the design parameters in consideration.

2.3.2.1 Fire design

While designing a structure to resist failure due to fire exposure, it becomes imperative to choose a proper design fire. Literature suggests three established methods for obtaining design fires.

2.3.2.1.1 Hand methods

This is the simplest but approximate method, where in the fire is assumed to have a constant temperature throughout the exposure time. The maximum temperature (T_{max}) to which the structure is to be exposed as per this method is calculated using the equation (2.1). The duration of the fire exposure/burning period (t_b) can be calculated using the equation (2.2). These equations have been established by Kawagoe (1958). The time- temperature curve for such a fire can be shown as in Fig. 2.30

$$T_{max} = 6000(1 - e^{-0.1\Omega})/\sqrt{\Omega} \quad (2.1)$$

Where,

$$\Omega = \frac{A_t - A_v}{A_v \sqrt{H_v}}$$

T_{max} is the maximum temperature in $^{\circ}C$

A_t is the total internal surface area of the room (m^2)

A_v is the area of the ventilation opening (m)

H_v is the height of the ventilation opening (m)

$$t_b = E/Q_{vent} \quad (2.2)$$

E is the energy content of the fuel available for the combustion (MJ)

Q_{vent} is corresponding ventilation controlled heat release rate (MW)

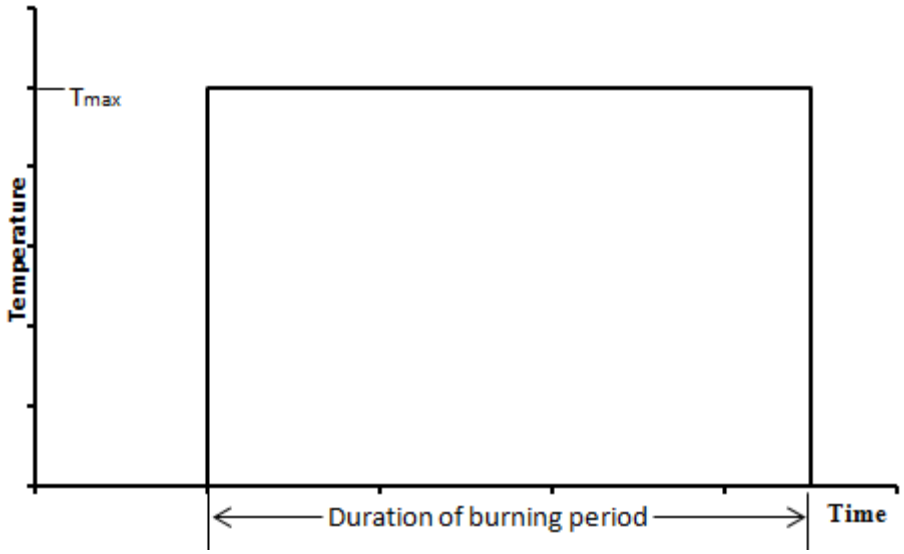

Fig.2.30: Design fire with constant temperature

2.3.2.1.2 Temperature- time curves as per standards

Another way of testing structures at elevated temperatures is the use of the temperature build up patterns as specified by different Standards and Codes. These curves are mostly used to determine the fire ratings of different structural elements. The fires developed using these curves are also referred to as the "parametric fires" or "standard fires". Some of the standard temperature- time curves are mentioned by ISO 834 (ISO, 1975) British Standard BS 476 Part 20-23(BSI 1987), Eurocode 1 (ENV 1995), Australian Standard AS 1530, Part 4 (SAA, 1990) and American Standard ASTM E119 (ASTM, 2001) However the most frequently used curves are ASTM E119 and ISO 834 (ISO, 1975). Fig. 2.31 shows the comparison of the temperature build up as given by these standards. At the outset, the build up of the temperature in the ISO 834 and ASTM E119 curves is similar. However as the time increases the temperatures vary between the two and the ISO 834 curve supersedes the ASTM E119 curve. A simple approach was established by Lie (Lie, 1992) and is denoted by equation (2.3).

$$T = 750\left[1 - e^{-3.79553\sqrt{t_h}}\right] + 170.41\sqrt{t_h} + T_0 \qquad (2.3)$$

Where

t_h is the time (hours)

T_0 is the ambient temperature in $^{\circ}$C.

Equation 2.4 denotes the Temperature- time curve of ISO 834

$$T = 345\log_{10}(8t + 1) + T_0 \qquad (2.4)$$

Where

t is the time in minutes.

Hydrocarbon fire, which attains a rapid flashover is given by the Eurocode and is denoted by the equation (2.5). Eurocode also gives an equation (2.6) for consideration of external fire for the fire design of facades as the temperatures calculated from the equation (2.5) are considered too severe for this purpose.

$$T = T_0 + 1100[1 - 0.325e^{-0.1667t} - 0.204e^{-1.417t} - 0.471e^{-15.833t}] \quad (2.5)$$

$$T = T_0 + 660(1 - 0.687e^{-0.32t} - 0.313e^{-3.8t}) \quad (2.6)$$

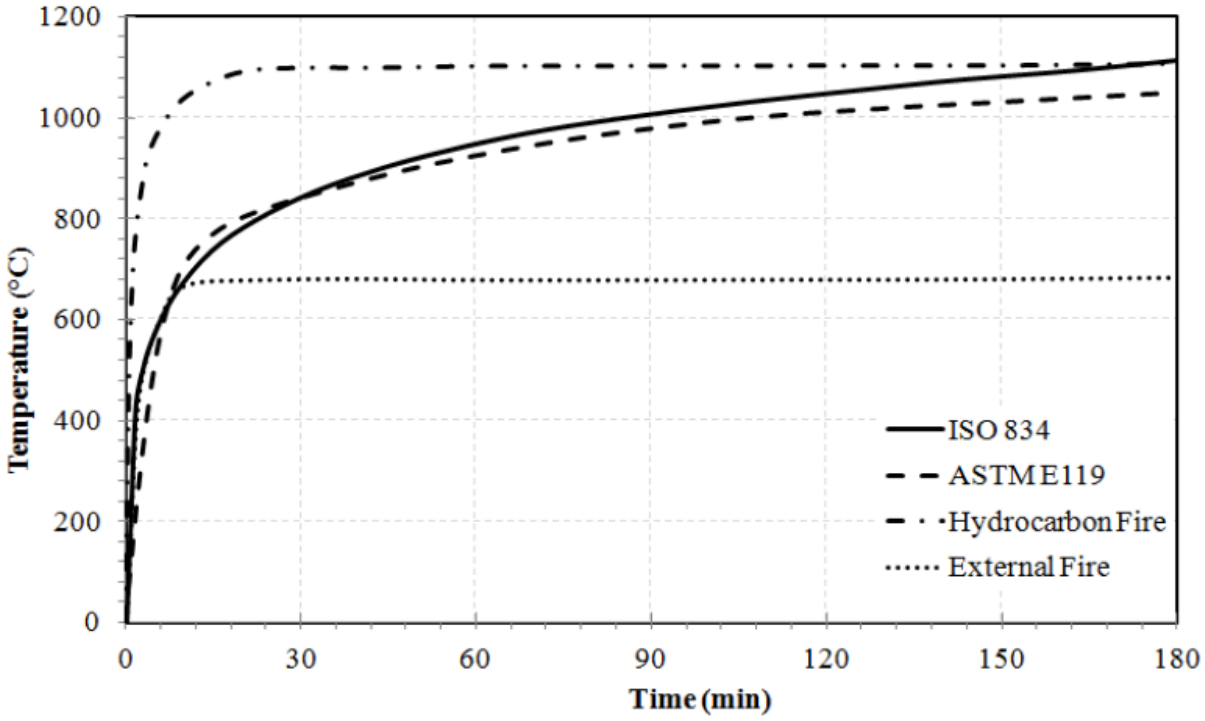

Fig.2.31: Different parametric fire curves.

2.3.2.1.3 Temperatures from the mock post flashover fire tests.

The most realistic data is the data from the actual test and is obtained by conducting the mock tests before the actual structure is exposed to the fire characteristics which are obtained by adjusting the data as acquired from these mock tests. Temperatures in most post-flashover fires are usually at least 1000 ºC. The temperature during the fire at any instant is determined by the balance between the heat released inside the compartment due to the fire load and all the heat losses; through ventilation by radiation and convection, and by conduction into the different elements of the compartment; walls, floor and ceiling (Feasey & Buchanan, 2002). The temperature characteristics of a real scale fire depend mainly on three parameters: size of ventilation, surface characteristics of the lining material of the compartment and the fire load. A number of tests have been performed to measure temperatures in post-flashover fires. The

results of these tests show a considerable scatter. Law (1983) developed an empirical relation for the maximum temperature for a large fire load of wood crib under steady burning rate in small scale compartments. This was based on the tests carried out by Thomas and Heseldon (1972). Based on Kawagoe's (1958) equation, Magnusson and Thelandersson (1970) developed the time- temperature curves for real fire exposure. These are also referred to as the "Swedish" fire curves and are the most widely referred curves for the real fire exposure. The curves are shown in Fig. 2.32. Each group of the curves is representative for a different ventilation factor F_v with fuel load as indication. As representative of the fully developed post- flashover fires, these curves have a descending branch also. Also the noteworthy point is the rising branch of the curve with a ventilation factor of 0.04 is quite similar to the ISO 834 curve.

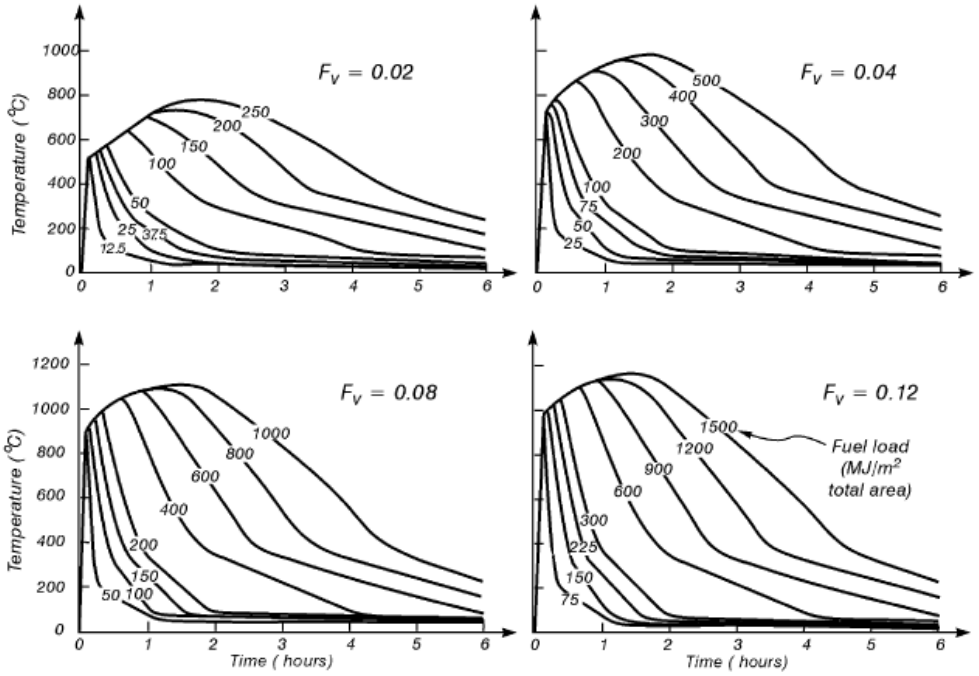

Fig.2.32: Time- Temperature curves for different ventilation factors and fuel loads

2.3.2.1.4 Compartment fire design for the current test

For uniformity and comparison purposes the fire design for the fire test was same as that of Sharma et al (2012) and Kamath (2014). A series of mock tests were conducted, using kerosene as the fire load, to arrive at the fire design with an objective to maintain the temperatures within the compartment at an average of 900-1000 °C for a period of one hour. The fire was designed as per Thomas and Heseldon (1972) and modified to allow rapid accumulation of smoke in order to enhance the flashover. With these modifications a compartment size of 3m × 3m × 3m was arrived at with an opening of 1 m height by 3 m length. The opening was kept low to enhance the accumulation of smoke for the rapid

flashover. The peak burning rate of kerosene oil was kept approximately 0.117 kg/m^2/s for maintaining a post flashover temperature of 900°C to 1000°C. A peak fuel flow rate of 1.43 x 10^{-4} m^3/s which corresponds to 9 litres/minute was maintained using a fixed head. Hence, a reasonably simple technique was adopted to attain gas temperature of about 1000°C within 5 minutes after ignition to simulate a realistic compartment fire (Kumar, 2012)

2.3.2.2 Fire test set up and the Fire test

Figures 2.33 to 2.37 show the different views of the frame before the fire test. The necessary fire enclosure was provided by four mild steel fire proof panels. In one of the panel a 1 m height by 3 m length opening was provided at the bottom to account for the ventilation as per the design. These mild steel panels were coated with a lining of fire proof glass wool material (0.0254 m thick) which was followed by the blocks of same material of size 0.3 m x 0.3 m x 0.20 m (thick) tied to the panels with the help of stainless steel rods. Extra care was taken to ensure that no smoke or flame leaks out of the compartment from any side except through the designed opening.

The fire load consisted of the kerosene oil supplied at a constant rate of 1.43x10^{-4} m^3/s through galvanised iron (GI) pipes of diameter 0.254 m. A fire pool was developed using a stainless steel tray of size 1m × 1m × 0.05 m which was positioned at the centre of the floor area. The fuel tray was embedded in the sand with the top of the tray flushed with the sand. The fuel tray was connected to the fuel supply which was maintained at a predetermined fixed head using galvanised iron pipes. In order to avoid the back flow of the oil, which could a major accident, a one way valve was attached to the GI pipe before being connected to the tray. The unutilised fuel from the tray was collected into another tank through GI pipe on the other side of the tray from where it was again transferred back to the source using an electric motor pump. As mentioned earlier both the compartment and the frame were adequately instrumented to capture the gas temperatures and the element temperatures respectively. The compartment was instrumented with the thermocouple trees placed at five different plan locations, each near the four corners and one at the centre. Each thermocouple tree consisted of five 6 mm diameter metal insulated (MI) thermocouples positioned at different heights, of 0.20 m, 0.90 m, 1.60 m, 2.30 m and 2.90 m from the floor level of the compartment, to obtain the thermal profiles inside the compartment.

After damaging the frame by subjecting it to the simulated seismic loading the RC test frame assemblage was exposed to one hour fire. As shown in Fig. 2.36, a full blown fire with a clear flashover was achieved in 4-5 minutes as required in the fire design. In case of the test

reported by Sharma et al (2012) and Kumar (2012) the flashover was achieved within 5-7 minutes, while in case of the test reported by Kamath (2014) the time to attain the flashover was 8-10 minutes. A close agreement of the flashover with the design suggests the robustness of the compartment built for the fire test. The fuel supply was cut exactly one hour after ignition and the data was recorded for the complete heating and cooling phase.

Fig.2.33: The test frame before the fire test with fire enclosure

Fig.2.34: Top view of the frame

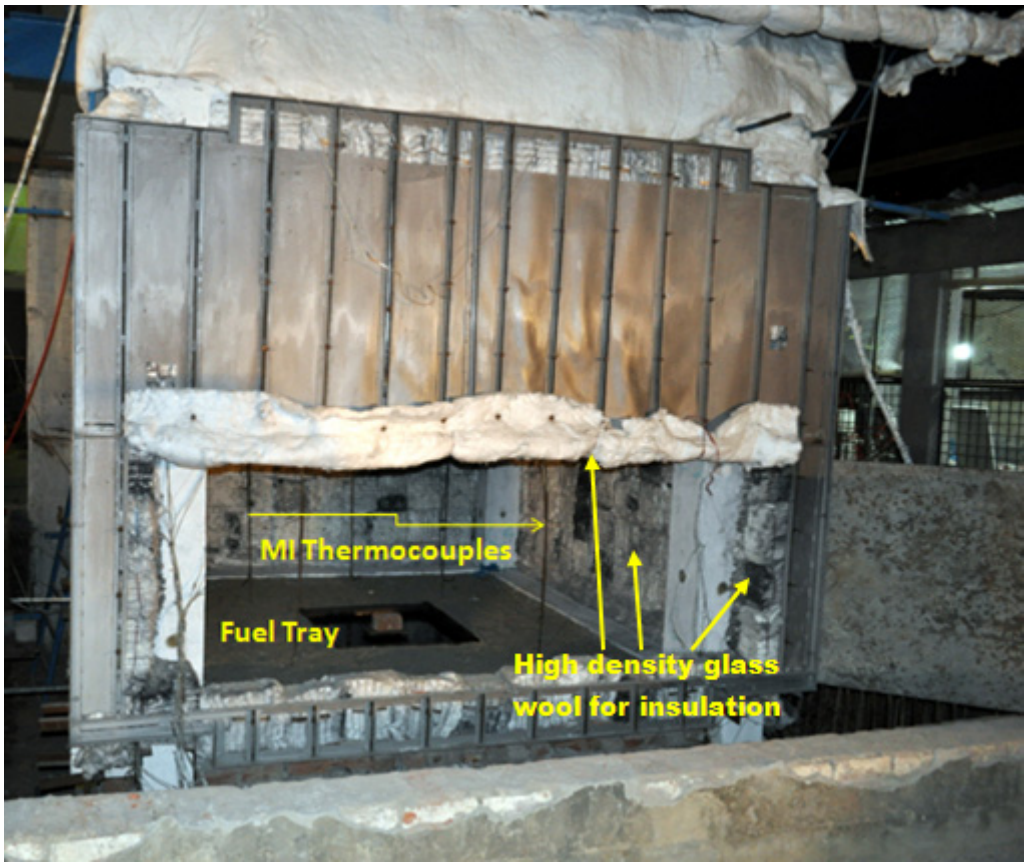

Fig. 2.35: The compartment opening, fuel tray and MI thermocouples inside the fire compartment

Fig.2.36: Attainment of flashover

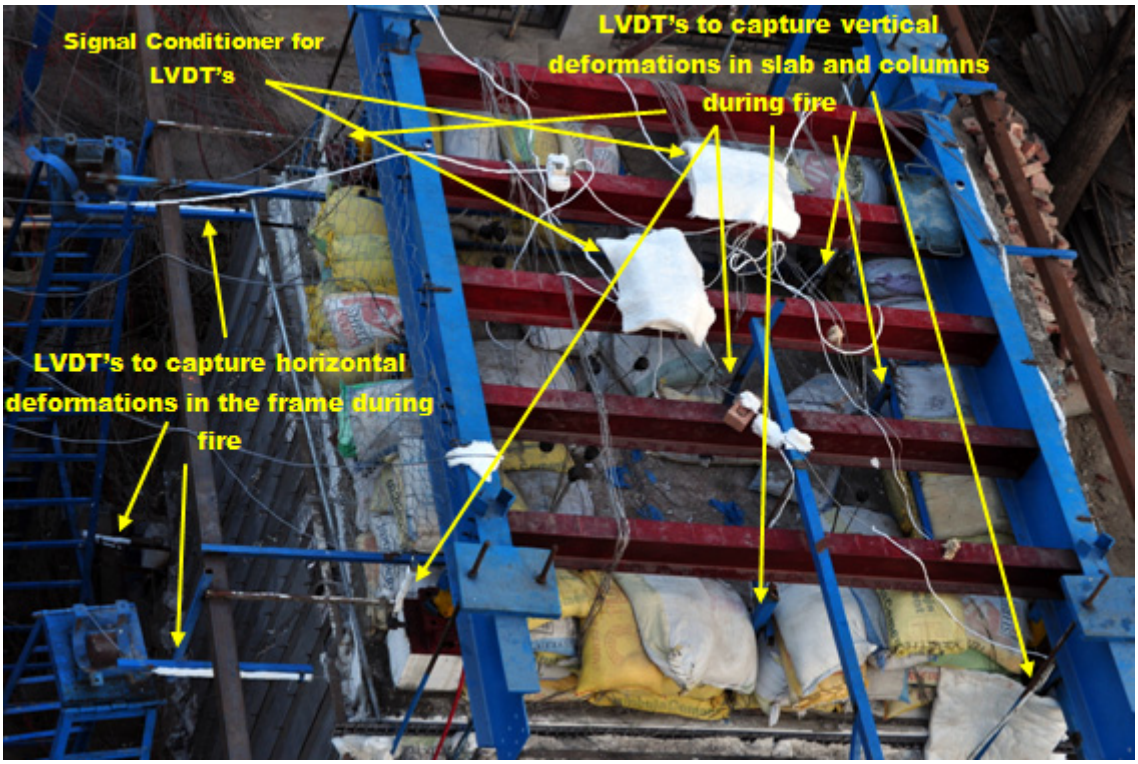

Fig.2.36: Zoomed view of the frame slab showing instrumentation

2.3.3 Results

2.3.3.1 Gas/Compartment temperatures

Fig 2.38 shows the evolution of the gas phase temperatures at the five key locations within the fire compartment. While Figs.2.38 (b) and (c) show an 18 hour log with complete heating and cooling phases, Figs.2.38 (a), (d) and (e) show only the one hour log of the compartment temperature because of the thermocouple trees at these locations got damaged during the course of fire. Figure 2.38 (f) and (g) show the 5 hour log of the compartment temperature to get an insight of the fire behaviour. The ISO 834 time- temperature curve is also shown as a benchmark for comparison with the experimental results. As are the characteristics of a full blown fire and the post flashover fires, the temperature profiles of this compartment fire had three main phases which are:

(a) the growth period, ending with flashover 4-5 minutes after the ignition,

(b) the fully developed fire during which the temperatures crossed the 1300 $^{\circ}$C mark. The behaviour of the fire changed dramatically in this phase due to the flow of air and combustion gases turning very turbulent. The sound of concrete spalling to was clearly audible during this phase. During this period the temperature remained in the range of 800- 1371°C,

(c) fuel supply was cut at 60 minutes, after which the temperatures decayed and the fire was left to extinguish on its own.

During the course of fire, considerable spatial variation in gas temperatures and the incident heat fluxes across the surfaces of different structural elements was seen. The variation in the fire spread and the fire flow can be attributed to many factors not limited to the direction of the wind and the fire dynamics.

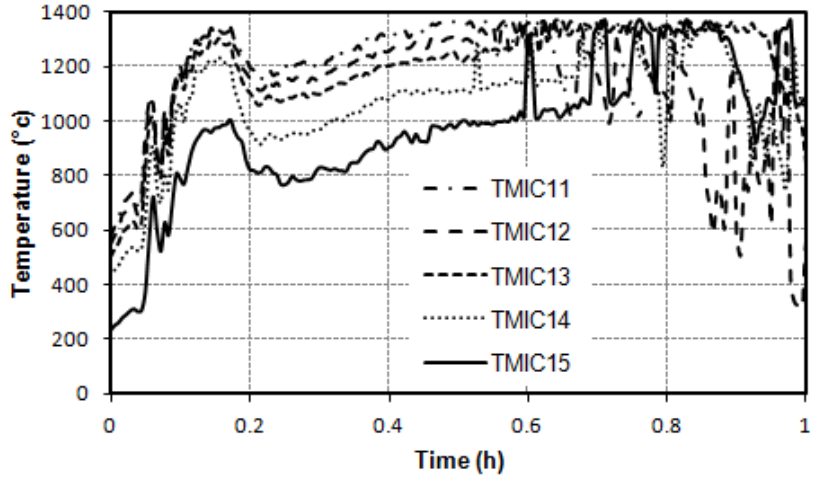

(a)

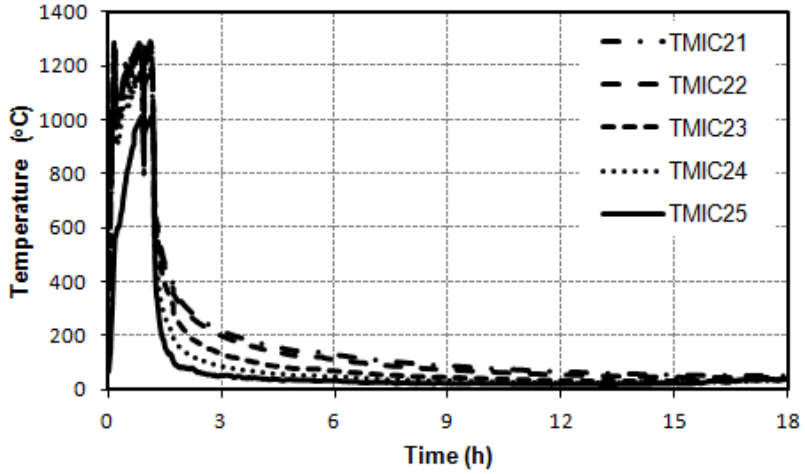

(b)

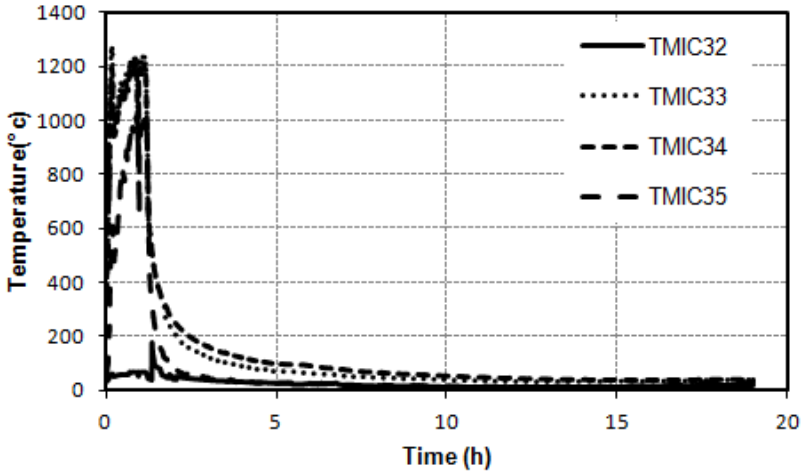

(c)

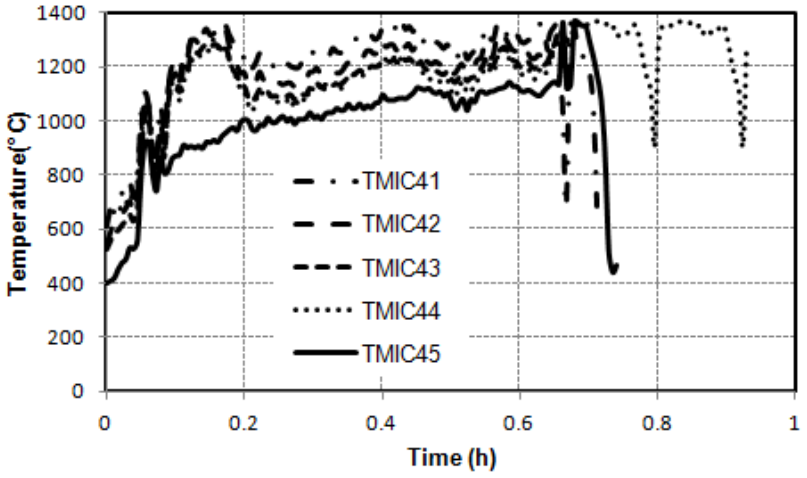

(d)

Fig.2.38: Variation of temperature within the compartment (Contd.)

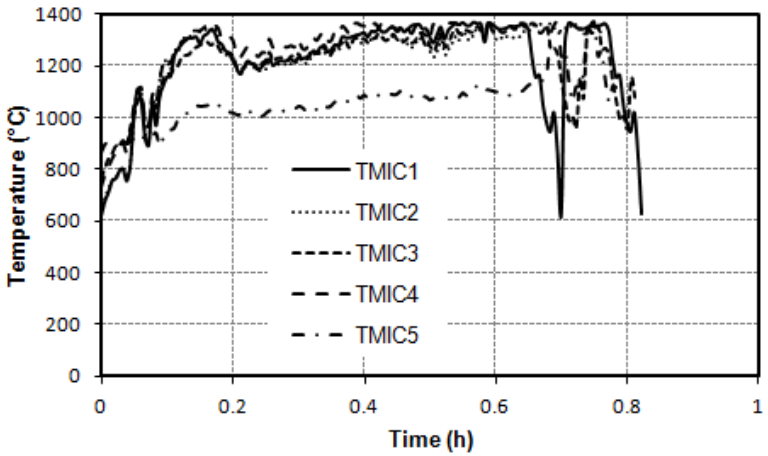

(e)

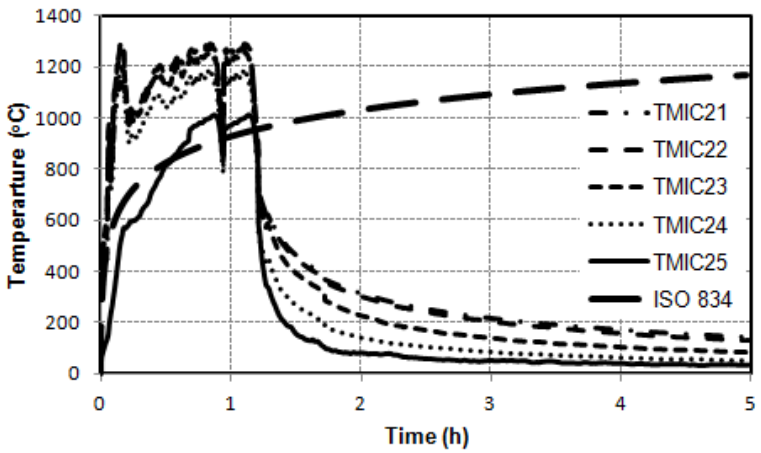

(f)

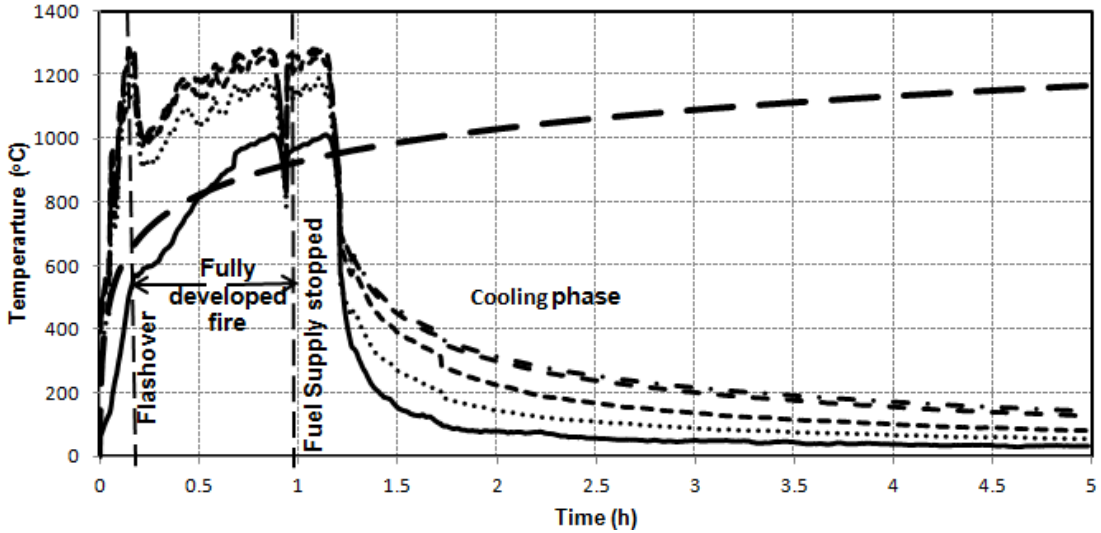

(g)

Fig.2.38: Variation of temperature within the compartment.

2.3.3.2 Observation during and after fire test

The different elements of the RC frame assemblage began to spall within 3 minutes of the fire test. The slab experienced spalling accompanied with intense bullet shot sound heard at 5 minutes. The spalling was quite intense at 6 minutes which corresponded to the compartment temperature of about 1100 $^{\circ}$C. Spalling occurred throughout the first 30 minutes of the fire with clear marked sound of spalling being heard at 6, 8, 12, 14 and 16 minutes after the ignition. The floor of the compartment got filled with the spalled concrete pieces during the fire as shown in Fig.2.39. It was also observed during the fire that the gravity loads on columns C1 and C2, which was applied through the hydraulic jacks kept atop the columns, increased from 10 ton to a maximum of 13 ton at 7 minutes after ignition.

Fig.2.39: Spalled concrete from the elements of the frame during fire

The structure was inspected after the test to have an idea about of its global performance and the behaviour of the different structural elements during fire. The column C1 was found to have numerous thermal cracks throughout its length with even the sintering of the aggregates at some places. The corners of the column were found to be disintegrated. The exposed corner of the upper half portion of the column was completely burnt rendering the column cross section reduced. A 5.5 mm wide crack was measured at the mid height of this column. The concrete had disintegrated with crumbling of the mortar into powder. Fig 2.40 shows the condition of the column C1 after the fire. The column C2, which was just adjacent to the ventilation opening, had undergone thermal cracking with delamination and degradation of concrete. However the cross section of the column was not reduced and no spalling was observed in this column as shown in the Fig 2.41. The column C3 underwent extensive thermal cracking with severe damage at the mid height of the column. The concrete at the mid height was observed to be very loose and delaminated as shown in the Fig 2.42. The column at the mid height had cracked and the crack divided the column section into almost two equal halves. The cracks penetrated deep into the section rendering the exposed corner of the column delaminated and bulged out.

In spite of the extensive thermal cracking and deterioration of the concrete of the columns C2 and C3, the sintering of the aggregate was not found in these columns suggesting that these columns were not directly exposed to the flame for larger periods due to the drifting of the flame away from the opening. Similar kind of behaviour was noted in the columns adjacent to the ventilation in the test conducted by Kumar (2012).

The column C4 was found to have extensively sintered and damaged with the loss of cross section at the mid height. The top half portion of the column had badly sintered and spalled with the corner having a delaminating depth of 110 mm in a length of about 1040 mm as shown in the Fig. 2.44. It is important to note that the portions of the columns, where the cracking and distress was observed during the simulated earthquake load test, underwent more thermal damage compared to the other portions where relatively negligible damage was noted during the initial lateral load test.

The damage observed in various structural elements due to fire was directly proportional to the damage caused to the members in the simulated earthquake load test as well as the fire exposure conditions. The plinth beams were exposed to the fire on one face only and thus the fire damage was minimal in these beams. The beam B1 had no signs of delamination or spalling, however some thermal cracking in the form of surface crazing was noticed. In the beam B2 the concrete cover at the mid-span was delaminated and spalled as shown in the Fig. 2.43. The cover concrete throughout the length of the beam had damaged with thermal cracks. Similarly the mid-span of the beam B3 was damaged by spalling. The cracks which were developed in the earthquake loading test had further aggravated during the fire test causing the delamination and the explosive spalling of the cover concrete as seen in Fig. 2.45. A number of thermal cracks also got developed across the cross section of the beam. Beam B4 was observed to have sintered at top surface however, the sintered material was believed to be from the molten aggregate of the roof beam B8 and the slab.

The beam B5 had damaged with thermal cracks all over the length of the beam. The portion of the beam near the beam-column joint near the column C1 had sintered and spalled. The beam column joint at C1 had already undergone spalling during the earthquake load test, thus exposing the rebars to the direct flame. Spalling of corners was witnessed in beam B6 near the column C2 although there was no damage in terms of sintering of the aggregate. This beam was just at the top of the ventilation window which caused the flame to move towards the opposite side. The thermal cracks and the concrete deterioration had rendered the beam weak. The beam B7 was observed to have spalled with damaged corners. This beam also witnessed

the sintering of aggregates in a length of 1.7 m from the column, where the aggregates had melted as shown in the Fig. 2.46. The beam column joint of the beam B7 near column C3 was already spalled during the earthquake loading with the rebars exposed and buckled also. Thus the rebars got directly exposed to the fire during the fire test as seen in Fig. 2.47. During the fire test the beam spalled at a number of places rendering the reinforcement exposed. The beam B8 was the worst affected in terms of the fire induced spalling and the sintering of the aggregates and the mortar. The cover concrete of the beam had spalled almost all over its length leaving the reinforcement exposed. The sintered and the molten material from the beam B8 was lying on the beam B4. The solidification of the molten material could also be observed as shown in the Fig. 2.48

As evident in Fig.2.49, the roof slab spalled extensively with most of the cover concrete lost exposing the reinforcement. This may be attributed to high temperature gradients across the slab cross section. At some places in the slab, as shown in the Fig. 2.50, the steel reinforcement was observed to have undergone loss in the cross section due to the melting of the steel. The reinforcement being directly exposed to the high temperatures as high as 1370 ^{o}C caused the reduction in the strength of the steel. This phenomenon is important from the safety point of view as this would cause considerable loss in the tensile capacity of the steel and thus the flexural capacity of the slab element. While drawing the attention towards addressing the issues of fire following earthquakes, the melting of reinforcement after spalling of thin elements like slab and shells needs to be considered in design codes. Spalling of depths ranging from 9 mm to 45 mm was observed in the slab. The slab also witnessed the formation of cracks other than those formed due to the mechanical loads. These cracks were mostly with the lines at which the reinforcement in the upper part of the slab was curtailed. The spalling contour of the slab is shown in the Fig. 2.51. The spalling depths in slab were manually measured with the help of a steel scale ruler. The slab was divided into a number of points and the loss of concrete at each point was measured with the help of the steel scale ruler. The loss of concrete was plotted across the slab area and same is reproduced in Fig. 2.51.

Fig. 2.40: Fire damage in Column C1

Fig. 2.41: Fire damage in Column C2

Fig.2.42: Fire damage in Column C3

Fig.2.43: Delamination of concrete cover in beam B2

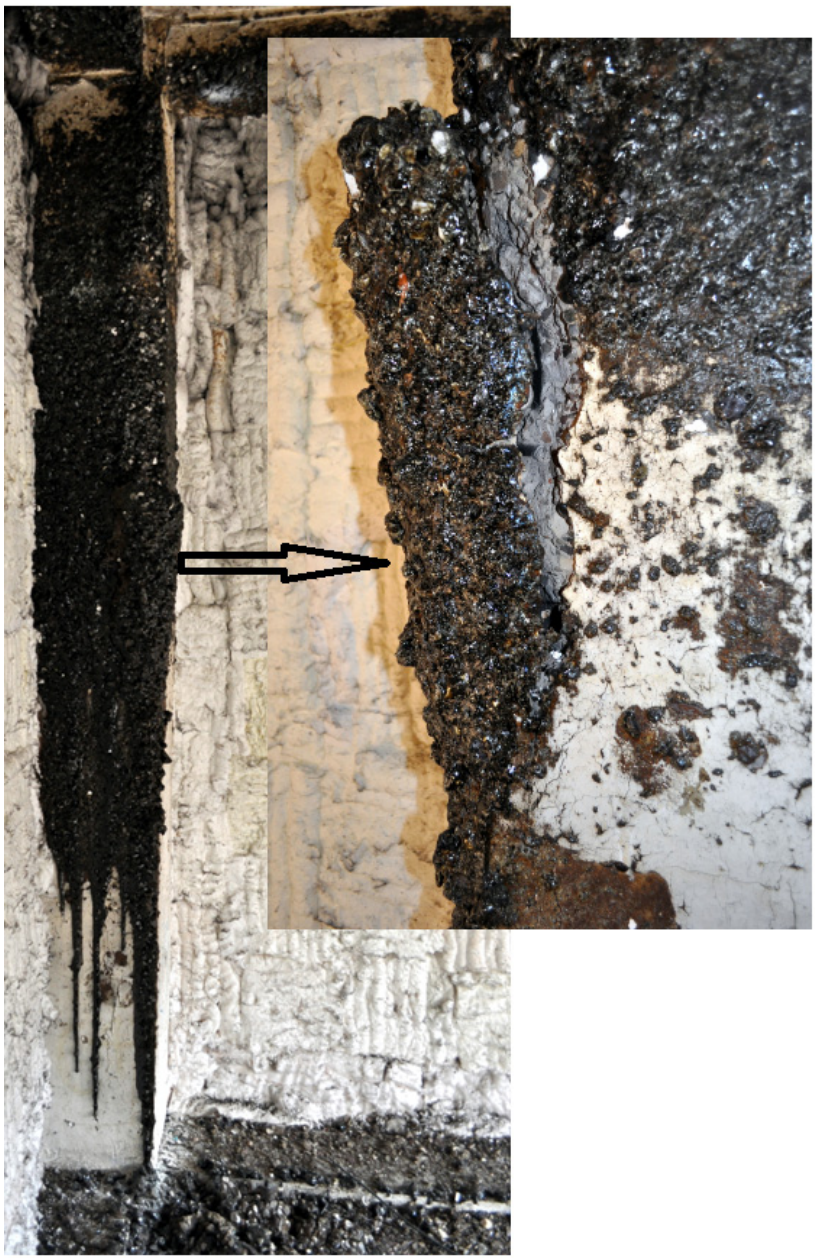

Fig.2.44: Fire damage in Column C4

Fig.2.45: The delamination of the cover concrete in Beam B3

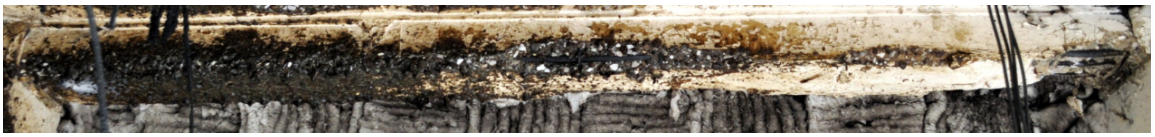

Fig. 2.46: The sintering of aggregate and the spalling in Beam B7

Fig. 2.47: Buckled reinforcement bars (Beam B7) exposed to direct flame

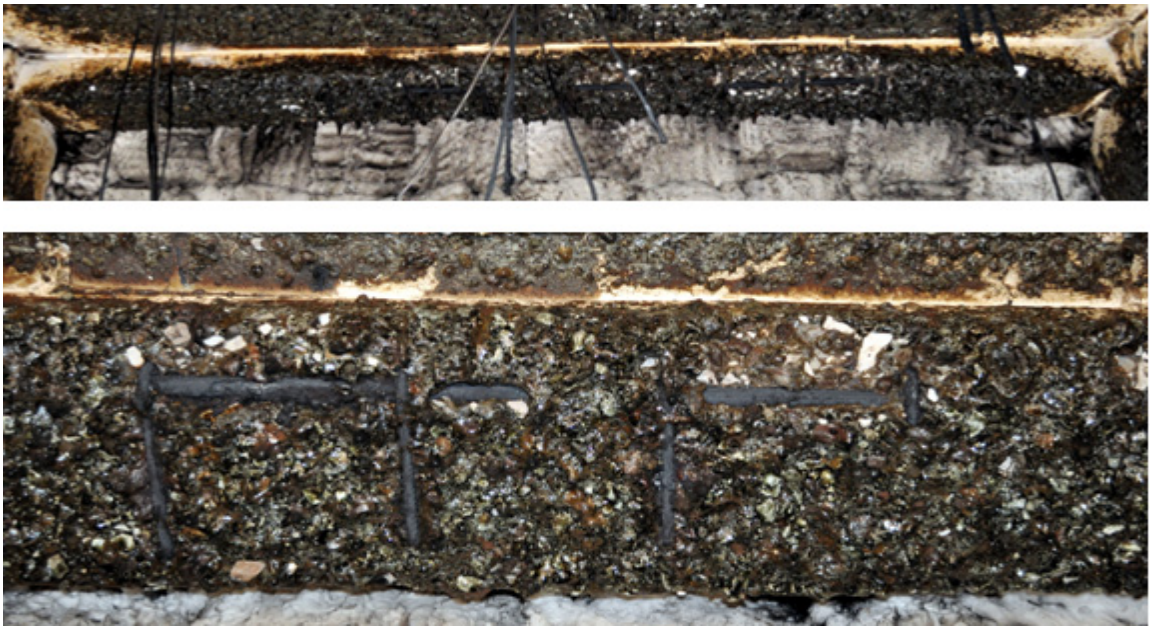

Fig. 2.48: A view of Beam B8 showing sintering and spalling of concrete along the length of the beam

Fig.2.49: Spalling in slab

Fig. 2.50: Reduced cross section of the reinforcement of slab due to fire exposure.

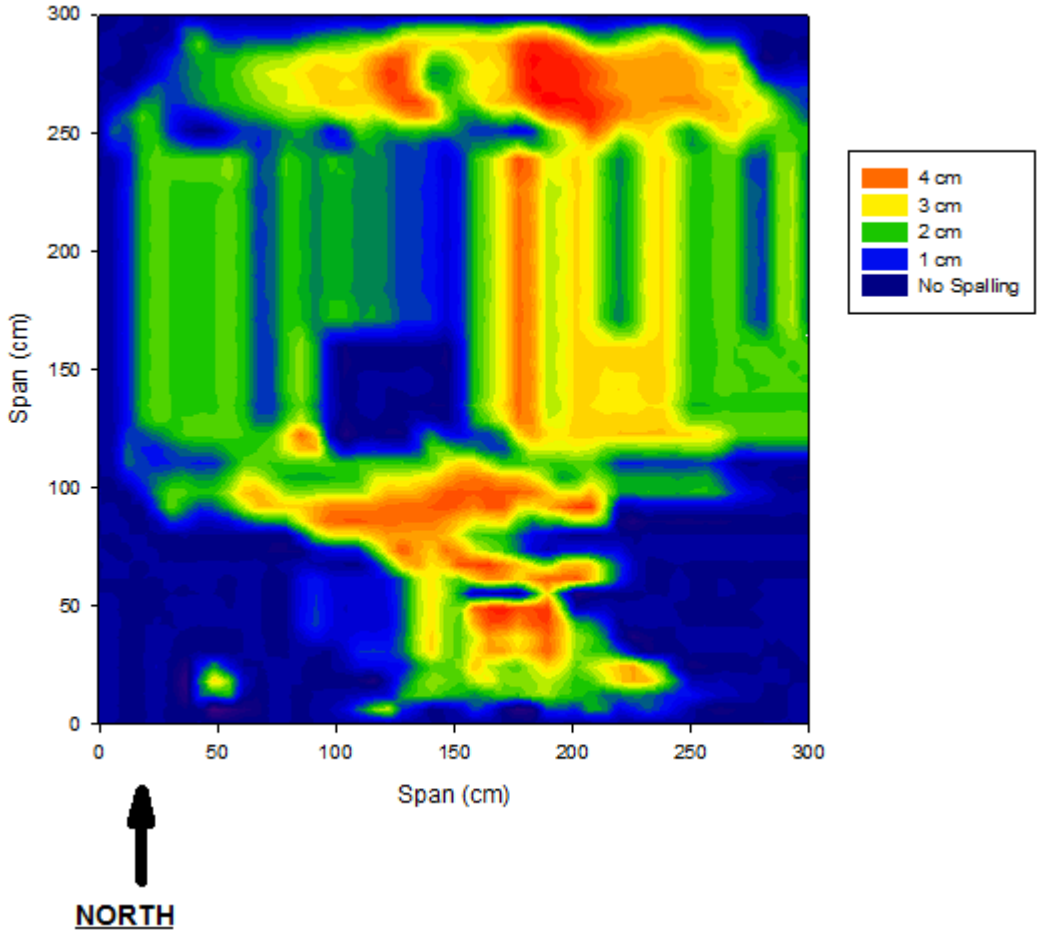

Fig.2.51: The spalling contour map for the slab.

2.3.3.3 Slab deflections

A number of LVDT's were installed to measure the deflections of the slab, beams and columns during the fire test. Fig. 2.52 shows the vertical deflections of the ceiling slab during fire. The figure shows the variation in deflection with time illustrating the deflection profiles of the slab at five locations, both during the heating and the cooling phase. At all the points, except at SC4, rapid downward deflection was observed initially. This phase of deflection is likely dependent on thermal bowing of concrete which is influenced by increasing thermal gradients with time (> 350 ^{o}C) and the resulting differential thermal expansion of the concrete through its thickness. The peak deflection at the centre of the slab (LVDT SC0) was around 21 mm, which recovered to 10 mm after cooling. The peak deflection was measured at a time of about 73 minutes that is about 13 minutes after the fuel supply was cut off. This infers that the temperatures inside the concrete elements reached their maximum values after the fuel supply was cut which is also implied by the temperature profiles of different members. Since the fire duration was long and high temperatures penetrated into the concrete slab, the majority of the

deflections recorded will have resulted from both thermal curvatures as well as from the loss of material stiffness or strength.

The centre of the slab sagged due to the exposure to elevated temperatures and as the temperatures regained to the normal, residual sag of 10 mm was registered at the end of 18 hours. This trend of deflection of slab can be explained on the basis of the concrete deterioration and the load induced thermal straining. This phase of deflection showing the upward deflection of slab can be explained on the basis of the concrete mechanical deterioration and the load induced thermal strains. With the loss in stiffness of concrete, when the temperatures on the exposed soffit of slab ranges from 400 to 500 ^{o}C, an upward movement of the effective neutral axis of bending is possible, which causes the slab to bend upwards (Gales and Bisby, 2014). Moreover, the heat-induced thermal dilation turns partially into unrecoverable (plastic) strain. The layers exposed to the fire during the heating phase become colder than the core (where the temperature is still increasing) in the cooling phase and therefore shrinks, forcing the slab to bend upwards. Since part of the thermal dilation during the heating phase is unrecoverable, it causes a residual displacement after cooling.

The deflections reduced towards the corners as expected. While as a sagging deflection of 3.7 mm was measured at the corner location near column C1 (LVDT SC1) at the time of about 55 minutes, the deflection profile changed and the corner registered a hogging deflection which remained in the slab portion with a maximum hogging deflection of 1.5 mm. However, on complete cooling, sag of about 0.05 mm was registered. This change from sagging to hogging can also be attributed to the formation of the hogging cracks in the slab. The hogging deflection at the corner can also be attributed to the axial deformation of the columns. The column C1, as shown in Fig. 2.51, expanded axially by about 2.2 mm during the fire which got manifested in the nearby slab region also. Similar behaviour was seen at the deflection point near column C2 (LVDT SC2), where a kink in the deflection profile indicates the formation of another hogging crack. A maximum sagging deflection of 3.2 mm was measured before the deflection pattern changes and a permanent hog of 1.58 mm was registered upon cooling. The LVDT SC3 installed at the deflection point near C3 recorded maximum sag of 2.5 mm, however during the cooling stage. This unexpected behaviour picked up by the LVDT can be an experimental anomaly. The deflection profile captured at the deflection point near column C4 (LVDT SC4) exhibited a trend opposite to both C1 and C2 columns. An initial hog of about 1.02 mm was registered during the early stages of the fire. At about 56 minutes the deflection profile changed and slab started to sag. Till the end of data logging the slab registered a sag of 3.13 mm at this point near column C4. This can be attributed to extensive spalling and sintering

of the slab at this location. A spall depth of about 40 mm was measured at this location, which would have caused this type of behaviour. While drawing the attention towards addressing the issues of fire following earthquakes, the melting of reinforcement after spalling of thin elements like slab and shells needs to be considered in design codes.

2.3.3.4 Axial Deformations of columns

All the columns were instrumented with LVDT's to measure the axial deformation during the fire test. The columns were extended above the slab and above each column an insert plate was cast during the construction stage. LVDT's were placed on the steel insert plates during fire to capture the deflections. The LVDT's were properly insulated to avoid any damage due to fire as shown in the Fig.2.37, yet the LVDT mounted on column C2 malfunctioned during the test and the axial deformation for this column could not be captured. The axial deformations as measured by other LVDT's are shown in the Fig. 2.53. All the four columns underwent thermal expansion as the temperatures increased. The column C1 and C4 can be seen to have experienced the thermal expansion of 2.27 mm at 46 minutes after the ignition. In the cooling stage the columns seem to come back to normal before undergoing the decrease in length. The net decrease in length at the end of 18 hours is 2.3 mm in column C1 and 1.65 mm in column C4. The increase in the loads on the columns during the fire can be attributed to this behaviour. The column C3 attainted an expansion of about 8 mm at 58 minutes after ignition, which on cooling decreases and the ultimate expansion of 1 mm was registered in the column C3 at 18 hours. This expansion of the column in early stages is due to the thermal expansion of concrete and the steel bars and in the later stages, the columns contract because of the deterioration of the material's mechanical properties.

2.3.3.5 Beam vertical deflections

All the roof beams were instrumented with LVDT's at the midpoint to capture their behaviour during fire. The vertical deflections of the beams B5, B6, B7 and B8 are shown in Fig. 2.54. These deflections profiles show the variations of deflection of the midpoints of the beams with the time. Each of the three beams B5, B6 and B8 had initial downward sag corresponding to the thermal expansion of concrete and steel bars. The deflections in beams recover as the temperatures decrease and the deterioration of concrete sets in. The beam B5 had a maximum sag of 1.05 mm and the maximum hogging deflection of 1.5 mm. The Beam B6 experienced a sag of 5.5 mm and it finally recovered to have a permanent hogging deflection of 7.19 mm. The Beam B7 underwent an initial sag of 1.05 mm during the temperature build up

stage and had a maximum hog of 6.8 mm. In the case of beam B8, unlike other beams the initial sag was absent and the beam is bent upwards with a deflection of 5.3 mm. This complex behaviour is due to the interaction the beams with the columns. Due to their different thermal responses, beams and columns framing together in structures are constrained from free elongation when a localised fire occurs. The axial restrain plays an important role in the behaviour of the framing elements like beams and columns. The larger deflections of the beam B7 and B6 can also be attributed to the larger thermal expansion of the column C3 which caused the beams B6 and B7 to hog upwards by a larger value.

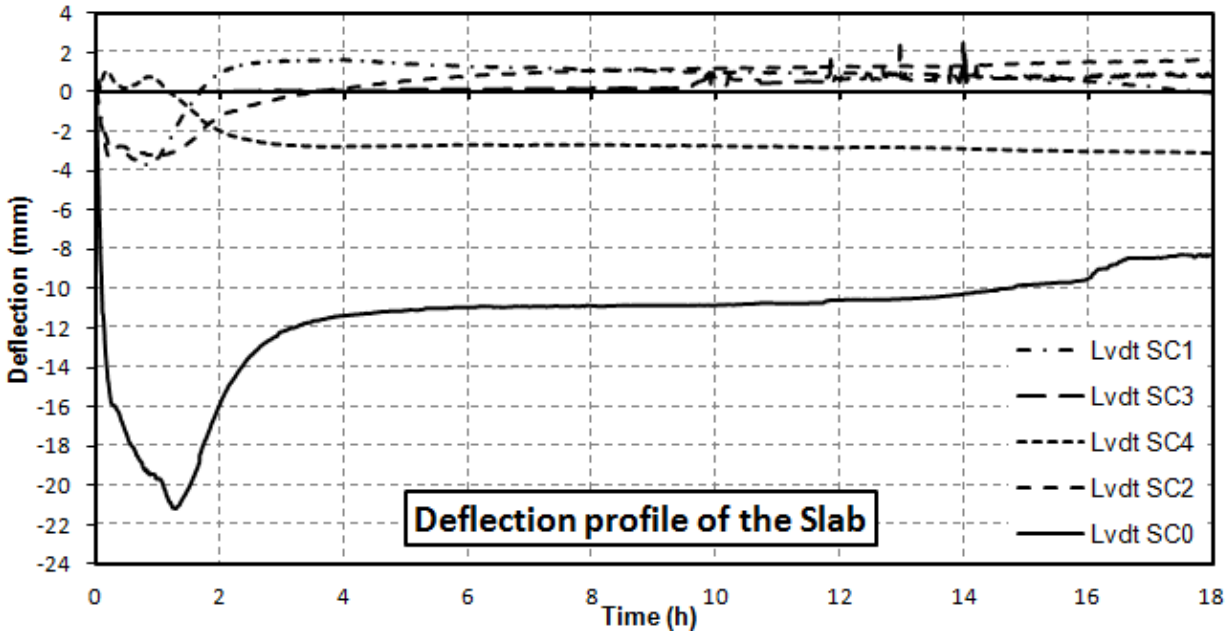

Fig.2.52: Deflection profile of the slab in fire

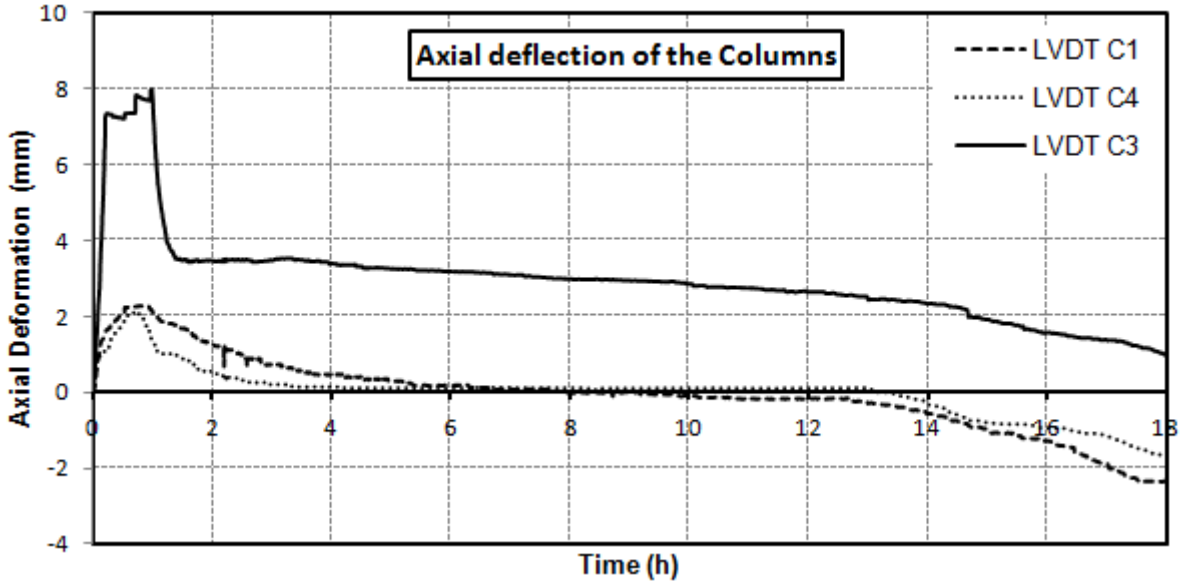

Fig.2.53: Axial deformations of the columns of the frame in fire.

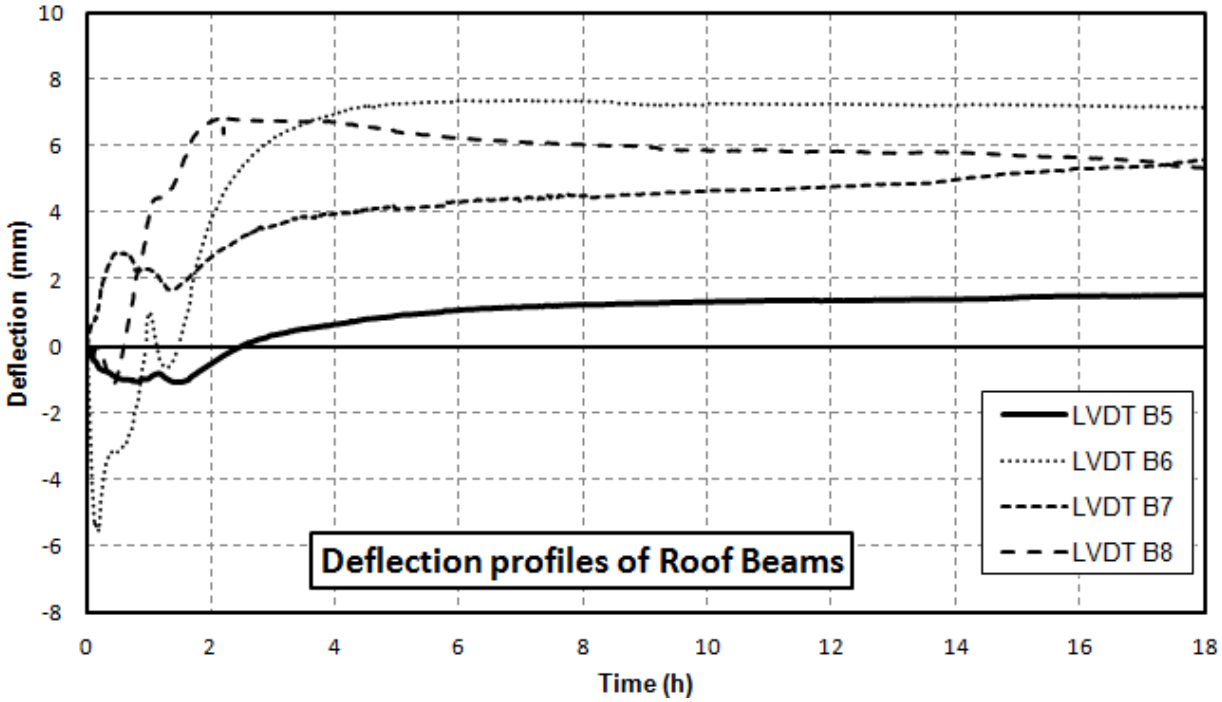

Fig. 2.54: The deflection profiles of the roof beams in fire.

2.3.3.6 Thermal strains

Figs. 2.55 to 2.59 show the variation in the strains with time as recorded during fire. As mentioned earlier strain gauges were attached to the reinforcement at different locations in all the structural elements. The strains in the structural members resulted from two phenomena: thermal expansion of the heated rebars and deformation of the surrounding members. Each surrounding element not only experienced thermal deformation, but also restrained the deformation of the corresponding element. Although strain gauges were encapsulated in high temperature protective coatings, very few gauges survived the high temperature and logged the strains. It is observed that the strains increased rapidly during the heating phase and the locations where the sharp increase in temperature was seen also showed a sharp increase in strains. In column C1 at its mid height on the exposed face (C1ME) the strains reached a maximum value of 2115 micron at 1.02 hours which is also the time when the temperature was maximum here. The strains increased due to the thermal expansion of the rebars and showed a declining trend due to the axial restraint and the cooling of the rebars. The strains measured on the unexposed face at mid height in column C1 (C1MU) (as shown in Fig. 2.55 (c)) also showed similar trend with a sharp increase in the strains till 1 hour where the maximum strain value of 1335 microns was registered. The strains decreased subsequently due to decrease in the temperature until the time 13 hours from the ignition at which the strains increase first with a sharp gain until the value again reaches 1163 microns at 18 hours. This unexpected increase in

the strain value can be attributed to the decrease in the length of the column as shown in the Fig.2.53. Around this time the column C1 experienced a reduction in its original length due to the thermal contraction in the cooling phase causing the strains to increase. Also this may be attributed to the restrained thermal effects of the column. In the strain plot shown in the Fig 2.55 (a) the rebar towards the exposed face in column C1 at the bottom section (C1BE), the strains change from tensile to compressive which may be primarily due to the bending moments induced by the beam at the beam column joint. Figs. 2.55 (d) and 2.56 (a) show the strain time plot in column C4 at top (C4TE) and mid height (C4ME) respectively. The strains increased as the temperature increased due to the thermal deformations.

Figs. 2.56 to 2.58 show the strain time plots for different beams. Higher strain values were registered in some of the plinth beams as well as in the roof beams. These higher values of strain can be attributed to the thermal effects caused by the higher temperatures attained by these elements. Figs. 2.58 (d) and 2.59, show the strain development in roof slab. It can be observed that strains increased and then decreased changing into compressive strains. The compressive strains then increased till the strain gauge underwent de-bonding (SC1D1, SC3D1). The large compressive strains recorded on the top of the slab were dominated by geometrical compatibility with the surrounding elements and due to the internal self equilibrating stresses created due to the thermal profile through the depth of the slab.

The general trends captured by the strain gauges are always difficult to interpret. Some results might at first seem anomalous, but are the result of non-uniform heating, complex boundary conditions and the extensive cracks present in these structural elements. Also the use of more reliable high temperature strain gauges, which are very expansive, was not in the scope of the budget allotted to the project. In the future tests it is recommended that indirect means of strain measurement, namely, digital image correlation may be used to trace the development of strains in the structural members of an RC framed structure during the event of fire. However, it is a challenging task since the smoke from fire and the hazing effect from high temperature may interrupt clear view or the image resolution of the demarcated area of focus.

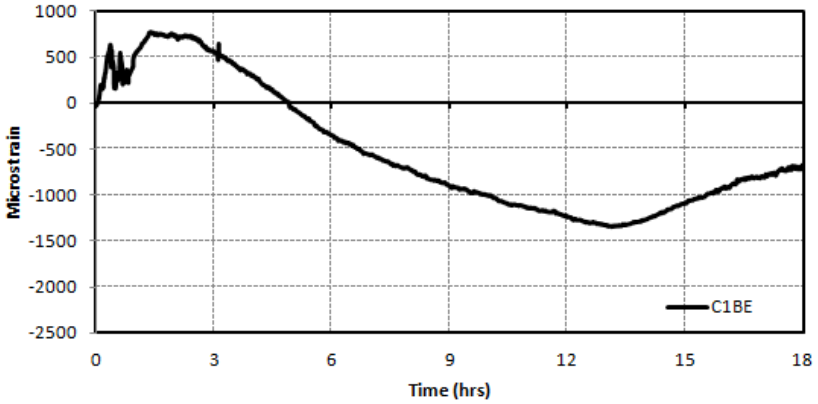

(a)

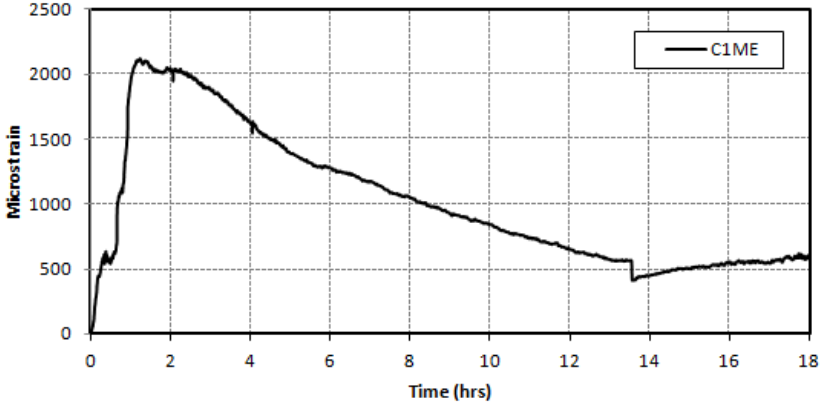

(b)

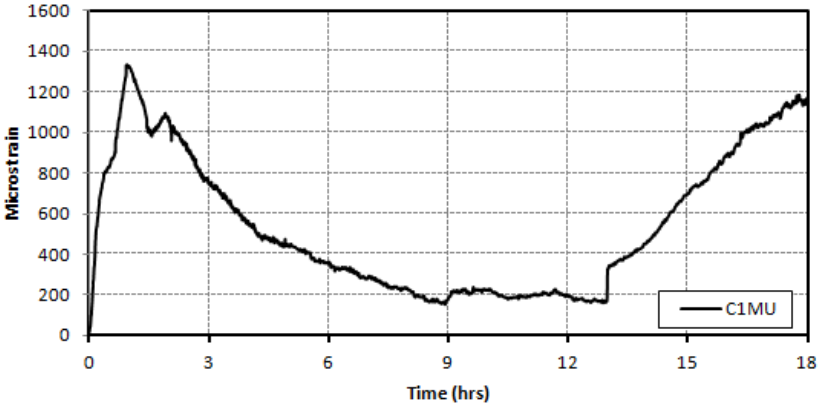

(c)

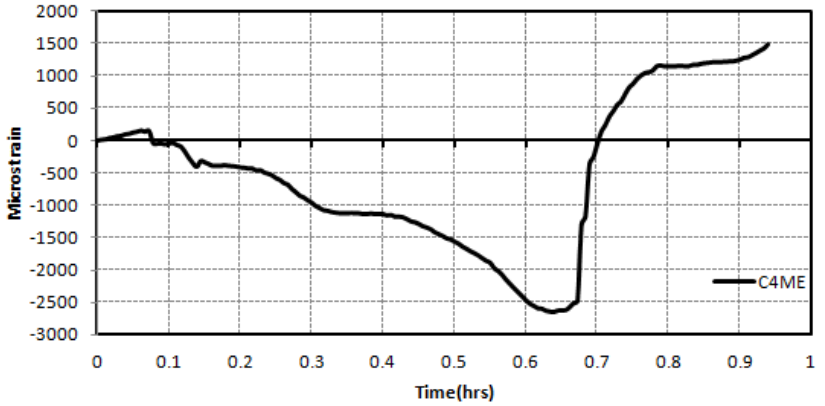

(d)

Fig. 2.55 (a)-(d): Thermal strains in Columns

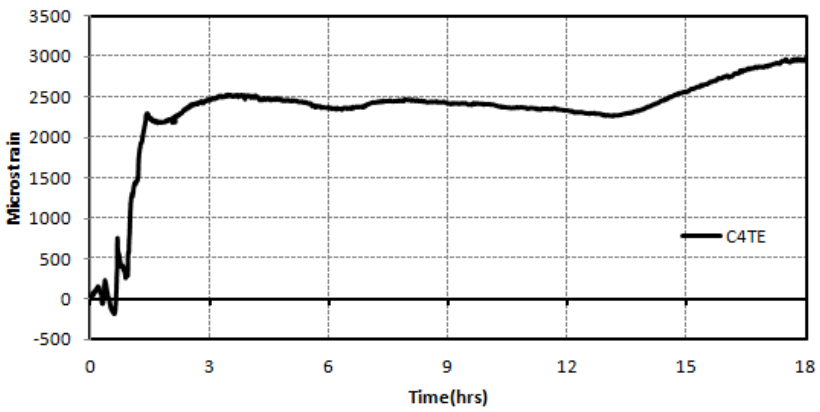

(a)

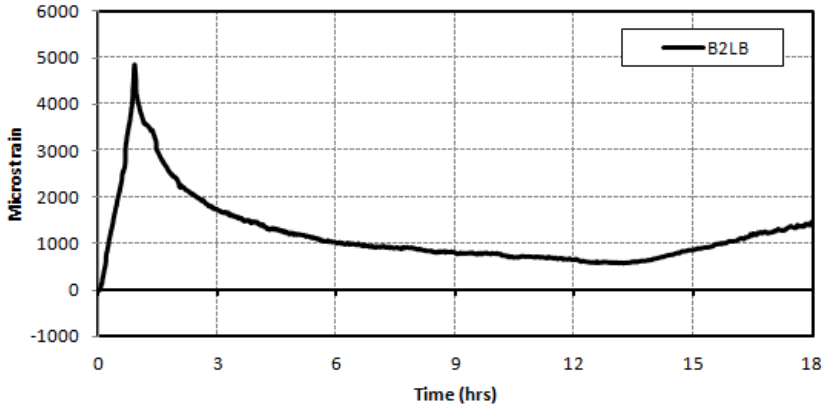

(b)

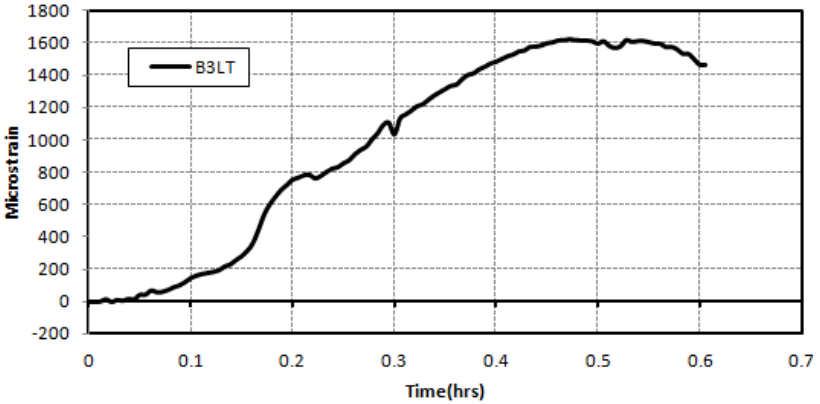

(c)

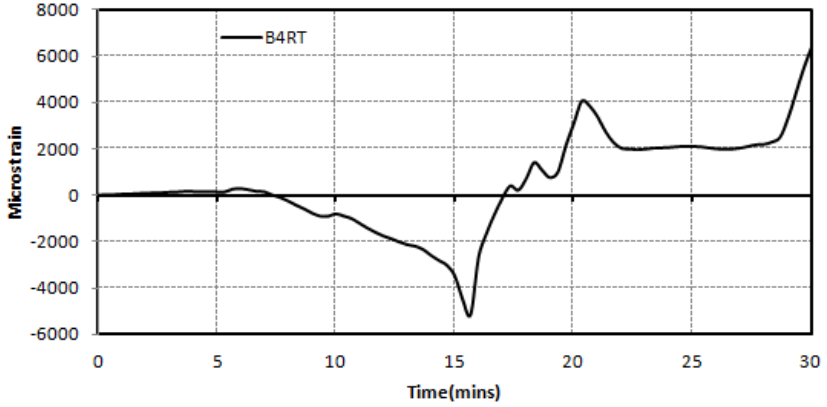

(d)

Fig.2.56: Thermal strains in (a) Column C4, (b) - (d) Beams

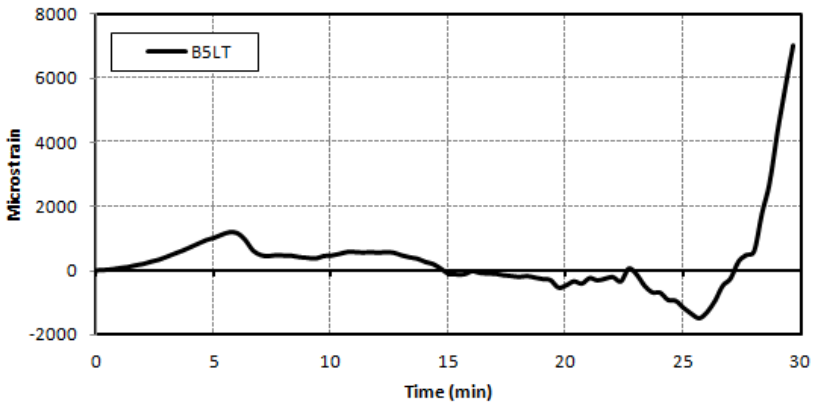

(a)

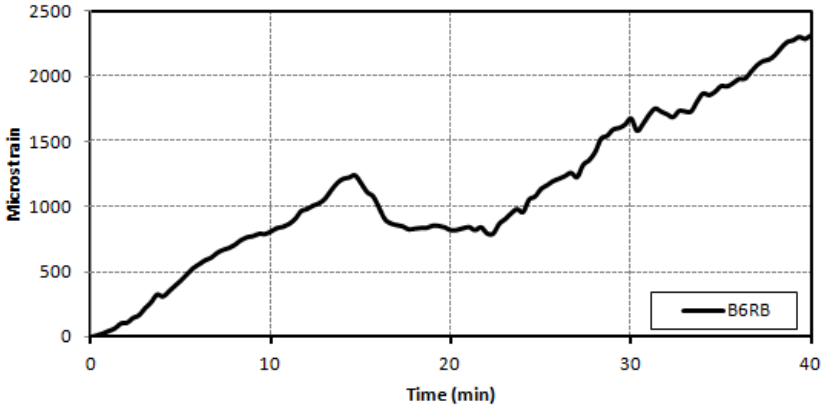

(b)

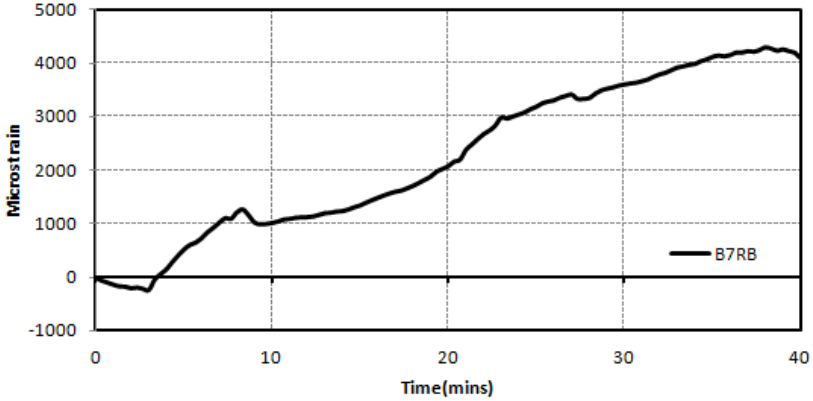

(c)

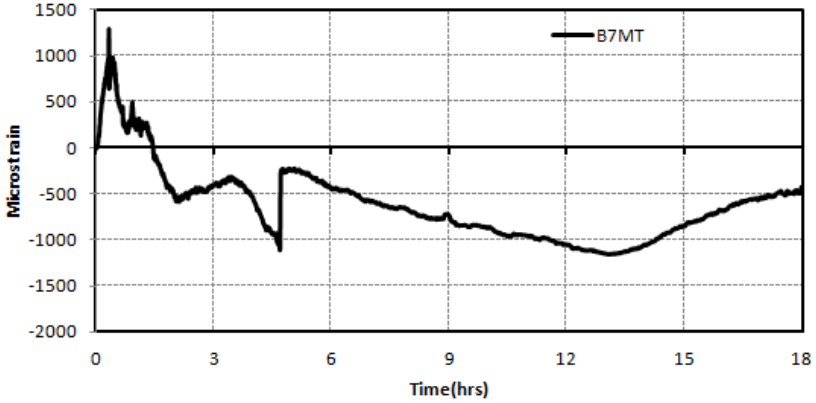

(d)

Fig 2.57 (a) – (d): Thermal strains in Beams

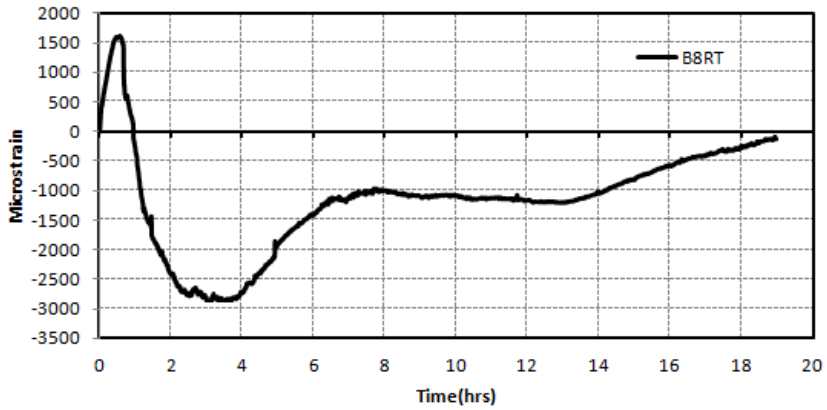

(a)

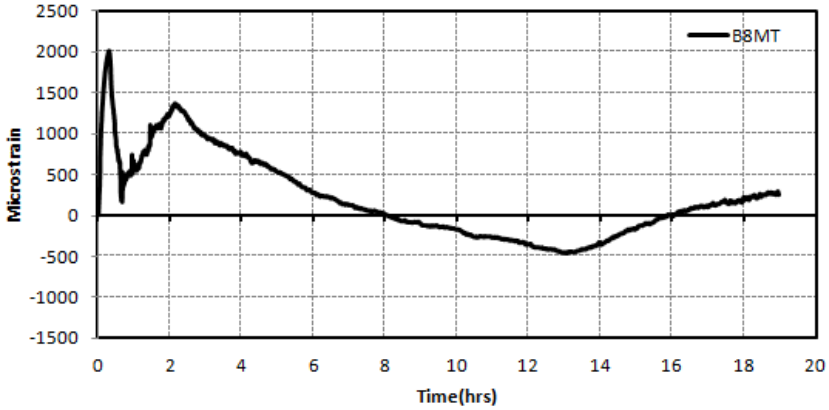

(b)

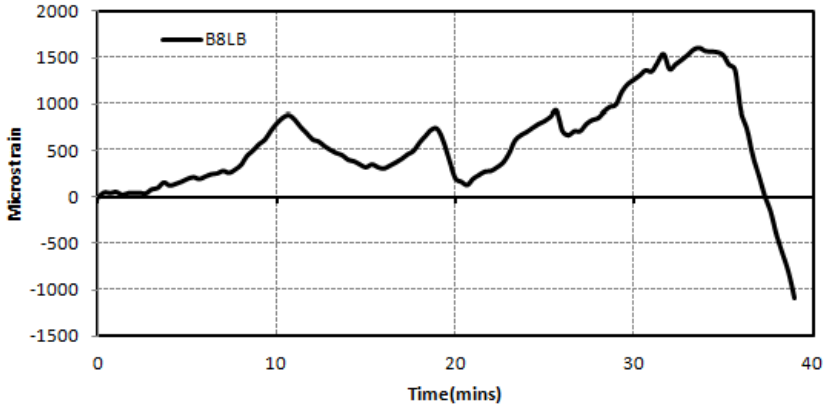

(c)

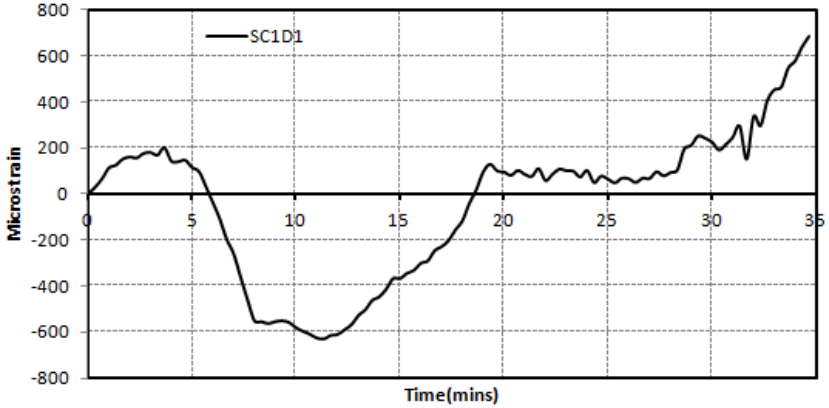

(d)

Fig. 2.58 (a) –(c): Thermal strains in Beams (d) Slab

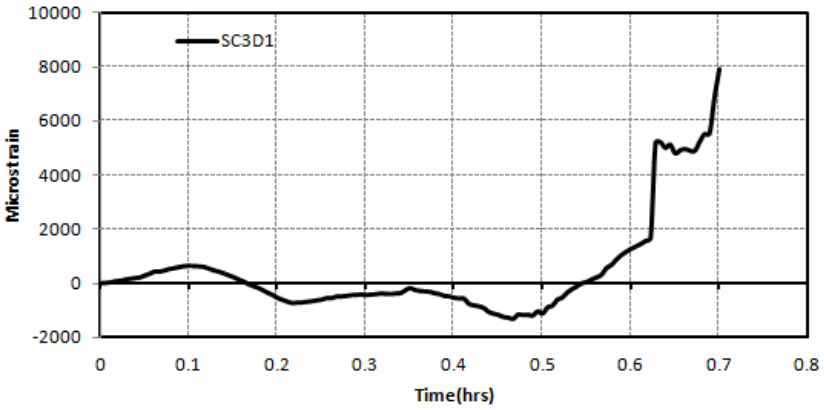

Figure 2.59: Thermal strain profile in slab.

2.3.3.7 Temperature Histories of the Various Structural Elements

In order to record the temperature profiles as developed in beams, columns and the slab, thermocouples were embedded in the concrete while casting. The temperatures were recorded at five sections each in beams and columns and at nine sections in slab as shown in Fig.2.6. Each section in plinth beams was instrumented with three thermocouples along the depth at 25 mm, 115 mm and 205 mm from the exposed face. In case of columns the thermocouples were embedded along two directions, both depth wise and breadth wise. The sections were instrumented with three thermocouples along the depth at 40 mm, 150 mm and 260 mm and two thermocouples along the breadth at 40 mm and 150 mm from the exposed faces. This was done to record temperatures along both the exposed faces of the columns. Each section in the roof beams was also instrumented with five thermocouples, three along the depth and two along the breadth at 25 mm, 115 mm and 205 mm. Nine points were chosen for instrumentation for measuring the slab temperatures. Each section was instrumented with three thermocouples along the depth at 30 mm, 60 mm and 115 mm from the exposed surface.

The recorded temperature data is presented to understand the thermal behaviour of the RC test frame assemblage.

2.3.3.7.1 Plinth Beam temperatures

Fig. 2.61 (a) - (t) shows the thermocouple readings from within the plinth beam B1, B2, B3 and B4 along the depth of the beam at different sections. The maximum temperature in the concrete members was achieved at the time when the fuel supply was cut. The profiles showed a clear increase in the temperatures to a distinct peak value which was followed by a gradual decrease in the temperature during the cooling phase. As expected the thermocouples embedded near the surface registered higher temperatures. The maximum temperature in beam B1 was measured to be 1200 ^{o}C by the thermocouple embedded at 25 mm from the surface at left

quarter section (TB1LQD1). This unexpectedly higher temperature may be attributed to the direct exposure of the thermocouple due to the damage caused at this place during the seismic load test. The plinth beam B2 attained relatively lower temperatures than the other three plinths beams with the maximum temperature of 328 ^{o}C measured by the thermocouple embedded at 115 mm from the surface at the right quarter section (TB2RQD2). The relatively lower temperature built up in the plinth beam B2 can be attributed to two main factors; (a) being adjacent to the compartment opening the beam B2 was not exposed to the flame for longer durations as the air inflow through the opening caused the flame to drift away from the beam B2 and (b) the beam B2 being perpendicular to the axis of loading witnessed very less damage in terms of concrete cracking and spalling during the simulated earthquake loading and thus the penetration of heat through the cracks was restricted in this beam. It is noteworthy that the effect of the later in experiencing lower temperatures is lesser than the former as is exhibited by the higher temperatures in beam B4 even though the damage in this beam was also very less due to its position.

The plinth beam B3 underwent very high exposure which was indicated by the temperatures measured by the thermocouples embedded in the beam B3. While as a temperature of 960 ^{o}C was registered at left quarter section (TB3LQD1), a temperature of 1184 ^{o}C was recorded at middle section (TB3MD1). At the right section (TB3RD1) also a high temperature of 1180 ^{o}C was recorded. The high temperature build up can be attributed to the penetration of the heat through the wider cracks and the spalled cover concrete. Further, the temperature increases from the left to the right section which is due to the drifting of the flame towards the right hand section of the beam.

The maximum temperature attained in plinth beams was recorded in beam B4 which was positioned just opposite to the compartment opening. A temperature of 1355 ^{o}C was measured at the right section of the beam. It is to be noted that at this section the beam achieved very high temperatures in its almost entire depth at 48 minutes. At 50 minutes the temperatures recorded at 25 mm, 115 mm and 205 mm were 865 ^{o}C, 1257 ^{o}C and 1280 ^{o}C respectively at right hand section (TB4RD1, TB4RD2, and TB4RD3). It is also important to note that the temperatures of the exposed surface of the beam dropped after the fuel supply to the fire was stopped however the temperatures inside the beam continued to increase. This is due to the fact that the rate of heat transfer inside the concrete gradually increases with time. The temperature development is dependent on many factors with the ventilation and the flame drift having a major contribution. This can be gauged from the fact that the rate of temperature increase was much higher in beam

B4 than the other beams with the maximum temperatures throughout the length of beam B4 being achieved earlier than in other beams.

2.3.3.7.2 Column temperatures

Fig. 2.60 (a) – (r) shows the temperatures recorded at various sections within the columns along their lateral dimensions. The position of thermocouples is shown in the Fig 2.6. As expected, the temperatures at locations farther from the exposed surface were lower than those closer to the exposed surface. As in the case of plinth beams the temperature rose till the fuel supply was cut after which the temperatures decrease gradually. In column C1 the maximum temperature recorded was 441 ^{o}C in the top quarter section (TC1TQP1) at 40 mm from the exposed surface. As shown in Fig. 2.60 (d) at 60 minutes when the fuel supply was cut the temperatures of the concrete layer at 40 mm started decreasing till it again increased to reach the maximum. This phenomenon can be attributed to the gas temperature variation and the concrete thermal conductivity. As the fuel supply was stopped the gas temperatures decreased which was captured by the thermocouples placed in the cover concrete. However due to the thermal conductivity of the concrete the temperatures of the layers inside increased as the heat penetrated inside which is shown by the kinks in the plots. Another aspect to be noted in column C1 is the occurrence of the spalling. During the post fire inspection the column C1 was seen to have spalled extensively which cannot be explained on the basis of the maximum temperatures attained in the column. After closely inspecting the temperature plots it can be seen that the difference in the temperature between the cover concrete and the core concrete, in the heating stage and some part of the cooling stage, is very large which gave rise to higher thermal gradients. This huge thermal gradient caused the cover concrete to undergo spalling.

The column C2 witnessed relatively higher maximum temperature at the mid section with the maximum temperature being 995 ^{o}C (TC2ML3) at 58 minutes just before the fuel supply was stopped. Apart from this section, the other instrumented portions of the column witnessed the temperatures between 350 to 500 ^{o}C which is also reflected by the type and extent of damage as shown in the Fig. 2.40. The spalling in column C2 was low which was also manifested by the lower temperature gradients along the depths of the sections.

In case of the column C3 only 9 of the 25 thermocouples could give reasonable data. The temperatures at the mid section could not be recorded which could be due to the damage to the thermocouples due to spalling and cracking of the section. The irregular plot (TC3TQP1) can also be attributed to spalling and cracking in the top quarter section. The maximum temperature recorded in the column was 716 ^{o}C at 48 minutes from the ignition at the top quarter section. It can be anticipated from the damage at the midsection that the temperatures would have crossed

the 1000 °C at the mid-section however unfortunately could not be captured due to the malfunctioning of the thermocouples. The irregular time temperature curves registered in column C4 can be attributed to heavy spalling experienced at the various sections of the column as shown in Fig. 2.44. The maximum temperature was measured to be 622 °C at the top quarter section (TC4TQL1).

2.3.3.7.3 Roof Beams

The time- temperature distribution curves along the two lateral directions of the roof beams (B5, B6, B7, and B8) are shown in Fig. 2.62 (a) – (t). In Beam B5 it can be seen that the temperature build up varied from highest at the left end which decreased towards right. A maximum temperature of 565 °C was recorded at 60 minutes at a depth of 25 mm from the exposed face at the left end of the beam (TB5LD1). While as a temperature of 523 °C was measured at the midsection (TB5MD1), it reduced to 382 °C at the right end section of the beam. The results indicate that the temperature build up was influenced by the presence of pre-damage in terms of cracks in the end regions of the beams and also the location of the sections relative to the fire source and the compartment opening. The left end section of the beam was damaged during the simulated earthquake loading and thus the hot gases and the flame directly penetrated inside the concrete section causing the rise in temperature. Moreover, the direction of flame also has the effect on the temperature build-up in the beam. The flame and the hot gases were directed towards the left end due to the ventilation opening, which also contributed to high build up of temperatures in the beam sections towards the left end. Another thing to be noticed is that at a section the outer layers reached their maximum at around 60 minutes. This is the time when the fuel supply was stopped. The temperature for inner layers of the concrete sections went on increasing and the maxima were achieved after 120 minutes. In some cases the temperature inside the concrete reached to the maximum at 225 minutes (TB5RQD3, T_{max}= 138°C). This phenomenon is due to the thermal conductivity of the concrete and the heat penetration inside the concrete section didn't stop even after the fuel supply is stopped.

The beam B6 was positioned directly above the ventilation opening in the fire compartment. A maximum temperature of 626 °C was measured in left quarter section (TB6LQB2) of this beam. The beam B6 didn't spall much due to the low thermal gradients noted in this. While as a maximum temperature of about 350 °C was recorded at the left section (TB6LB1), the midsection of the beam witnessed a maximum of 431 °C at 115 mm from the exposed face.

The beam B7 witnessed a very high rise in temperatures. The maximum temperature recorded in the beam was 863 °C recorded at 25 mm (TB7LD1) from the exposed face at the left end section of the beam. This section was heavily damaged during the simulated earthquake loading and witnessed mechanical spalling. The reinforcement bars at this section (Fig.2.47) got buckled and exposed during the mechanical loading phase. Thus the bars at this section got directly exposed to the high temperatures during the fire test. The right end sections were also exposed to high temperatures to the level of 555 °C (TB7RB1). However at the midsection of the beam relatively lower temperatures were measured. The maximum temperature recorded at the midsection was 397 °C (TB7MB1). The occurrence of high temperatures in the left end and the right end regions of the beam also prove the direct influence of initial damage on the temperature build up in the structural elements.

Beam B8 witnessed very high temperatures in all its five instrumented sections. A maximum temperature of 959 °C was measured at 25 mm from the exposed face at right end section (TB8RD1). At midsection the maximum temperature went up to 863 °C where as the maximum temperature recorded at the left quarter section was 630 °C. Beam B8 was worst hit in terms of spalling and thermal deterioration which rendered the reinforcement exposed to the direct flame thereby causing the melting of the steel reinforcement. The beam was found to be sintered throughout its length.

2.3.3.7.4 Roof Slab

The maximum temperatures as recorded at the nine instrumented locations of roof slab along the depth are shown in Table 2.8.

Table 2.8: Maximum Temperatures and temperature gradients in Slab

Member	Maximum temperature gradient (ºC/mm)								
	TSC1	TSC2	TSC3	TSC4	TSB5	TSB6	TSB7	TSB8	TSC
Slab	19.36	3.8	5.4	15.73	8.53	15.1	15.03	14.99	11
	Maximum Temperatures (ºC)								
	845	298	365	790	656	925	834	626	769

The time-temperature curves for the entire test duration at these locations are shown in Fig. 2.63 (a) – (i).High temperatures ranging from 626 °C to 925 °C were recorded after about 70 to 75 minutes. Relatively lower temperatures were recorded in the slab near column C2 and

C3. It was observed that the north half portion of the slab experienced more temperatures than the southern half of the slab. Further, in the north half portion, the west side quarter portion had more temperatures than the eastern quarter portion. Table 2.8 provides the thermal gradients at various locations, which were computed from the temperature data. It can be noted that quite high thermal gradients were observed in the roof slab. A maximum gradient of 19.36 ºC/mm was recorded near column C1, which explains the reason for severe spalling of the cover concrete in the corresponding location of roof slab. However, despite the considerable damage, the roof slab remained structurally intact and continued to carry superimposed loads.

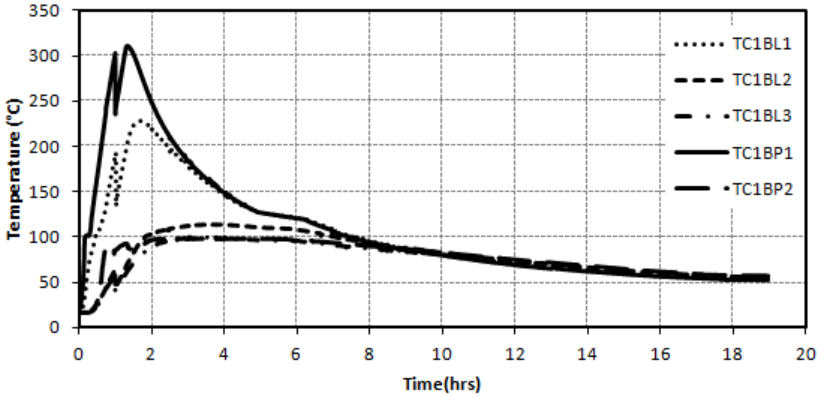

(a)

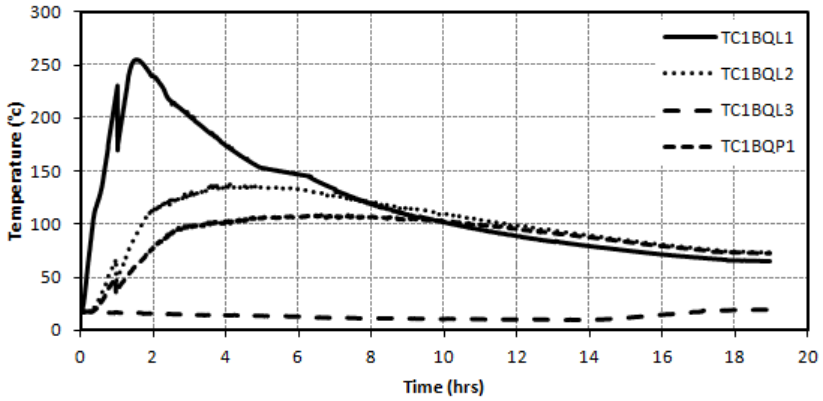

(b)

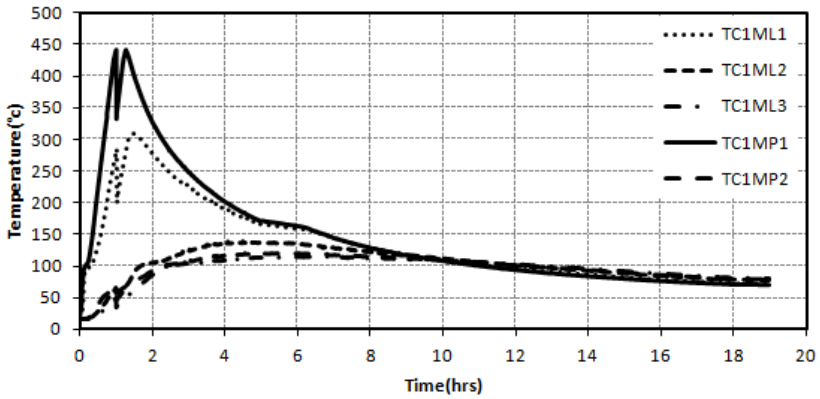

(c)

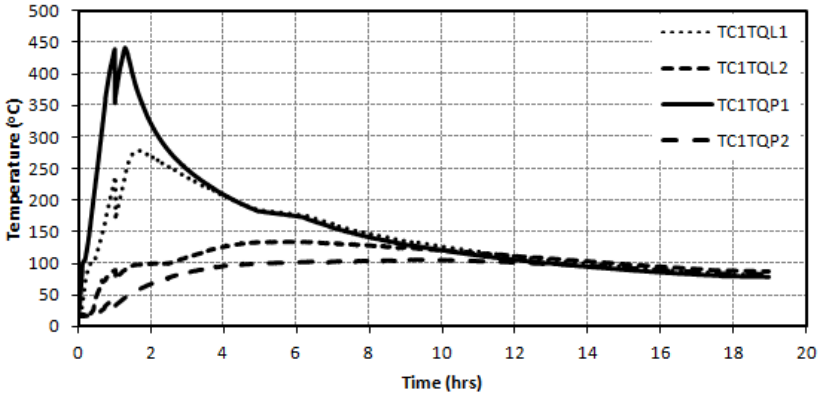

(d)

Fig.2.60: (a)-(r) Time- Temperature curves for columns (contd.)

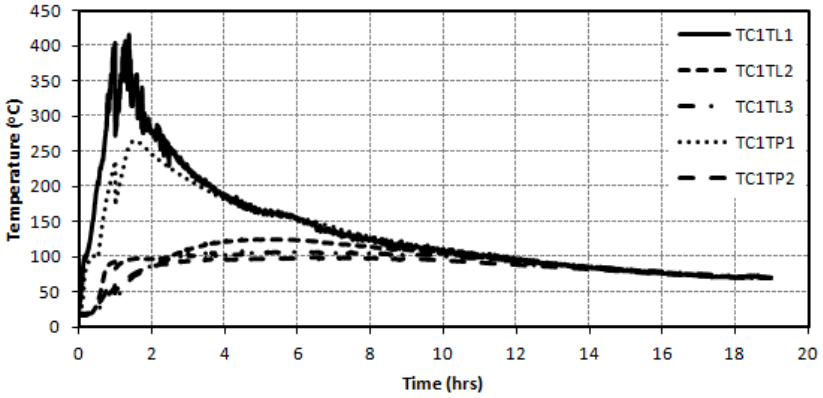

(e)

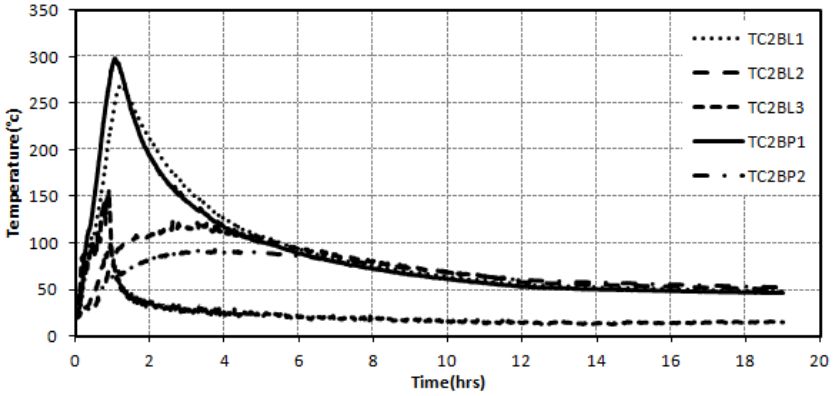

(f)

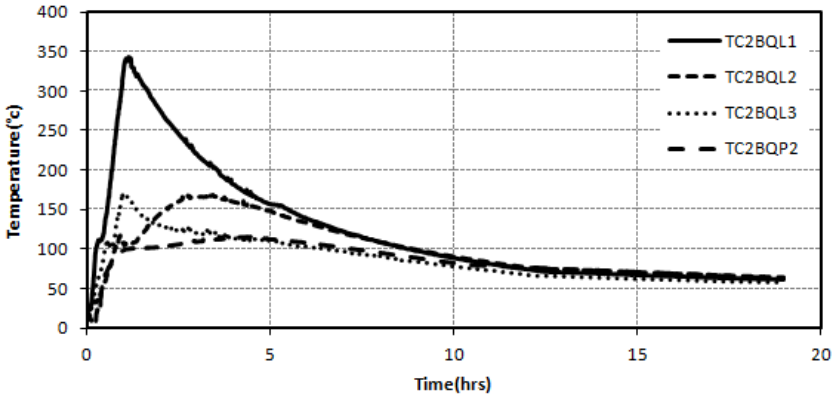

(g)

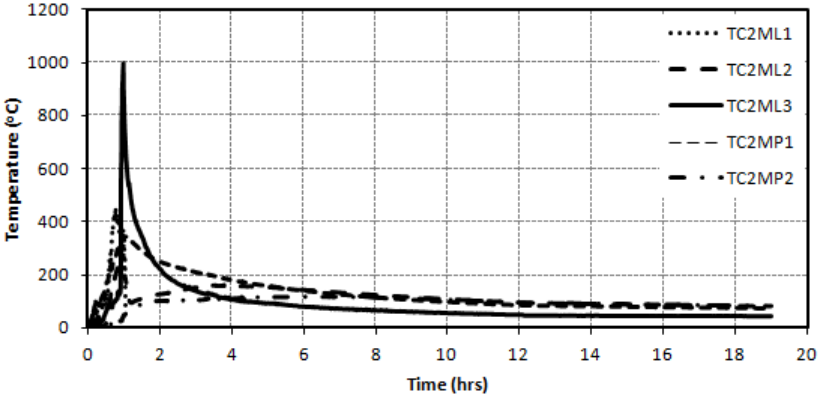

(h)

Fig.2.60: (a)-(r) Time- Temperature curves for columns (contd.)

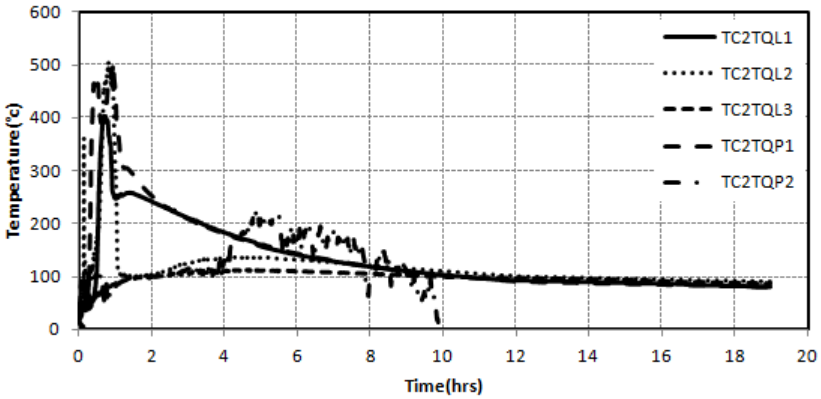

(i)

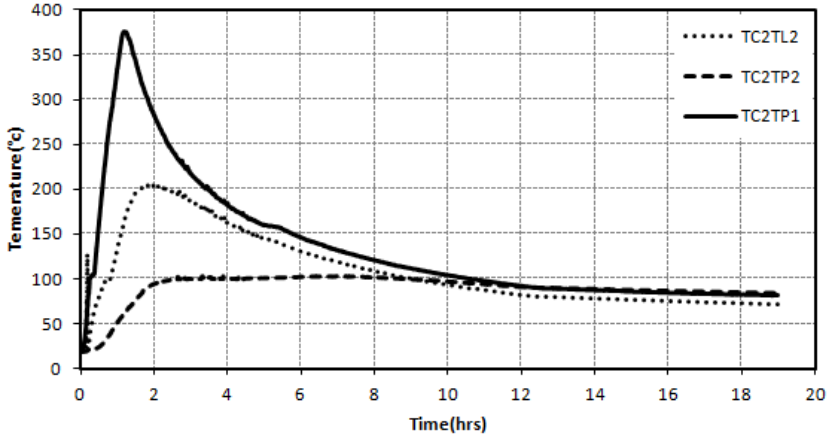

(j)

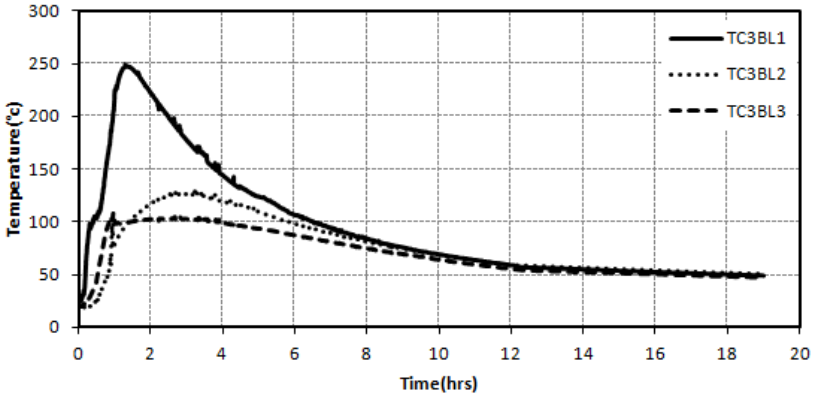

(k)

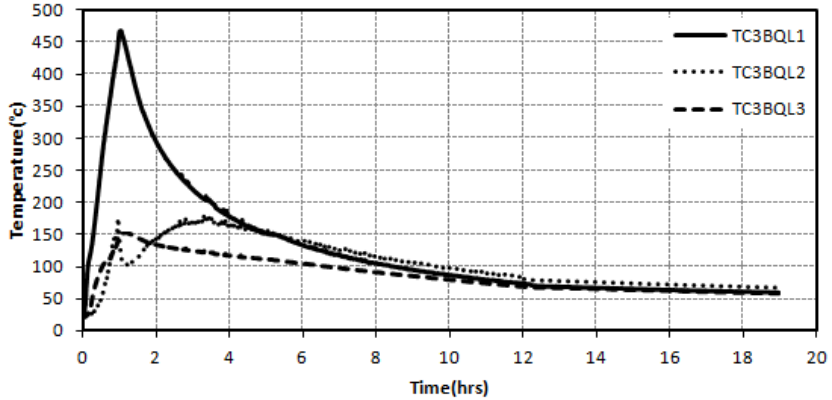

(l)

Fig.2.60: (a)-(r) Time- Temperature curves for columns (contd.)

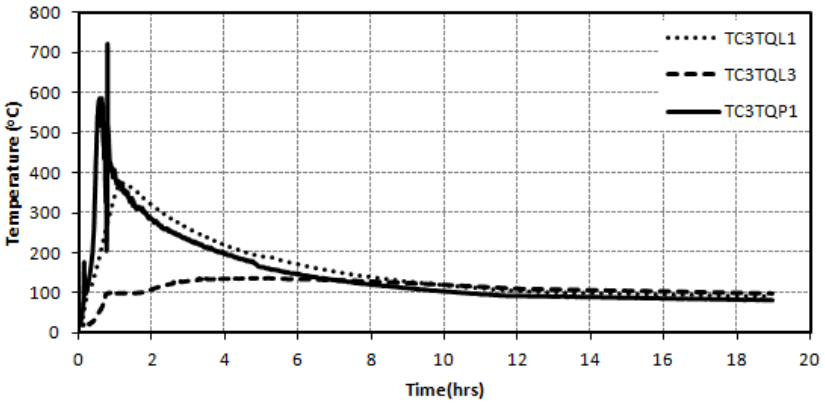

(m)

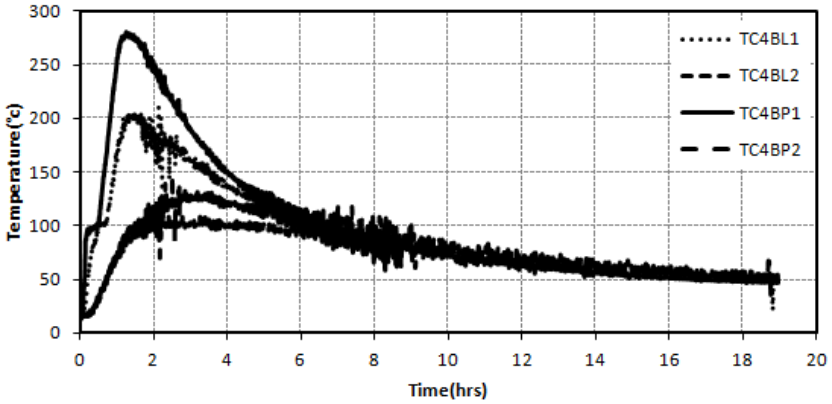

(n)

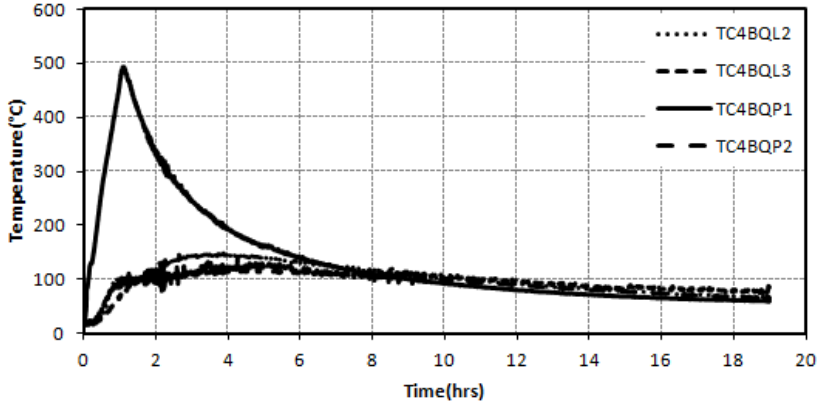

(o)

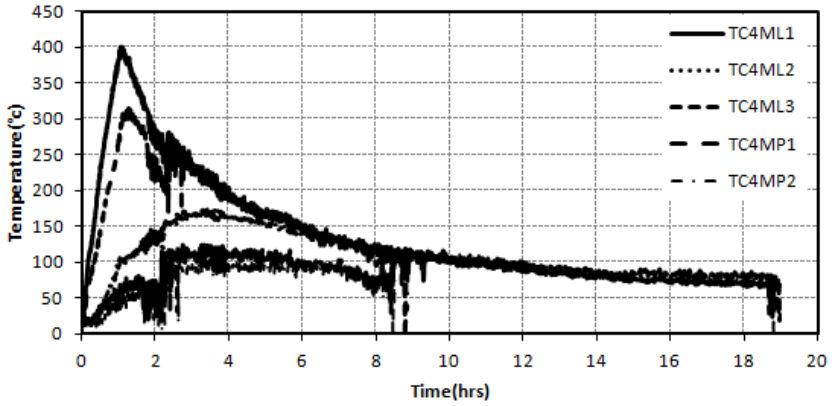

(p)

Fig.2.60: (a)-(r) Time- Temperature curves for columns (contd.)

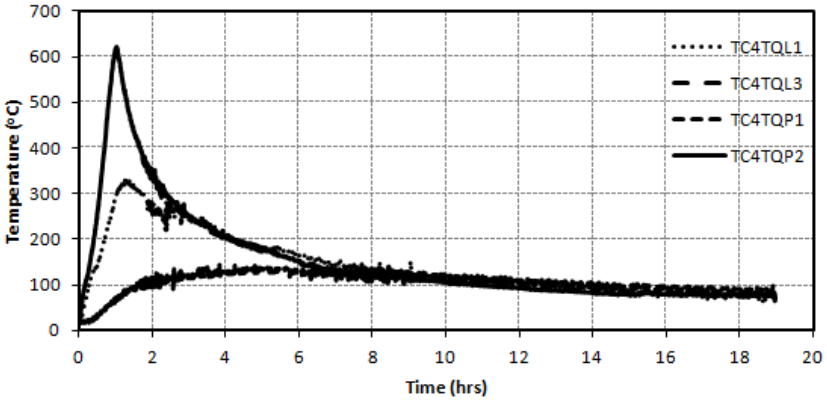

(q)

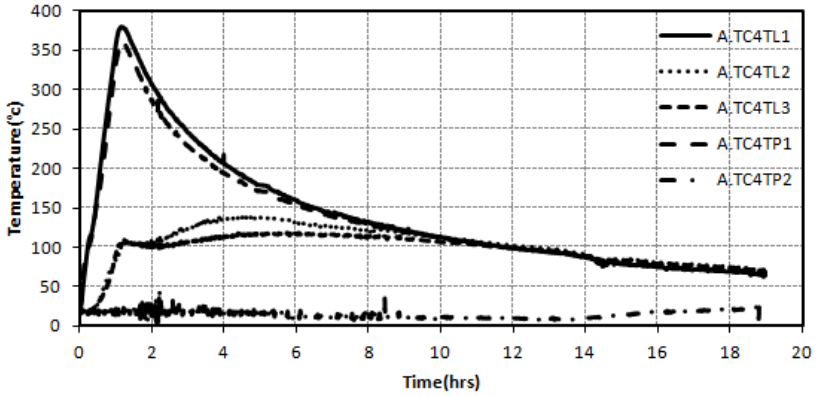

(r)

Fig.2.60: (a)-(r) Time- Temperature curves for columns (contd.)

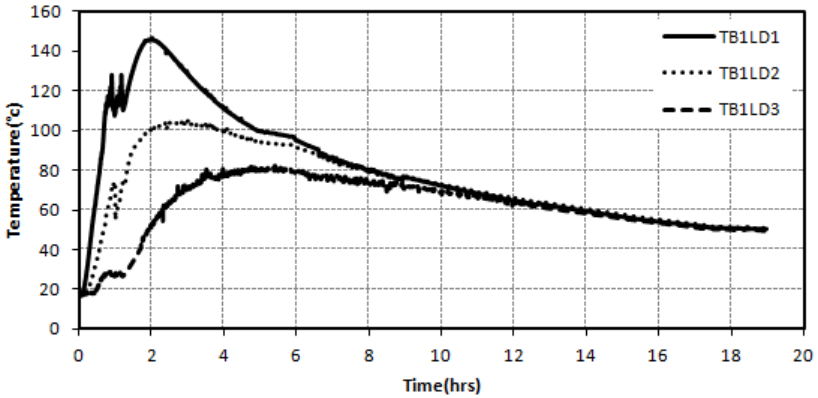

(a)

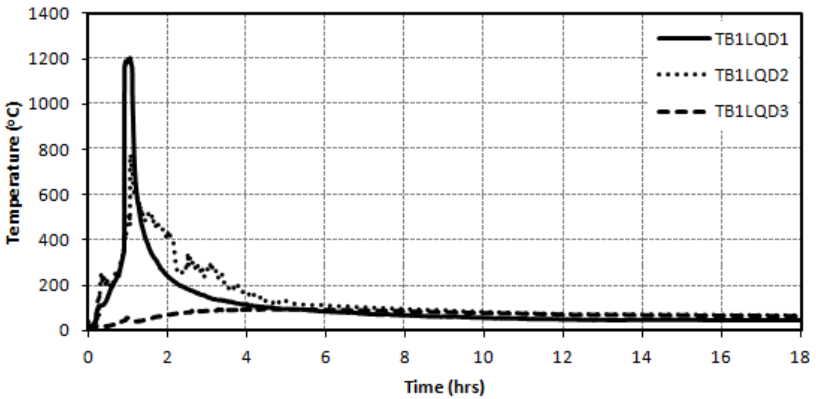

(b)

Fig.2.61: (a)-(t) Time- Temperature curves for Plinth Beams (contd.)

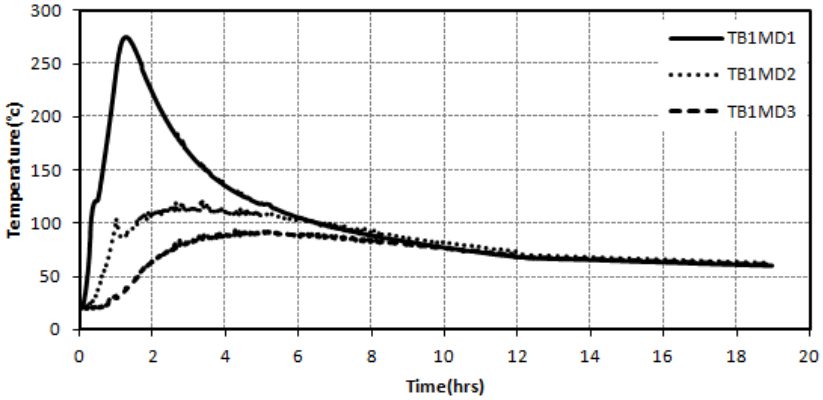

(c)

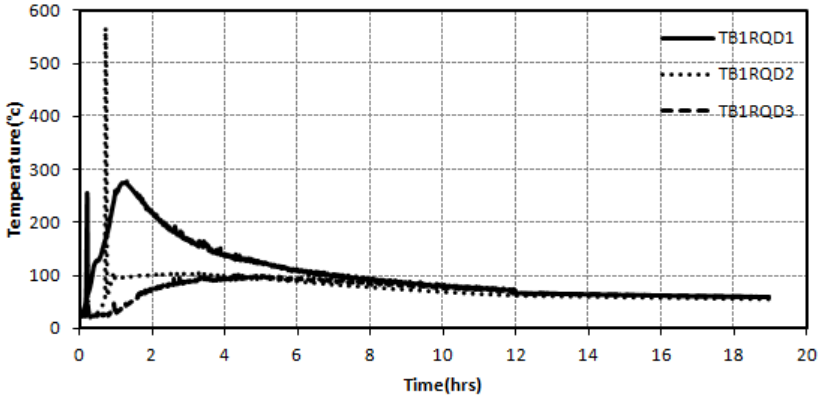

(d)

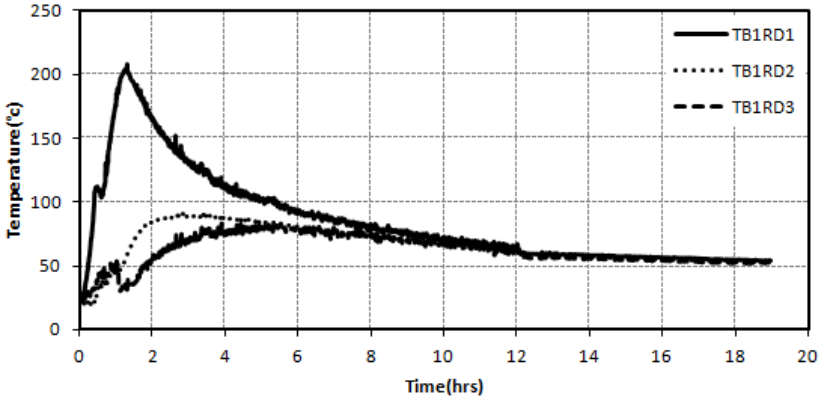

(e)

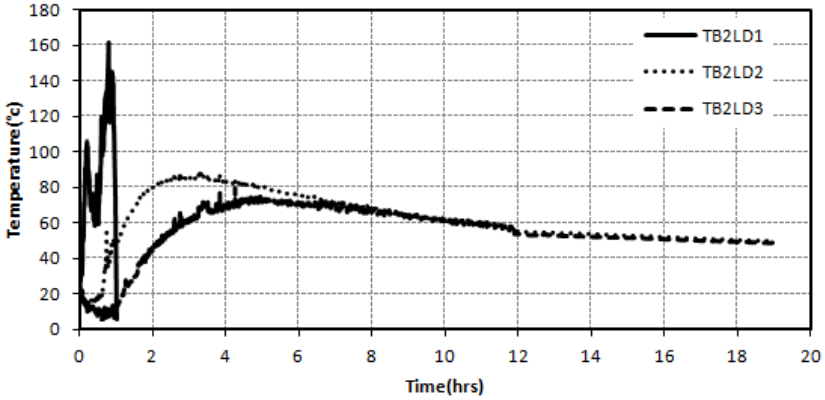

(f)

Fig.2.61: (a)-(t) Time- Temperature curves for Plinth Beams (contd.)

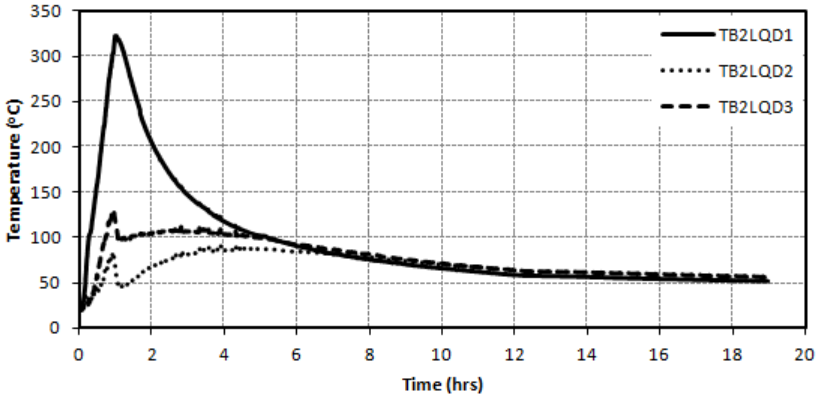

(g)

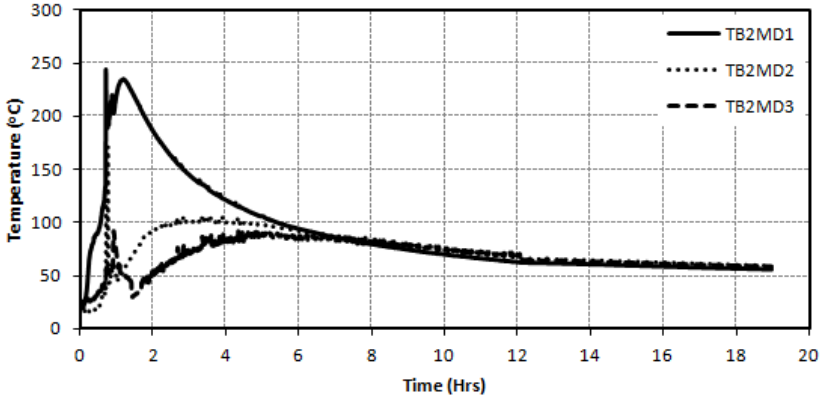

(h)

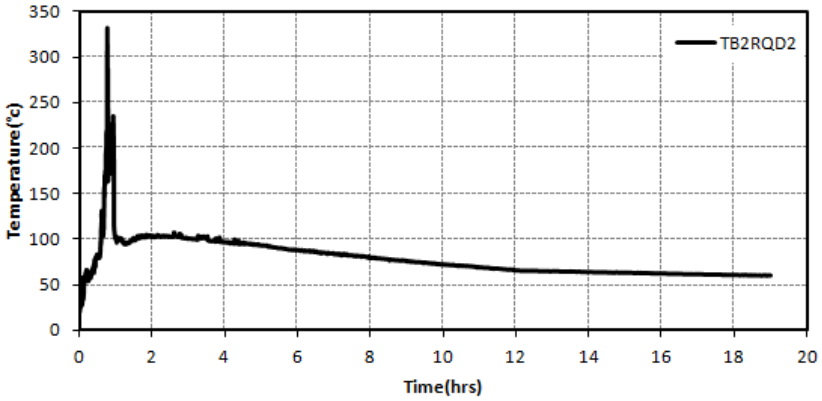

(i)

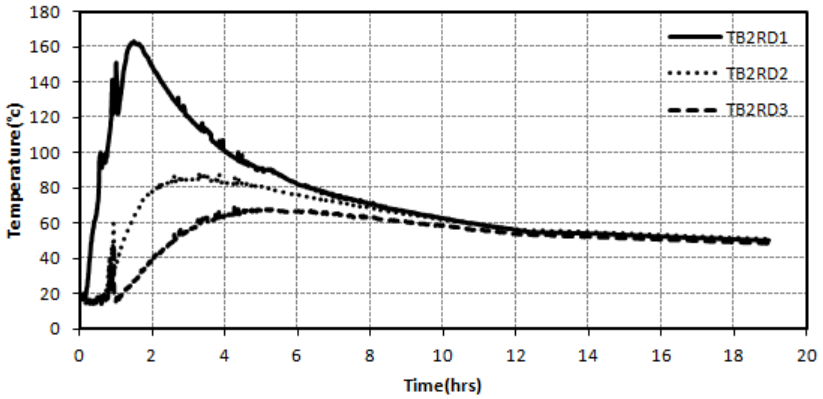

(j)

Fig.2.61: (a)-(t) Time- Temperature curves for Plinth Beams (contd.)

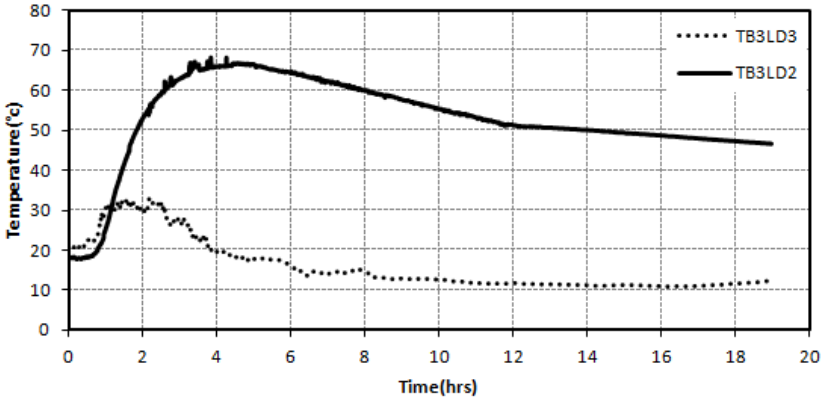

(k)

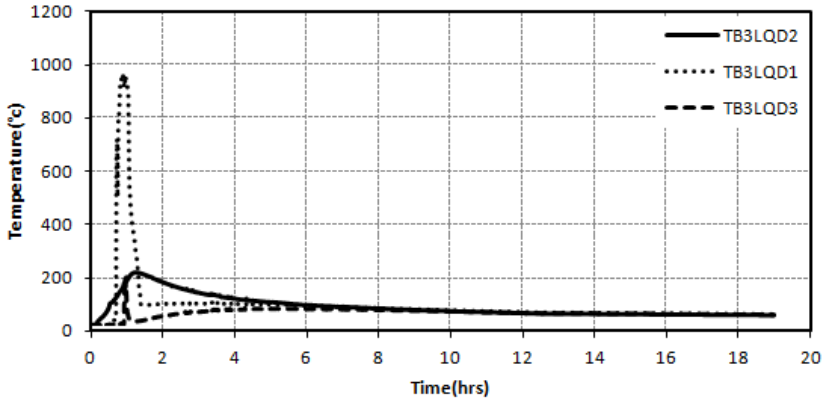

(l)

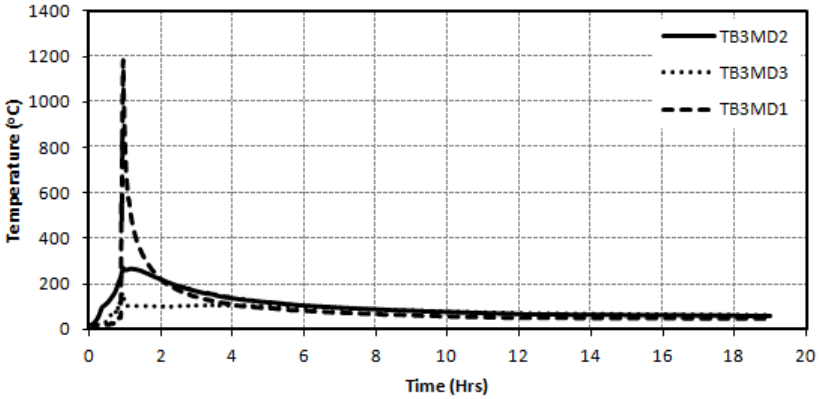

(m)

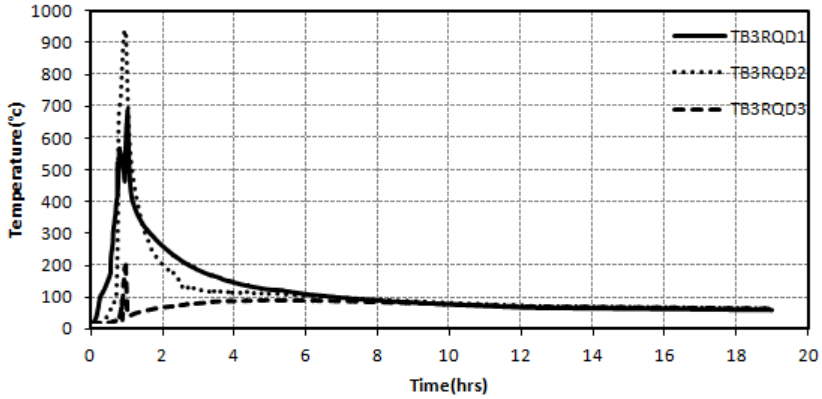

(n)

Fig.2.61: (a)-(t) Time- Temperature curves for Plinth Beams (contd.)

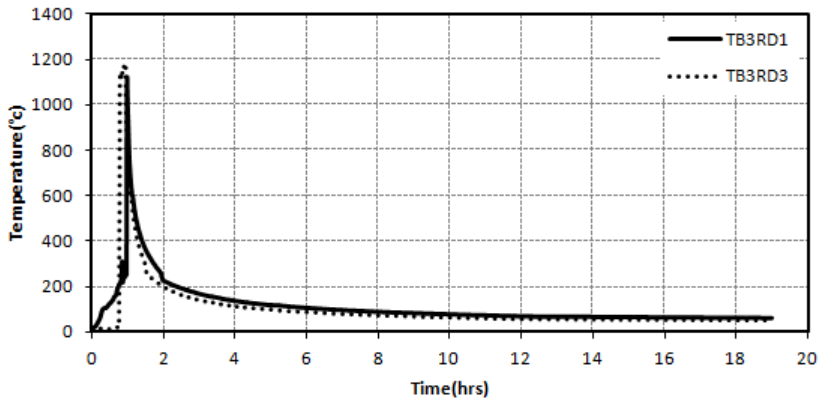

(o)

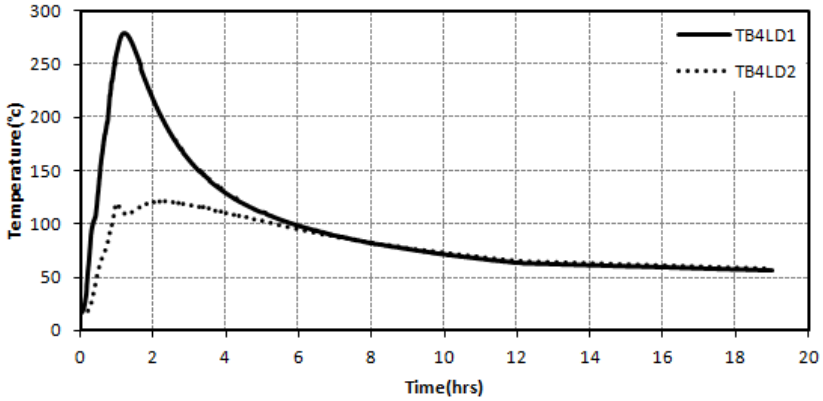

(p)

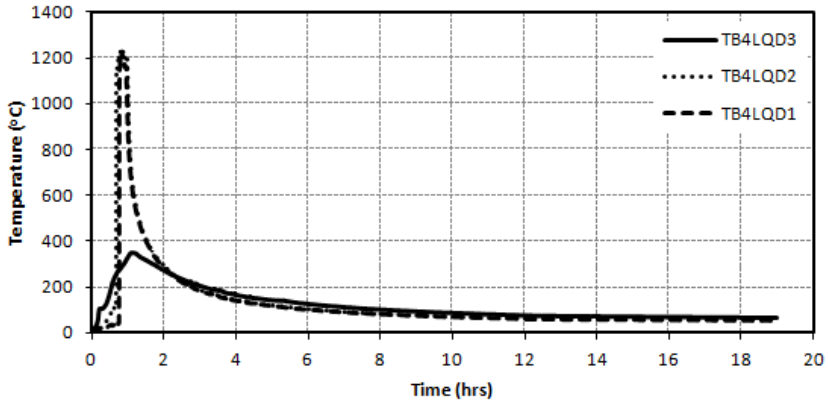

(q)

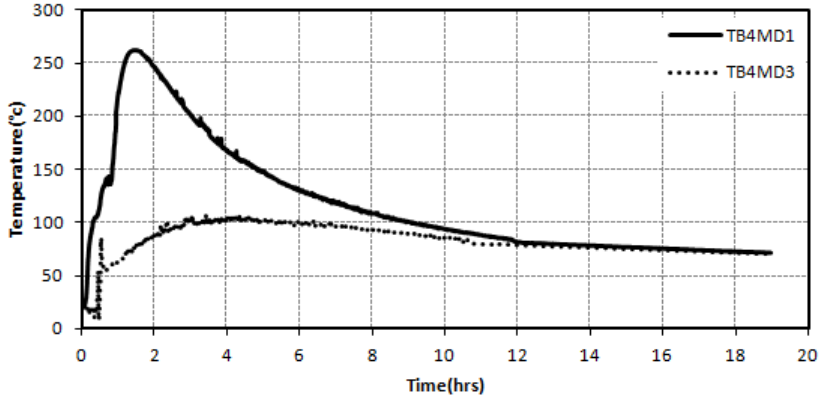

(r)

Fig.2.61: (a)-(t) Time- Temperature curves for Plinth Beams (contd.)

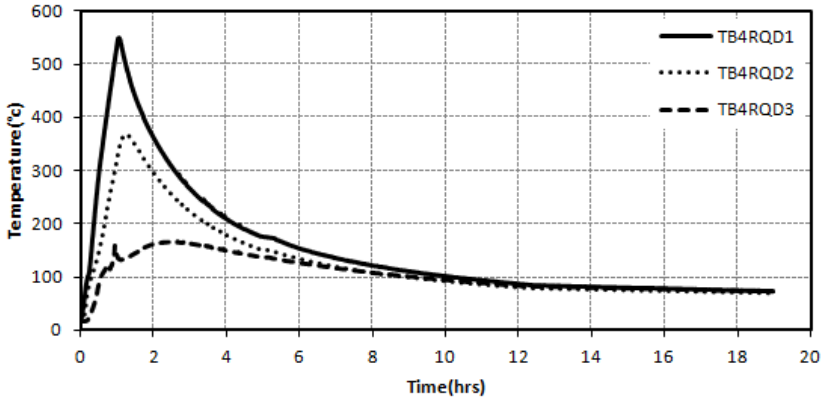

(s)

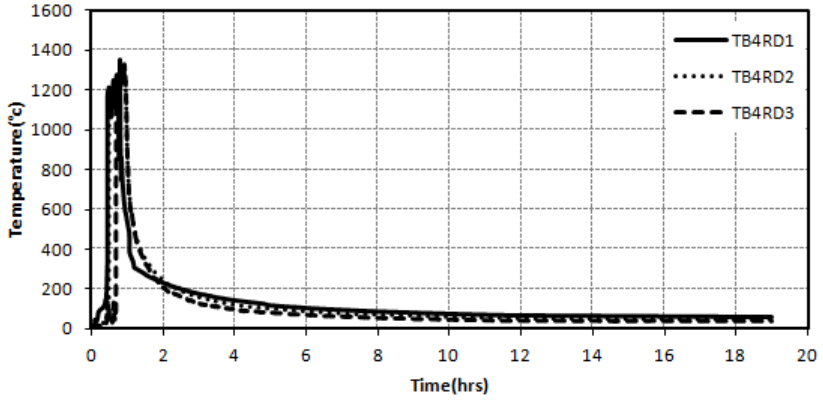

(t)

Fig.2.61: (a)-(t) Time- Temperature curves for Plinth Beams.

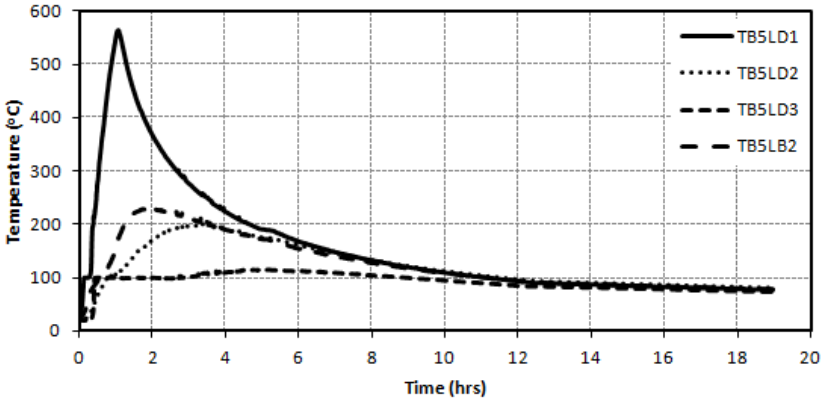

(a)

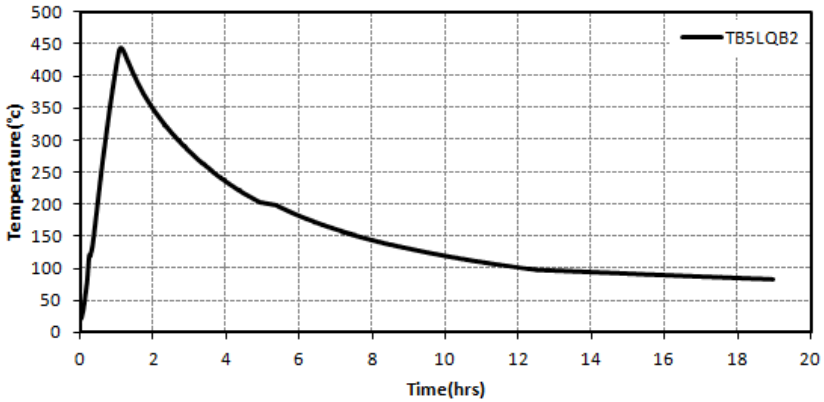

(b)

Fig.2.62: (a)-(t) Time- Temperature curves for Roof Beams (contd.)

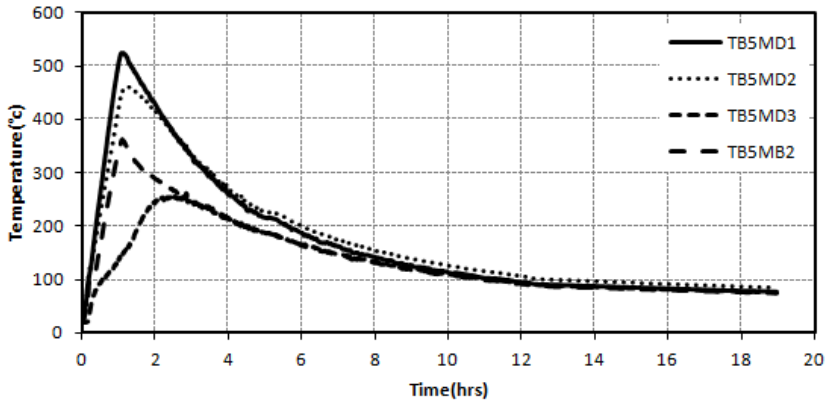

(c)

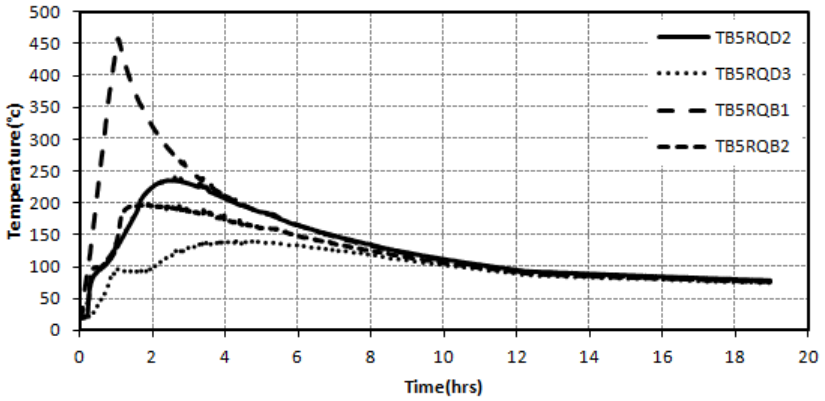

(d)

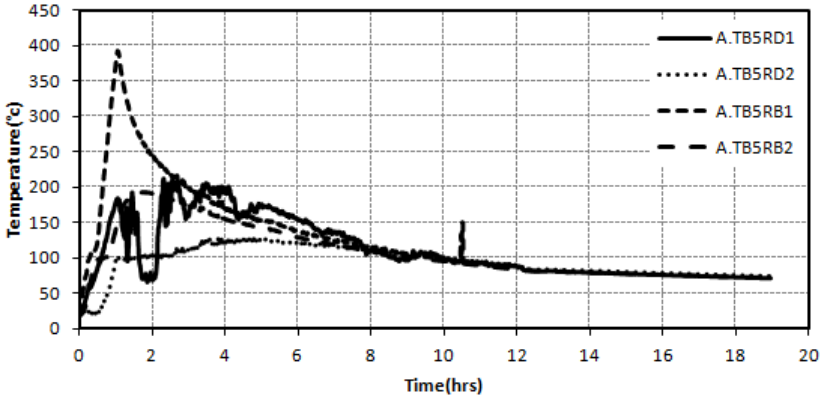

(e)

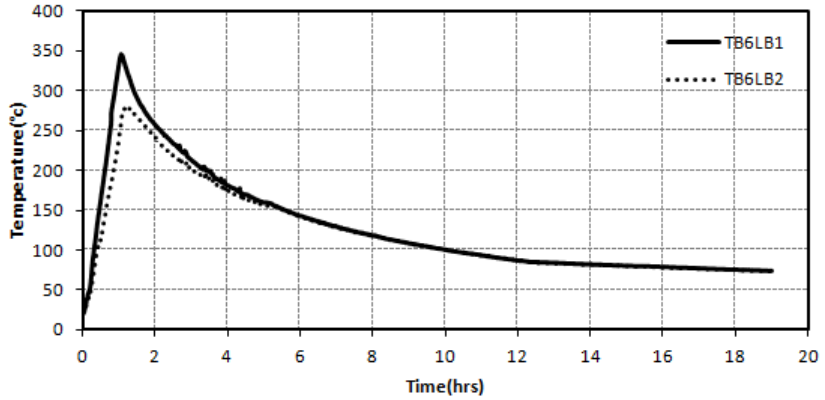

(f)

Fig.2.62: (a)-(t) Time- Temperature curves for Roof Beams (contd.)

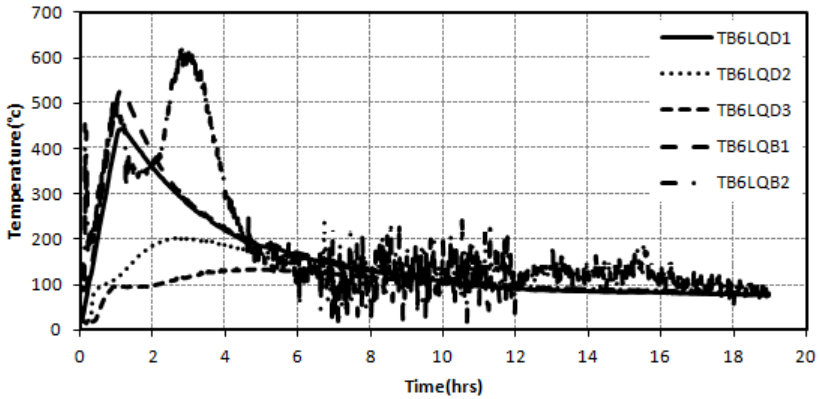

(g)

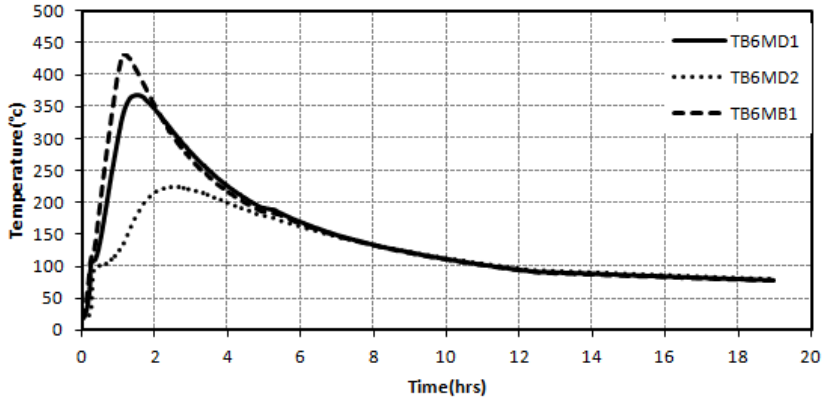

(h)

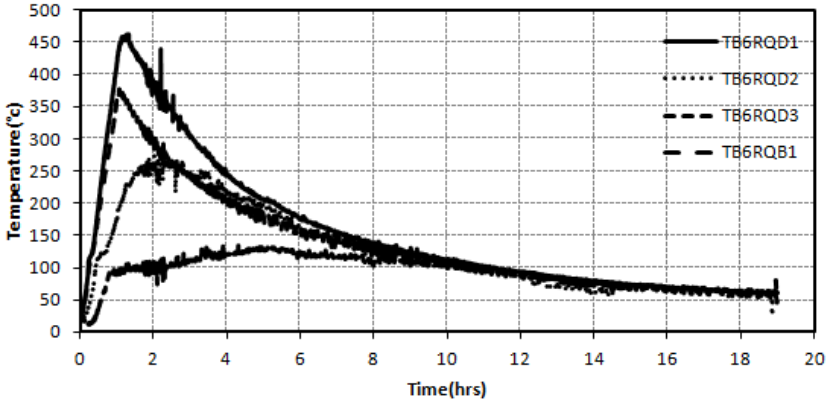

(i)

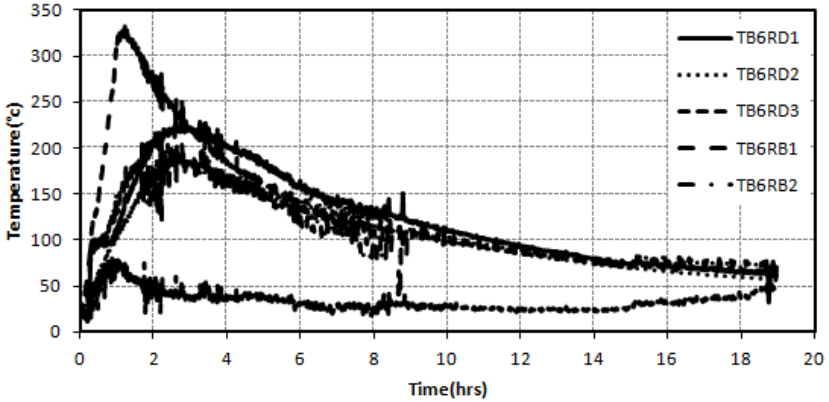

(j)

Fig.2.62: (a)-(t) Time- Temperature curves for Roof Beams (contd.)

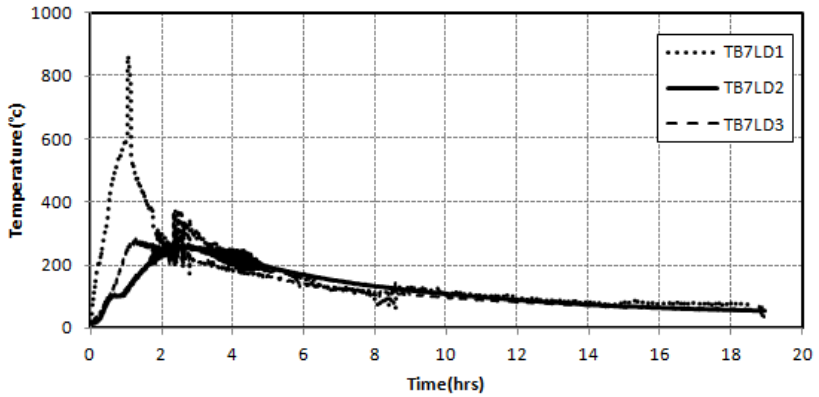

(k)

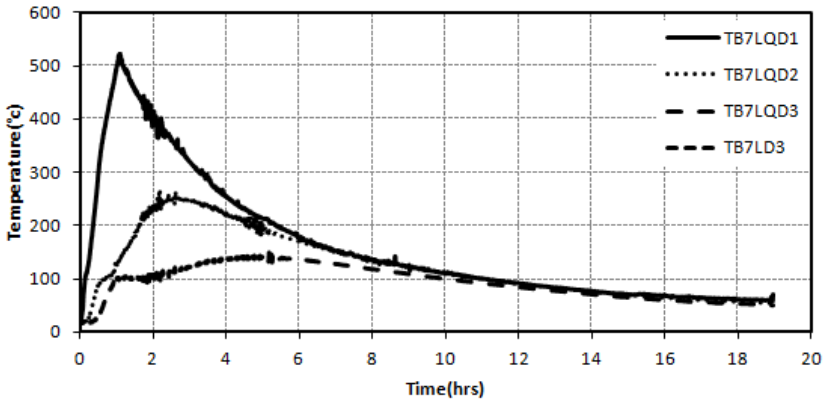

(l)

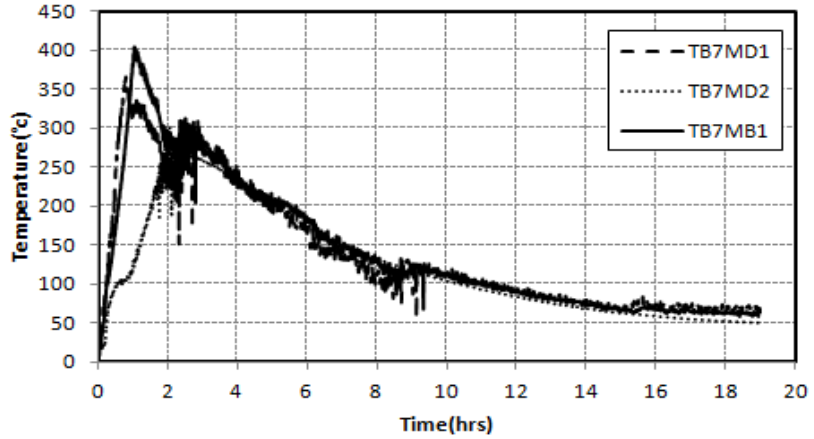

(m)

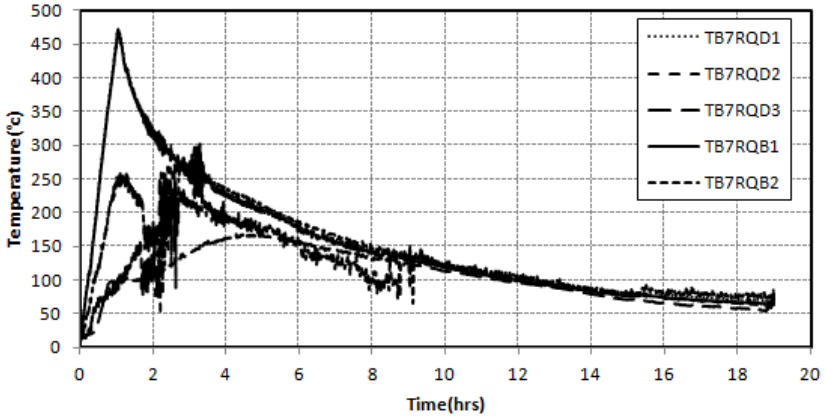

(n)

Fig.2.62: (a)-(t) Time- Temperature curves for Roof Beams (contd.)

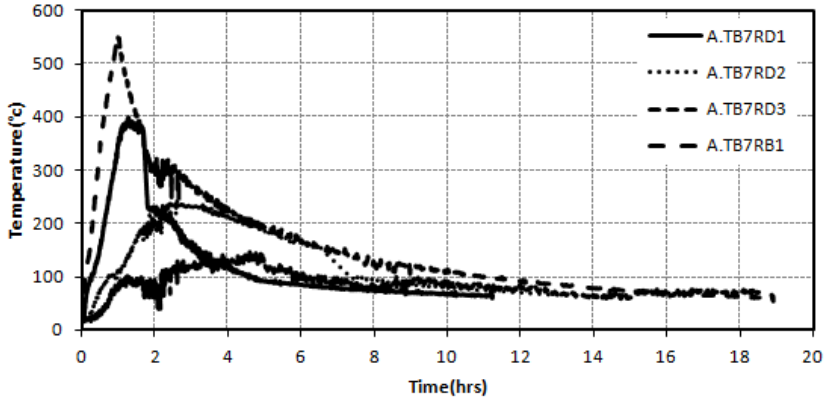

(o)

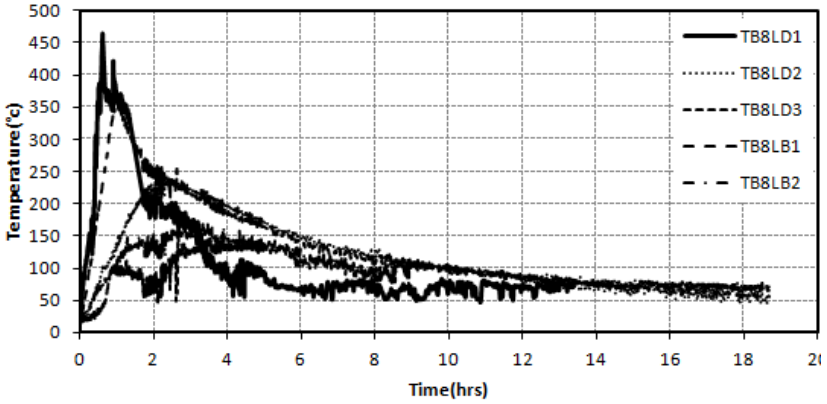

(p)

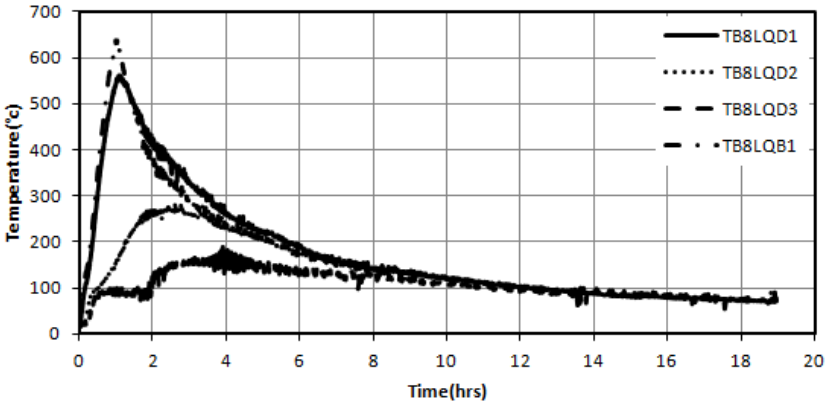

(q)

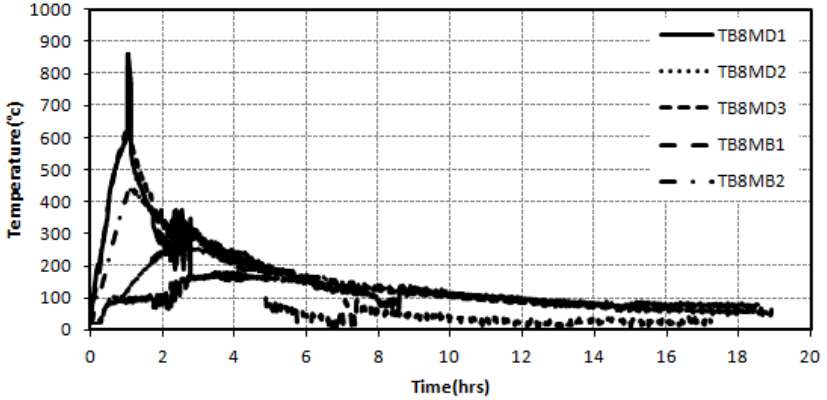

(r)

Fig.2.62: (a)-(t) Time- Temperature curves for Roof Beams (contd.)

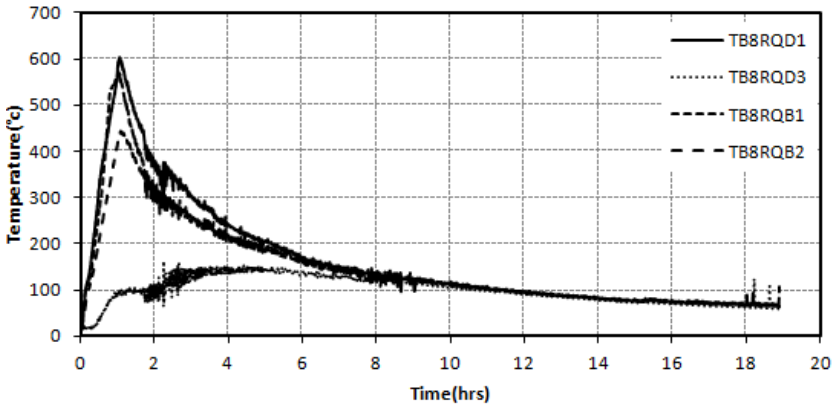

(s)

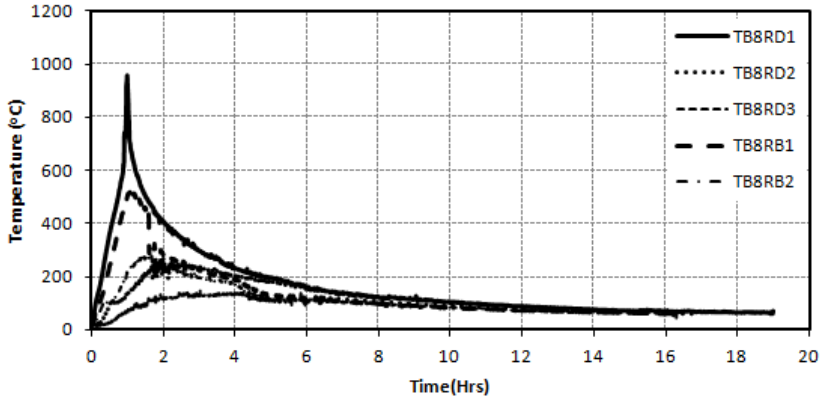

(t)

Fig.2.62: (a)-(t) Time- Temperature curves for Roof Beams.

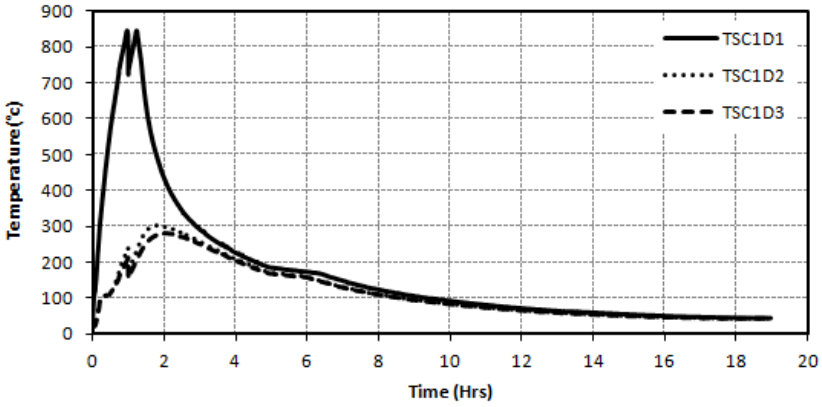

(a)

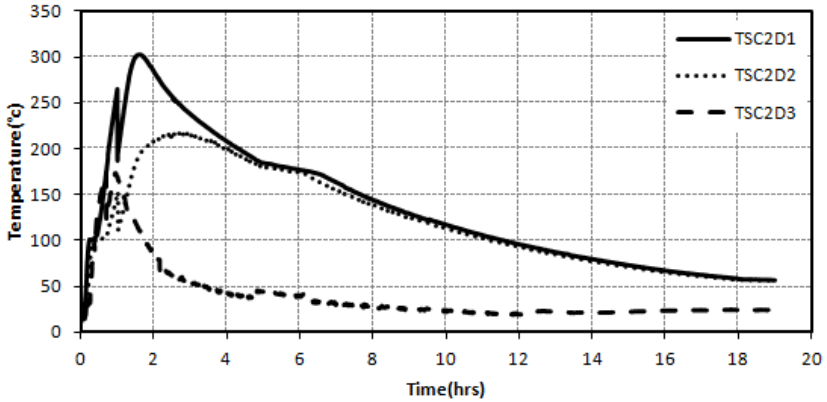

(b)

Fig.2.63: (a)-(i) Time- Temperature curves for Roof slab(contd.)

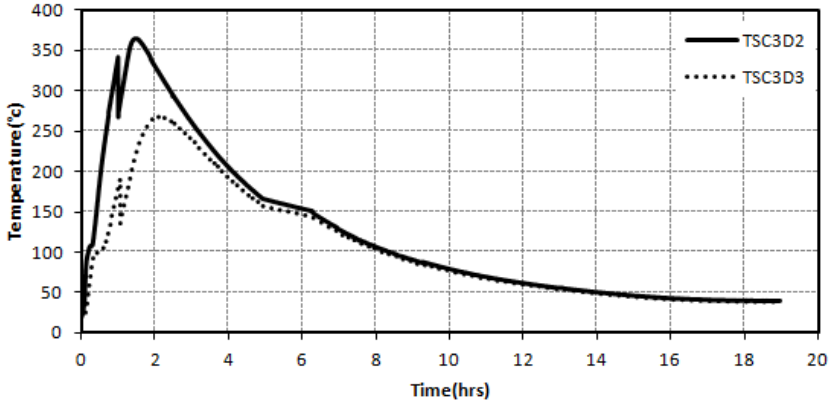

(c)

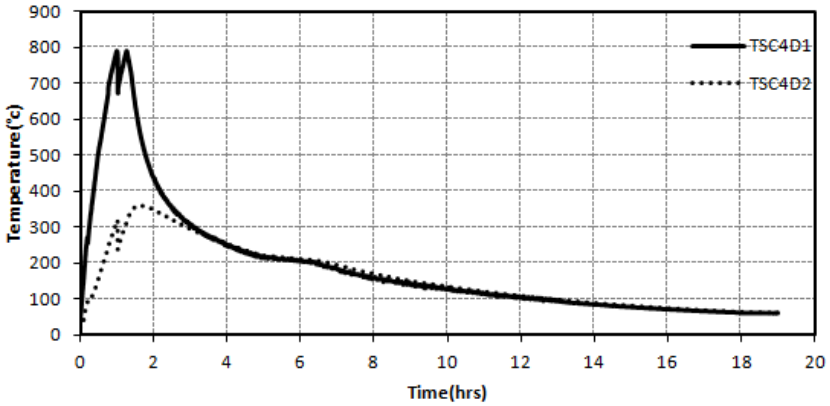

(d)

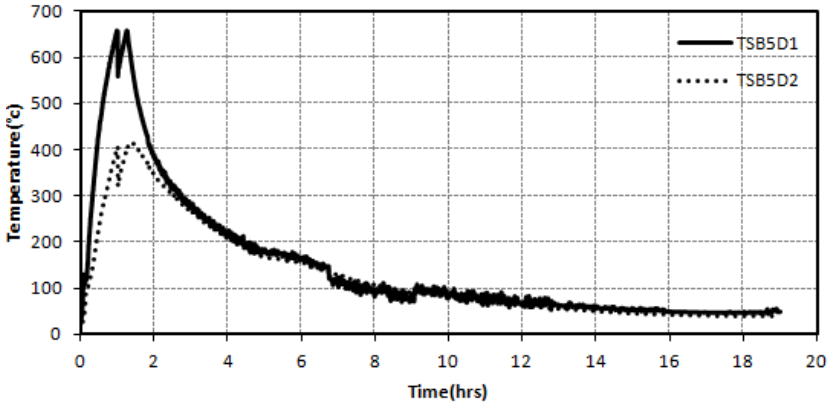

(e)

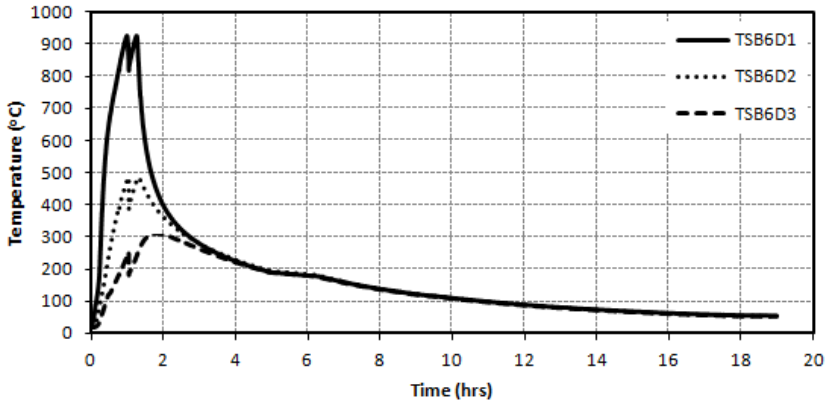

(f)

Fig.2.63: (a)-(i) Time- Temperature curves for Roof slab(contd.)

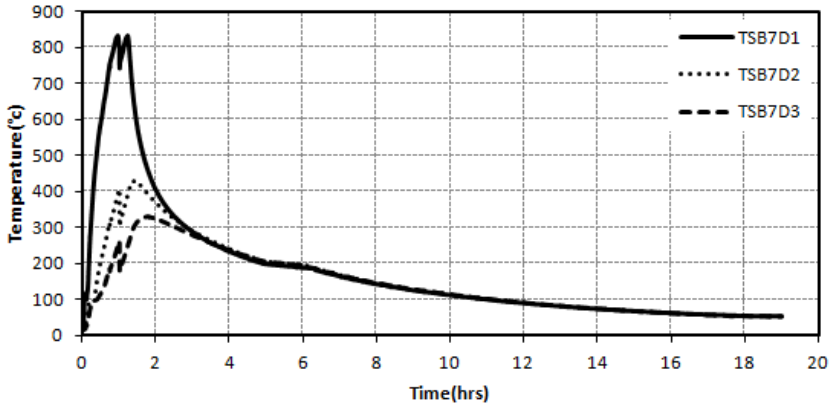

(g)

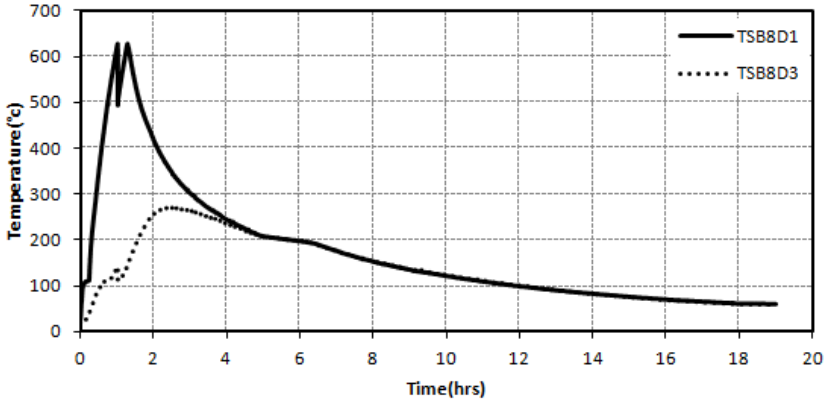

(h)

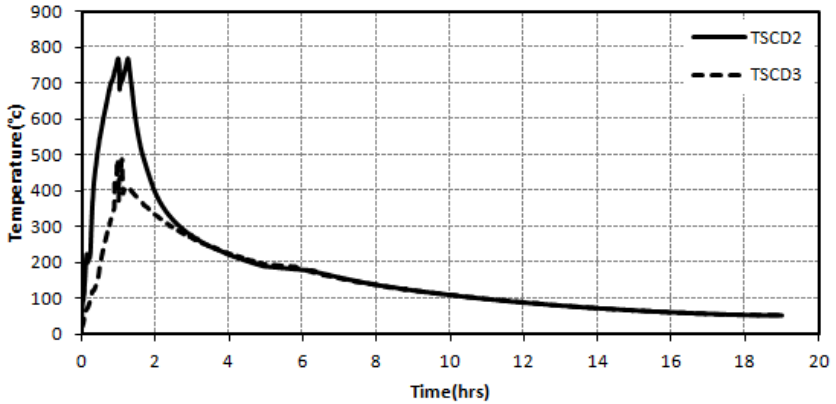

(i)

Fig.2.63: (a)-(i) Time- Temperature curves for Roof slab.

2.3.3 Test phase III: The Residual load test

After the fire test the RC frame was subjected to cyclic lateral loading excursion in order to evaluate its residual lateral load capacity. Fig. 2.64 shows the load displacement hysteresis loop for the residual test. A large reduction in lateral capacity was observed during the initial stages of loading. Chunks of loose concrete fell from the roof slab, beams and the columns. The deteriorated concrete from the columns especially near the beam column joints fell apart rendering the core concrete exposed. It was observed that the concrete was damaged though the chunks of concrete were held together by the confining reinforcement as shown in Fig 2.65. The reinforcement was rendered exposed with cracks and damage in the core concrete. In the already spalled portion of the beam B7, the vertical leg of a shear stirrup was observed to fail. A residual lateral capacity of 46%, of the capacity before fire, was observed at the displacement of 20 mm. At 80 mm displacement, the frame showed a residual lateral capacity of 53% of the capacity before fire. An average reduction in the load carrying capacity of 51% was observed at displacement of 100 mm. The final reduction in the lateral load carrying capacity of the frame was measured to be 35% at 150 mm displacement. Fig. 2.66 gives a comparison of the initial and the residual lateral load carrying capacity of the test frame. The lower residual strength at initial stages of loading was due to the damages in the concrete section and loss in concrete material stiffness. However, during the higher displacement cycles the effect of low concrete material stiffness was minimal. The contribution of concrete material stiffness at higher lateral displacement diminished due to initiation and widening of cracks. The stiffness was provided by the steel reinforcement. The frame was subjected to a lateral displacement of 270 mm corresponding to a drift ratio of 7.2 %. The frame witnessed substantial amount of loss in material stiffness and strength, however the frame remained intact without collapse.

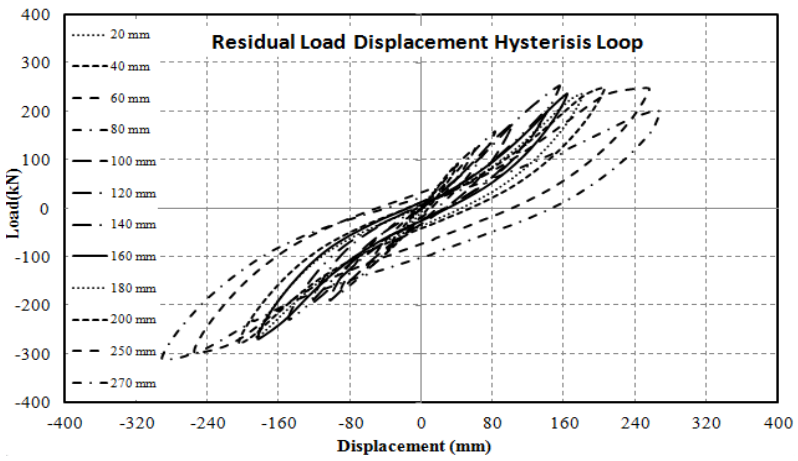

Fig.2.64 Residual Load Displacement Hysteresis of the test frame

(a)

(b)

(c)

Fig. 2.65: (a) Damaged core concrete in Beam B7 (b) failed shear stirrup in beam B7 (c) view of a column

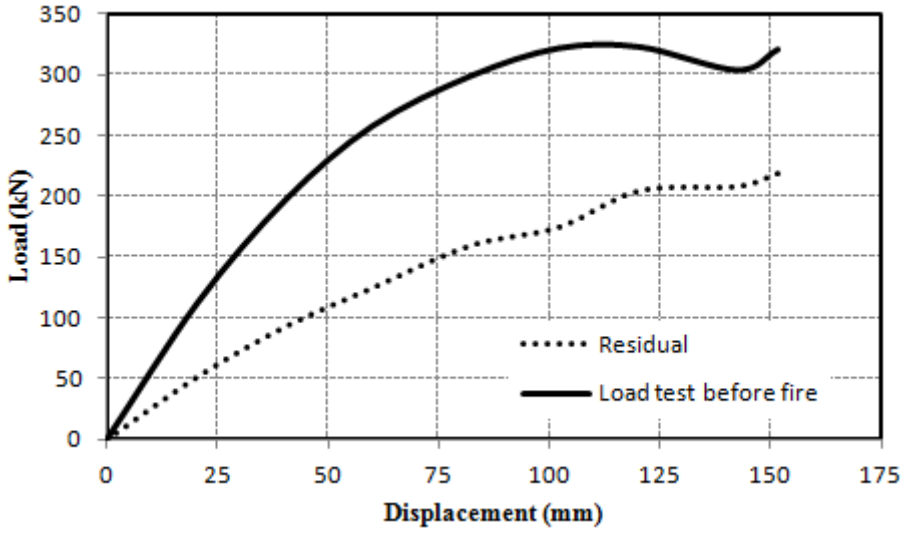

Fig.2.66: Load carrying capacity before and after fire

2.3.4 Effect of Ductile Detailing on the Post- Earthquake Fire Behaviour of the Frame

In this section a comparison of the overall behaviour of the non-ductile frame is presented with the tests conducted by Kamath (2014) on the ductile frame. The comparison will give an insight on the effect of the reinforcement detailing on the Post earthquake fire resistance of reinforced concrete frames. As explained in the introductory part of this chapter, there is a need to study the effect of ductile detailing on the post earthquake fire performance of the buildings. The typical reinforcement details of the ductile detailed frame tested by Kamath (2014) are shown in Fig. 2.65. All the parameters during the testing were identical to the present frame except the reinforcement detailing. The frame tested in the present study was designed with non-seismic detailing and the frame tested by Kamath (2014) was designed as a ductile frame conforming to the guidelines of the Indian Code – IS 19320. Both the frames were subjected to a simulated earthquake loading corresponding to the to the collapse prevention structural performance level (S-5) of FEMA 356:2000. The damage level was ensured by subjecting the RC frame to a maximum roof level lateral displacement of 150 mm corresponding to a roof drift ratio of 4%.

In the frame with ductile detailing as tested and reported by Kamath (2014), the nucleation and propagation of cracks did not initiate up to 20 mm displacement cycles. Cracks on columns and beams initiated during 20 mm and 30 mm push cycles respectively. Mostly the cracks got initiated in the planes perpendicular to the loading direction and these cracks further propagated in the subsequent cycles.

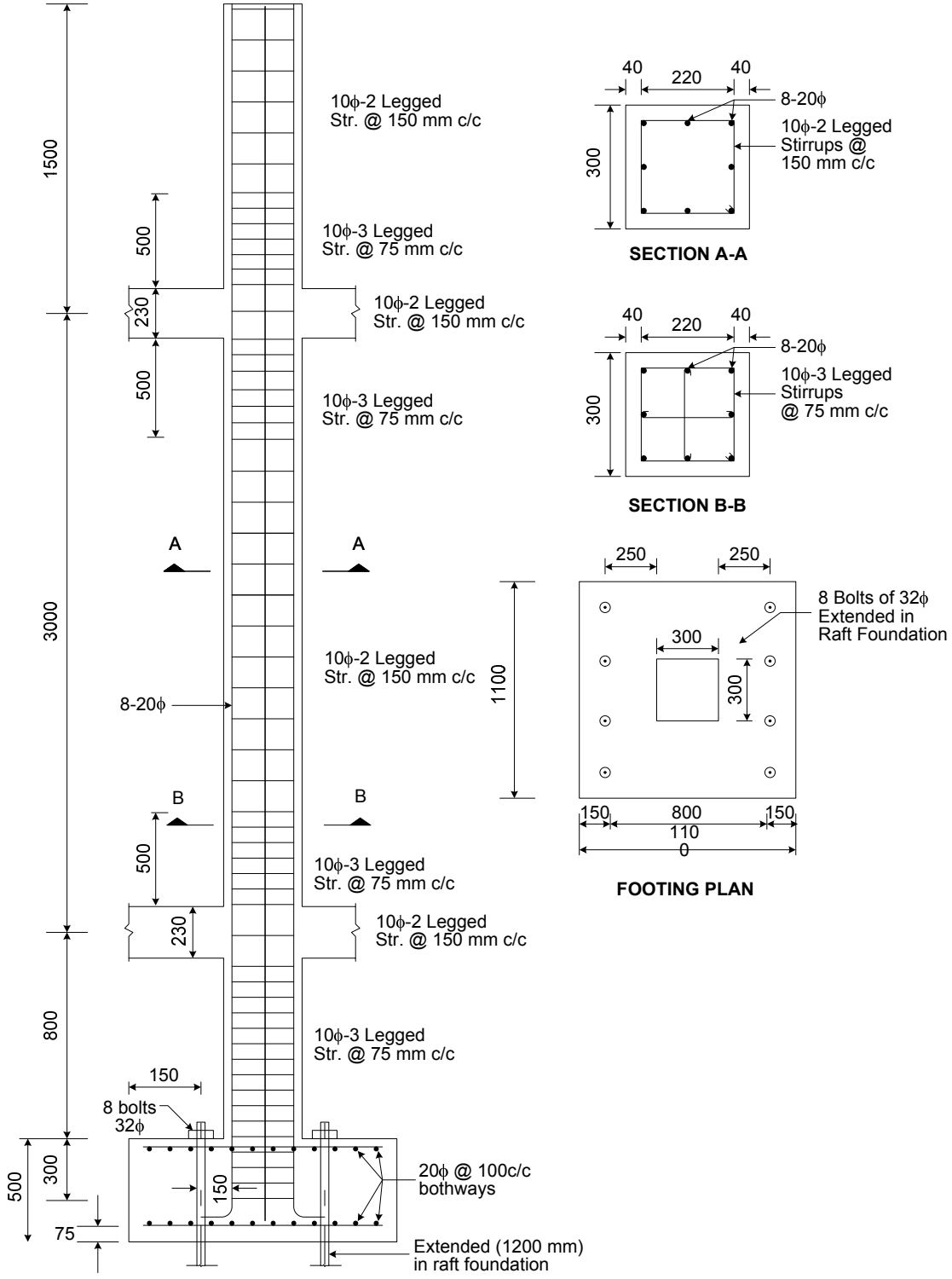

Fig. 2.67: The typical reinforcement details in the different elements of the test frame. (a) Column detailing. (b) Beam reinforcement (Ductile detailed frame tested by Kamath (2014)) (contd.)

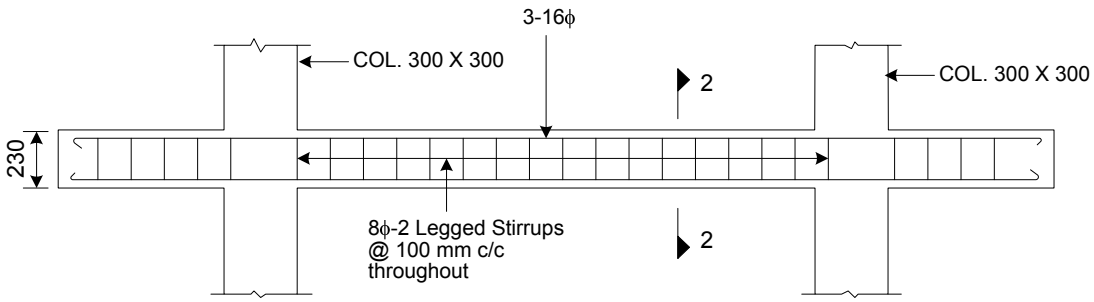

L-SECTION OF BEAM (230 X 230)

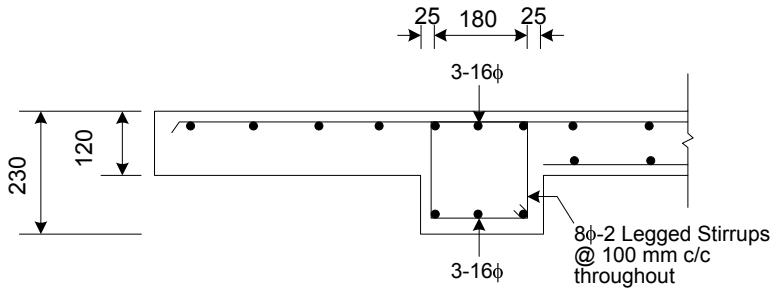

SECTION 2-2

(b) : TYPICAL DETAILING OF BEAMS

ALL DIMENSIONS ARE IN mm

Fig. 2.67: The typical reinforcement details in the different elements of the test frame. (a) Column detailing. (b) Beam reinforcement (Ductile detailed frame tested by Kamath (2014))

Numerous fine cracks were observed in the RC frame with ductile detailing, with the crack widths in different members varying from 0.1 mm to 2.4 mm with no spalling at the joints as in Fig. 2.68 (a, b). Neither was any spalling observed in columns and beams nor was any reinforcement found to be buckled in the ductile detailed frame. At the end of the mechanical loading the residual plastic displacement of 19 mm was recorded upon unloading in the RC frame constructed with ductile detailing.

The degradation of the RC test frame with non ductile detailing due to the cracks, spalling and delamination was also shown by the load displacement history in Fig. 2.15, where in a clear decrease in stiffness and pinching of the hysteresis loops can be seen. However, in the case of ductile detailed frame tested by Kamath (2014) no such effect was seen (Fig. 2.69). The pinching effect as seen in the non ductile detailed frame is the direct manifestation of the deviation of the steel reinforcement direction from the coordinate of the principal stresses,

which was caused in the structural elements of the RC test frame assemblage due to the extensive cracking of the various structural elements of the frame. The pinching effect can also be attributed to the rapid increase in the shear strains which is evident from the wide shear cracks formed in the roof beams B5, B7 and plinth beams B1, B3 (Mansour and Hsu,2002). A large number of shear cracks formed during loading in different elements of the non-ductile frame indicates a build up of large vertical strains. From compatibility, the large vertical strains produce a large increase of strain in steel bars. From equilibrium, the large stresses in the steel bars and in the vertical concrete produce a large shear stress causing the pinched shape of the hysteretic loops. Figs. 2.70 and 2.71 give a comparison of the lateral load capacities of the two RC test frames before and after fire.

(a)

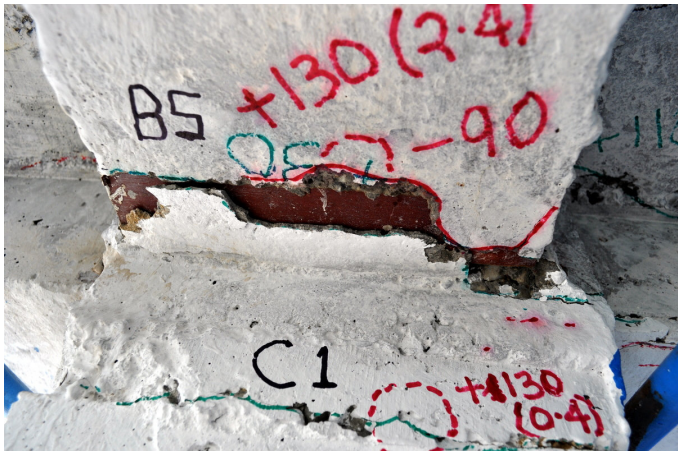

(b)

Fig.2.68: (a) & (b) Fine cracks in the elements of frame with ductile detailing tested by Kamath (2014)

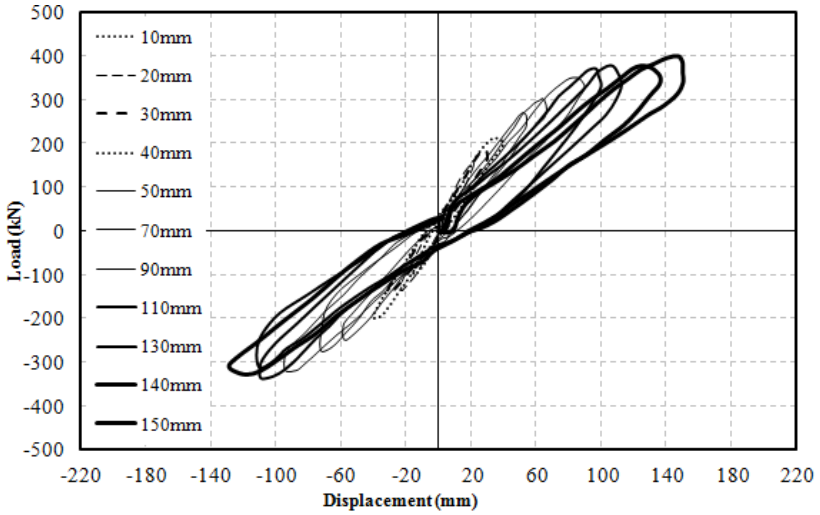

Fig.2.69: Load displacement hysteresis curve of the test frame tested by Kamath (2014).

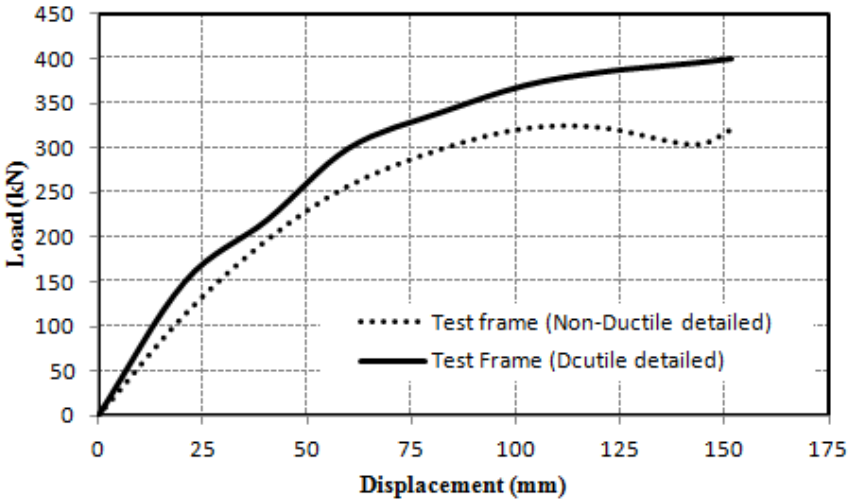

Fig. 2.70 Load envelops (before fire) of the two frames with different detailing

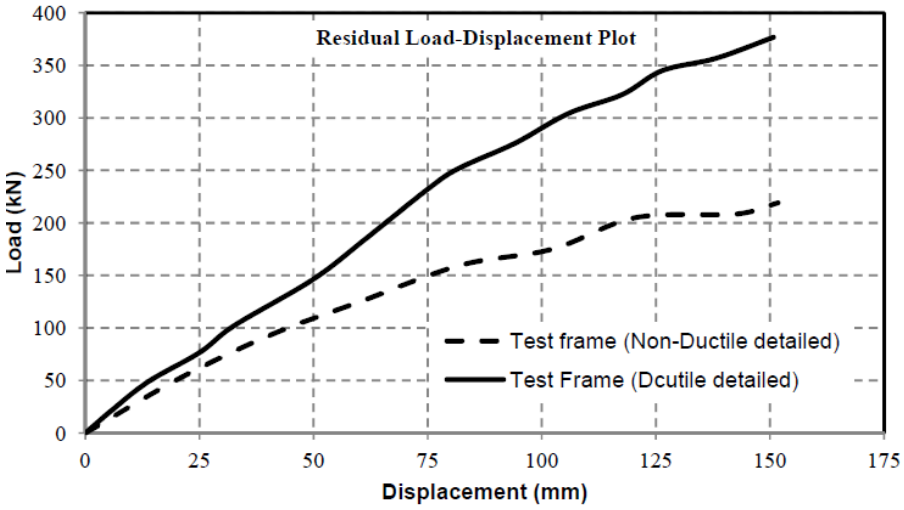

Fig. 2.71 Comparison of residual load envelops of the two test frames

The Figs. 2.72 (a) to 2.72 (j) give an insight into the effect of confining reinforcement on the temperature build up in the structural elements of the RC framed structures in post earthquake fire. It is seen that at any given location, the temperatures were much higher in non-ductile frame than those reported by Kamath (2014) for ductile detailed frame. It is due to the more pre-damage caused during the seismic loading in non-ductile frame than in ductile detailed frame. At some locations however, the temperatures reported by Kamath (2014) are higher. This can be attributed to the effect of crack widths. It was seen that the locations which had finer cracks attained less temperatures than un-cracked sections. However the sections with wider cracks attained more temperatures than the un-cracked sections. This behaviour is due to the vapour transport through the cracks. The finer cracks provide a path for hot vapours to escape leading to less build up of the temperature. However if the cracks are wider and large, though the hot gases leave the concrete sections but the wider cracks provide a path for the flames and hot gases to penetrate into the concrete thereby causing the temperatures to rise. This is the reason why some sections reported in ductile detailed frame had more temperatures even when it was less damaged. It is to be noted that the critical crack width below which the temperatures fall and above which the temperatures rise is still unknown and more tests need to be carried out to have a clear idea about the critical width of the crack.

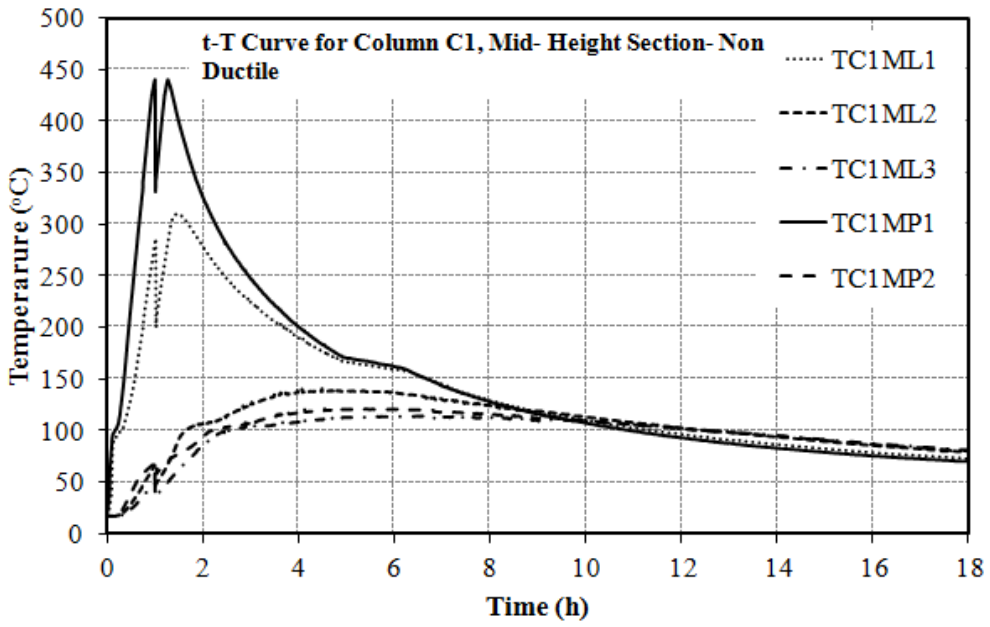

(a)

Fig.2.72: Comparison of the temperature development for different elements for the test frame with the ductile detailed frame tested by Kamath (2014). (contd.)

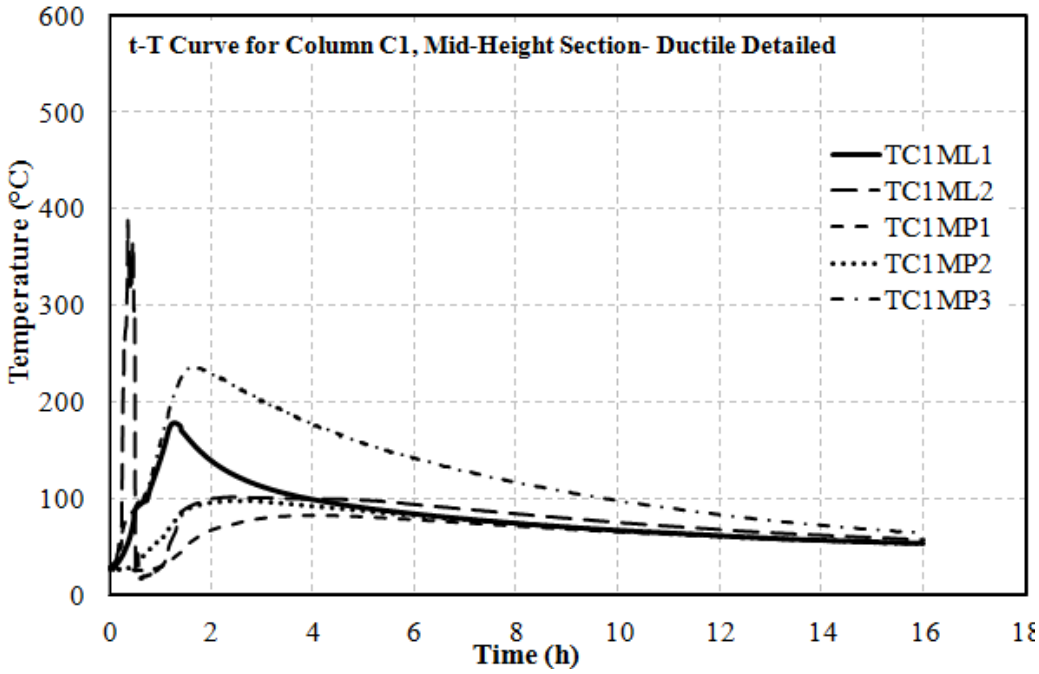

(b)

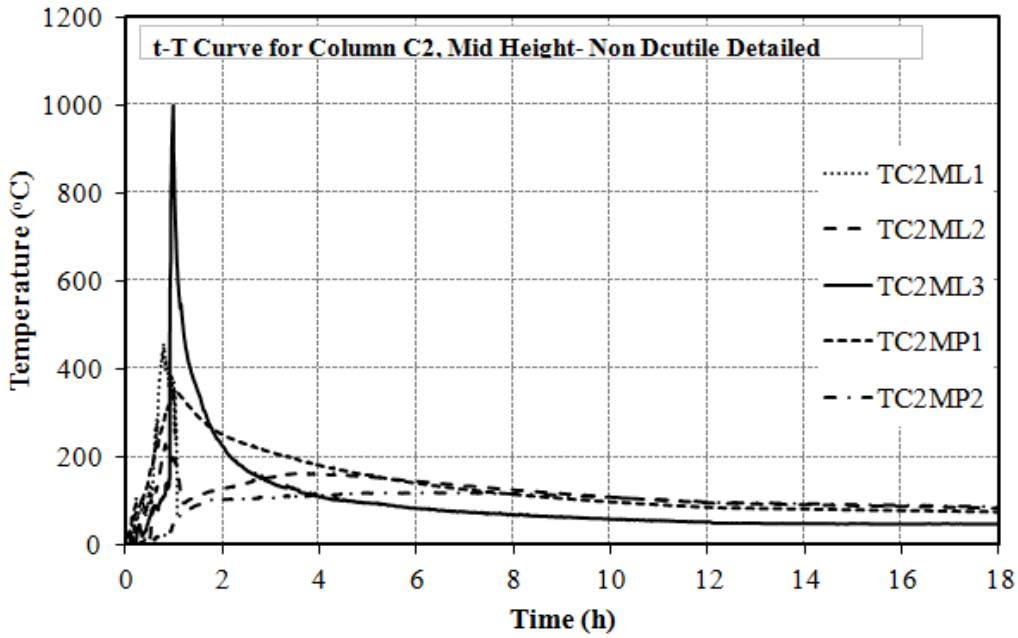

(c)

Fig.2.72: Comparison of the temperature development for different elements for the test frame with the ductile detailed frame tested by Kamath (2014). (contd.)

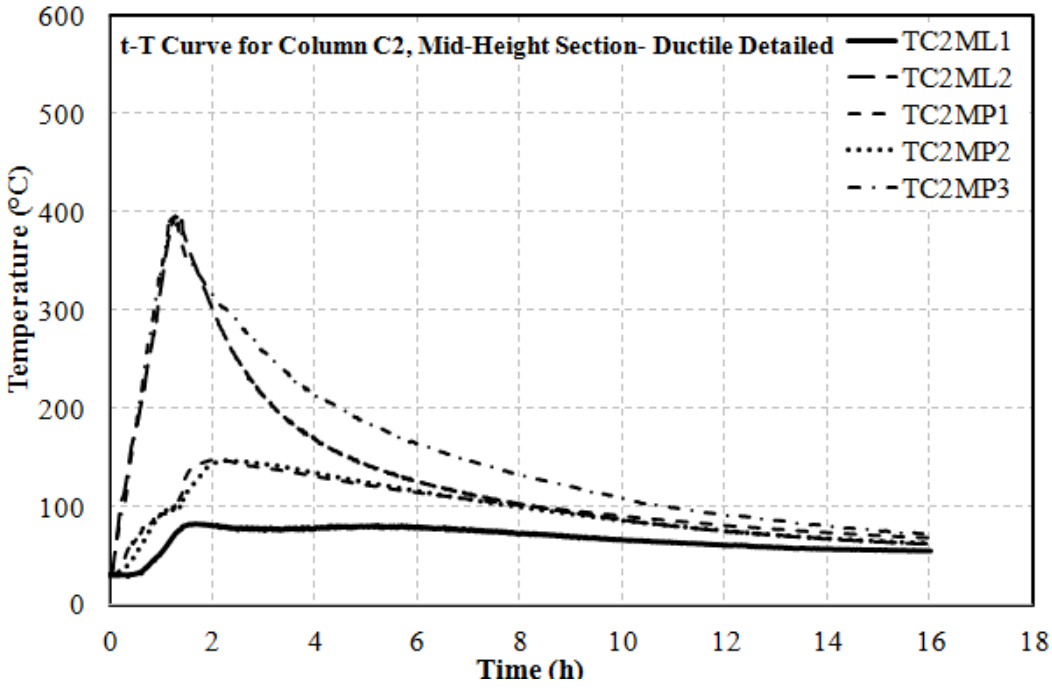

(d)

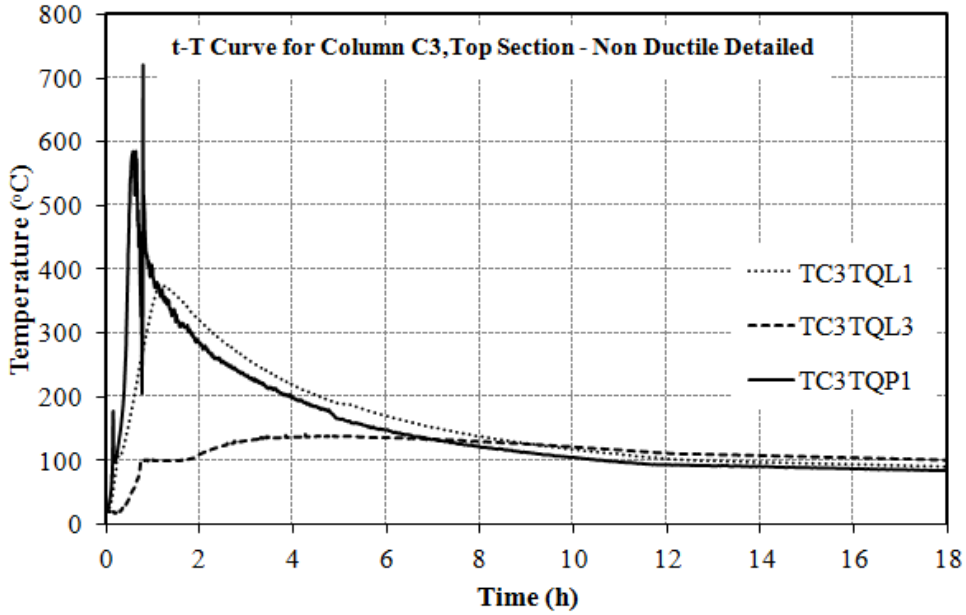

(e)

Fig.2.72: Comparison of the temperature development for different elements for the test frame with the ductile detailed frame tested by Kamath (2014). (contd.)

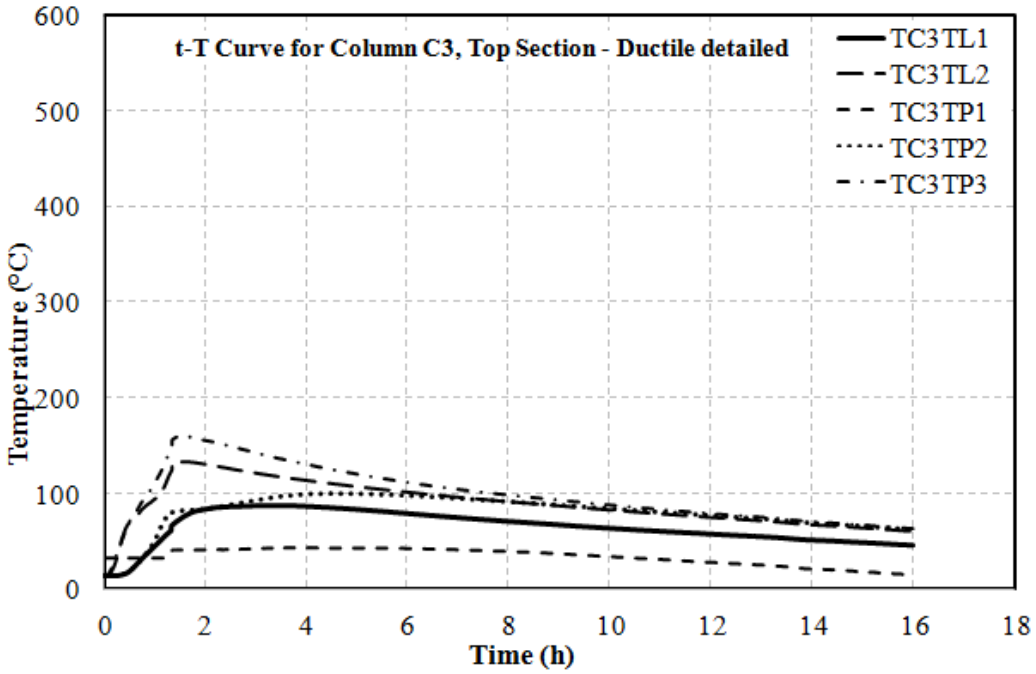

(f)

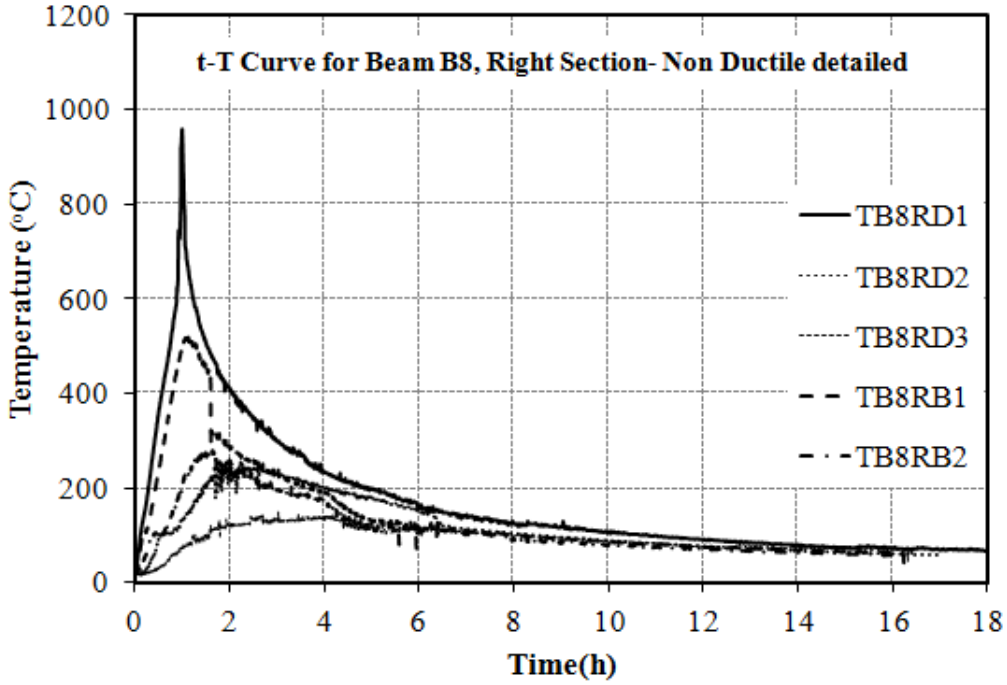

(g)

Fig.2.72: Comparison of the temperature development for different elements for the test frame with the ductile detailed frame tested by Kamath (2014). (contd.)

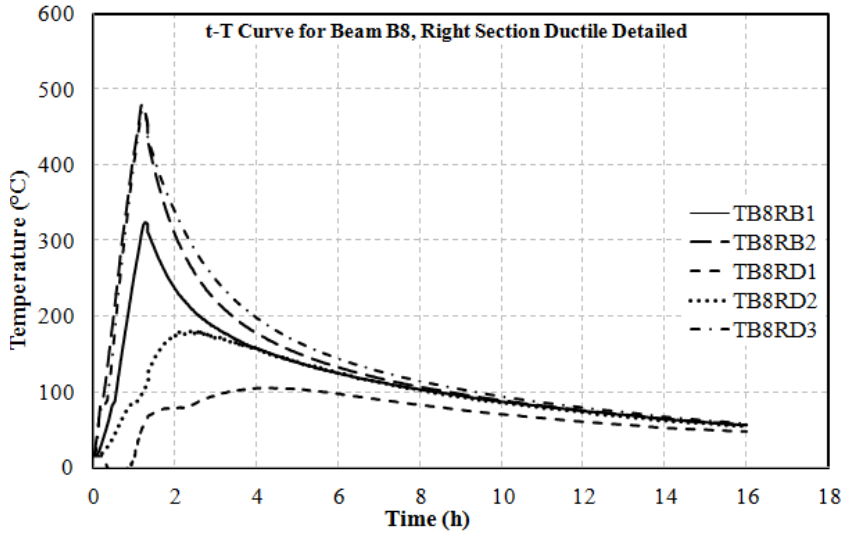

(h)

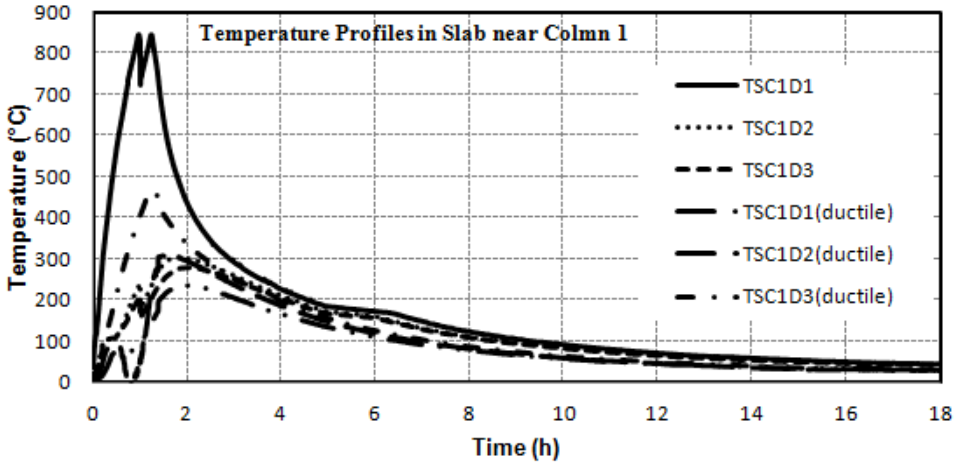

(i)

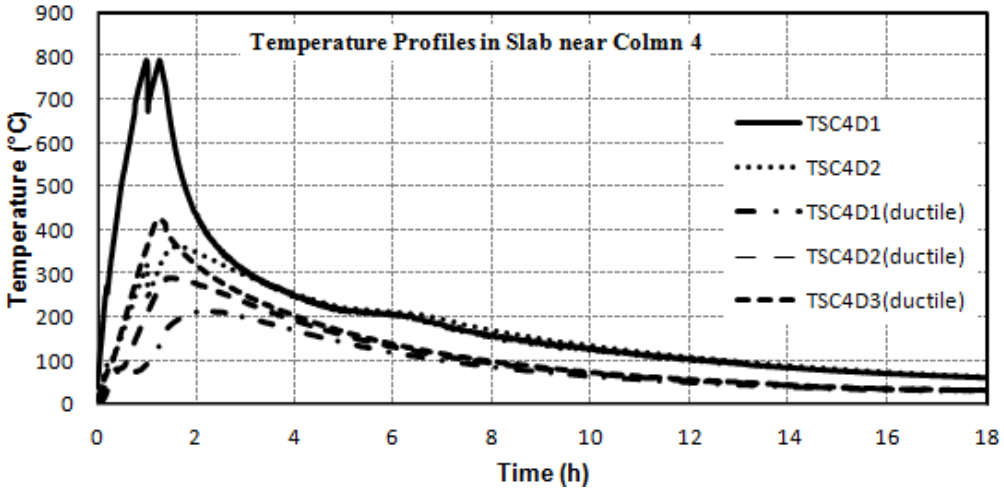

(j)

Fig.2.72: Comparison of the temperature development for different elements for the test frame with the ductile detailed frame tested by Kamath (2014).

2.4 CONCLUDING REMARKS

An account of a full scale fire test on a damaged RC frame has been presented. The aim of test was to assess the global behaviour of a damaged RC frame with non-ductile detailing and to generate a large database of results consisting of temperature profiles, displacements and strains and thereby to compare the results with a previous frame constructed with ductile detailing. Within the scope of the present study the following conclusions may be drawn. A novel test setup has been developed and tested which gives an understanding of the global behaviour of a concrete structure in post earthquake fire. The sequential loading was devised in the form of a three phase testing procedure – simulated earthquake loading facilitated by cyclic quasi-static lateral loads; followed by a compartment fire; and finally by subjecting the earthquake and fire damaged frame to a another cyclic loading to assess its residual capacity. The structure subjected to the tests was a symmetric RC frame and consisted of four columns, four plinth beams, four roof beams and a roof slab. The reinforced concrete frame was carefully instrumented with numerous sensors, consisting of thermocouples strain gauges, LVDTs. A large database of results consisting of temperature profiles, displacements and strains has been generated and salient observations have been made during each stage of loading.

CHAPTER – 3

BEHAVIOUR OF A MASONRY INFILLED RC FRAME UNDER POST-EARTHQUAKE FIRE

3.1 INTRODUCTION

Reinforced concrete buildings have been the emerging building stock since mid nineteenth century. Whereas the design philosophies for reinforced concrete evolved since then, the infills were always utilized in the construction of the RC framed structures. In these RC framed structures, exterior walls and/or interior walls/partitions are built as an infill between the frame members. These infills are usually regarded as non-structural architectural elements or functional elements. Among a number of materials, which are being used for constructing the infills in RC framed structures, masonry is the most famous and cost effective. Often it is used for infill walls in frame structures. In such cases, the masonry is mostly not considered to take part in the lateral force resisting system. For this reason masonry infill panels are considered as simply an environmental divider that forms the envelope of a building. Thus the usual practice in the structural design of masonry infill-frames has been to ignore the structural interaction between the frame and infill. It could be deduced that the infill contribution on the structural behaviour is nil except for its mass. However this would have been the case if a sufficient gap was being provided between the frame and the infill material. Contrary to this, the gaps between the infill and the frame members are usually nonexistent and the actual behaviour of infill frames observed during past earthquakes shows that their response is sometimes wrongly predicted (Kermani et al, 2008). The masonry infill panels intend to interact with the bounding frame when the structure is exposed to strong lateral actions like earthquakes. In some countries, masonry infill panels have been used as a means to strengthen existing moment-resisting frames, and there is evidence that they improved the performance of structures under severe earthquake loads (Amrhein et al, 1985). Several dozen investigations, which included both experimental and analytical investigations, of infilled structures have been conducted over the past 50 years, and important advances have been made for both steel and RC frames infilled with masonry (Al-chaar et al. 2002). However no study has been carried on the fire performance of pre-damaged masonry infilled RC framed structures.

In view of the work carried out on bare RC frames, as presented in the previous chapter, it also becomes necessary to study the effect of the masonry infills on the behaviour of an RC

structure. This chapter includes the experimental study on a full scale brick masonry infilled RC structure subjected to a fire following earthquake.

3.2 TEST ARRANGEMENT

The structure constructed and tested for the fire following earthquake was an RC frame sub assemblage similar to the structure tested and presented in chapter 2. The test frame was similar in all the aspects except that it was infilled with brick masonry. The test frame consists of four 300 x 300 mm columns at 3000 mm centres in both the N-S and E-W directions supporting a grid of four 230 x 230 mm beams underlying a 120 mm thick RC slab. Plinth beams were provided at the level of the ground floor and their size and configuration was similar to the roof beams of the building. All the elements of the test frame were cast monolithically with the column fixity at the base being provided by the termination of all the four columns into a 900 mm thick RC raft foundation of plan size 6900 x 8700 mm. A detailed description of the bare frame is given in chapter 2 of this thesis.

A normal strength concrete with 28 day cube strength of 30 MPa was employed in the present study. The concrete mix was designed using ordinary Portland cement of 43-grade, fine aggregate, coarse aggregate and tap water. The materials, in general, conformed to the requirements of the specifications laid down in the relevant Indian Standard Codes. The properties of the materials are described in detail in the previous chapter.

Solid burnt clay brick units were used for the infill walls. The brick units had a compressive strength in range of 13 MPa. The compressive strength was measured as per IS 3495 (Part 1): 1992 (BIS 1992). Cement- sand mortar in the ratio of 1:6 with a compressive strength 3.68 MPa was used as a binder for the brick units. The thickness of the masonry infill walls was kept as 230 mm which is a standard in Indian construction.

Figs. 2.6 to 2.9 give an insight into the instrumentation developed for the testing. The main aim of testing the RC frame sub assemblage was to derive an in depth understand of the behaviour of structures in post earthquake fire. Data which was planned to be recorded during all the phases of the tests for the structural aspects consisted of temperatures within the roof slab, columns, beams, and the compartment ; strains on the rebars embedded in all the structural elements of the RC frames; deflections of the roof slab at different points both vertical as well as horizontal. Extensive instrumentation was planned for the test frame and a number of sensors were installed to record the data.

3.3 FRAME TEST STAGE I: SIMULATED EARTHQUAKE LOAD TEST

Test procedure adopted in this study was same as in the previous study on bare RC frame for comparison purposes. A three phase test procedure was adopted and followed in testing the RC frame. The test procedure consisted of subjecting the frame to a simulated cyclic lateral load in a quasi-static fashion followed by a one hour compartment fire and after which the frame was subjected to a residual load test. The simulated cyclic lateral load was applied onto the RC frame using two displacement controlled double acting hydraulic actuators acting in tandem with each other against a strong reaction wall. Fig. 3.1 shows the RC frame before the simulated earthquake load test.

Fig. 3.1 RC test frame before the test

The RC frame sub assemblage was subjected to a predefined seismic damage by subjecting the test setup to a simulated cyclic lateral load in a quasi-static manner with the help of two displacement controlled double acting hydraulic actuators. The jacks were having a capacity of producing the displacement of 300 mm in either direction. The initial seismic damage was achieved by inducing a pre-planned lateral displacement through applying lateral cyclic load corresponding to the collapse prevention structural performance level (S-5) of FEMA 356:2000 (FEMA 2000) as done in the previous study. The damage was kept same in order to study the effect of masonry infill on the behaviour of the RC frames.

The test was started by subjecting the frame to cyclic displacements starting with 2 mm. No sign of cracks or distress was observed in any structural member or masonry infill till the displacement of 6 mm. At the displacement of 8 mm corresponding to a drift of 0.21%, the cracks started getting developed in the masonry- beam interface. At the displacement of 10 mm (0.27 % drift), cracks started developing on infill walls. A brick in the in-plane wall was observed to be cracked in 10 mm (pull) displacement cycle. The mortar also started to get loosened up in 10 mm cycle. Cracks in in-plane walls started progressing in diagonal fashion towards the corners in 12 mm cycle. Spalling of mortar also started with 12 mm displacement which corresponds to 0.32 % drift ratio. However no signs of distress were found in any of the structural member of the RC frame. The cracks in the masonry started widening in 12 mm cycle and progressed in diagonal fashion towards the corners. No cracks were observed in out of plane walls and structural elements. With a displacement of 25 mm (0.67% drift) a number of bricks cracked with wider cracks.

Separation of the bottom and top layers of the bricks in the in-plane masonry wall started in 30 mm cycle (0.81 % drift). With this displacement cycle the cracks in the masonry walls started widening. The cracks were formed in a diagonal fashion with symmetry followed in push and pull events of the cycle. At a drift of 0.81 %, cracks were observed in beams and columns also. Hairline cracks were formed in beam B1, B5, B3 and B7 at beam column joints. Flexure cracks were also observed in column C3 at the secondary beam joint.

40 mm (1.08% drift) displacement cycle caused the shear cracks to get developed in beam B1 and B3 which were placed along the direction of force. The width of these shear cracks in beam B1 at beam column joints near column C1 and C2 was measured to be 0.1 mm. A 0.2 mm wide flexural crack was also observed at the centre of beam B1and B3. At column C3 a 1 mm wide shear crack was measured in beam B3. Cracks in the masonry started widening in this displacement cycle and spalling of mortar was also observed.

More number of bricks cracked in 50 mm (1.37 % drift) displacement cycle with chunks of mortar coming out from the bonds of masonry in the in-plane walls. The out of plane walls were still intact with no signs of distress and cracks. The diagonal cracks in the two opposite in-plane walls widened and extended more towards the corners of the walls. A new 1.2 mm wide shear crack was measured in beam B3 at column C3. This crack originated from the bottom corner of the beam and met the top section at 100 mm from the column C3. The first crack in slab appeared in this cycle and 0.06 mm wide crack was measured in slab parallel to beam B8.

Diagonal cracks in the in-plane walls started widening in the 60 mm displacement cycle (1.6% drift). A 1.5 mm wide shear crack was observed in beam B1 at column C1 and 1.4 mm wide crack at column C2. At the displacement of 70 mm i.e. 1.9 % drift, shear cracks in beam B1 and B3 traversed into the brick walls also. Flexure cracks also started widening.

At the displacement of 90 mm which corresponded to a drift of 2.4%, loss of cover in beam B1 was observed at column C1, the shear cracks widened abruptly. Similar observation was noticed in beam B3. More number of cracks in slab were observed which were oriented perpendicular to the loading.

Complete shear failure of beam B1 and B3 was observed at the displacement of 100 mm (2.7 % drift). Crushing of concrete was observed and the reinforcement was exposed at this drift. Further displacement caused widening of cracks. At the displacement of 120 mm corresponding to a drift of 3.2 %, buckling of longitudinal reinforcement was observed. Shear stirrups were also observed to buckle at this drift. At the end of the loading excursion it was noticed that the out-of-plane masonry walls were unaffected with no visible damage on any of the two walls. Figs. 3.3 and 3.4 show the in-plane wall after the test. Figs. 3.5 and 4.6 show the shear failures in beams B1 and B3. The frame was subjected to a total of 23 push pull displacement cycles and targeted for 150 mm displacement. A maximum load of 565 kN was observed at a displacement of 120 mm. A load of 540 kN was measured at the lateral displacement of 150 mm. Fig. 3.7 shows the load-displacement hysteresis.

Fig.3.2 gives a comparison between the load- deflection behaviour of the test frame with the bare frame. The presence of infill increased the lateral load carrying capacity of the test frame. The peak load was obtained at almost same displacement i.e. 120 mm in both the frames. At a displacement of 20 mm the load carrying capacity of infilled frame was 305% of the bare frame. As the masonry started cracking, the load carrying capacity as compared to the bare frame started reducing. At the displacement of 40 mm the lateral capacity of the test frame was 266 % of the bare frame which further reduced to 212 % at 60 mm. At the peak displacement of 150 mm the lateral strength of the frame was 168% of the capacity of bare frame at the same displacement.

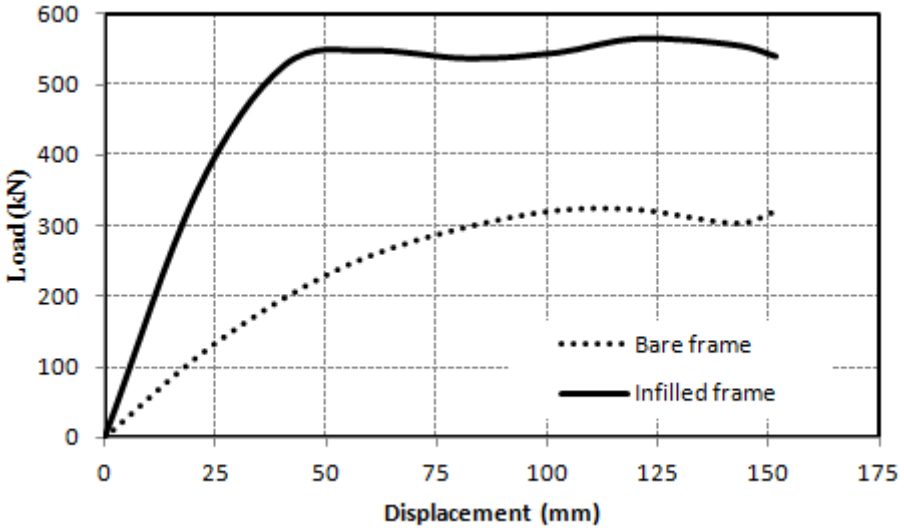

Fig.3.2: Comparison of the loading envelops of the two test frames.

Fig. 3.3 View of the In-plane wall after the test

Fig. 3.4: A close up image of In-plane wall after the test

Fig.3.5: Shear failure in beam B1 with buckled reinforcement

Fig 3.6: Shear failure in beam B3.

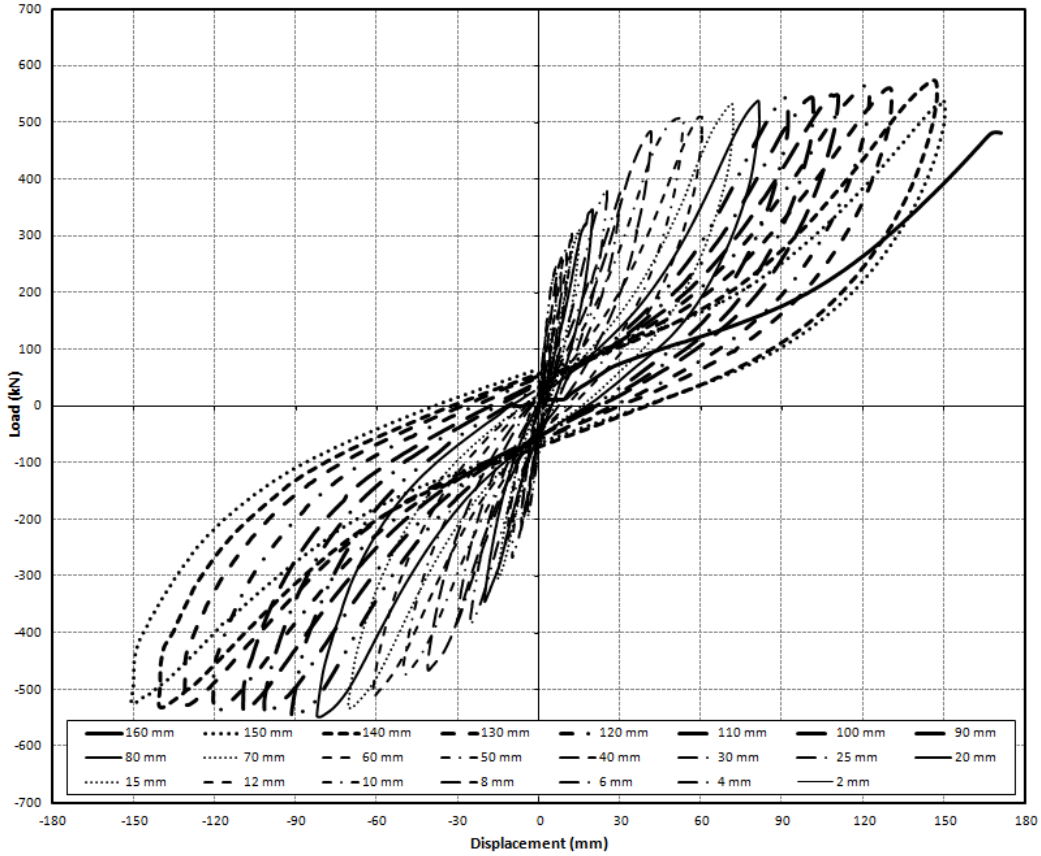

Fig.3.7: Load displacement hysteresis curve of the test frame.

3.4 FRAME TEST STAGE II: FIRE TEST

After inducing the damage corresponding to a drift of 4%, the test frame was subjected to a one hour designed compartment fire. The design parameters of the fire and the compartment size were kept same as in the previous test on the bare RC frame. Fig 3.8 shows the test setup before the fire test.

Fig. 3.8: RC frame with fire enclosure.

Figure 3.9 shows the temperatures inside the compartment during the fire and cooling phases of the test. These temperatures were obtained at five different locations inside the compartment as shown in Fig. 4.8. Unlike in the bare RC frame, the attainment of flashover was delayed in this test. A full blown flashover was attained in 10-11 minutes after the start of the fire. In case of the bare frame, the same was attained in 4-5 minutes. The delay in the flashover can be attributed to the moisture evolution from the masonry walls which delayed the rise in temperature inside the compartment. A maximum temperature of 1363 $^{\circ}$C was registered inside the compartment at 62 minutes from the ignition. The temperature thus attained was almost similar to what was attained during the fire test on the bare frame. The fuel supply was stopped after a period of 60 minutes from the ignition. Subsequently, the temperature dropped down to about 500 °C after the lapse of 90 minutes indicating that the test frame experienced a sharp decline in temperature during the cooling phase within a period of about 30 minutes after the oil supply was shut.

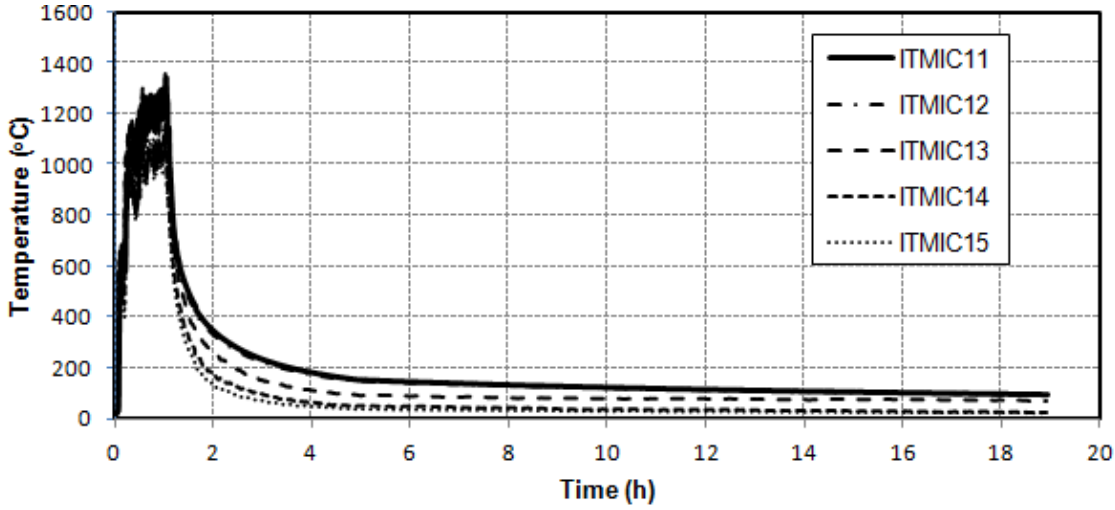

(a)

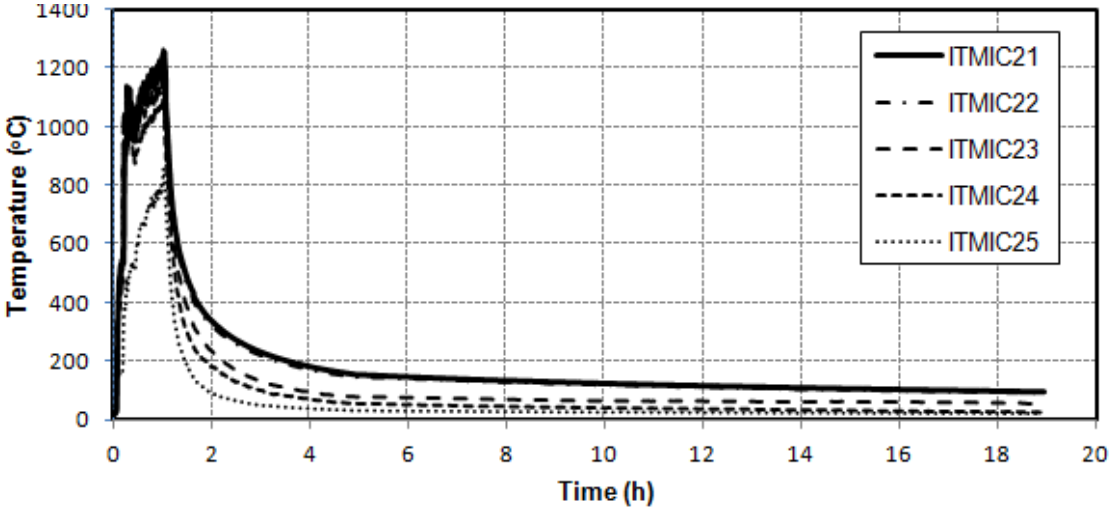

(b)

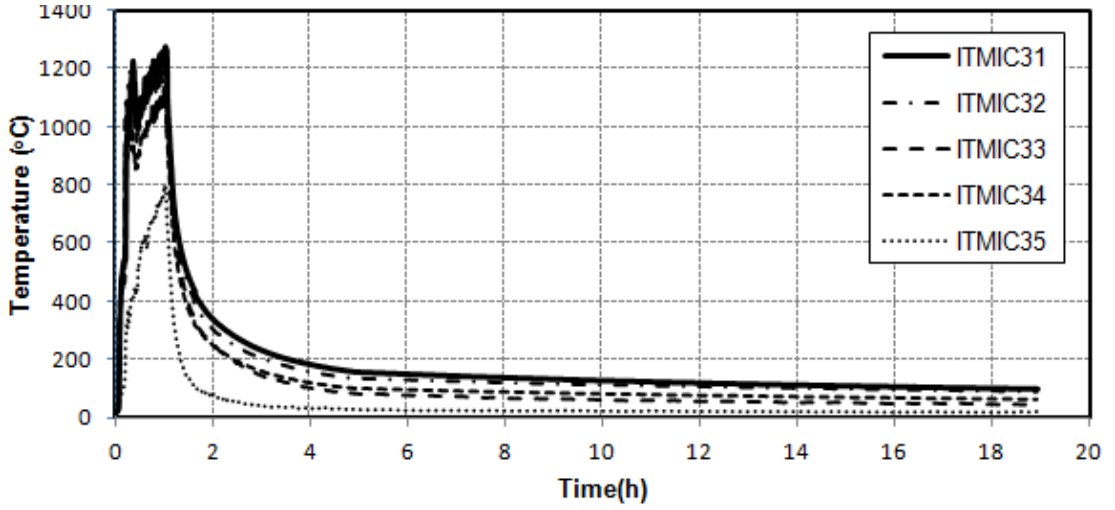

(c)

Fig.3.9: (a-e) Variation of temperature within the compartment.(Contd.)

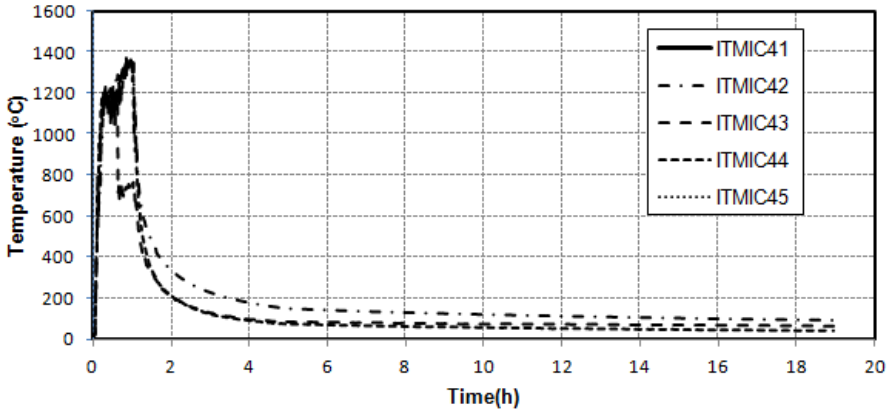

(d)

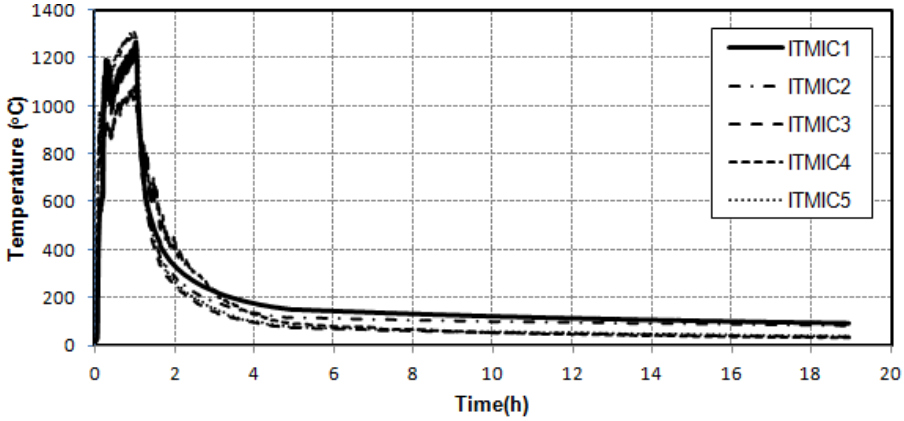

(e)

Fig.3.9: (a-e) Variation of temperature within the compartment.

3.4.1 Observations during and after the fire

The slab began to spall within 4-5 minutes of the test. The spalling aggravated at about 8-9 minutes after ignition that was just before the flashover. As in case of bare frame intense bullet shot sound was heard around this time. The spalling aggravated at 11 minutes which corresponded to the compartment temperature of about 1250 °C. The spalled concrete from slab can be seen lying on the floor in Fig. 3.10.

Fig. 3.10: Spalled concrete from the slab of the RC frame: (left) before flashover; (right) at the end of the test

After the fire test, the RC test frame was inspected to have an idea about its behaviour and the behaviour of different structural and non structural elements in fire. It must be noted that among all the structural elements slab soffit was directly exposed to fire. The columns C1 and C4 were insulated with the brick infill walls with only corners exposed to direct fire. Similarly the columns C2 and C3 were also insulated except with bottom 1m on one of the faces which was directly exposed to fire due to the provision of ventilation window. The plinth beams were insulated, so were the top beams. Only a small portion of about 110 mm (towards the inner side of the enclosure) of the top beams was exposed to direct flame.

Figure 3.11 shows the view of the slab soffit after the fire test. Extensive spalling was observed to have occurred in slab. This was due to the direct exposure of the slab to the flame which caused development of very high temperatures across the slab cross section. The spalling led to the exposure of the reinforcement to the direct flame. The spall depths ranging from 6 mm to 48 mm were observed in the slab.

Fig. 3.11 Spalled soffit of the slab.

Extensive thermal cracking, as seen in Fig. 3.12, was observed in the unspalled portions of the slab. Spalling also exposed some deeper flexural cracks in the slab cross section as seen in Fig. 3.13.

Fig.3.12. Thermal cracking in slab soffit

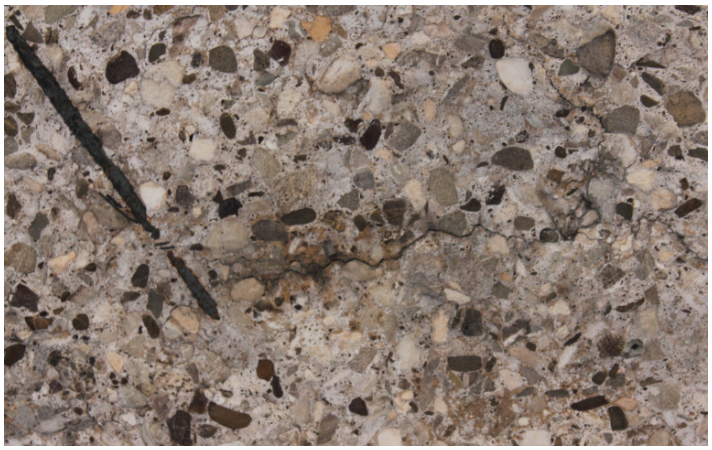

Fig.3.13: Exposed reinforcement in slab and the flexural cracks.

The masonry was found to be burnt and sintered on the wall opposite to the ventilation opening. The solidified molten mass was also observed on the masonry walls as seen in the Fig. 3.14. The masonry walls were intact even after the fire.

Fig. 3.14: Solidified molten mass from masonry walls

As stated earlier in this section that the columns and beams were mostly insulated with the brick infills and thus it was not possible to examine them for the damage due to the fire.

However the exposed portions of columns C2 and C3 had underwent thermal cracking and thermal cracks having a width of .8 mm were noticed on these faces. Fig.3.15 shows the thermal cracking on the exposed face of the column C2.

Fig.3.15: Thermal cracking in Column C2

Similar thermal cracks were also observed on the exposed face of column C3. The corners of the columns C1 and C4 were deteriorated and spalling was noticed in both the columns.

Fig. 3.16 shows the vertical deflections of the slab during the fire test including the cooling phase. The figure shows the variation in deflection with time illustrating the deflection profiles of the slab at four locations. As was observed in the bare frame tested and reported in previous chapter, a rapid downward deflection was observed initially. This phase of deflection is likely dependent on thermal bowing of concrete which is influenced by increasing thermal gradients with time (> 350 ^{o}C) and the resulting differential thermal expansion of the concrete through its thickness. The behaviour of the slab in this frame was almost similar to that of the bare frame. However the deflections were low. While as the centre of the slab was found to have sagged by 21 mm in bare frame, it was only 8 mm in the masonry infilled frame.

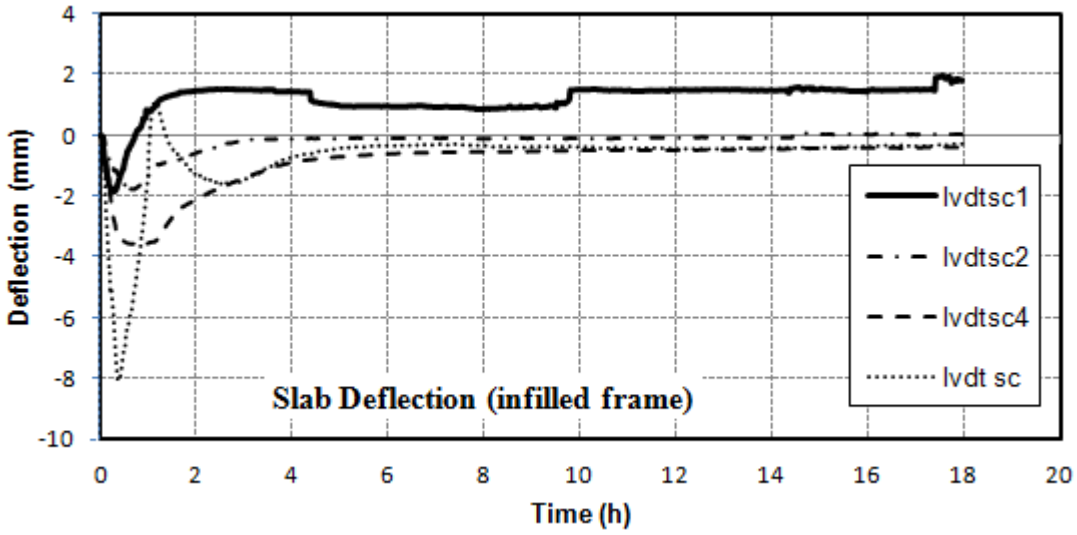

Fig.3.16: Deflection profile of the slab in fire

Columns were also instrumented with displacement transducers to capture the axial deformation during the fire test. The axial deformations are shown in Fig. 3.16. All the columns underwent thermal expansion as the temperatures increased, however the expansion was also very less as compared to the bare frame. The lower displacements can be explained due to the lower temperatures attained in the columns as will be explained in later sections. The columns underwent thermal expansion of about 1.2 to 15 mm at about 60 minutes after the ignition. In the cooling stage the columns again seem to come back to normal before undergoing the decrease in length. While a net reduction of about 0.6 mm was observed in column C1, a net expansion of 1 mm was registered in column C3. Column C4 almost regained the equilibrium position. This expansion of the column in early stages is due to the thermal expansion of concrete and the steel bars and in the later stages, the columns contract because of the deterioration of the material's mechanical properties.

Roof beams were also instrumented to measure the vertical displacements during fire. Fig. 3.18 shows the vertical deflections of the midpoints of the roof beams during the fire. While as the beams B7 and B5 experienced rapid sag during the fire test, the beams B6 and B8 underwent hogging. This behaviour could be attributed to the composite action of the beams and slab. The beam B7 had a maximum sag of 6.2 mm and recovered in cooling stage to have a permanent hog of about 1.9 mm. the beam B5 underwent a sag of 1.9 mm during fire and experienced a permanent hogging deflection of 1 mm at the end of 18 hours. Similarly the beams B6 and B8 underwent a maximum hogging deflection 2.2 mm and 4.1 mm respectively during the fire and recovered to have residual hogging deflections of 0.2 and 1.8 mm respectively in the cooling stage.

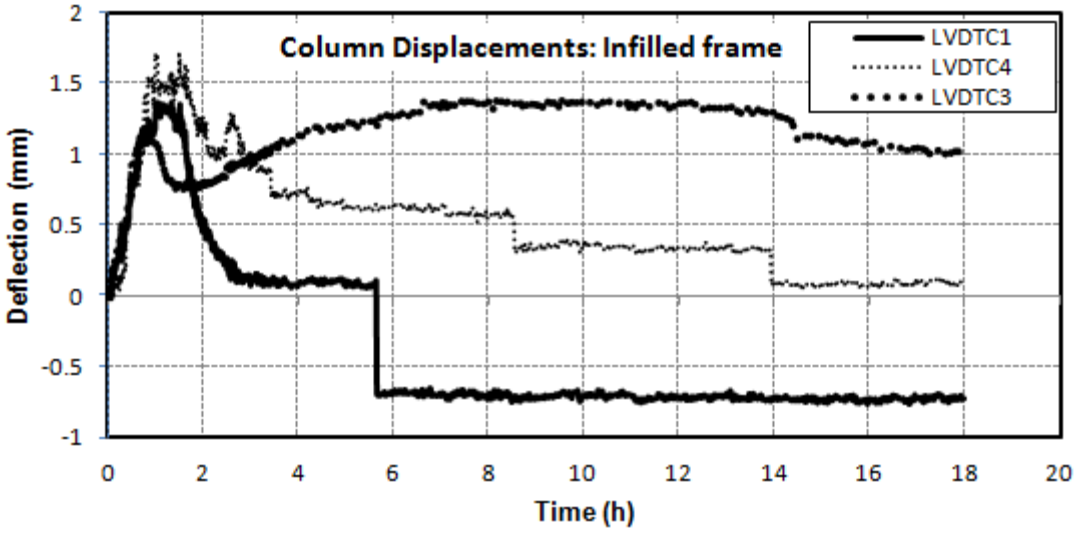

Fig.3.17: Axial deflection profiles of the columns in fire

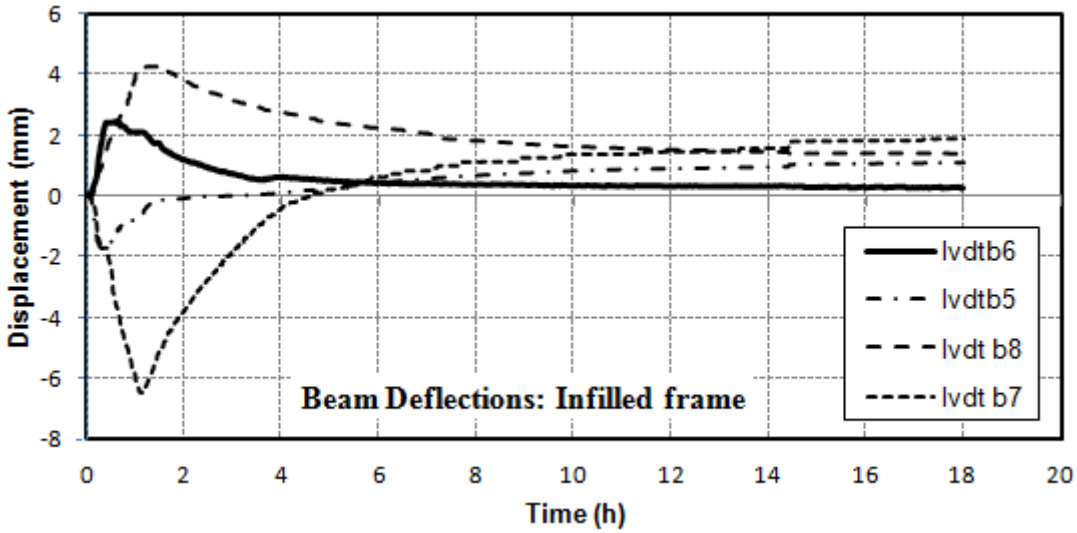

Fig.3.18: The deflection profiles of the roof beams in fire.

3.4.2 Temperature Histories of the Structural Elements

Fig.3.6 shows the instrumentation details of different elements of the test frame. The plinth beams, roof beams, columns and the slab were instrumented with thermocouples to record the temperatures during the fire and the cooling stage. The recorded temperature data is presented in following sections to understand the thermal behaviour of the elements.

3.4.2.1 Plinth Beam temperatures

Fig.3.19 (a-m) shows the time- temperature variations from within the plinth beams B1, B2, B3 and B4. The curves show a record of temperatures during the fire test and the cooling stage. It is evident from the temperature record of these beams that very lower temperatures were attained in the plinth beams as compared to the plinth beams of the bare frame. While as

the maximum temperature in beam B1 of the bare frame was 1200°C, the maximum temperature in beam B1 in the masonry infilled frame was only 68 °C. Similarly the maximum temperatures in beams B2, B3 and B4 were only 33, 5.5 and 6.6 % respectively of the maximum temperatures attained in plinth beams of the bare frame. An important observation from the curves points to the time at which the maximum temperature was attained in these beams. The maximum temperature was reached between 2-4 hours from the time to ignition, whereas the maximum was attained at almost 1 hour in bare frame. This phenomenon can be attributed to the insulating properties of the brick masonry units. The masonry units not only provided the insulation and slowed down the penetration of the heat into the beams.

3.4.2.2 Roof beam temperatures

Fig. 3.20(a-s) shows the temperatures recorded at various sections within the roof beams along the two lateral directions. The beam B5 witnessed a maximum temperature of 485 °C at 1.3 hours from the time of ignition. This temperature was recorded at the midpoint of the beam. Similarly the maximum temperatures at different locations in beam B5 were 250, 400, 277 and 291 °C at left, left quarter, right quarter and right sections respectively. This beam also witnessed lower temperatures than the beam B5 of the bare frame.

Beam B6 was positioned directly above the ventilation opening in the fire compartment. A maximum temperature of 474 °C was measured in right section (ITB6RD1) of this beam. At the other sections the maximum temperatures were of the order of 432, 140, 300 and 150 °C respectively at left, left quarter, midsection and right quarter sections of the beam.

Beam B7 also witnessed relatively lower temperatures than what was recorded in the bare frame. The maximum temperature recorded in the beam was 550 °C recorded at the midpoint of the beam (ITB7MD1). The temperature gradients were also lower than those recorded in the bare frame elements.

Beam B8 was the worst hit roof beam in the RC frame without infill walls with the maximum temperatures reaching about 960 °C. however in the frame with infill walls the maximum temperature reached up to 525 °C which was recorded at the midpoint of the beam. Though the flame was driven towards the beam B8 but the insulating properties of the brick masonry stopped the penetration of the heat.

3.4.2.3 Column temperatures

Fig. 3.21 (a-r) shows the temperatures recorded at various sections within the columns. Among all the structural elements the columns were least affected by the fire. The maximum temperatures recorded in the columns C1, C2, C3 and C4 were 101, 140, 376 and 107 ^{o}C respectively. The relatively higher temperatures in columns C2 and C3 were due to the fact that the lower 1m of one of the faces of these columns was exposed to direct flame. Moreover the maximum temperatures in the columns were attained between 2-4 hours after the ignition. This is due to the thermal conductively of the masonry units. The respective temperatures in the columns of the bare frame were 441, 995, 716 and 622 ^{o}C. The lower temperatures in the main structural elements of the test frame were also reflected by the lower thermal damage and deterioration.

3.4.2.4 Slab temperatures

The time-temperature curves for the nine sections of the slab are shown in Fig. 3.22(a-i). The maximum temperatures of 350, 564, 289, 531, 1083, 600, 586, 840, and 800 ^{o}C were recorded at the selected nine locations of the roof slab. The thermal gradients obtained in the slab were very high which led to the spalling of the concrete.

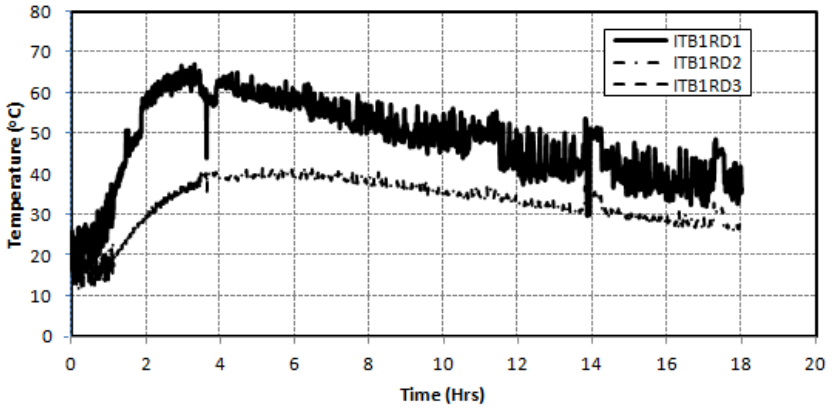

(a)

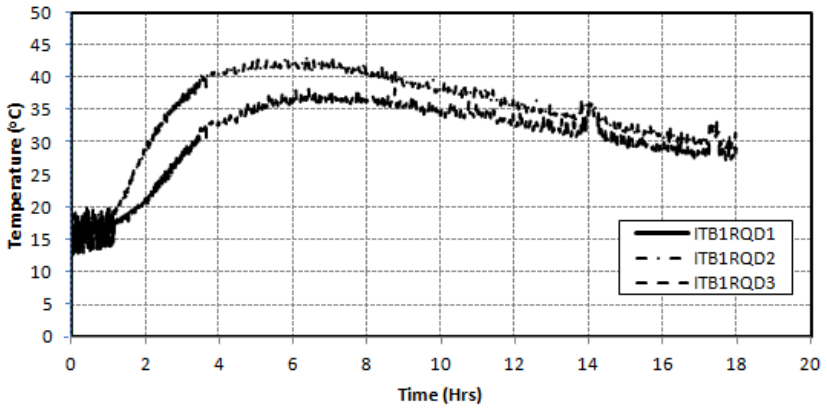

(b)

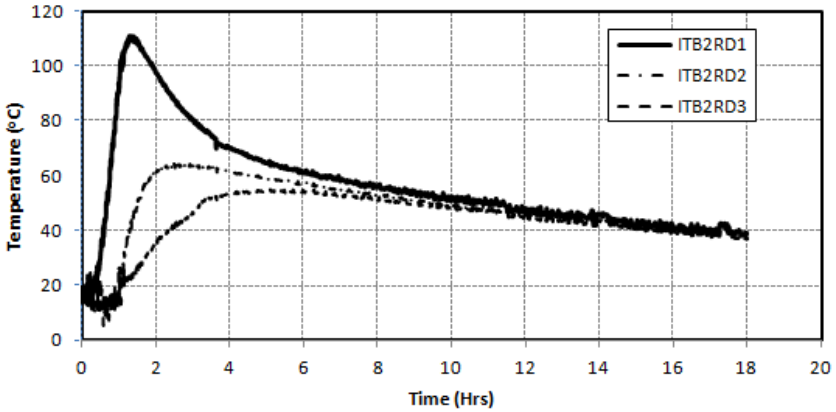

(b)

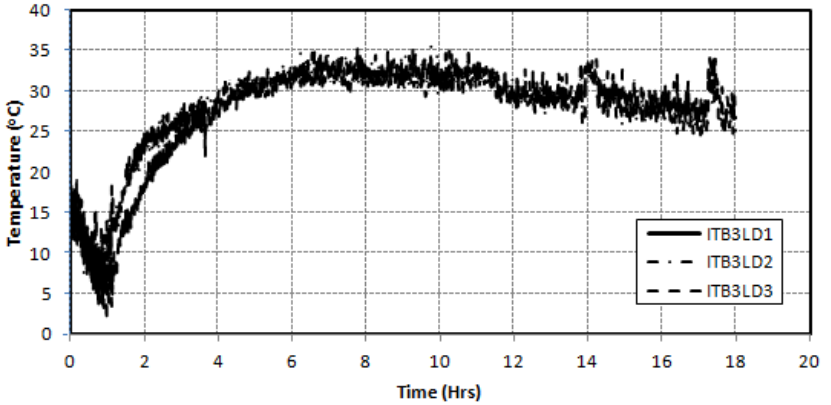

(d)

Fig. 3.19: (a-m) Time-Temperature curves for Plinth beams (Contd.)

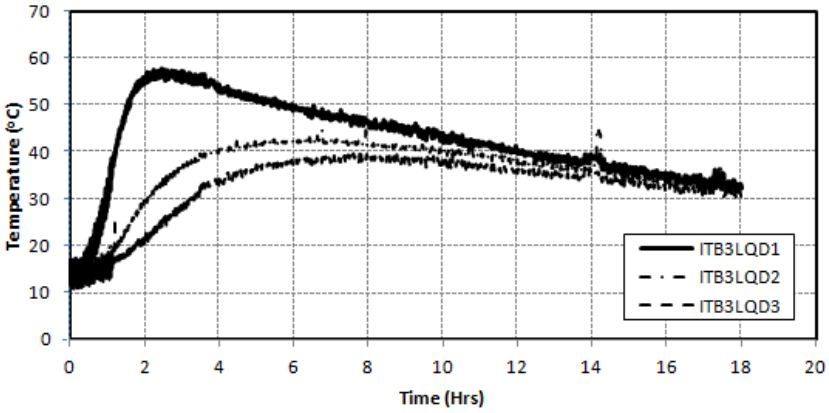

(e)

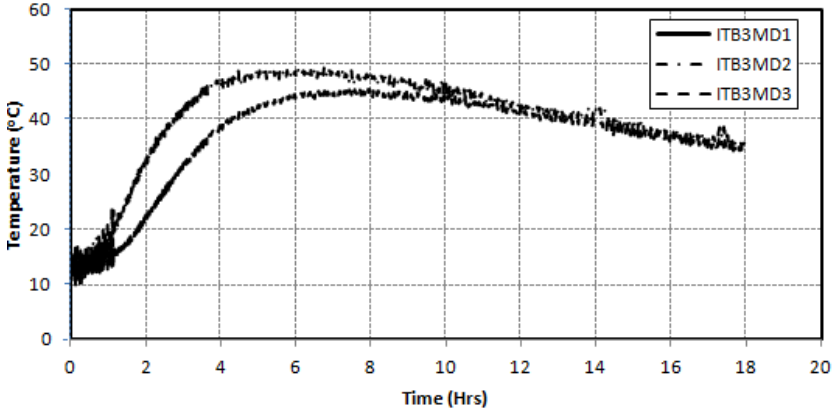

(f)

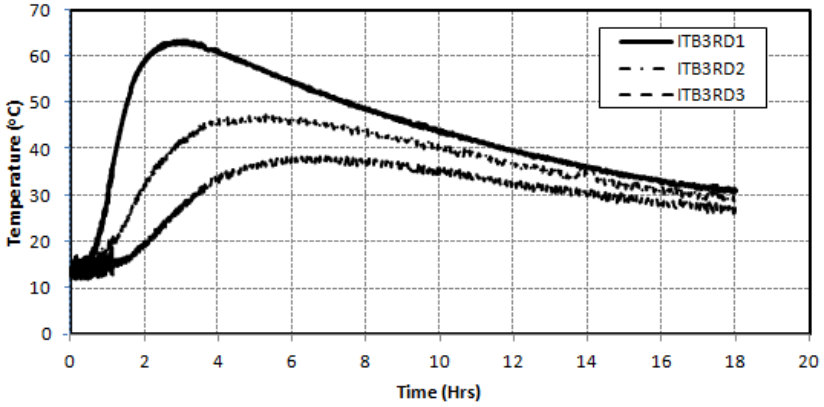

(g)

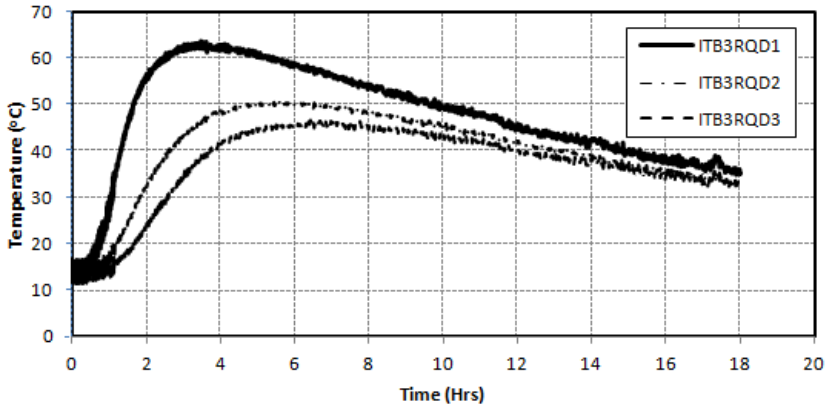

(h)

Fig. 3.19: (a-m) Time-Temperature curves for Plinth beams (Contd.)

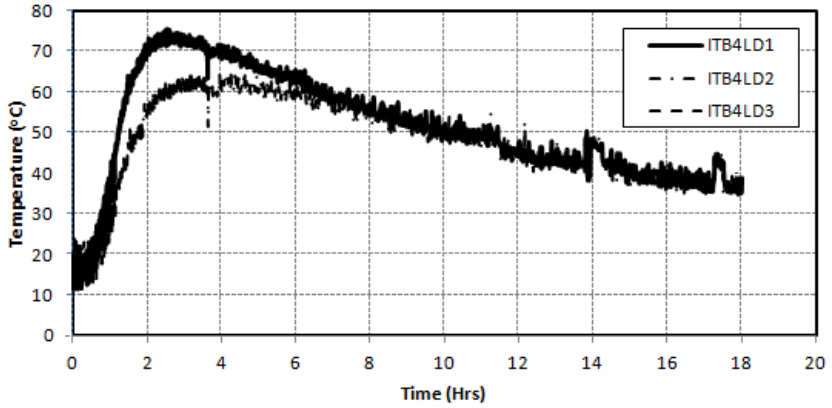

(i)

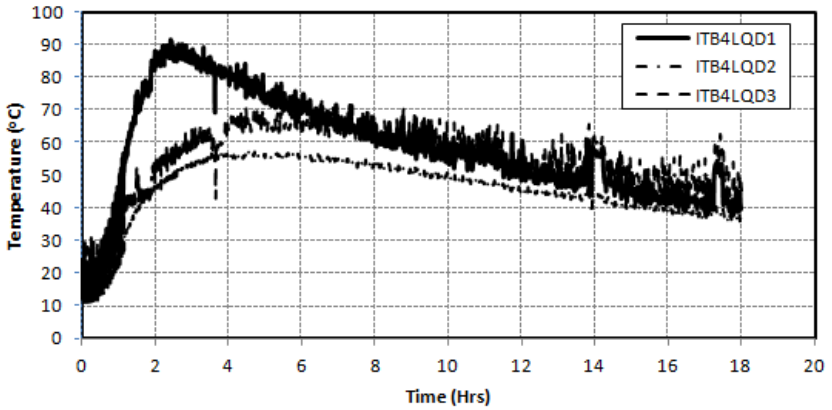

(j)

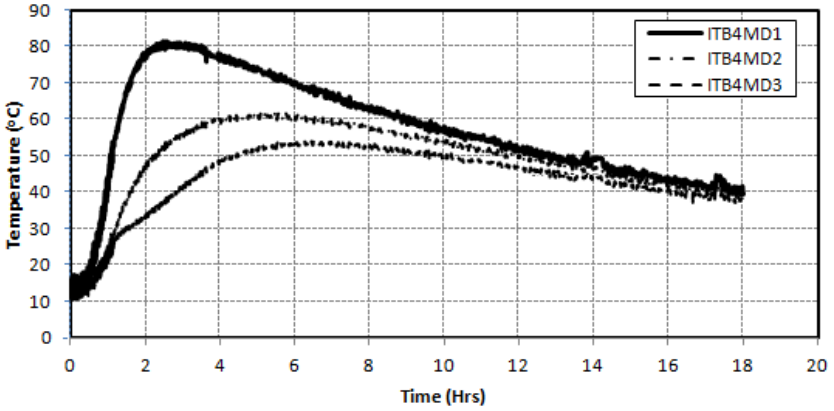

(l)

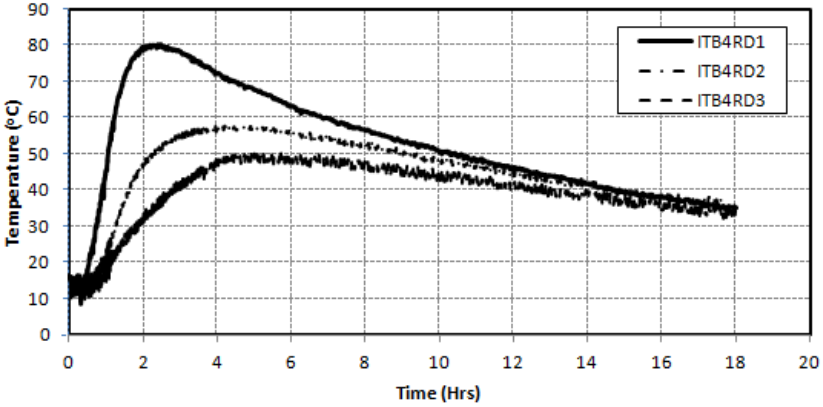

(m)

Fig. 3.19: (a-m) Time-Temperature curves for Plinth beams.

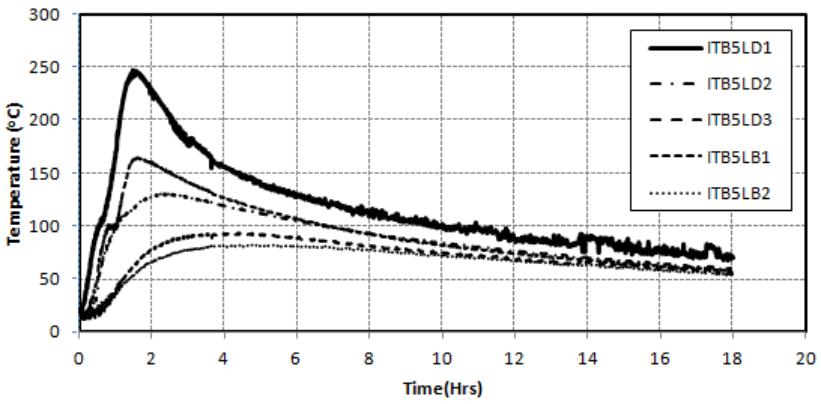

(a)

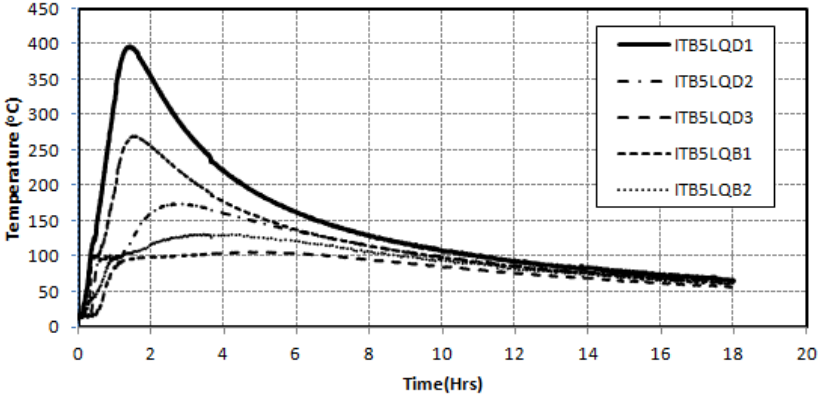

(b)

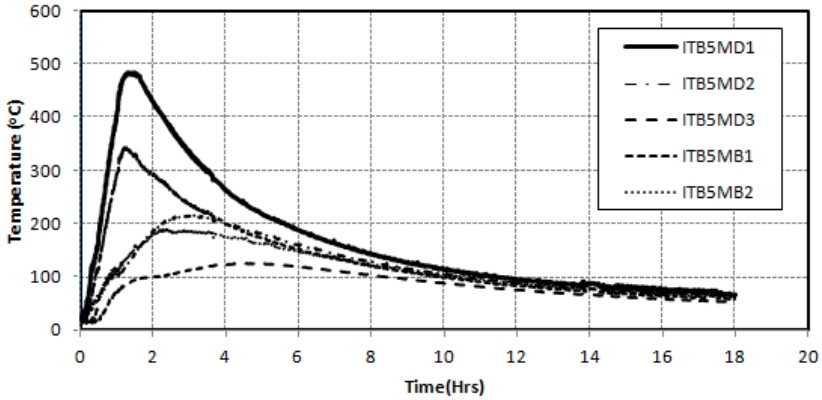

(b)

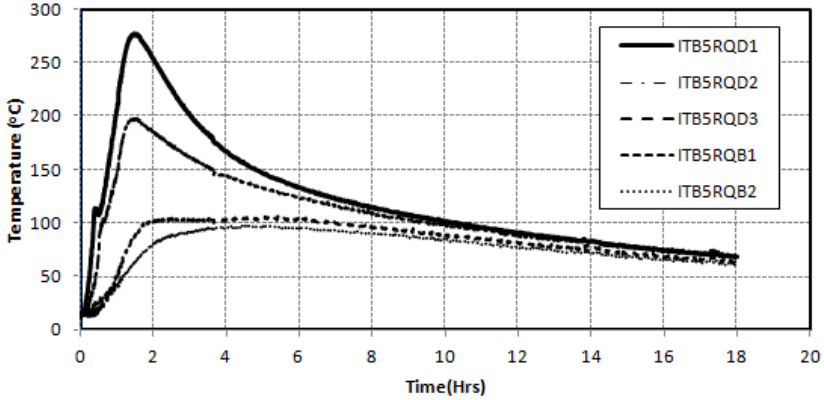

(d)

Fig. 3.20: (a-s) Time-Temperature curves for roof beams (Contd.)

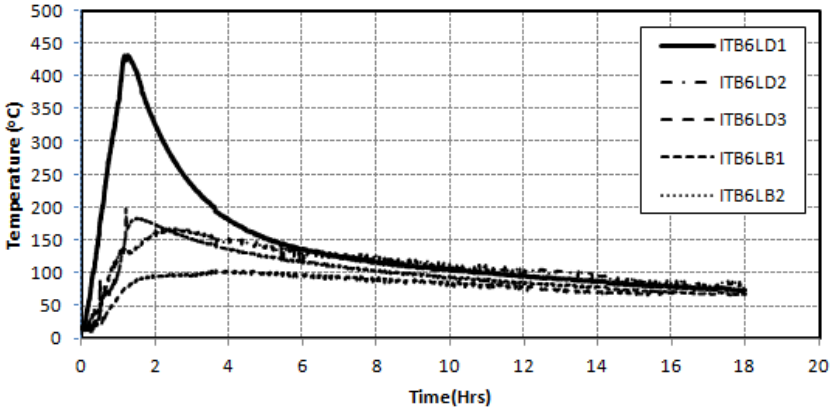

(e)

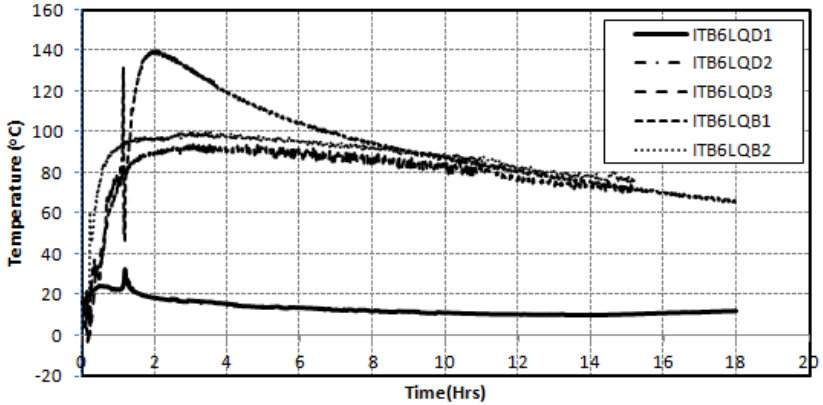

(f)

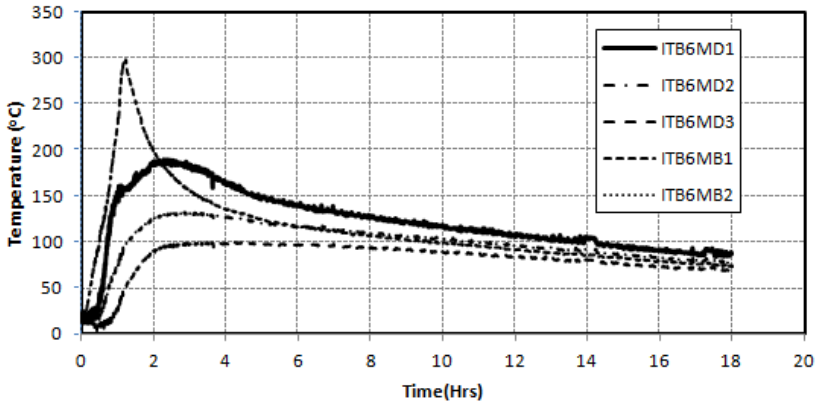

(g)

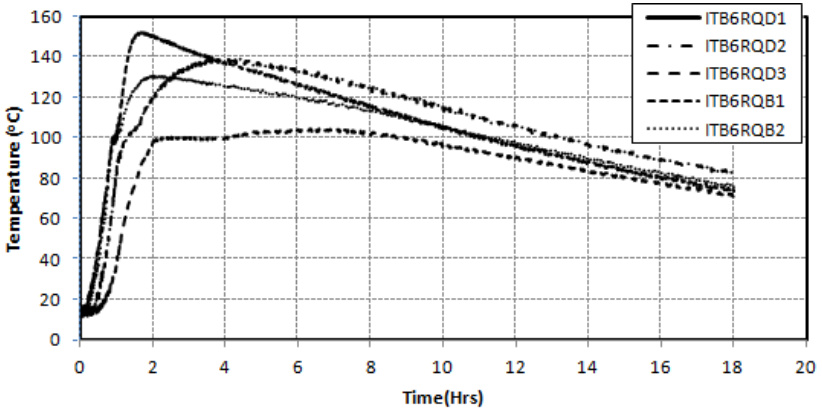

(h)

Fig. 3.20: (a-s) Time-Temperature curves for roof beams (Contd.)

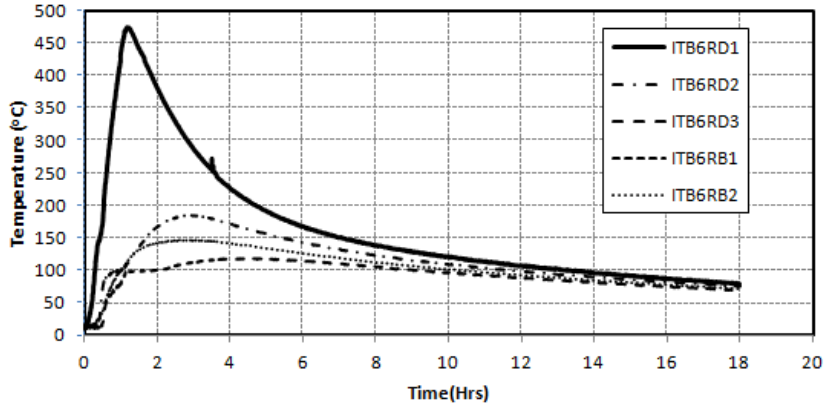

(i)

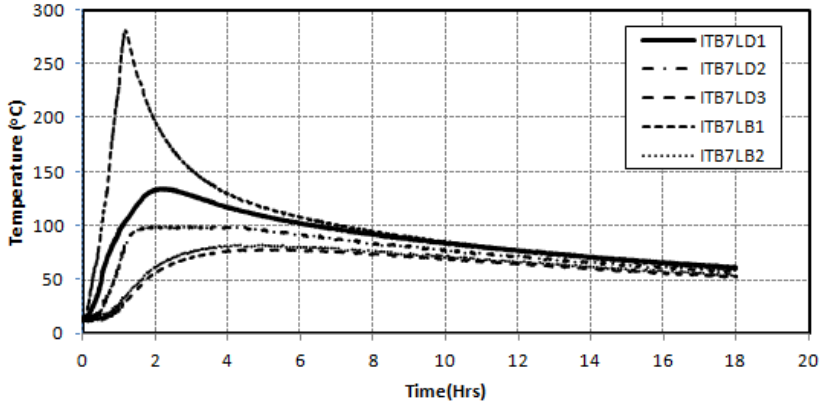

(j)

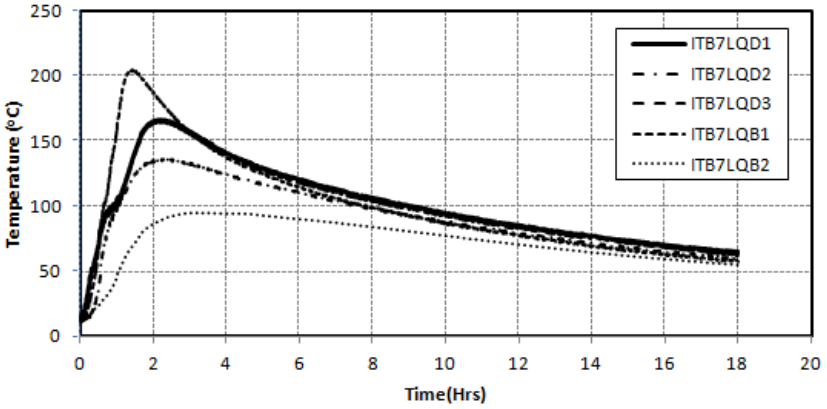

(k)

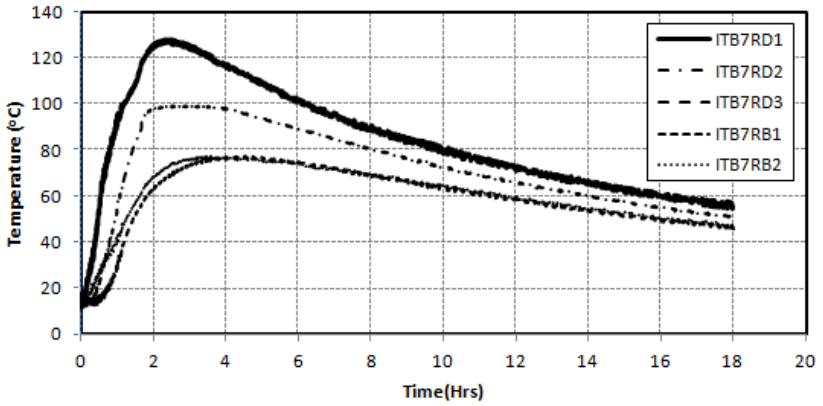

(l)

Fig. 3.20: (a-s) Time-Temperature curves for roof beams (Contd.)

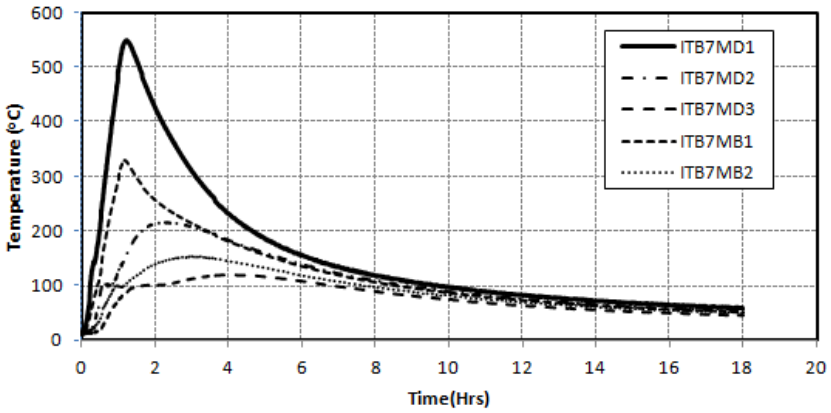

(m)

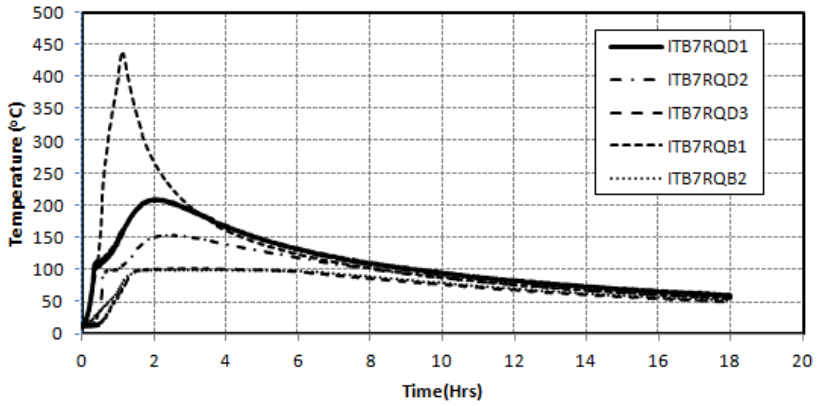

(n)

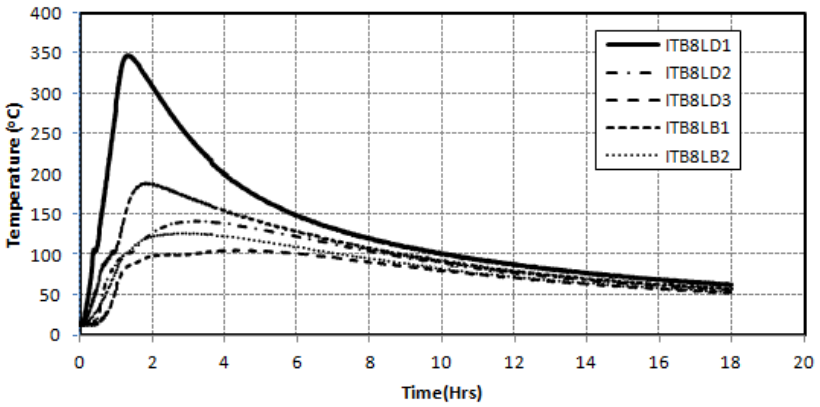

(o)

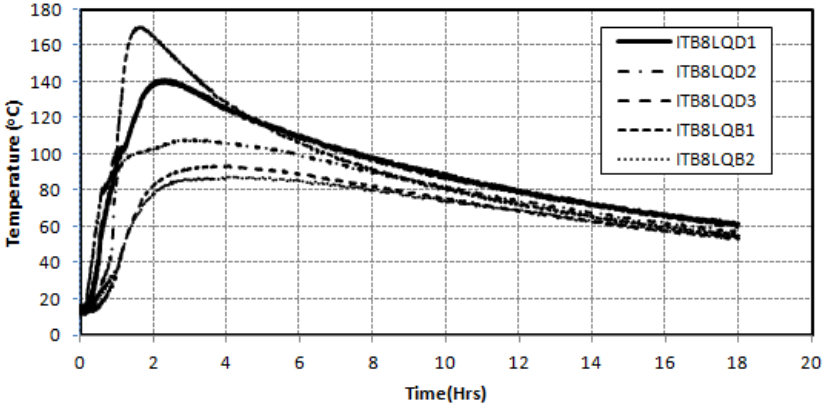

(p)

Fig. 3.20: (a-s) Time-Temperature curves for roof beams (Contd.)

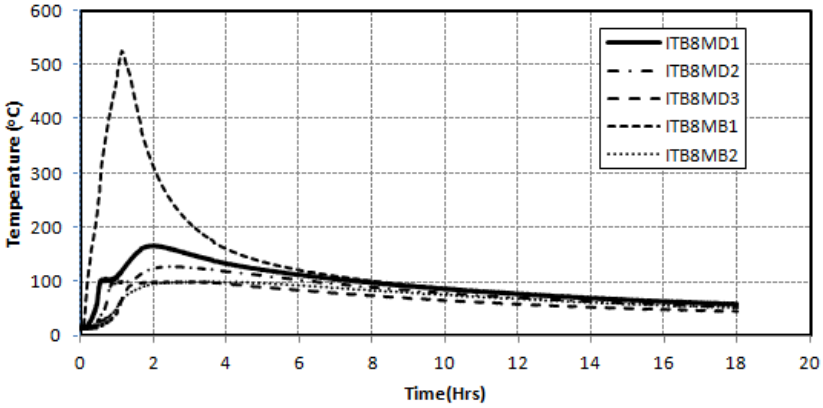

(q)

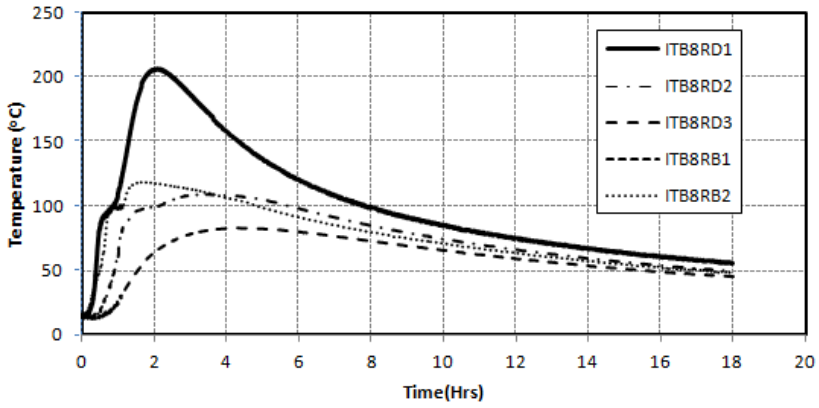

(r)

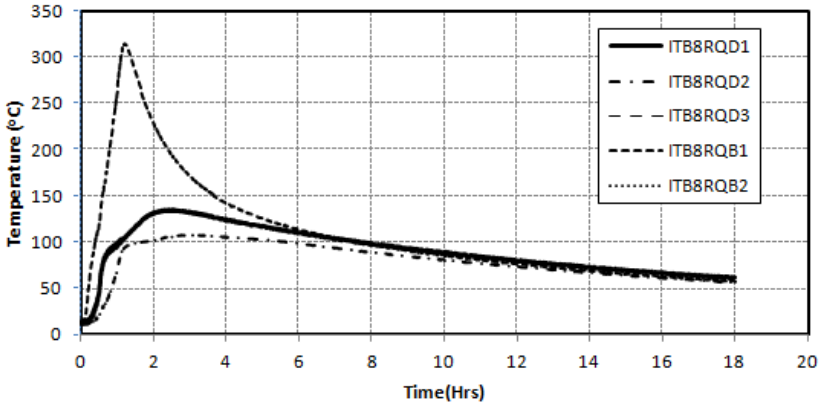

(s)

Fig. 3.20: (a-s) Time-Temperature curves for roof beams.

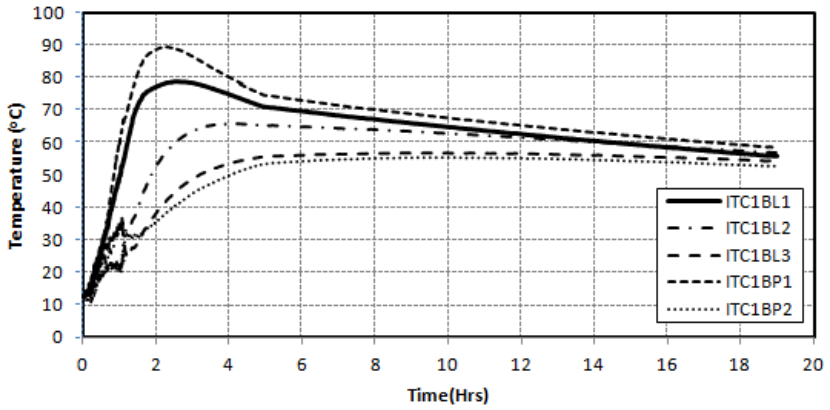

(a)

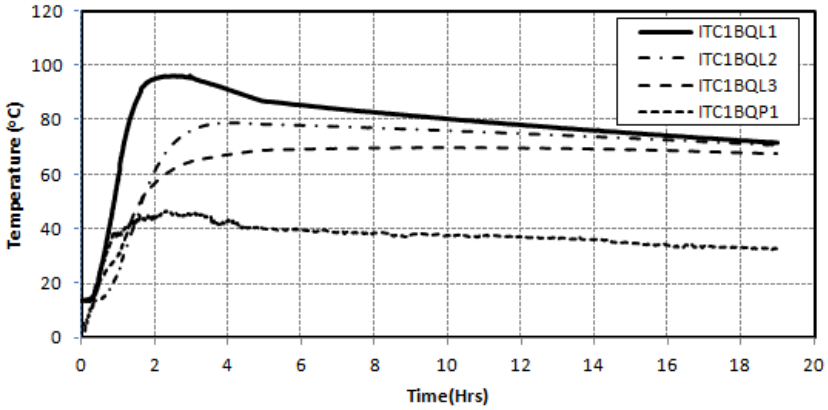

(b)

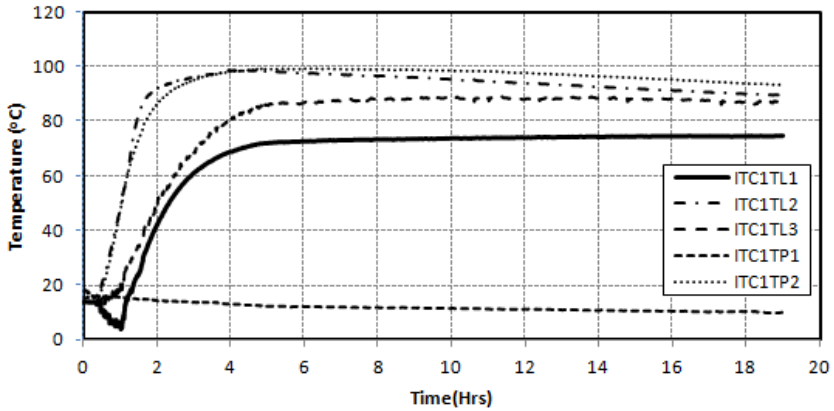

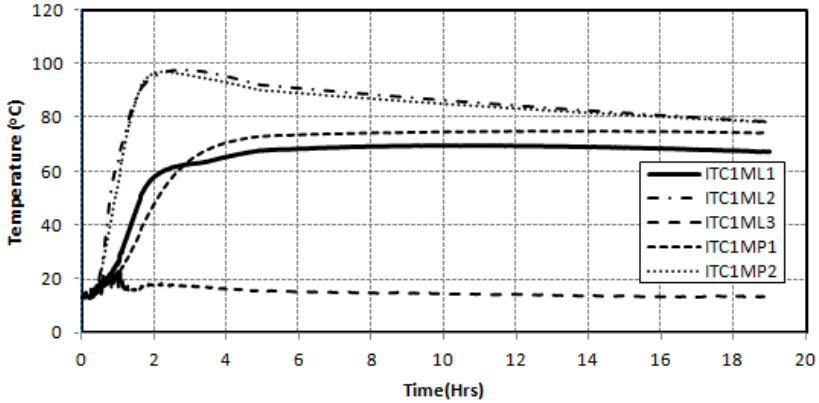

Fig. 3.21: (a-r) Time-Temperature curves for Columns (Contd.)

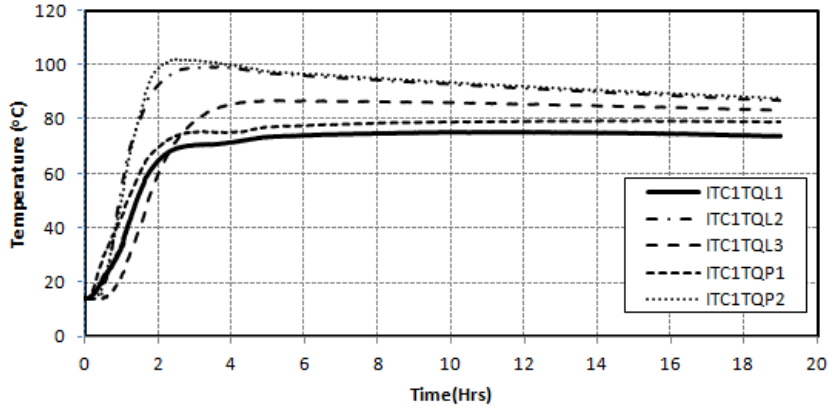

(e)

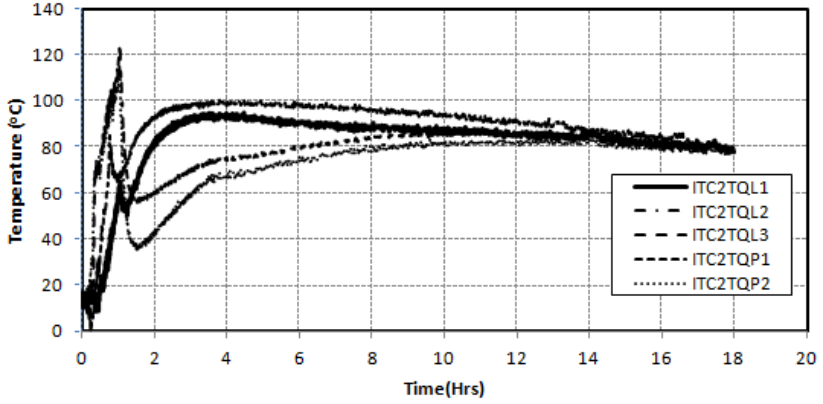

(f)

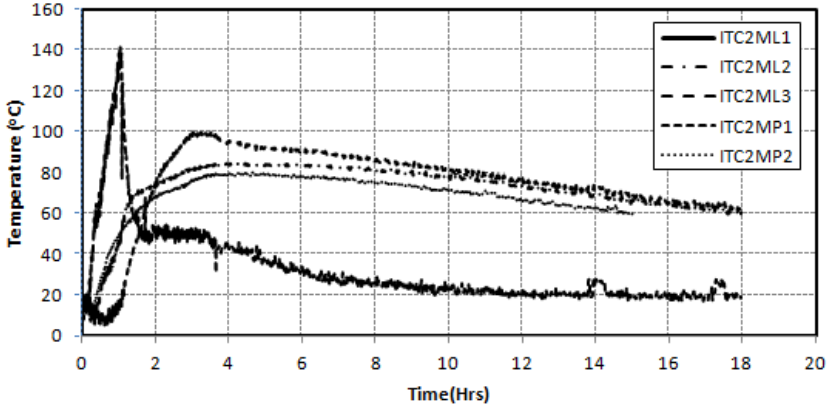

(g)

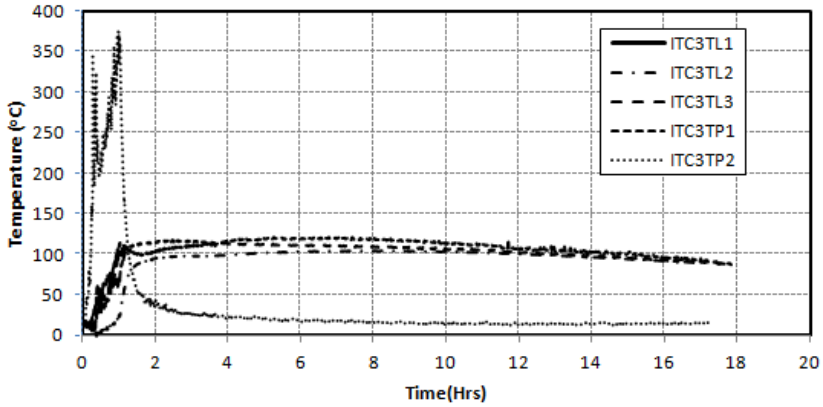

(h)

Fig. 3.21: (a-r) Time-Temperature curves for Columns (Contd.)

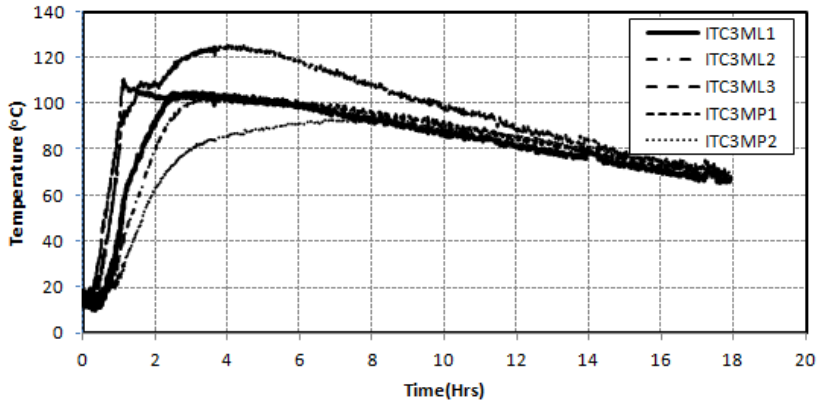

(i)

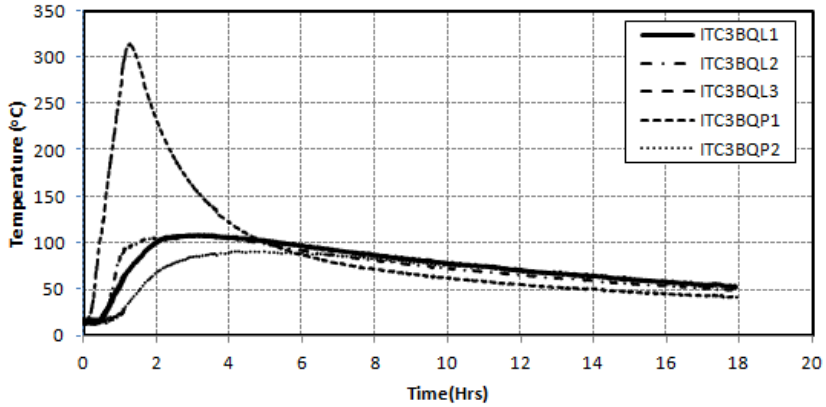

(j)

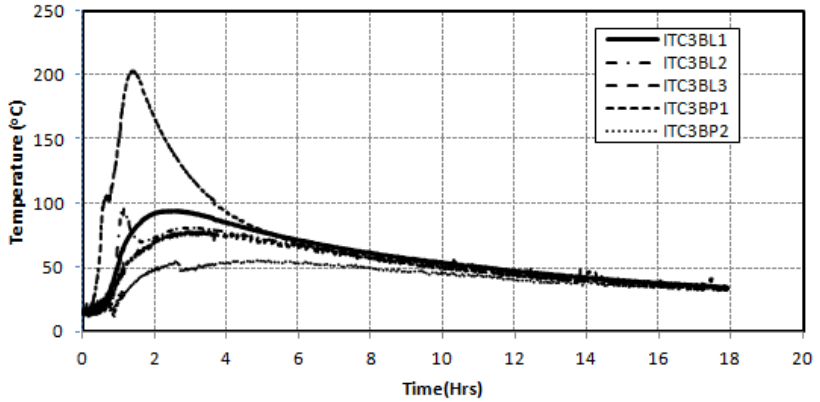

(k)

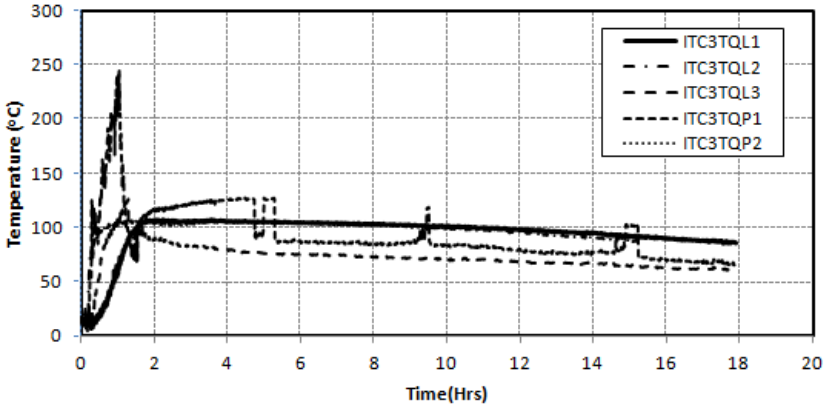

(l)

Fig. 3.21: (a-r) Time-Temperature curves for Columns (Contd.)

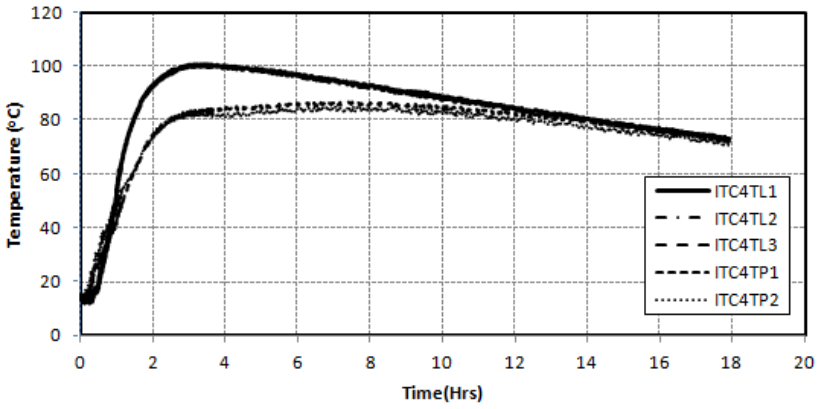

(m)

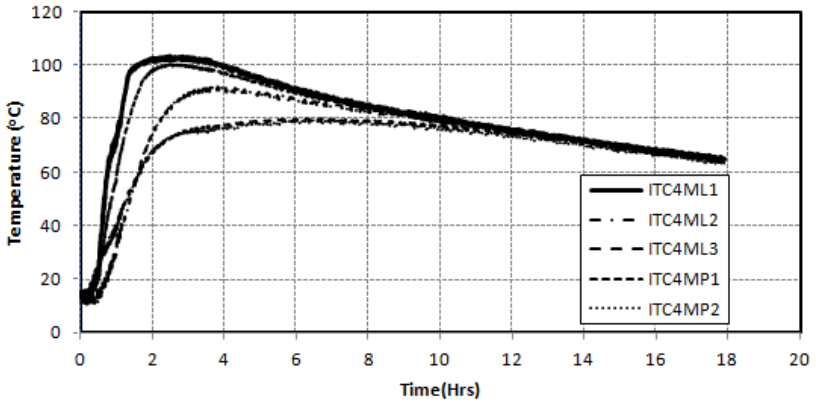

(n)

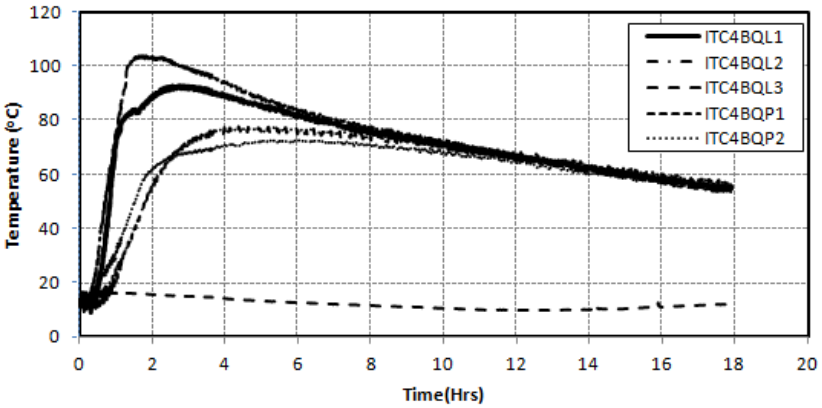

(o)

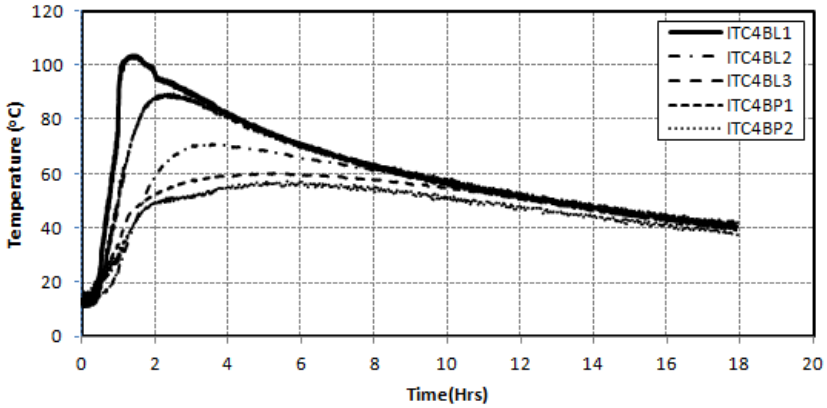

(q)

Fig. 3.21: (a-r) Time-Temperature curves for Columns (Contd.)

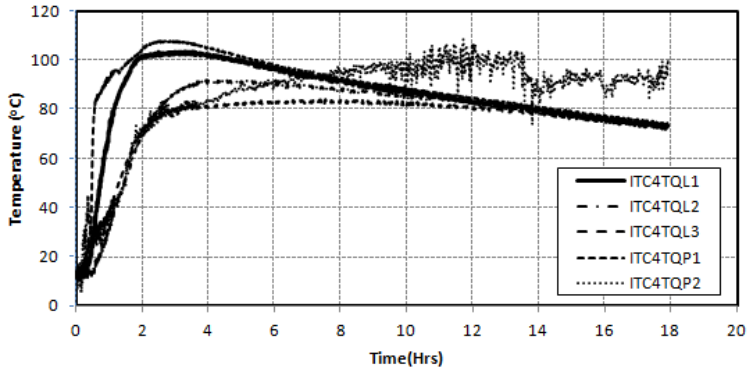

(r)

Fig. 3.21: (a-r) Time-Temperature curves for Columns

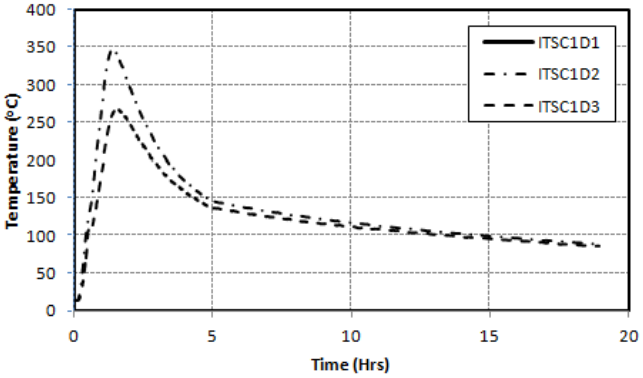

(a)

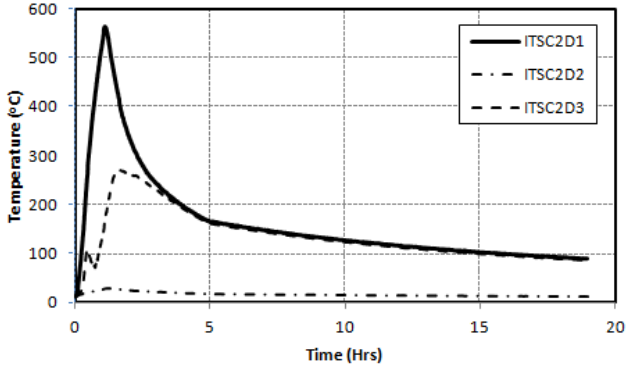

(b)

Fig. 3.22: (a-i) Time-Temperature curves for Slab (Contd.)

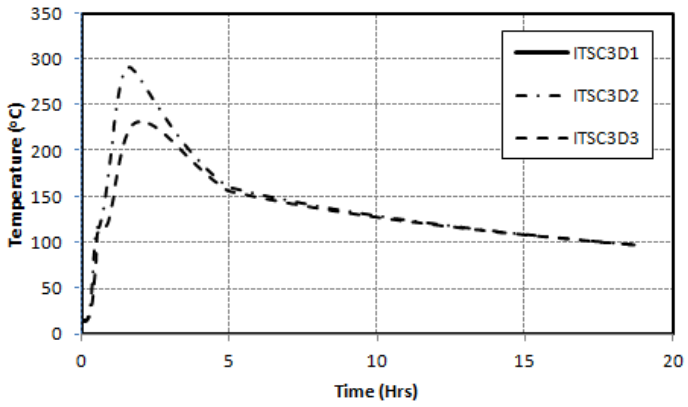

(c)

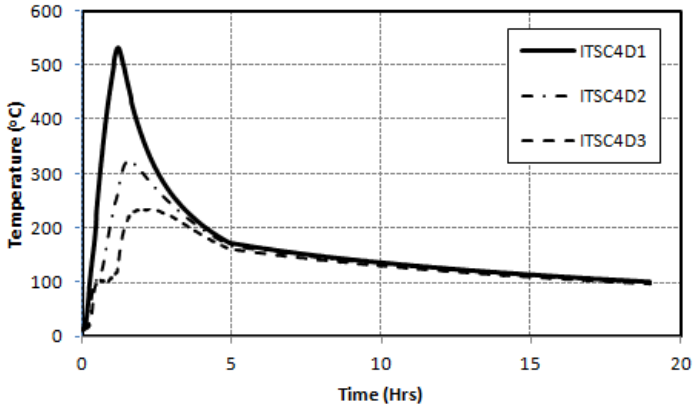

(d)

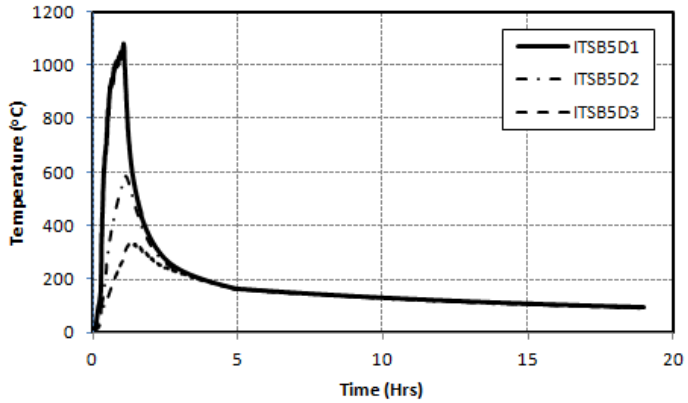

(e)

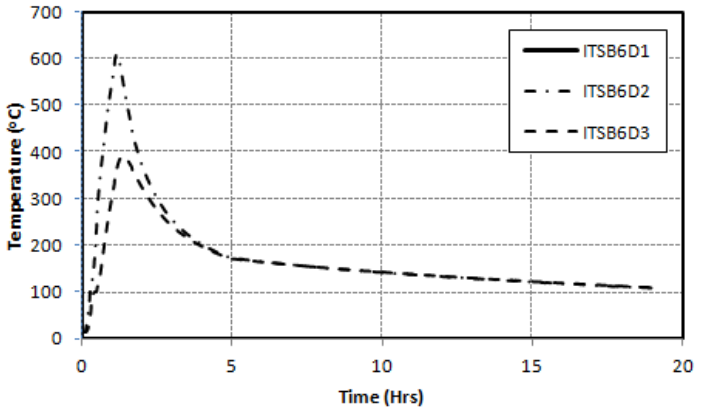

(f)

Fig. 3.22: (a-i) Time-Temperature curves for Slab (Contd.)

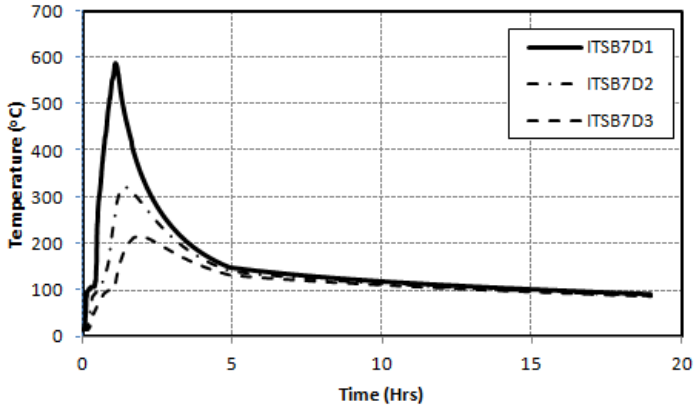

(g)

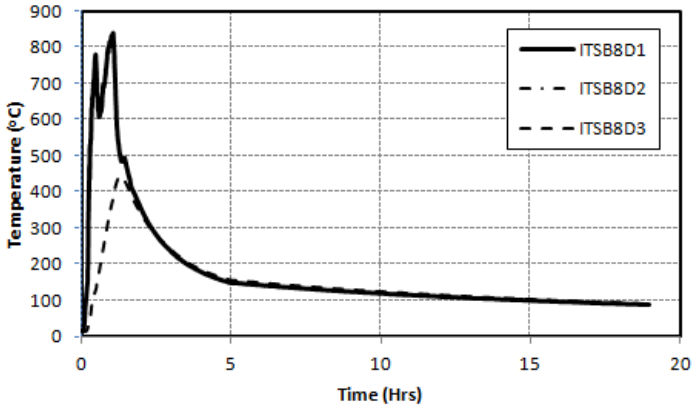

(h)

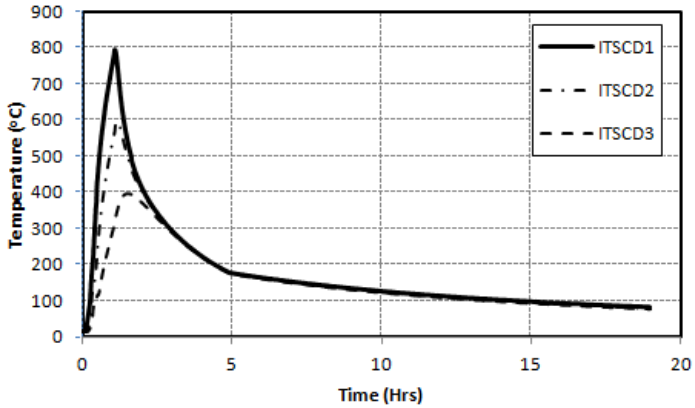

(i)

Fig. 3.22: (a-i) Time-Temperature curves for Slab

3.5 FRAME TEST STAGE III: RESIDUAL LOAD TEST

After subjecting the RC frame to simulated seismic load test and the fire test, it was subjected to a cyclic lateral loading excursion for its residual lateral load capacity. Fig. 3.23 shows the load displacement hysteresis loop for the residual load test. As in case of the bare frame a large reduction in lateral capacity was observed during the initial stages of the loading. However the reduction in the lateral load capacity was larger than in the bare frame. A residual lateral capacity of 18.2 % of the original capacity was observed at the displacement of 20 mm. However the same in case of the bare frame was 46%. The higher loss of strengths at the initial stages in the infilled frame can be attributed to the shear failure which the plinth beams (placed along the loading) suffered during the initial load test before fire. At a displacement of 40 mm, the residual capacity of the frame was 22% of the original capacity. At 100 mm displacement, the frame exhibited a residual lateral capacity of 59% of the original strength. The overall reduction in the lateral load carrying capacity of the frame was measured to be 37% at 140 mm displacement. Fig. 3.24 gives a comparison of the initial and the residual lateral load carrying capacity of the test frame. Fig. 3.25 shows the frame during the residual load test.

Although the frame witnessed a considerable loss in the lateral load capacity, the RC test frame remained intact with all its in-plane and out-of-plane masonry walls. Fig. 3.26 - 3.30 show the test frame after the load test. Although the frame witnesses loss in strength and stiffness, it could withstand the tests without collapse.

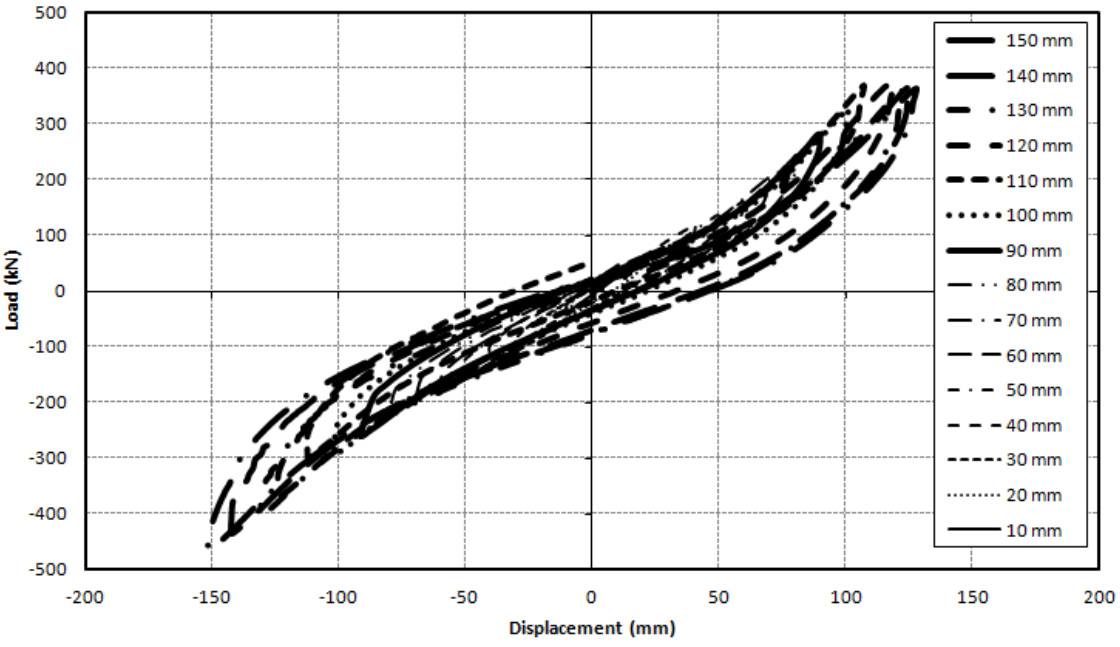

Fig.3.23 Residual Load Displacement Hysteresis of the test frame with masonry infills

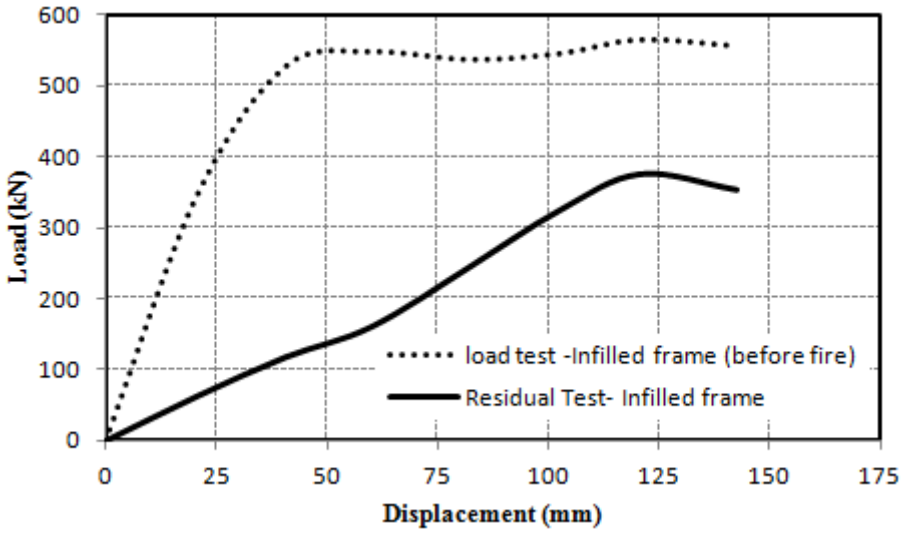

Fig.3.24 Load carrying capacity before and after fire

Fig. 3.25: The test frame during the residual load test.

After subjecting the frame to the residual test, the infill walls were removed to observe the damage to the structural elements. As can be seen in Fig. 3.29, the elements had undergone very less thermal damage due to the insulation provided by the masonry walls. The effect of the masonry can be also gauged by the colour difference in the cross-section of the column C4.

Fig.3.26: A view of the frame after residual test

Fig. 3.27: A view of the frame after residual test

Fig 3.28: A closer view of the beam B1 showing damaged portion

Fig. 3.29: A view of the frame after removal of infill walls

Fig. 3.30: Column C4 after removal of infill walls

3.6 CONCLUDING REMARKS

This study attempts to investigate the performance of earthquake damaged masonry in-filled reinforced concrete frame under fire. The construction, instrumentation and testing of a full scale reinforced concrete frame was a challenging job. Important observations have been made about the behaviour of frame during the initial simulated seismic loading and later during the fire testing. Understanding the build-up of temperatures in the pre-damaged reinforced concrete sections of beams and columns of a masonry in-filled building frame during a real compartment fire is another key highlight of this research. As there is no current guidance on fire resistance of earthquake damaged structures, the outcome of this study will help formulating the design guidelines for the earthquake damaged reinforced concrete structures.

CHAPTER – 4
EFFECT OF CONFINING REINFORCEMENT ON FIRE RESISTANCE OF RC COLUMNS

4.1 INTRODUCTION

Much attention has been attached in the past to the fundamental properties of concrete at room temperature. The research on the behaviour of concrete under elevated temperatures has only recently increased because many modern concrete structures are frequently subjected to elevated temperatures due to exposure to an aggressive fire or heat. The extent of concrete property variation due to high temperature depends on many internal and external parameters, such as concrete mix design, properties of the constituents, heating rate, peak temperature, cooling rate, thermal incompatibility between aggregate and cement paste, type of aggregate, shape and size of member, moisture content, presence of admixtures, presence of fibres, methods of heating and cooling etc (Khoury 2000). It is generally assumed that the reinforced concrete elements behave satisfactorily under fire. However the phenomenon of spalling can sometimes cause the failure prematurely due to the loss of concrete cover and the steel strength (Franssen and Dotreppe, 2003).

In buildings, the columns form the main load bearing components and hence to safeguard the building from the effects of fire the columns must be able to withstand a design fire. The serviceability criteria of the structural design demand that the concrete columns be designed to resist the failure against fire for a predetermined period of time. The satisfactory performance of a structural member exposed to fire is measured in terms of fire resistance. Fire resistance is defined as the duration during which a structural member exhibits adequate resistance with respect to structural integrity, stability and temperature transmission under fire conditions. The objectives for providing the fire resistance need to be established before making any design, recognizing that fire resistance is only one component of overall safety strategy. To prevent structural collapse, structural elements must be provided with sufficient fire resistance to maintain stability for the fire design time (Buchanan, 2002). Fire resistance rating requirements are specified in building codes and these provisions are based on standard fire tests carried out on a limited number of specimens.

The provision of appropriate fire safety measures for the columns is one of the major safety requirements in building design. The basis for this requirement can be attributed to the fact that when all other measures for containing the fire fail, structural integrity is the last line of defense (Kodur and Raut 2007).The most common approach for evaluating the fire resistance of RC columns is through fire tests under standard fire conditions. For fire resistance testing, many countries use the International Standard ISO 834 (ISO, 1975) or have national standards based on ISO 834 (for example AS 1530 Part 4(SAA, 1990(c)). Most European countries have standards similar to ISO 834. The standard used in the United States and some other countries is ASTM E119 (ASTM, 1988(a)), which was first published in 1918. The Canadian standard (ULC, 1989) is based on ASTM E119. The corresponding British Standards are BS 476 Parts 20-23 (BSI, 1987). The Indian standard 3809-1979 (BIS, 1979) is also based on ISO 834 and was first adopted in 1979. These standards are more concerned with the fire temperatures to be followed during the test and the failure criteria.

Most of the building codes provide the fire resistance ratings of the structural elements based on the standard fire tests. These ratings are usually based on the dimensions of the members and the cover to the reinforcement. However the effects of the factors like the load level, fire exposure, material strength, slenderness ratio and the reinforcement detailing are not accounted for. For example as per ACI 216.1 standard (ACI, 2006), a concrete column made with carbonate aggregate and with dimensions 300 × 300 mm^2 and cover to the reinforcement 40 mm, shall have a fire rating of 4 hours irrespective of the load level, slenderness ratio or the reinforcement detailing.

During the last four decades RC columns have been tested for fire ratings by different researchers under different conditions. A number of studies have been carried across the globe by the researchers on the performance of RC columns in standard fires. The objectives of these tests included; capturing the overall behaviour under a standard fire curve; measuring the time to failure under the standard fire exposure (fire ratings); generating data for different variables to carry out parametric studies through analytical and software tools; studying the effects of various additives in the concrete on the fire ratings and investigating the phenomenon of spalling in the fire exposed columns.

The outcome of the past tests has been the fire resistance ratings of the structural elements based on these standard tests. These ratings have been documented in the building codes and are usually based on the dimensions of the members and the cover to the

reinforcement. Apart from the tabulated fire resistance ratings an important outcome of the standard fire tests on the columns has been the development of simple calculation methods as given in Eurocode 2 (EN 1992-1-2 2004), Australian code (AS-3600, 2001) and those developed by different researchers (Kodur and Raut 2009; Frenssen and Dotreppe 2003). Whereas the fire resistance ratings given in different building codes are usually based on the dimensions of the members and the cover to the reinforcement, the effects of the factors like the load level, fire exposure, material strength, slenderness ratio and the reinforcement detailing are not accounted for in these stipulations. Similar is the case with the different calculation methods which although take the effect of a number of factors but an important influencing factor of confinement has been missed out by the researchers.

In view of the above discussion an experimental study was carried out involving testing of eight full scale RC columns in a fire furnace exposed to a standard fire. The columns were constructed using different confinement levels and concrete strength and exposed to standard fire. The results of the experiments are used to trace the behaviour of the RC columns at elevated temperatures. An empirical equation has also been arrived at, which incorporates the effect of a number of parameters including that of confining reinforcement.

Although the researchers have studied a number of parameters affecting the fire resistance of RC columns, however no such study has been carried out to the best knowledge of the authors that takes into consideration the effect of the confining reinforcement on the fire resistance of RC columns. It is hoped that the present study addresses this gap in the literature.

4.1.1 Summary of Factors governing fire resistance

A number of researchers have documented the effect of various factors on the fire resistance of the columns. Results from fire tests clearly illustrate that load intensity has a significant influence on fire resistance of RC columns. The fire resistance decreases with the increase in load ratio (Kodur and Raut 2009, Kodur and Phan 2007, Kodur and McGrath 2003, Kodur et al 2004, Kodur et al 2003, Ali et al 2004, Kodur and McGrath 2006).

Results from fire tests show that the geometric properties, mainly cross-sectional dimensions, length and support conditions, play a significant role in determining the fire resistance of RC columns. This could be attributed to the fact that buckling becomes a prominent factor with deteriorating stiffness (with increased fire exposure duration). As slenderness increases, the fire resistance of the column decreases owing to decreased resistance to buckling (Kodur and Raut 2009). While as a larger cross section leads to decreased fire

resistance in HSC columns due to higher spalling due to explosive thermal spalling, the fire resistance increases with the size of the members in NSC columns (Kodur and Phan 2007).

The strength of concrete has significant influence on the fire performance of concrete structures. The rate of loss of strength in HSC columns is more as compared to NSC columns (Phan 1996). Results indicate that the HSC columns exhibit lower fire resistance than the NSC columns due to explosive spalling (Kodur and McGrath 2003, Kodur et al 2003).

Concrete moisture also influences the behaviour of RC columns in fire by influencing the extent of spalling. Higher moisture content leads to more spalling and a reduction in fire resistance. Fire tests on RC columns revealed that significant spalling takes place when relative humidity is higher than 80% (Bilodeau et al 2004).

The ratio of longitudinal reinforcement also influences the fire resistance of the RC columns. An increase in the reinforcement ratio leads to lower fire resistance in RC columns. This can be attributed to the fact that for the same cross-sectional area of column there is more steel present, the properties of which deteriorate quickly with temperature. Steel loses its strength with the rise in its temperature at a faster rate than concrete. This leads to reduction in fire resistance of the RC columns (Kodur and Raut 2009).

Generally the building codes relate the fire resistance property of a structural element to its concrete cover. It is well established that the fire resistance increases with cover thickness. This is due to the fact that the cover protects the steel from rise in temperature and the increased cover thickness causes delay in temperature rise in reinforcing steel and thus the time to failure gets enhanced.

4.1.2 Research Significance

Inelastic deformability of reinforced concrete elements is essential for the overall stability of structures in order to sustain various natural and man-made hazards. The desired deformability of reinforced concrete structural components is generally achieved through proper confinement of the core concrete **(**Sheikh and Uzumeri, 1980, Mander et al., 1988, Saatcioglu, and Razvi, 1992). The effects of various key parameters of confinement on the strength and ductility of confined concrete at ambient temperatures are well documented now (Sargin, 1971, Park and Sampson, 1972, Sheikh and Uzumeri, 1980, Mander et al., 1988, Saatcioglu and Razvi, 1992, Sheikh and Toklucu, 1993, Srinivasan and Menon, 2003, Sharma et al., 2005). With the increasing use of confined concrete in the potential plastic hinge regions of disaster resistant structures, concern has developed regarding the post-fire behavior of such

confined concrete elements. The effects of high temperatures on the mechanical properties of concrete have been investigated by many researchers in the past. Upon exposure to high temperature, concrete undergoes changes in its chemical composition, physical structure and water content. These changes are reflected by a reduction in various mechanical properties of concrete. However, most of the earlier studies were carried on unconfined concrete only and there are only very few studies in the existing literature related to the behavior of confined concrete exposed to elevated temperatures (Terro and Hamoush, 1997, Wu et al., 2002, Kodur and McGrath, 2006).

The design and detailing of critical hinge regions of concrete columns has been of great concern to engineers and designers in the recent past with respect to their performance during earthquakes only. On the contrary, little research has been undertaken to investigate the significance of confined end regions of reinforced concrete columns during fire. Therefore, there is a need to account for the confinement provided by ties in the procedures for fire resistant design of reinforced concrete columns. Thus it becomes important to evaluate the effectiveness of confinement reinforcement in confining core concrete after exposure to elevated temperatures. It also remains to be seen that how the various parameters of confinement would affect the behavior of concrete after exposure to elevated temperatures experienced during fire.

4.2 EXPERIMENTAL PROGRAM

4.2.1 Specimen details

The experimental program consisted of conducting fire resistance tests on eight reinforced concrete columns as shown in Table 4.1. Six of these columns, M3S50, M3S75, M3S100, M3S150, M3ST150 and M3S200, were of normal strength concrete (NSC) while two of them, M6S150 and M6ST150 were made with high strength concrete (HSC). All columns were 2,800 mm long and of square cross section of 300 mm. The dimensions of the column cross section and other details of the columns are given in Fig.4.1.

All the columns had eight, sixteen mm diameter longitudinal bars. The confinement was provided by using ten mm diameter ties placed at different spacing. The spacing of the confining ties varied from 50 mm to 200 mm as per the column type. The main reinforcing bars and ties had yield strength of 569 MPa. Two columns, M3ST150 and M6ST150 were provided with additional confinement by using additional cross ties. Table 4.1 also gives the details of the transverse and longitudinal steel in all the columns.

Table 4.1 RC Column specimen details

Specimens	f'_c (MPa)	Longitudinal steel			Transverse Steel			
		Number & Diameter(mm)	Spl %	f_{yl} (Mpa)	Diameter (mm)	Spacings (mm)	ρ_s %	f_{yh} (MPa)
M3S500	34	8 No's 16	1.7863	569	10	200	0.75	569
M3S150						150	1	
M3S75						75	2	
M3ST150						150	1.49	
M3S100						100	1.5	
M3S50						50	3	
M6S150	63					150	1	
M6ST150						150	1.49	

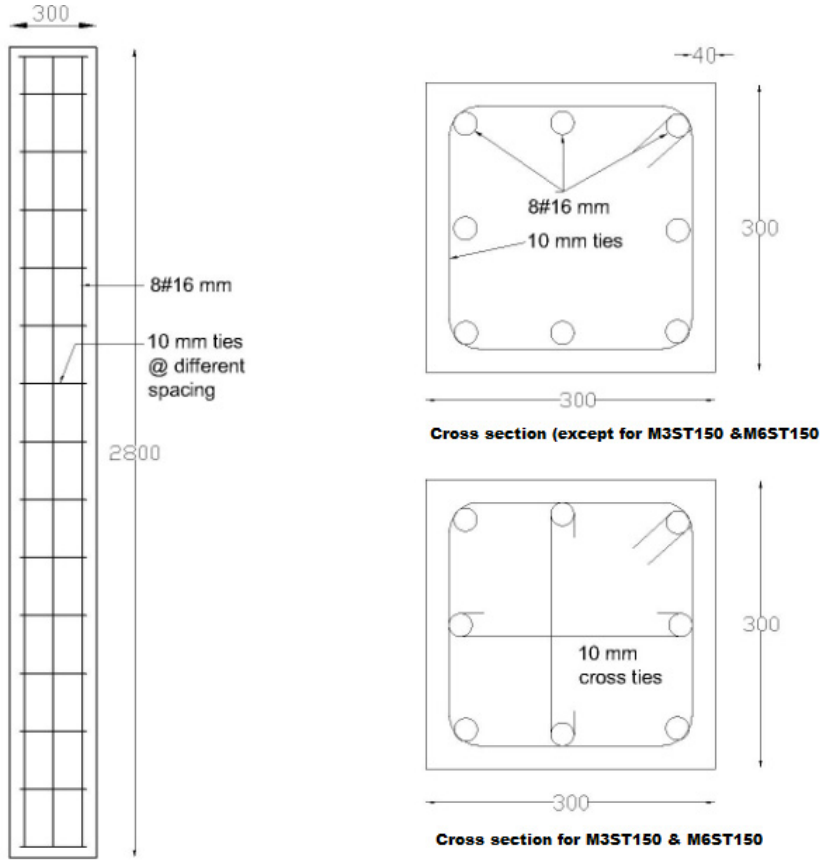

Fig. 4.1 Elevation and cross section of columns

The aggregate, cement and water used to develop the concrete mix was same as used in Chapter 2 of the thesis. Two batches of concrete were used in fabricating the columns. The

concrete mix for Batch 1 was of NSC, while the mix for Batch 2 was of HSC. The coarse aggregate used in all the batches was of carbonate type. Columns M3S50, M3S75, M3S100, M3S150, M3ST150 and M3S200, were fabricated from Batch 1 while the columns M6S150 and M6ST150 were manufactured from Batch 2. All the batches of concrete were made with, Ordinary Portland cement. The mix proportions, of the various batches are given in Table 4.2. The average compressive cylinder strength of the concrete, measured 28 days after pouring is also given in Table 4.2. The moisture condition of the columns was also measured on the day of the test. The relative humidity of the Columns M3S50, M3S75, M3S100, M3S150, M3ST150 M3S200, M6S150 and M6ST150 was approximately, 56, 55, 56, 56, 59, 55, 48, and 49% respectively.

Table 4.2: Concrete Mix proportions

Mix Type	**Cement (kg/m^3)**	**Water (kg/m^3)**	**Coarse aggregates (kg/m^3)**	**Sand (kg/m^3)**	**Micro Silica (kg/m^3)**	**Super Plasticizer (kg/m^3)**	**characteristic compressive strength at 28 days, f_c (MPa)**
Normal Strength Concrete (NSC)	435	195	1183	539	-	-	34
High Strength Concrete (HSC)	500	150	1045	618	51	5.18	64

4.2.2 Instrumentation

To measure the temperatures inside the RC columns K-type chromel-alumel thermocouples of 0.5 mm thickness were installed at three different elevations namely mid-height, top three-quarter and bottom one quarter cross-section in the fire exposed portion of the columns. A total of 13 thermocouples were placed in each of the column specimens to measure the temperatures at different locations along the length of the column. Figure 4.2 shows the thermocouples in the RC column. Figure 4.3 illustrates the position of the three instrumented cross sections and precise location of thermocouples in each cross section. To compare the results, the location and the arrangement of the thermocouples was kept same in all the eight columns. At Section AA, thermocouples TC 1 to TC 3 were attached to record longitudinal

rebar temperatures, while as TC 4 and TC 5 were attached to record concrete cover temperatures. TC 6 and TC 7 were used to record the concrete temperatures at center and quarter depth of the cross-section AA. At the section BB, TC 8 was attached to record longitudinal rebar temperature, while TC 9 and TC 10 were installed to record temperatures of center the cross-section and confining tie respectively. At Section CC, TC 11, TC 12, and TC 13 were attached to record longitudinal rebar temperature, concrete temperature at quarter depth and confining tie temperatures respectively.

Fig. 4.2: Reinforcement cage with thermocouples in mould.

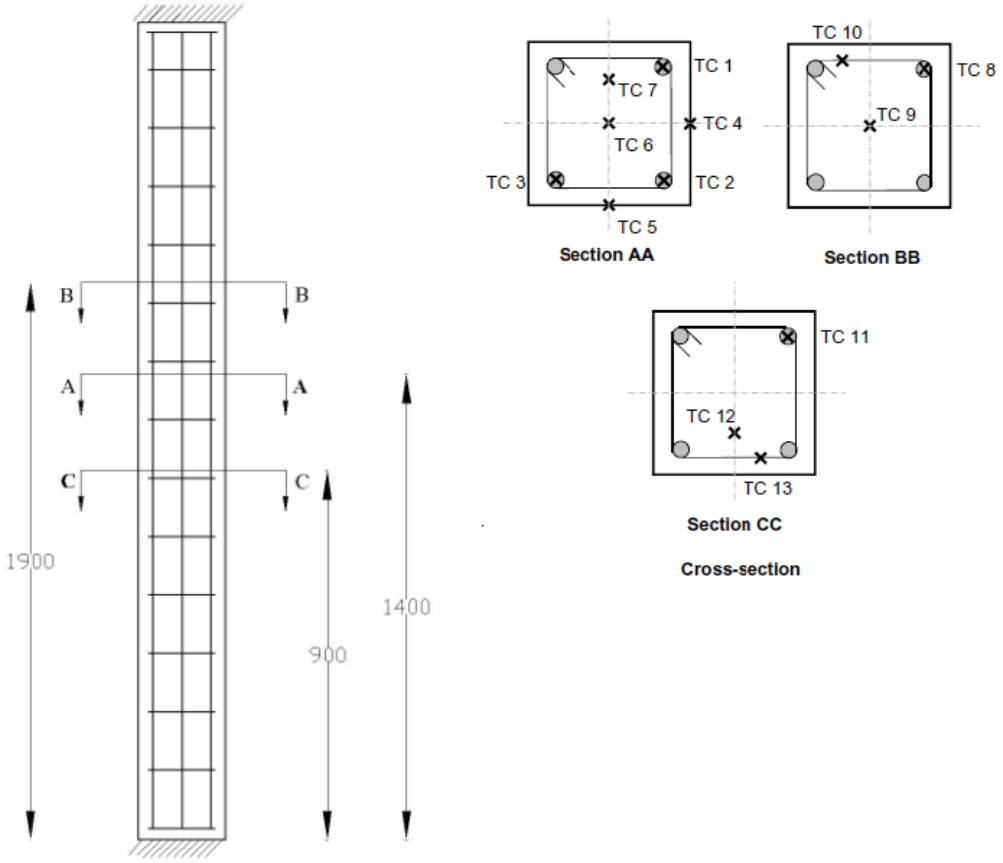

Fig. 4.3: Location of thermocouples in columns

Figure 4.4 shows the RC columns after casting. The columns were wet cured for 28 days after casting and were tested for fire resistance after about 90-110 days of casting.

Fig.4.4: RC columns after casting.

4.2.3 Test Setup

A new test facility was developed at the Civil Engineering Department, Indian Institute of Technology Roorkee for carrying out the full scale fire tests on RC columns. First of its kind in the country, the test furnace was designed and built to produce conditions such as temperature, loads and heat transfer to which a column might be exposed during a fire event. The furnace being a split type and integrated with a reaction frame having a capacity of 300 Ton has been specially designed to supply both heat and applied loads to which a column might be subjected during a fire. With an internal hot zone size of 2 m x 1 m x 1 m, the inside of the furnace is insulated with ceramic fibre roll and *Face Kyanite* (HFK) bricks. A total of four burners have been installed in the furnace to provide the thermal energy. The furnace is diesel driven and the fuel supply is regulated by a 3hp motor pump attached to a 1000 liter fuel tank. The furnace has a 3hp air blower which helps control the temperature development. The fuel supply to the burners is also regulated by the butterfly valves attached to each of the burners. In order to monitor the furnace temperature during the test, eight K-type metal insulated (MI) thermocouples are distributed throughout the test chamber. The furnace temperature is taken as the average of these eight thermocouples. During the fire test, the temperatures from these MI thermocouples are used to adjust the fuel and air supply to maintain the standard temperatures.

In the present test the furnace was adjusted to produce the temperature profile as per the ISO 834: 1975 fire curve. At least five small view ports are also provided in the furnace wall which enables monitoring of the working of the four burners and also for the visual monitoring of the fire-exposed specimens during the test.

The external dimensions of the furnace are 2.5 m x 1. 5m x 1. 5m. Fig.4.5 shows the elevation of the furnace along with the loading reaction frame. Fig. 4.6 shows the actual view of the furnace. The furnace is square in plan with a central opening of 400 mm × 400 mm. The length of the column can be up to 4 m with an exposed length of 2 m. A 300 ton capacity hydraulic jack is also attached to the loading frame for loading the columns under compression. The axial deformation of the test specimen was determined by measuring the displacement of the girder that supports the jack. The displacement was measured using transducers.

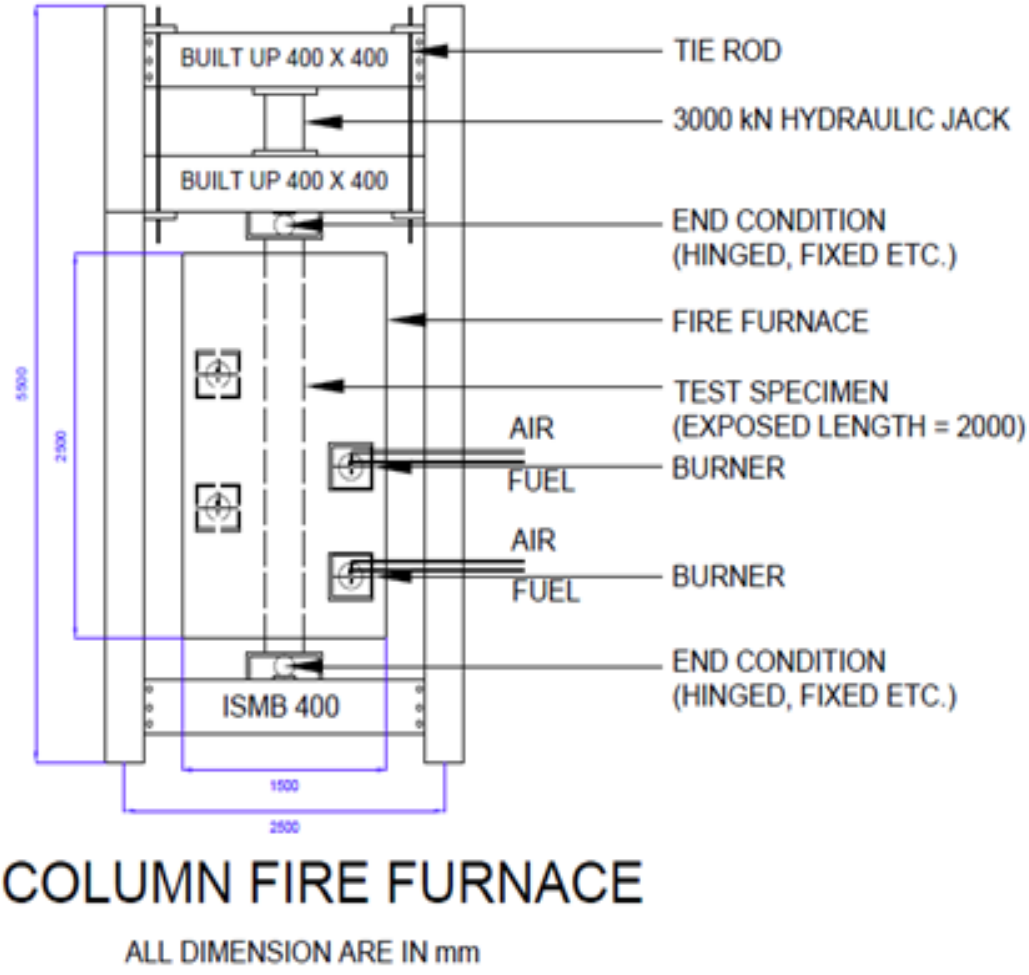

Figure 4.5: Furnace elevation

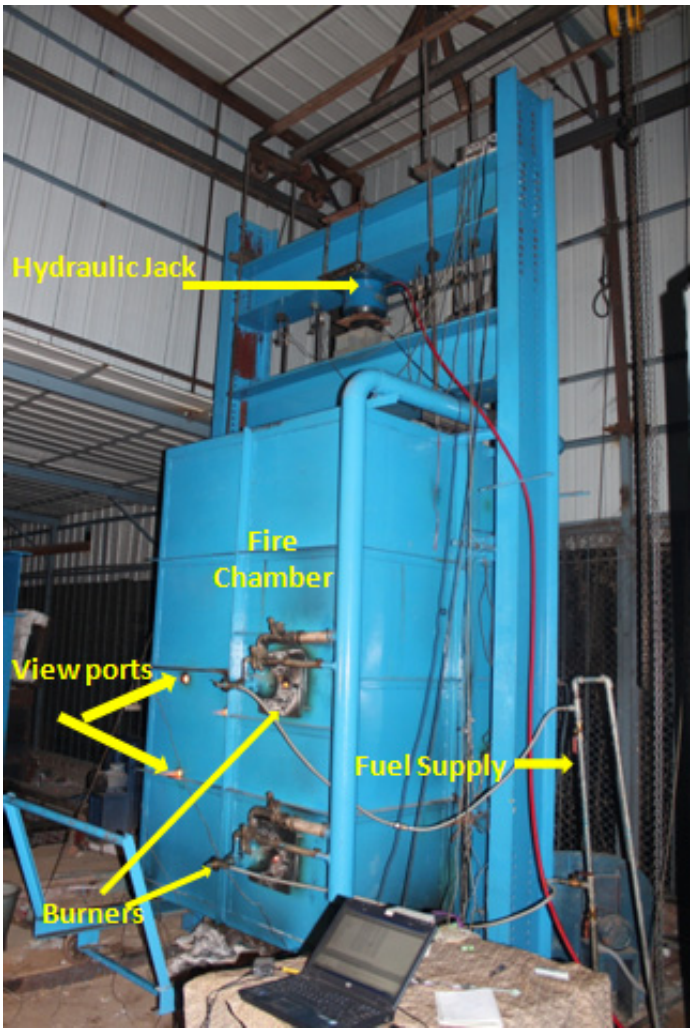

Fig. 4.6: The test arrangement

4.2.4 Test Condition and Procedure

The columns were installed in the furnace by fastening the top and bottom of the columns to the steel girders of the loading frame. The end conditions of the columns were kept as fixed-fixed for all the tests. The columns were fixed supported at the top and bottom girders of the reaction frame. The fixity was achieved by using 100×100×12 mm angles at the ends of the columns. These angles were bolt connected to the two girders. The top girder was made to rest on the column and was kept free to move in vertical direction. This was done to capture the vertical displacements of the columns during fire. The hydraulic jack, attached to another steel girder fixed with the loading frame, was used to apply a pre-load on the columns. The columns were tested under a concentric axial load with fixed supports. The length of the column exposed to the fire during the tests was 2000 mm.

All columns were tested for fire resistance under constant concentric loads. The NSC Columns M3S50, M3S75, M3S100, M3S150, M3ST150 and M3S200 were subjected to a load of 1170 kN, which is equal to 40% of the design load according to IS 456 (BIS 2002). Similarly HSC columns, M6S150 and M6ST150 were subjected a load of 1858 kN corresponding to 40% of the design load.

The axial load was applied to the columns about 60 minutes before the fire test. During the test, the column was exposed to the standard fire controlled in such a way that the temperature profile matches, as closely as possible, the targeted fire curve (i.e. ISO 834: 1975 fire curve). The load was maintained constant throughout the test duration. The columns were considered to have failed and the testing was stopped when any of the following conditions took place; (a) hydraulic jack could no longer resist the load, (b) if the RC columns contract axially by 28 mm (corresponding to 0.01L mm) or (c) if the rate of contraction reached 8.4 mm/min (0.003L/min). However, in all the columns it was found that the criteria of the hydraulic jack ceasing to maintain the load determined the failure of the columns.

4.3 BEHAVIOUR OF COLUMNS IN STANDARD FIRE

4.3.1 Variation of Temperatures

Fig. 4.7 shows the average furnace temperature attained in the fire tests of different columns. The temperatures at various depths in concrete and steel rebars are plotted in Figs. 4.8 -4.15 for all the columns tested. The temperature profile in the furnace followed approximately the standard temperature-time curve as per ISO 834 standard. For all the RC columns temperatures reached rapidly above 100 $^{\circ}$C. This phenomenon has been reported by a number of researchers (Lie and Celikkol 1991, Kodur et al 2003) and is due to the heat being utilized for evaporation of free water in concrete.

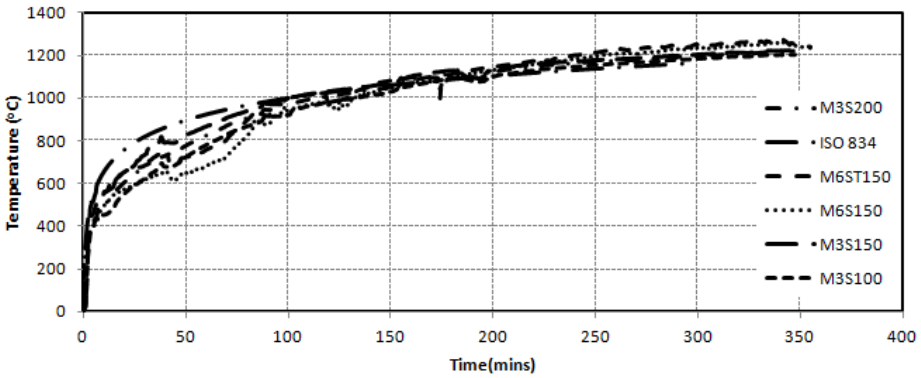

Fig.4.7: Temperature profile in furnace during the tests

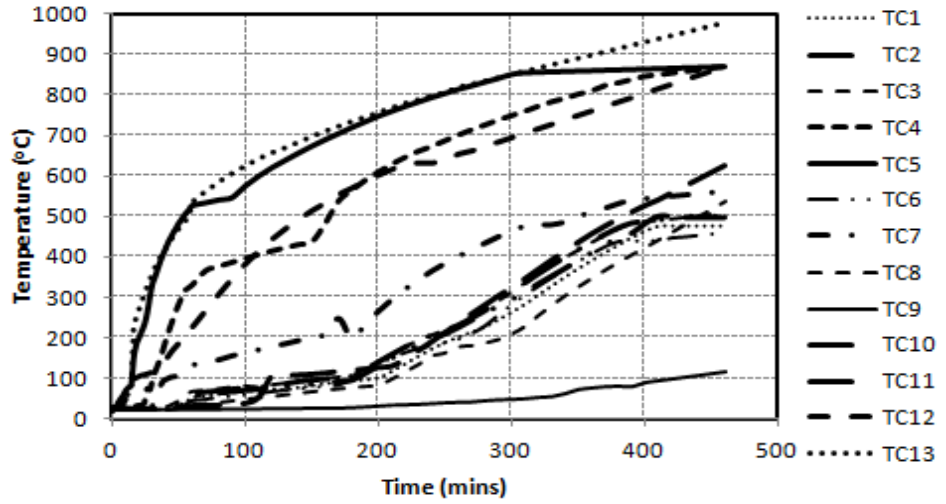

Fig. 4.8: Temperature distribution at various depths in Column M3S50

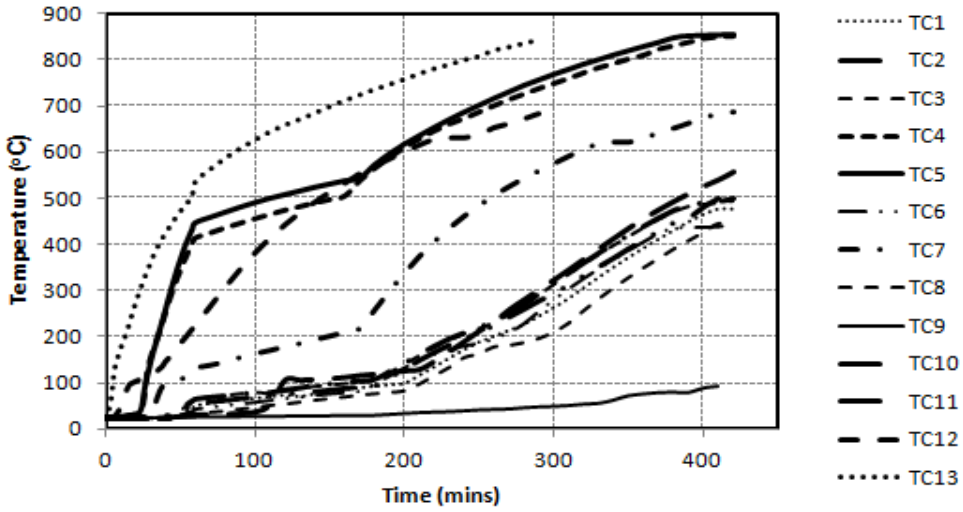

Fig 4.9: Temperature distribution at various depths in Column M3S75

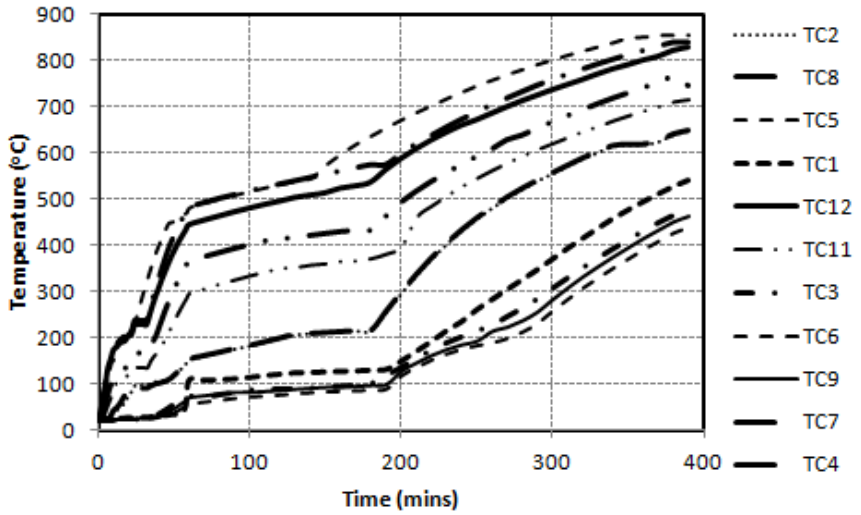

Fig. 4.10: Temperature distribution at various depths in Column M3S100

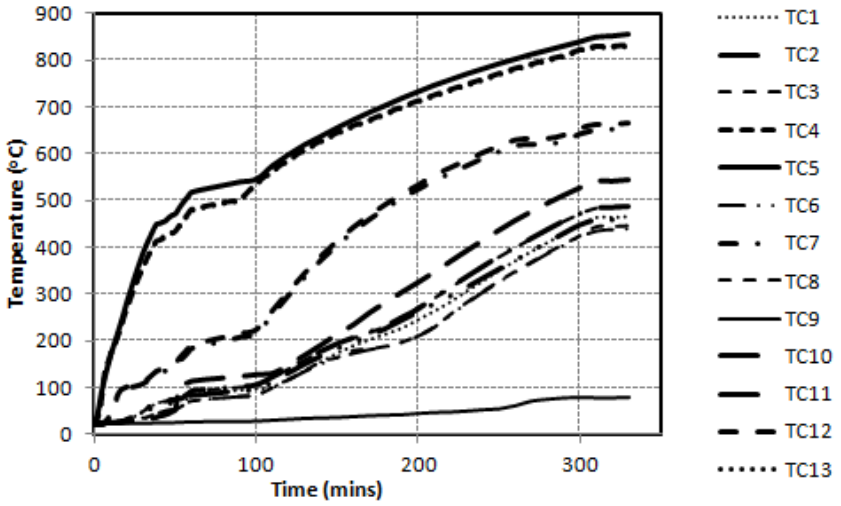

Fig.4.11: Temperature distribution at various depths in Column M3S150

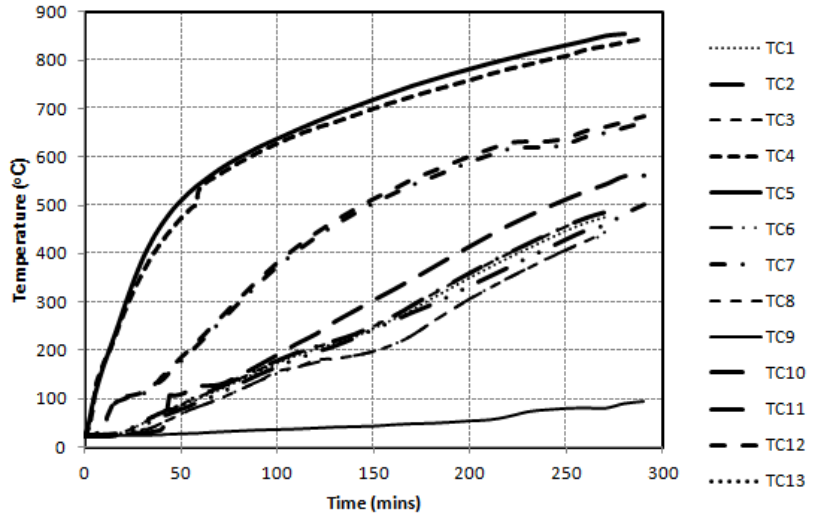

Fig.4.12: Temperature distribution at various depths in Column M3S200

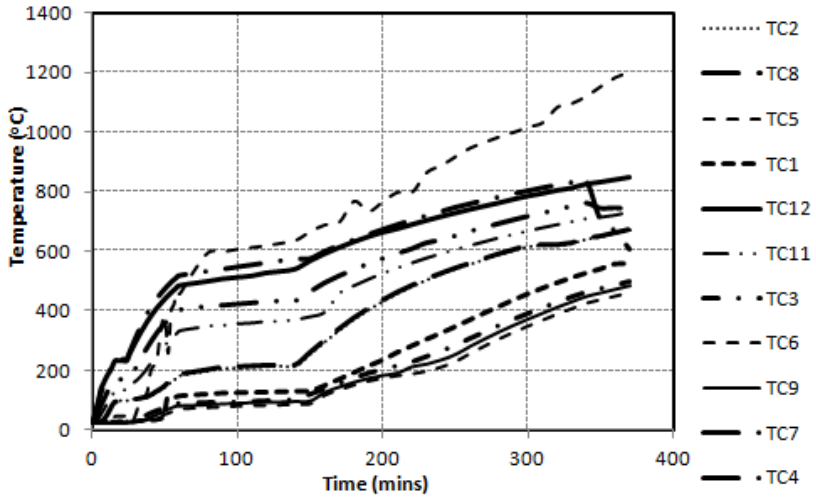

Fig.4.13: Temperature distribution at various depths in Column M3ST150

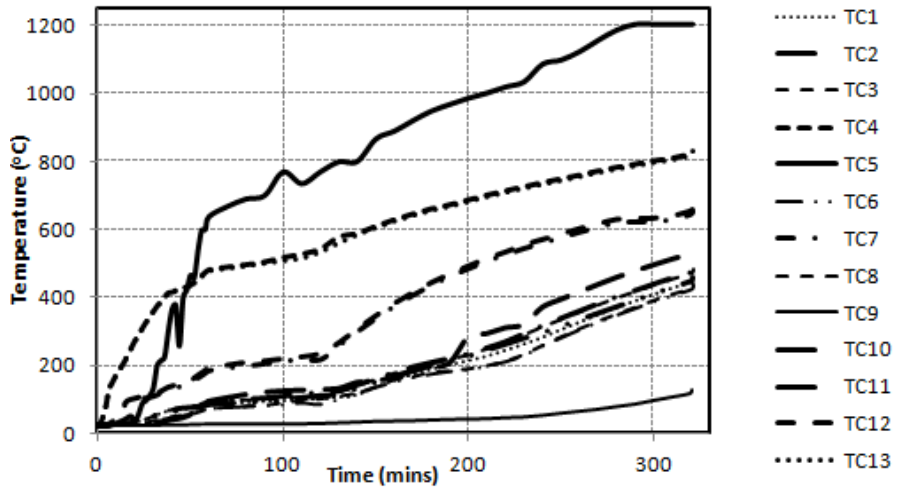

Fig.4.14 Temperature distribution at various depths in Column M6S150

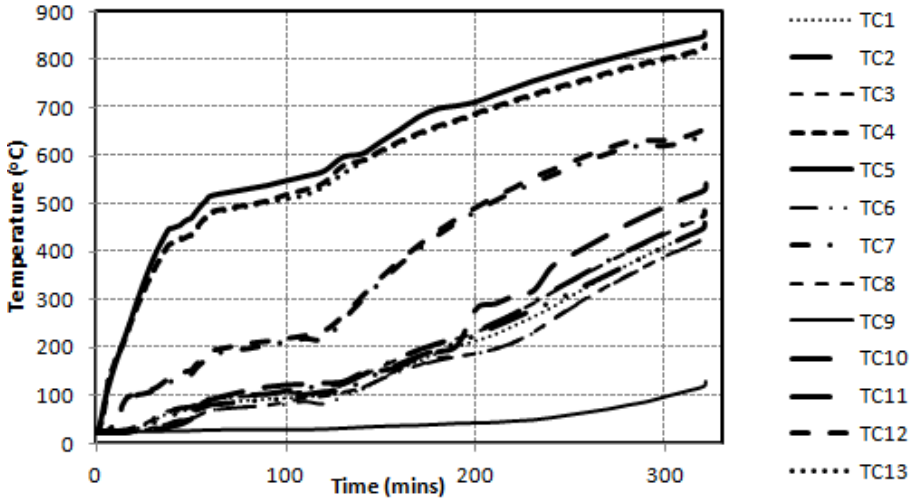

Fig.4.15 Temperature distribution at various depths in Column M6ST150

It can be seen from Figs. 4.8- 4.15 that the temperatures in the NSC columns are generally lower than the corresponding temperatures in the HSC column throughout the fire exposure. This variation can be attributed partly to the variation in thermal properties of the two concrete and to the higher compactness (lower porosity) of HSC. The lower porosity of HSC affects the rate of increase of temperature until the cracks widen and spalling occurs (Kodur et al 2003). The temperature profiles at different sections reveal that the temperature at the centre of concrete core is lower than that at the rebars which is due to lower concrete thermal conductivity and high thermal capacity which causes the slowdown in heat penetration.

The temperatures across the instrumented sections in RC columns indicate that the temperatures in less confined columns are higher than that in more confined columns. This can be attributed to the occurrence of fire induced spalling leading to the loss of concrete cross

section in the columns having lower confinement. All the columns failed when the rebar temperatures reached to about 750^{o}C. However the time to reach this temperature varied with the confinement. The closely placed ties protected the core concrete and increased the time to failure as can be seen in Fig. 4.16. Both the NSC and HSC columns experienced axial expansion until the reinforcement yielded and then contracted leading to failure. It can be seen from the Fig.5.16 that the overall deformation behaviour of HSC columns was similar to that of the NSC columns. The failure patterns in all the columns is similar except that the time taken by the steel to undergo yielding increases as the confinement increases. This is due to the better protection of core concrete due to higher confinement which keeps the steel temperatures lower till the spalling takes place and thus increasing the time to failure.

4.3.2 Spalling, Failure and Fire Resistance

The columns were regarded to have failed when the hydraulic jack could no longer resist the load. The spalling pattern varied according to the confinement levels. Fig. 4.16 shows the load variations in the RC columns during the fire test. Fig. 4.17 shows the different columns after the test. While the NSC columns M3S50, M3S75, M3S100 and M3ST150 which had the confining tie spacing of 50, 75, 100 and 150 mm respectively showed no spalling, significant spalling was observed during the later stages of the test in the NSC columns M3S150, M3S200 and the HSC column M6S150, which had the confining tie spacing of 150, 200 and 150 mm respectively. The spalling in the HSC column M6ST150, which had additional cross ties, was however less than that in the column M6S150. As the time of exposure increased cracks began to appear, which further propagated resulting in spalling. The cracks in the columns progressed at the corners of the cross section and led to the spalling of chunks of concrete. HSC columns M6S150 and M6ST150 were having similar properties and same tie spacing of 150 mm except that the M6ST150 had additional cross ties. The column M6ST150 performed better due to the extra confinement because of the provision of the cross ties. The HSC columns though susceptible to thermal spalling can be safeguarded by using extra confinement. Uniform spalling along the length was observed in the columns. While minute (hair line) Cracks could be noticed in about 20 to 30 min the widening of these cracks occurred after about 60 min or so.

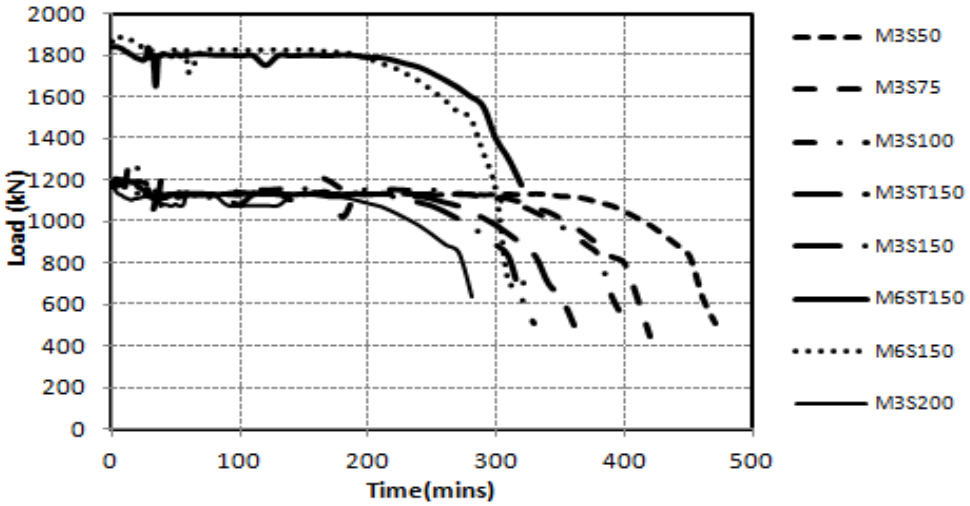

Fig.4.16: Load variations in RC columns during fire exposure

A comparison of fire resistance of the eight columns is given in Table 4.3. The time to reach failure is defined as the fire resistance for the column. For the NSC Columns, M3S50, M3S75, M3S100, M3S150, M3ST150 and M3S200 the fire resistance was approximately 456, 415, 390, 325, 366 and 298 minutes, respectively. For HSC columns M6S150 and M6ST150, the fire resistance was approximately 310 and 321 minutes respectively. The reduced fire resistance for HSC columns as compared to the NSC column can be attributed to the thermal and mechanical properties of HSC.

Fig. 4.17: RC columns after the fire exposure

The columns M3S150 & M6S150 had similar properties except the concrete strength. Similarly M3ST150 & M6ST150 also had similar properties including the confinement and tie configuration but different concrete strengths. Further, spalling which results in the decrease in the cross section at later stages of fire exposure, also contributed to lowering the fire resistance in the HSC columns. The layout of ties and confinement of columns had a marked influence on the fire performance of both the NSC and HSC columns. The provision of cross ties also helps increase in the fire resistance. This is mainly due to reduced spalling because of the ties holding the longitudinal rebars firmly in place. This mechanism effectively reduces the movement and buckling of longitudinal reinforcement and thus helps reduce the concrete strains (Kodur and Phan 2007). However the present study reveals an important observation that the effect of confinement is more pronounced in NSC columns than in HSC. Increase in the confinement by 100 % increased the fire resistance by 90 minutes in NSC columns. Increasing the confinement by 50 % increased the fire resistance by 41 and 11 minutes respectively respectively in NSC and HSC columns respectively. The increase in confinement by giving additional cross ties had more effect in NSC than in HSC columns. While an increase of 41 minutes in fire resistance can be seen in NSC columns due to additional cross ties, the same is only 11 minutes in HSC.

4.4 DESIGN EQUATION

Results from the tests were analyzed and the trends were studied to develop an equation for evaluating the fire resistance of the RC columns. Results of some of the fire resistance tests were also taken from the literature, Kodur et.al (2000). The data from these tests and the present results indicate that load ratio, slenderness ratio, the percentage of longitudinal reinforcement and the confining reinforcement plays an important role in the fire resistance of RC columns. The present study shows that the confinement has a marked role in the fire resistance of RC columns. The analysis of the results of the present study and those taken from the literature revealed the effectiveness of the extra confinement in enhancing the fire resistance of the RC columns.

The effect of confinement (K_{cf}) is a function of both, the confinement spacing (K_s) as well as the confinement configuration (K_e). The confinement spacing parameter can be defined in terms of the volumetric ratio of the transverse reinforcement $\rho_{s,}$ the yield stress of the transverse reinforcement f_{yh} and the cylinder compressive strength of the concrete f'_c.

The volumetric ratio of transverse reinforcement, ρ_s is given as

$$\rho_s = \frac{A_{stv} \times L_{stv}}{A_{core} \times S^*} \tag{4.1}$$

Where A_{stv} is the area of transverse steel, L_{stv} is the length of the transverse tie at any cross section.

$$K_s = \frac{\rho_s \times f_{yh}}{f'_c} \tag{4.2}$$

The effect of the confinement configuration was taken from a study on RC columns (Sheikh and Uzumeri, 1982). To take into account the role of efficiency of transverse reinforcement configuration, the confinement spacing parameter, *Ks* is multiplied by a second parameter, K_e, representing the confinement efficiency of lateral steel arrangement.

$$Ke = \left((1 - \frac{1}{\alpha A_{core}} \sum_{i=1}^{n} w_i^2) \times (1 - \frac{s^*}{2b_c}) \right) \times \left(1 - \frac{s^*}{2d_c} \right) \tag{4.3}$$

Where, *Ke* = confinement effectiveness coefficient ($Ke \leq 1$); s* = clear spacing between the ties or spirals; *wi* = ith clear distance between adjacent tied longitudinal bars; bc and dc = core dimensions to the centreline of the ties across the width and depth of the section, respectively; $A_{core} = b_c d_c$; n = number of spaces between tied longitudinal bars; and α = constant. If the arches of the effectively confined core are parabolic and have an initial tangent slope of 45° (Sheikh and Uzumeri, 1982), a = 6

Thus

$$K_{cf} = Ks \times Ke \tag{4.4}$$

The values for the confinement parameters Ks, Ke Kcf for all the columns of the present study and those taken from the literature were calculated and are given in Table 4.3. An equation was aimed at which would take the parameters like confinement, slenderness ratio, load ratio and the longitudinal reinforcement into account. Non-linear regression analysis of the data presented in the Table 4.3 was carried out using method of least squares. The variables were first logarithmically transformed and then the regression analysis was carried out. Logarithmically transforming variables in a regression model is a very common way to handle situations where a non-linear relationship exists between the independent and dependent

variables. Using the logarithm of one or more variables instead of the un-logged form makes the effective relationship non-linear, while still preserving the linear model. The regression of the data was carried out to arrive at the following design equation for the fire resistance

$$FR = \frac{Kcf^{0.218} Spl^{1.67} Sr^{4.09} Lr^{-0.87}}{831.76} \quad (4.5)$$

Where,

FR is the fire resistance in minutes,
Spl accounts for the longitudinal reinforcement percentage and is ratio of area of steel to the total gross area of the cross section.
Sr is the slenderness ratio of the column and Lr is the load ratio of the column i.e. the ratio of the applied load to the design carrying capacity of the column.
The value of coefficient of determination (R^2) was found to be 0.89.

Data from the fire tests on four columns from previous study, by Kodur et.al (2000), was used to validate the proposed equation. The predicted fire resistances from the equation were compared with the measured fire resistances from the tests and it was observed that the results almost match with the experimental results. The properties of the columns and the measured resistances from tests and the values from the equation are given in the Table 4.3. The data in bold was used to validate the equation. Fig. 4.18 shows the comparison of the measured fire ratings from furnace tests and the predicted values from the proposed equation. The data points in black ink show the results of the columns which were used to validate the equation. It can be seen that most of the predicted values either lie on or below the line of agreement. The agreement line in the figure represents the condition where the measured values exactly match the predicted values. Any value below the line represents the conservative condition and hence underestimation of the fire rating. It should be noted that more data could not be validated due to the missing data regarding the confinement parameters in existing literature. Also the equation has been validated only for the columns made with carbonate aggregate due to non availability of other parameters in the tests carried on the RC columns with siliceous aggregate. The comparison of the predictions with the measured test data shows that the predictions match well and are conservative for most of the columns. To enhance the applicability of the proposed equation more tests need to be carried out with other parameters like eccentric loading and aggregate type.

Table 4.3: Fire resistance data on RC columns used for developing and validating the proposed equation

Column ID	ρs (%)	CF	ke	keCF	Spl	Sr	Load Ratio (Lr)	Fire resistance (min)	
								Measured	Predicted
M3S200	0.75	0.125515	0.228	0.028617	1.786311	16.16581	0.4	298	284
M3S150	1	0.167353	0.344	0.057569	1.786311	16.16581	0.4	325	331
M3S75	2	0.334706	0.562	0.188105	1.786311	16.16581	0.4	415	428
M3ST150	1.49	0.249356	0.378	0.094257	1.786311	16.16581	0.4	366	368
M3S100	1.5	0.251029	0.483	0.121247	1.786311	16.16581	0.4	390	389
M3S50	3	0.502059	0.646	0.32433	1.786311	16.16581	0.4	456	482
M6S150	1	0.090317	0.344	0.031069	1.786311	16.16581	0.4	310	289
M6ST150	1.49	0.134573	0.378	0.050869	1.786311	16.16581	0.4	321	322
HS2*	0.15	0.004762	0.13	0.000619	2.381155	16.25397	0.46	204	180
HS3*	0.15	0.006061	0.13	0.000788	2.381155	16.25397	0.47	239	186
HS4*	0.15	0.006742	0.13	0.000876	2.381155	16.25397	0.57	145	161
HS5*	**0.15**	**0.006977**	**0.13**	**0.000907**	**2.381155**	**16.25397**	**0.4**	**224**	**221**
HS6*	**0.15**	**0.00625**	**0.13**	**0.000813**	**2.381155**	**16.25397**	**0.66**	**104**	**139**
HS7*	**0.34**	**0.011429**	**0.351**	**0.004011**	**1.518947**	**21.63644**	**0.63**	**266**	**313**
HS8*	**0.69**	**0.023193**	**0.566**	**0.013127**	**1.518947**	**21.63644**	**0.93**	**290**	**289**

(*results from Kodur et al. 2000)

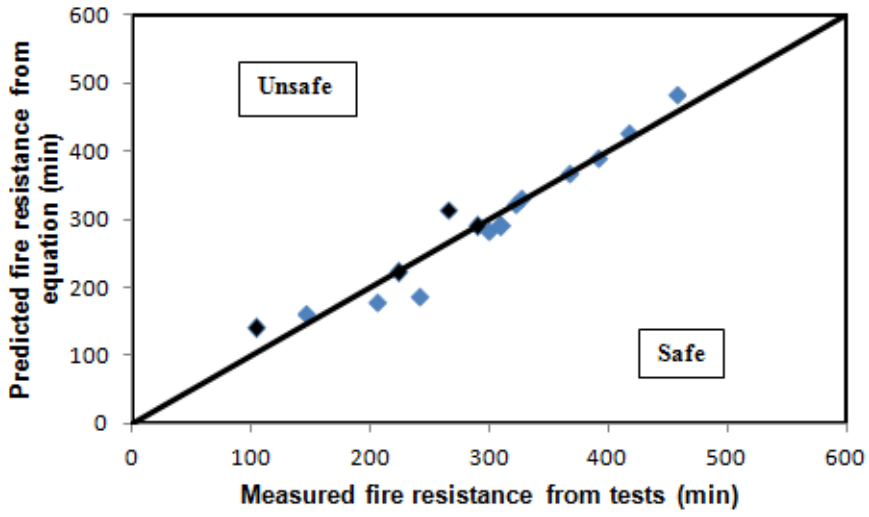

Fig. 4.18: Comparison of predicted and measured values of fire resistance

4.5 CONCLUDING REMARKS

Eight full scale RC columns with different confining reinforcement were tested for fire resistances in a fire furnace under standard fire scenario. The study was undertaken to study the effect of concrete strength, confining reinforcement and the configuration of confining reinforcement on the fire resistance of RC columns. The results show that these parameters of confinement have a marked role to play in the fire rating of the reinforced concrete columns. The disadvantage of high strength concrete being prone to spalling can be mitigated by the enhanced confinement of the RC columns. A simplified design equation, to determine effect of confinement on fire resistance of RC columns, has been arrived at.

CHAPTER - 5
CONCLUSIONS

5.1 GENERAL

The present research was carried out to study the behavior of reinforced concrete structures under post earthquake fire. In the first part of the study, an RC frame constructed with non-ductile detailing was subjected to a post earthquake fire and then also tested for its residual lateral capacity. The aim was to study the effect of earthquake and fire on such non-ductile detailed RC frames and also thereby to compare the behavior of non-ductile frame with ductile detailed frame tested in a previous study. In the second part of the study, a brick masonry in-filled RC frame was tested under post earthquake fire conditions. The aim was to study the effect of masonry in-fills on the post earthquake fire performance of RC frames. Finally, a study was carried out on full scale RC columns to study the influence of confining reinforcement on the fire resistance of the RC columns. It is believed that this research program will contribute to the fundamental understanding of the behavior of RC framed structures in post earthquake fire at the structural as well as at the elemental level.

5.2 CONCLUSIONS

On the basis of the experimental investigations carried out in this study, the following conclusions may be drawn:

1. The bare RC test frame was subjected to a target displacement of 150 mm, which corresponds to “Collapse prevention” structural performance level (S5) according to FEMA 356 (2000). Ideally, the performance of RC frames under earthquakes should be investigated using dynamic seismic loads. However, some initial observations can even be made from this study on the basis of static cyclic load tests. The present study reveals the conservativeness of the damage levels specified in Table C1-2 of FEMA 356 (2000) vis-à-vis both the RC frames (ductile and non-ductile). The overall damage in the test frame was not severe as anticipated in the Table C1-2. However the damage caused in the non-ductile detailed frame was in line with the expected damage specified by C1-3 of FEMA 356.

2. Present study also reveals overestimation of permanent drifts given in FEMA 356. However the permanent drift in non-ductile detailed RC frames is higher than in ductile detailed frames.
3. The investigation validates the time-temperature curve designed according to the fire design equation of Thomas and Heseldon (1972). The repeatability of the time-temperature curve proves the robustness of the fire design equation. The same could be used for future fire tests.
4. The tests reveal the vulnerability of thin elements like slabs and shells of non-ductile RC frames to spalling in post earthquake fire events. While drawing the attention towards addressing the issues of fire following earthquakes, the melting of reinforcement after spalling of thin elements like slab and shells needs to be considered in design codes.
5. Generally the normal strength concrete doesn't spall. However the present study reveals that the damaged concrete members (particularly with non-ductile detailing) having normal strength concrete are also susceptible to spalling. This is an important issue which must be taken into account while dealing with fire ratings of such elements.
6. The maximum deflection recorded in the columns was 8 mm. Similarly some of the beams underwent the change in deflection profiles as the cooling took place. The centre of the slab sagged at high temperatures and a maximum deflection/span ratio of 0.7% was registered in fire. After cooling, the residual sag was 0.37%. This data along with the other deflection profiles measured in this investigation can be used for the validation of numerical and theoretical models.
7. The measured results show that the position of the opening in the compartment and the resulting movement of fire plume also have an influence on the damage and buildup of the temperatures in the structural elements of the structure**.**
8. The test revealed the disadvantage of using standard fire curve as different elements revealed different temperature profiles. The uniform heating of structures as given in codes does not hold valid in real fire scenarios.
9. The cracks that appeared on the different elements of the test structure suggest that detailing of reinforcement has implications on the global behaviour of the structure when exposed to fire. In about 80 % of the structural members the temperatures in the RC frame with non-ductile detailing were much higher than those in the ductile detailed frame.

10. The test reflects the better performance of the RC frames with ductile detailing. Thus recommendations generally used in the seismic resistant design may also be helpful in enhancing the fire resistance of the RCC structures.
11. This study indicates that for a frame that is properly designed for seismic loads, infill panels will most likely have a beneficial influence on its performance. The study reveals that infill panels can be used to improve the performance of existing non-ductile frames. For this purpose, methods should be developed to enhance the shear resistance of non-ductile structural elements to avoid irreparable damage and catastrophic failure.
12. The masonry infill helps in delaying the flashover. The time taken to reach the maximum temperature is higher in masonry in-filled frames.
13. The brick infill walls provided insulation to the RC structural elements and slowed the transmission of heat to these elements. This beneficial effect of masonry walls should be considered while designing the columns and beams which are integrated in the masonry walls.
14. Despite losing two-thirds of its lateral load carrying capacity, the test frames showed no signs of collapse. The frames were in retrievable state. This implies that even after earthquake and fire the RC framed structures can be retrofitted.
15. This study shows that the layout of ties and confinement of columns has a marked influence on the fire performance of both the NSC and HSC columns. With the increase in the confining reinforcement factor, the fire resistance of the RC columns gets enhanced.
16. The effect of confinement is more pronounced in normal strength concrete columns than in high strength concrete columns. Higher grade of concrete in RC columns leads to lower fire resistance. For same fire rating in high strength columns the confinement to be provided has to be more than in normal strength columns.
17. An empirical equation has been proposed for evaluating the fire resistance of RC columns. The equation can be integrated in design standards to arrive at fire ratings of confined columns without being dependent on prescriptive methods.

5.3 FUTURE SCOPE

It is desirable that, more number of full-scale RC frame sub-assemblages subjected to higher level of simulated earthquake pre-damage and then exposed to compartment fire should be investigated for broader simulation of fires following earthquake scenarios. The data from the tests presented in this study can be utilized to develop numerical and analytical models to

study the effect of various parameters viz. confinement levels, reinforcement details, fire scenarios, fire duration, simulated mechanical pre-damage, number of storeys etc on the post earthquake fire performance of the RC structures. Based on such a comprehensive testing programme, suitable guidelines for designing new structures and retrofitting existing structures can be proposed. Since fire performance of structural members under FFE events depends on the properties of the constituent materials like concrete and reinforcing bars, knowledge of high-temperature material properties is critical for advancing the state-of-the-art in the science of fire engineering. The effect of the crack widths on the temperature build up in the structure elements of any structure also needs to be studied. Similar to develop a robust design tool for the fire design of RC columns, more experimental studies need to be carried out on the RC columns. The important parameters like the aggregate type, the load eccentricities etc also need to be incorporated in the design equations.

REFERENCES

1. Abu, A.K., Burgess, I.W. and Plank, R.J. (2013) Tensile Membrane Action of Thin Slabs Exposed to Thermal Gradients. Journal of Engineering Mechanics 139(11): 1497-1507
2. Abu, A.K., Ramanitrarivo, V. and Burgess, I.W. (2011) Collapse Mechanisms of Composite Slab Panels in Fire. Journal of Structural Fire Engineering 2(3): 205-216.
3. Abrams, M. S. (1971), "Compressive strength of concrete at temperatures to 1600 F", Temperature and concrete, Detroit (MI): American Concrete Institute, SP-25, pp.33–59.
4. Abrams, M. S. (1978), "Behaviour of inorganic materials in fire", In: ASTM symposium on design of buildings for fire safety, Boston (MA) (special publication 685).
5. Ahmed, A. E., Al-Shaikh, A. H., Arafat, T. I. (1992), "Residual compressive and bond strengths of limestone aggregate concrete subjected to elevated temperatures", Magazine of Concrete Research, 44, No. 159, June, 1 17-125.
6. Aiello, M. A., Focacci, F. and Nann, A. (2001), "Effects of thermal loads on concrete cover of fiber- reinforced polymer reinforced elements: theoretical and experimental analysis", ACI Materials Journal, V. 98, No. 4, pp. 332-339.
7. Al-Chaar, G., Issa, M., & Sweeney, S. (2002). Behavior of masonry-infilled nonductile reinforced concrete frames. Journal of Structural Engineering, 128(8), 1055-1063.
8. Aldea, C. M., J. M. Franssen, et al. (1977). Fire test on normal and high strength reinforced concrete columns. National Institute of Science and Technology Gaithersburg, Maryland, USA.
9. Ali, F., Nadjai, A., Silcock, G. & Abu-Tair, A. (2004), "Outcomes of a major research on fire resistance of concrete columns", Fire Safety J., 39(6), pp. 433-445.
10. Anderberg, Y. (1978), "Analytical fire engineering design of reinforced concrete structures based on real fire conditions", in: Proceeding of the FIP Congress, London, Part I, pp. 112-121.
11. Arlekar, J. N., Jain, S. K., & Murty, C. V. R. (1997, November). Seismic response of RC frame buildings with soft first storeys. In Proceedings of the CBRI Golden Jubilee Conference on Natural Hazards in Urban Habitat (pp. 10-11).

12. Aschl, H. and Mooseeker, W. (1979), "Mechanical Properties at Elevated temperatures and Residual Mechanical Behaviour after Tri-axial Pre loading", Transactions of the International Conference on Structural Mechanics in Reactor Technology, V.H. pp.1-10.

13. Aslani, F. and Bastami, M. (2011), "Constitutive Relationships for Normal- and High-Strength Concrete at Elevated Temperatures", ACI Materials Journal, V. 108, No. 4, pp. 355-364.

14. ASTM Test Method E119-01 (2001), "Standard Methods of Fire Test of Building Construction and Materials", American Society for Testing and Materials.

15. Bailey, C. (2002), "Holistic behaviour of concrete buildings in fire", Proceedings, Institute of Civil Engineers: Structures & Buildings, V.152, Issue 3, pp. 199-212.

16. Bailey, C.G. (2004), "Membrane action of slab/beam composite floor systems in fire", Engineering Structures, 16, pp. 1691-1703.

17. Bailey, C.G., Toh, W.S. (2007), "Behaviour of concrete floor slabs at ambient and elevated temperatures", Fire Safety Journal, V. 42, pp. 425–436.

18. Bamonte, P. Gambarova P. G. and Meda, A. (2008), "Today's concretes exposed to fire-test results and sectional analysis", Thomas Telford and fib. Structural Concrete, V. 9, No 1, pp.19-29.

19. Baruah, P. and Talukdar, S. (2007), "A Comparative Study of Compressive, Flexural, Tensile and Shear Strength of Concrete with fibres of different origins", Indian Concrete Journal, 81 (7), pp. 17-24.

20. Bastami, M. and Aslani, F. (2010), "Preloaded High-Temperature Constitutive Models and Relationships for Concrete", Transaction A: Civil Engineering Vol. 17, No. 1, pp. 11{25).

21. Bayasi, Z. and Dhaheri, M.A. (2002), "Effect of Exposure to Elevated Temperature on Polypropylene Fiber-Reinforced Concrete", ACI Materials Journal, V. 99, No. 1, pp. 22-26.

22. Bazant, Z.P. and Kaplan, M.F. (1996), "Concrete at High Temperature", Material Properties and Mathematical Models. Longman Group Limited, London, pp. 196.

23. Behnooda, A. and Ghandehari, M. (2009), "Comparison of compressive and splitting tensile strength of high-strength concrete with and without polypropylene fibers heated to high temperatures", Fire Safety Journal 44, 1015–1022.

24. Beitel, J. and Iwankiw N. (2002), "Analysis of needs and existing capabilities for full-scale fire resistance testing", National Institute of Standards and Technology, NIST GCR 02-843, Hughes Associates, Inc., Baltimore, MD.

25. Benmarce, A. and Guenfoud, M. (2005), “Experimental behaviour of high strength concrete column in fire”, Magazine of Concrete Research, 57(5), pp. 283-287.

26. Berto, A. F. and Tomina, J. C., (1988), "Lessons From the Fire in the CESP Administration Headquarters" IPT Building Technologies, Sao Paulo, Brazil.

27. Bingo, A.F., Gül, R. (2009), “Residual bond strength between steel bars and concrete after elevated temperatures”, Fire Safety Journal V. 44 pp. 854–859.

28. Bisby, L. A., Green, M. F. and Kodur, V. K. R. (2005), “Modeling the Behavior of Fiber Reinforced Polymer-Confined Concrete Columns Exposed to Fire”, ASCE, Journal of Composites for Construction, Vol. 9, No. 1, pp. 15-24.

29. Bisby, LA. , Chen, J. F., Li, S. Q., Stratford, T. J. , Cueva, N. & Crossling, K. (2011), “Strengthening fire damaged circular concrete columns with FRP”, Journal of Advanced Composites in Construction, Warwick : Net Composites Ltd., pp. 130-141.

30. Book, N. G A., Mirza, M. S. and Lie, T. T. (1990), “Response of direct models of reinforced concrete columns subjected to fire”, ACI Structural Journal, V. 87, No. 3, pp. 313-325.

31. Both, C., van de Haar, P., Tan, G. & Wolsink, G. (1999), “Evaluation of passive fire protection measures for concrete tunnel linings”, Proceedings, Int. Conf. on Tunnel Fires & Escape from Tunnels, Lyon, France, pp. 95-104.

32. BS 8110: Part 2: 1985: Structural use of concrete. Part 2: Code of practice for special circumstances, British Standards Institution, London.

33. BSI 1987. Fire tests on building materials and structures - Part 20: Method for determination of the fire resistance of elements of construction. Standard 20, British Standard Institution, UK.

34. BSI 1987. Fire tests on building materials and structures - Part 21: Methods for determination of the fire resistance of load bearing elements of construction. Standard 21, British Standard Institution, UK.

35. BSI 1987. Fire tests on building materials and structures - Part 22: Methods for determination of the fire resistance of non- load bearing elements of construction. Standard 22, British Standard Institution, UK.

36. Buchanan, A. H. (2001), “Structural design for fire safety”, John Wiley & Sons, 421pp.

37. Bureau of Indian Standards (2000), “Indian Standard Plain and Reinforced Concrete, Code of Practice, IS 456:2000, (Fourth Revision)”, BIS New Delhi, 100pp.

38. Bureau of Indian Standards (2002), "Indian Standard Specification for coarse and fine aggregate from natural sources for concrete, Code of Practice, IS 383:1970, (Reaffirmed 2002)", BIS New Delhi, 21pp.

39. Bureau of Indian Standards (2003), "Code of practice for design loads (other than earthquake) for buildings and structures: Part 1 Dead loads-Unit weight of building material and stored materials (Incorporating IS: 1911-1967), IS 875: (Part 1):1987, (Reaffirmed 2003)", BIS New Delhi, 37pp.

40. Bureau of Indian Standards (2003), "Code of practice for design loads (other than earthquake) for buildings and structures: Part 2 Imposed loads, IS 875: (Part 2):1987, (Reaffirmed 2003)", BIS New Delhi, 18pp.

41. Bureau of Indian Standards (2005), "Indian Standard 43 Grade Ordinary Portland Cement Specification, Code of Practice, IS 8112:1989, First revision, (Reaffirmed 2005)", New Delhi, 8 pp.

42. Bureau of Indian Standards (2005), "Methods of chemical analysis of hydraulic cement, IS 4032:1985, First Revision, (Reaffirmed 2005)", BIS New Delhi, 42pp.

43. Bureau of Indian Standards (2005), "Methods of physical tests for hydraulic cement: Part 3 Determination of soundness, IS 4031(Part 3):1988, (Reaffirmed 2005)", BIS New Delhi, 4pp.

44. Bureau of Indian Standards (2005), "Methods of physical tests for hydraulic cement: Part 4 Determination of consistency of standard cement paste, IS 4031(Part 4):1988, (Reaffirmed 2005)", BIS New Delhi, 2pp.

45. Bureau of Indian Standards (2005), "Methods of physical tests for hydraulic cement: Part 5 Determination of initial and final setting times, IS 4031(Part 5):1988, (Reaffirmed 2005)", BIS New Delhi, 2pp.

46. Bureau of Indian Standards (2005), "Methods of physical tests for hydraulic cement: Part 6 Determination of compressive strength of hydraulic cement (other than masonry cement), IS 4031(Part 6):1988, First revision (Reaffirmed 2005)", BIS New Delhi, 3pp.

47. Bureau of Indian Standards (2007), "Criteria for earthquake resistant design of structures: Part 1 General provisions and buildings, IS 1893:2002, (Reaffirmed 2007)", BIS New Delhi, 39pp.

48. Bureau of Indian Standards (2008), " Ductile detailing of reinforced concrete structures subjected to seismic forces-Code of practice, IS 13920:1993, (Reaffirmed 2008)", BIS New Delhi, 16pp.

49. Bureau of Indian Standards (2008), "High strength deformed steel bars and wires for concrete reinforcement-specification, IS 1786: 2008, (Fourth revision)", BIS New Delhi, 12 pp.

50. Bureau of Indian Standards (2009), "Recommended guidelines for concrete mix design, IS 10262:1982, (Reaffirmed 2009)", New Delhi, 21pp.

51. Canisius, T.D.G., Waleed, N. & Matthews, S.L. (2003), "Evaluation of effects of the fire test on Cardington concrete building", Proceedings (CIB Publication No. 290, eds. Shafi, F., Bukowski, R. & Klemencic, R.), CIB-CTBUH Int. Conf. on Tall Buildings, Kuala Lumpur, Malaysia, pp. 353-360.

52. Capote, J.A., Alvear, D., Lázaro, M., Espina, P., Fletcher, I.A., Welch, S. & Torero, J.L. (2006), "Analysis of thermal fields generated by natural fires on the structural elements of tall buildings", Proceedings, Int. Cong. Fire Safety in Tall Buildings, Santander, Spain, pp. 93-109.

53. Carvel, R. (2005), "Fire protection in concrete tunnels", The Handbook of Tunnel Fire Safety (Eds. Beard, A. & Carvel, R.) Thomas Telford, London.

54. Castillo, C. and Durani, A.J. (1990), "Effect of transient high temperature on high-strength concrete", ACI Material Journal, 87(1), 47-53.

55. Chakrabarti, S. C. and Jain, A. K. (1999), "Strength properties of concrete at elevated temperature, A review", The Indian Concrete Journal, pp. 495-500.

56. Chan, S.Y. N., Peng, G. F. and Anson, M. (1999), "Residual strength and pore structure of high-strength concrete and normal strength concrete after exposure to high temperatures", Cement Concrete Composite, 21, pp. 23-27.

57. Chan, S.Y.N., Luo, X. and Sun, W. (2000), "Effect of high temperature and coolind regimes on the compressive strength and pore properties of high performance concrete", Construction and Building Materials Journal, V. 14 pp. 261-266.

58. Chang, Y. F., Chen, Y. H. Shen, M. S. and Yao, G. C. (2006), "Residual stress strain relationship for concrete after exposure to high temperature", Cement and Concrete Research, 36, pp. 1999-2005.

59. Chen, B., Li, C. and Chen, L. (2009), "Experimental study of mechanical properties of normal strength concrete exposed to high temperatures at an early age", Fire Safety Journal, 44, pp. 997-1002.

60. Chen WF and Scawthorn C (2003). "New directions in civil engineering", Earthquake Engineering Handbook. CRC Press, Boca Raton, FL

61. Chen, J. and Young, B. (2006), "Stress-strain curves for stainless steel at elevated temperatures", Journal of Engineering Structures, Vol. 28, Issue 2, pp. 229-239.

62. Chen, Y. H., Chang, Y. F., Yao G. C. and Sheu, M. S. (2009), "Experimental research on post-fire behaviour of reinforced concrete columns", Fire Safety Journal, 44, pp. 741-748.

63. Cheng, F. P., Kodur, V. K. R. and Wang, T. C. (2004), "Stress Strain curves for high strength concrete at elevated temperatures", Journal of Materials in Civil Engineering ASCE, 16(1), pp. 84-90.

64. Chung, R.M., Jason, N.H., Mohraz, B., Mowrer, F.W. and Walton, W.D. (1995), "Proceeding of the post-earthquake fire and lifelines workshop, Long Beach, Calif., NIST SP 889. Building and Fire Research Laboratory, National Institute of Standards and Technology (NIST), Gaithersburg, Md.

65. Cioni, P., Croce, P. and Salvatore, W. (2001), "Assessing fire damage to R.C. elements", Fire Safety Journal, V. 36, pp. 181-199.

66. Cooke, G. M. E. (1988), "An Introduction to the mechanical properties of structural steel at elevated temperatures", Fire Safety Journal, 13 45 - 54 45.

67. Cooke, G.M.E. (2001), "Behaviour of precast concrete floor slabs exposed to standardised fires", Fire Safety Journal Vol. 36 pp. 459-475.

68. Cousins, W. J., Dowrick, D. J. and Sritharan, S. (1991), "Fire following earthquake", Proc. Institution of Fire Engineers Conference, New Plymouth.

69. Cusson, D. and Paultre, P. (1994), "High strength concrete columns confined by rectangular ties", Journal of Structural Engineering ASCE, 120(3), pp. 783-804.

70. Cusson, D. and Paultre, P. (1995), "Stress-strain model for confined high strength concrete", Journal of Structural Engineering ASCE, 121(3), pp. 468-477.

71. Della Corte, G., Landolfo, R. and Mazzolani, F.M. (2003), "Post-Earthquake Fire Resistance of Moment Resisting Steel Frames", Fire Safety Journal, V. 38(7) pp. 593-612.

72. Demirel, B. and Kelestemur, O. (2010), "Effect of elevated temperature on the mechanical properties of concrete produced with finely ground pumice and silica fume", Fire Safety Journal, V. 45, pp. 385–391.

73. Desai, S.B. (1998), "Design of reinforced concrete beams under fire exposure", Magazine of Concrete Research, V. 50, No. 1, pp. 75-83.

74. Diederichs, U. and Schneider, U. (1981),"Bond strength at high temperatures", Magazine of Concrete Research: Vol. 33, No. 1 15:pp. 75-84.

75. Diederichs, U., Jumppanes, U. M. and Penttala, V. (1988), "Materials properties of high strength concrete at elevated temperature", Transaction 13th IABSE Congress, Helsinki Finland, pp. 489-494.

76. Dong, Y. and Prasad, K. (2009), "Experimental study on the behavior of full-scale composite steel frames under furnace loading", ASCE, Journal of Structural Engineering, Vol. 135, No. 10, pp. 1278-1289.

77. Dong, Y.L. (2010), "Tensile membrane effects of concrete slabs in fire", Magazine of Concrete Research, V. 62, No. 7 pp. 497–505.

78. Dotreppe, I.C., Franssen, I. M., Bruls, A., Baus, R. Vandevelde, P., Minne, T. R. Nieuwenburg, D. V. and Lambotte, H. (1996), "Experimental research on the determination of the main parameters affecting the behaviour of reinforced concrete columns under fire conditions", Magazine of Concrete Research, V. 49, No. 179, pp. 117-127.

79. Dotreppe, J.C. (1997), "Mechanical properties of quenched and self-tempered reinforcing steel at elevated temperature compared with recommendation of Eurocode 2-Part 1-2", Materials and structures, Vol.30, pp. 430-8.

80. Dotreppe, J.C., Franssen, J.M. and Vanderzeypen, Y. (1999), "Calculation method for design of reinforced concrete, columns under fire conditions", ACI Structural Journal, V. 96, No. 1, pp.9-20.

81. Drysdale, D.D. (1999), "Introduction to Fire Dynamics", John Wiley and Sons.

82. Dwaikat, M. and Kodur V. (2008), "Fire performance of steel beam-columns under design fire exposures", Proceedings of the Fifth International Conference on Structures in Fire.

83. Dwaikat, M. B. and Kodur, V. K. R. (2009), "Response of restrained concrete beams under design fire exposure", Journal of Structural Engineering, Vol. 135, No. 11, pp. 1408-1417.

84. Ehm, C., Schneider, U. and Kordina, K. (1985), "Bi-axial testing of reactor concrete", Transactions of the International Conference on Structural Mechanics in Reactor Technology, V.H. pp.349-354.

85. Ehm, C., Schneider, U. and Kordina, K.(1986), "Effect of bi-axial loading on the high temperature behaviour of concrete", Fire Safety Science, Proceedings of the First international Symposium.pp.281-290.

86. Eidinger, J.M. (2004). "Fire following earthquake-flex hose" In 13th World Conference on Earthquake Engineering, Vancouver, B.C.,, Canadian Association for Earthquake Engineering (CAEE), Ottawa, Ont. Paper No. 3268.

87. Elghazouli, A. Y. and Izzuddin, B. A. (2004), "Realistic modeling of composite and reinforced concrete floor slabs under extreme loading. II: verification and application", Journal of Structural Engineering, Vol. 130, No. 12, pp. 1985-1996.

88. Elghazouli, A.Y. and Izzuddin, B.A. (2001), "Analytical assessment of the structural performance of composite floors subject to compartment fires", Fire Safety Journal V. 36(8), pp. 769–793.

89. Elghazouli, A.Y., Cashell, K.A. and Izzuddin, B.A. (2009), "Experimental evaluation of the mechanical properties of steel reinforcement at elevated temperature", Fire Safety Journal, V. 44, pp. 909-919.

90. ENV 1992-1-2, (1995). "Design of concrete structures-Part 1-2: General rules-structural fire design", European Committee for Standardization, Brussels.

91. Eurocode 2 (2004), "Design of concrete structures: Part 1-2: general rules- structural fire design", European Committee for Standardisation, Brussels, BS EN 1992-1-2, 2004.

92. Feasey, R., & Buchanan, A. (2002). Post-flashover fires for structural design.Fire Safety Journal, 37(1), 83-105.

93. Felicetti, R. and Gambarova, P.G. (1998), "Effects of high temperature on the residual compressive strength of high strength siliceous concretes", ACI Materials Journal, V. 95, No. 4, pp. 395-406.

94. Felicetti, R. Gambarova, P G and, Meda, A. (2009), "Residual behavior of steel rebars and R/C sections after a fire", Construction and Building Materials 23 3546–3555.

95. FEMA (2000), "Pre-standard and commentary for the Seismic rehabilitation of buildings / FEMA 356, 2000, Chapter 1: Rehabilitation Requirements", Table C1-3, pp. 14.

96. FEMA 356 (2000), "Prestandard and commentary for the seismic rehabilitation of buildings," 518pp.

97. Fitiany, S.F.E and Youssef, M.A. (2009), “Assessing the flexural and axial behaviour of reinforced concrete members at elevated temperatures using sectional analysis”, Fire Safety Journal, V. 44, pp. 691–703.

98. Fletcher, I. A., Welch, S., Terero, J. L., Carvel, R. O. and Usmani, A. (2007), “The Behaviour of concrete Structures in Fire”, Journal of Thermal Science, V. 11 (2), pp.33-57.

99. Flint, G., Usmani, A., Lamont, S., Lane, B. and Torero, J. (2007), “Structural response of tall buildings to multiple floor fires”, ASCE, Journal of Structural Engineering, Vol. 133, No. 12, pp.1719-1732.

100. Folic, R., Radonjanin, V., and Malesev, M. (2002), “The assessment of the structure of Novi Sad Open University damaged in a fire”, Elsevier, Construction and Building Materials V.16 (7), pp. 427–440.

101. Foster, S. J. (1999), “Design and detailing of high strength concrete columns”, Research report No. R-375, March, University of New South Wales, Sydney, Australia.

102. Foster, S. J., Liu, J. and Sheikh, S. A. (1998), “Cover spalling in HSC columns loaded in concentric compression”, Journal of Structural Engineering ASCE, 124(12), pp 1431-1437.

103. Foster, S., Chladna, M., Hsieh, C., Burgess, .I. and Plank, R. (2007), “Thermal and structural behaviour of a full-scale composite building subject to a severe compartment fire”, Fire Safety Journal V. 42(3), pp. 183–199.

104. Franssen, J.M. (2005), “Structures in Fire, Yesterday, Today and Tomorrow”, Proceedings, 8th Int. Symp. Fire Safety Science, Beijing, China, pp. 21-35.

105. Franssen, J. M. and Dotreppe, J. C (2003). Fire tests and calculation methods for circular concrete columns. Fire Technology, 39, No. 1, 89–97.

106. Franssen, J.M., Pintea, D. and Dotreppe, J.C. (2007), “Considering the effects of localised fires in the numerical analysis of a building structure”, Fire Safety Journal V.42 (6-7), pp. 473–481.

107. Freskakis, G.N. (1980), “Behaviour of reinforced concrete at elevated temperatures”, Paper 3-4, Second ASCE conf. on Civ. Eng. And nuclear power, Vol. 1, Paper 3-5, pp. 3-5-1 to 3-5-21, Knoxville, Tennessee.

108. Freskakis, G.N. et al., (1979), “Structural Properties of Concrete of Concrete at Elevated Temperature", Civil Engineering Nuclear Power, Vol. 1, ASCE Natl. Convention, Boston April 1979.

109. Fu, Y. F., Wong, Y. L. Poon, C. S. and Tang, C. A. (2005), "Stress–strain behaviour of high-strength concrete at elevated temperatures", Magazine of Concrete Research, 57(9), pp. 535–544.

110. Furumura, F., Abe, T. and Shinohara, Y. (1995), "Mechanical properties of high strength concrete at high temperature", Proceedings of the Fourth Weimar Workshop on High Performance Concrete: Material Properties and Design, Hochschule fuer Architektur und Bauwesen (HAB), Weimar, Germany, Oct., 237-254.

111. Gales, J. and Bisby, L. (2014), " Deformation and response of continous and restrained post-tensioned concrete slabs at high temperatures", Proceedings of 8th International conference on Structures in Fire, Shanghai China, June 11-13, pp. 305-312

112. Gary, M. (1916), "Fire tests on reinforced concrete buildings", Verlag Wilhelm Ernst und Sohn, Heft 11, Germany.

113. Georgali, B. and Tsakiridis, P.E. (2005), "Microstructure of fire-damaged concrete", Cem Concre Compos, V. 27 pp, 255-9.

114. Ghan, Y. N., Peng, G. F., Anson, M. (1999), "Residual strength and pore structure of high-strength concrete and normal strength concrete after exposure to high temperatures, Cement and Concrete Composites, V. 21, pp. 23-27.

115. Ghandehari, M. Behnood, A. and Khanzadi, M., (2010), "Residual Mechanical Properties of High-Strength Concretes after Exposure to Elevated Temperatures", Journal of Materials in Civil Engineering, Vol. 22, No. 1, pp. 59-64.

116. Ghoreishi, M., Bagchi, A. and Sultan, M.A. (2009), "Estimating the response of structural systems to fire exposure: state-of-the-art review", Fires and Materials -11th International Conference and Exhibition, January 2009.

117. Giroldo F. and Bailey, C. G. (2008), "Experimental bond behaviour of welded mesh reinforcement at elevated temperatures", Magazine of Concrete Research, 60, No. 1, February, 23–31.

118. Gustaferro A., Martin L.D. (1988), "Design for fire resistance of precast prestressed concrete," 2nd ed. Skokie, Illinois, USA: Prestressed Concrete Institute.

119. Haddad, R. H., Al-Saleh, R. J. and Al-Akhras, N. M. (2008), "Effect of elevated temperature on bond between steel reinforcement and fibre reinforced concrete", Fire Safety Journal, 43, pp. 334–343.

120. Hammer, T. A. (1995), "High Strength concrete phase 3, compressive strength and E-modulus at elevated temperatures", SP6 Fire resistance, Report 6.1, SINTEF Structure and concrete, STF70 A95023.

121. Han, C. G., Hwang, Y. S., Yang, S. H. and Gowripalan, N. (2005), "Performance of spalling resistance of high performance concrete with polypropylene fibre contents and lateral confinement", Cement and Concrete Research, 35, pp. 1747-1753.

122. Han, C.G., Han, N.C. and Heo, Y.S. (2009), "Improvement of residual compressive strength and spalling resistance of high-strength RC columns subjected to fire", Construction and Building Materials, 23, pp.107-116.

123. Han, C.G., Yang, S.H., Han M.C. and Pei, C.C. (2008), "Spalling prevention of high strength concrete with 60-100 MPa of the compressive strength corresponding to addition of polypropylene fibre", Archit. Inst. Korea 24, pp. 91-98.

124. Hansen G (2015). "Timeline of the San Francisco Earthquake", April 18 - 23, 1906 http://sfmuseum.net/hist10/06timeline.html Accessed 20 March 2015.

125. Harmathy, T. Z. and Stanzak, W. W. (1970), "Elevated-temperature tensile and creep properties of some structural and pre stressing steel", 464, American Society for Testing and Materials, pp. 186–208 [special technical publication].

126. Hertz, K. D. (2003), "Limits of spalling of fire exposed concrete", Fire Safety Journal, 38, pp. 103-116.

127. Hertz, K. D. (2004), "Reinforcement data for fire safety design", Magazine of Concrete Research, 56(8), pp. 455-459.

128. Hertz, K. D. (2005), "Concrete strength for fire safety design", Magazine of Concrete Research, 57(8), pp. 445-453.

129. Hoehler, M.S. and Stanton, J. F. (2006), "Simple phenomenological model for reinforcing steel under arbitrary load", J. of Structural Engineering, ASCE, 132(7), pp. 1061-1069.

130. Holmes, M., Anchor, R.D., Cook, G.M.E., and Crook, R.N. (1982), "The effects of elevated temperatures on the strength properties of reinforcing and prestressing steels", Structural Engineer, March, 60B (1), 7-13.

131. Hong, K. N., Han, S. H. and Tac-Yi, S. (2006), "High strength concrete column confined by low volumetric ratio lateral ties", Engineering Structure, 28, pp. 1346-1353.

132. Hopkin, D.J., Lennona, T., Rimawi, J. E. and Silberschmidt, V. (2011), "Full-scale natural fire tests on gypsum lined structural insulated panel (SIP) and engineered floor joist assemblies", Fire Safety Journal V.16 (8), pp. 528–542.

133. Huang, Z. (2010), "The behaviour of reinforced concrete slabs in fire", Fire Safety Journal V. 45, pp. 271–282.

134. Huang, Z. and Platten, A. (1997), "Nonlinear finite element analysis of planar reinforced concrete members subjected to fires", ACI Structural Journal, V. 94, No. 3, pp. 272-281.

135. Huang, Z., Burgess, I. W and Plank, R. J. (1999), "Nonlinear Analysis of Reinforced Concrete Slabs Subjected to Fires", ACI Structural Journal, V. 96, No. 1, pp. 127-136.

136. Huang, Z., Burgess, I. W. and Plank, R. J. (2003), "Modeling Membrane Action of Concrete Slabs in Composite Buildings in Fire. I: Theoretical Development", ASCE, Journal of Structural Engineering, Vol. 129, No. 8, pp. 1093-2003.

137. Huang, Z., Burgess, I.W. and Plank, R. J. (2004), "Fire resistance of composite floors subject to compartment fires", Elsevier Journal of Constructional Steel Research V. 60(2), pp. 339–360.

138. Huang, Z., Burgess, I.W. and Plank, R.J. (2009), "Three-dimensional analysis of reinforced concrete beam-column structures in fire", ASCE, Journal of Structural Engineering, Vol. 135, No. 10, pp. 1201-1212.

139. Hurst, J. P. and Ahmed, G. N. (1998), "Validation and application of a computer model for predicting the thermal response of concrete slabs subjected to fire", ACI Structural Journal, V. 95, No. 5, pp. 480-487.

140. Irfanoglu, A. and Hoffmann, C. M. (2008), "Engineering perspective of the collapse of WTC-I", ASCE, Journal of Performance of Constructed Facilities, Vol. 22, No. 1, pp. 62-67.

141. ISO (1975), "Fire Resistance Tests, Elements of Building Construction. ISO 834", International Organization for Standardization. Geneva.

142. Iwankiw, N., Beyler, C., Beitel, J. (2008), "Testing needs for advancement of structural fire engineering", Proceedings of the Fifth International Conference on Structures in Fire.

143. Izzuddin, B. A. and Elghazouli, A. Y. (2004), "Failure of lightly reinforced concrete members under fire.II: parametric studies and design considerations", ASCE, Journal of Structural Engineering, Vol. 130, No. 1, pp. 18-31.

144. Izzuddin, B. A. and Elghazouli, A. Y. (2004), "Failure of lightly reinforced concrete members under fire. I: analytical modeling", ASCE, Journal of Structural Engineering, Vol. 130, No. 1, pp. 3-17.

145. Jau, W.C. and Huang, K.L. (2008), "A study of reinforced concrete corner columns after fire", Cement & Concrete Composites, V. 30, pp. 622–638.

146. Jeffers, A. E. and Sotelino, E. D. (2009), “Fiber heat transfer element for modeling the thermal response of structures in fire”, Journal of Structural Engineering, Vol. 135, No. 10, pp.1191-1200.

147. Johnston, R. P. D., Sonebi, M., Lim, J. B. P., Armstrong, C. G., Wrzesien, A. M., Abdelal, G., & Hu, Y. (2015). The Collapse Behaviour of Cold-formed Steel Portal Frames at Elevated Temperatures. *Journal of Structural Fire Engineering, 6* (2), 77-102.

148. Kalifa, P., Chene, G. and Galle, C. (2001), “High-temperature behaviour of HPC with polypropylene fibres from spalling to microstructure”, Cement and Concrete Research, 31(10), pp. 1487-1499.

149. Kamath, P. (2014), “Response of RC framed structures subject to post - earthquake fire”, PhD Thesis, Department of Civil Engineering, IIT Roorkee, Roorkee India.

150. Kawagoe, K. (1958.) Fire behaviour in rooms. Report 27, Building Research Institute, Ministry of Construction, Tokyo, Japan,

151. Kent, D. C. and Park, R. (1971), “Flexural members with confined concrete”, Journal of Structural Division. ASCE, 97, pp.1969-1990.

152. Khan, M. R. and Royles, R. (1986), “Post heat exposure behaviour of reinforced concrete beams”, Magazine of Concrete Research, Vol. 38, No. 135, pp. 59-66.

153. Khoury, G. A. (1992), “Compressive strength of concrete at high temperature”, A Reassessment Magazine of Concrete Research, 44(161), pp. 291-309.

154. Khoury, G. A., Majorona C.E., Pesavento, F. and Schrefler, B.A. (2002), “Modeling of heated concrete”, Magazine of Concrete Research, 54(2), pp. 77-101.

155. Khoury, G.A. (2000), "Effect of Fire on Concrete and Concrete Structures", Progress in Structural Engineering and Materials, 2(4) pp. 429-447.

156. Khoury, G.A. and Anderberg, Y. (2000), “Concrete spalling review”, A report on Fire Safety Design, Swedish National Road Administration.

157. Khoury, G.A., Grainger, B.N. & Sullivan, P.J.E. (1985), “Transient thermal strain of concrete: literature review, conditions within specimen and behaviour of individual constituents”, Mag. Concrete Res., 37 (132), pp. 131-144.

158. Kim, G. Y., Kim, Y. S. and Lee, T. G. (2009), “Mechanical properties of high strength concrete subjected to high temperature by stressed method”, Transactions Nonferrous Metals Society of China, 19, pp. 128-133.

159. Knaack, A. M. Kurama, Y. C. and Kirkner, D. J. (2010), "Compressive Strength Relationships for Concrete under Elevated Temperatures", ACI Material Journal, V. 107, No. 2, pp. 164-175.

160. Knaack, A. M. Kurama, Y. C. and Kirkner, D. J. (2011), "Compressive Stress-Strain Relationships for North American Concrete under Elevated Temperatures", ACI Material Journal, V. 108, No. 3, pp.270-280.

161. Ko, J., Ryu D.and Noguchi, T. (2011), "The spalling mechanism of high- strength concrete under fire", Magazine of Concrete Research, 2011, 63(5), 357–370.

162. Kodur V.K.R. and Dwaikat, M.B., (2008), "Effect of Fire Induced Spalling on the Response of Reinforced Concrete Beams", International Journal of Concrete Structures and Materials Vol.2, No.2, pp. 71-81.

163. Kodur, V. R.; Mcgrath, et al (2000). Experimental Studies on the Fire Endurance of High-Strength Concrete Columns National Research Council, Canada: internal report 819.

164. Kodur, V. K. R. and Sultan, M. A. (2003), "Effect of Temperature on Thermal Properties of High-Strength Concrete", ASCE, Journal of Materials in Civil Engineering, Vol. 15, No. 2, April 1, pp. 793-801.

165. Kodur, V. K. R. and Bisby, L. A. (2005), "Evaluation of Fire Endurance of Concrete Slabs Reinforced with Fiber-Reinforced Polymer Bars", ASCE Journal of Structural Engineering, Vol. 131, No. 1, pp. 34-43.

166. Kodur, V. K. R. and Dwaikat, M. (2008), "Flexural response of reinforced concrete beams exposed to fire", Thomas Telford and fib, Structural Concrete", Vol. 9, No. 1 pp. 45-54.

167. Kodur, V. K. R. and McGrath, R. (2006), "Effect of silica fume and lateral confinement on fire endurance of high strength concrete columns", Canadian Journal Civil Engineering, 33, pp. 93-102.

168. Kodur, V. K. R. and Phan, L.T. (2007), "Critical factors governing the fire performance of high strength concrete systems", Fire Safety Journal, 42, pp. 482-488.

169. Kodur, V. K. R. and Sultan, M. A. (1998), "Structural behaviour of high strength concrete columns exposed to fire NRCC-41736", National Research Council Canada.

170. Kodur, V. K. R., Bisby, L. A. and Foo, S. H.C. (2005), "Thermal Behavior of Fire-Exposed Concrete Slabs Reinforced with Fiber-Reinforced Polymer Bars", ACI Structural Journal, V. 102, No. 6, pp. 799-807.

171. Kodur, V. K. R., Cheng, F. P., Wang, T. C. and Sultan, M. A. (2003), "Effect of strength and fibre reinforcement on fire resistance of high strength concrete columns", Journal of Structural Engineering, 129(2), pp. 253-259.

172. Kodur, V. K. R., Dwaikat, M. B. and Fike, R. S. (2010), "An approach for evaluating the residual strength of fire-exposed RC beams", Magazine of Concrete Research, V. 62, No. 7, pp. 479–488.

173. Kodur, V.K. and Dewaikat, M. (2012), "Fire-induced spalling in reinforced concrete beams", Structures and Buildings, Vol.165, Issue SB7, pp. 347-359.

174. Kodur, V.K.R., Bisby, L. A. and Green, M. F. (2006), "Experimental evaluation of the fire behaviour of insulated fibre-reinforced-polymer-strengthened reinforced concrete columns", Fire Safety Journal, V. 41, pp. 547–557.

175. Kodur, V.K.R., Dwaikat, M.M.S., and Dwaikat, M.B. (2008), "High-Temperature Properties of Concrete for Fire Resistance Modeling of Structures", ACI Materials Journal, 105(5), September-October, 517 – 527.

176. Kodur, V.K.R., Wang, T.C. and Cheng, F.P. (2004), "Predicting the fire resistance behaviour of high strength concrete columns, Cement & Concrete Composites, V. 26, pp. 141–153.

177. Kodur. V. K. R., Bisby, L. A. and Green, M. F. (2006), "Experimental evaluation of the fire behaviour of insulated fibre reinforced polymer strengthened reinforced concrete columns", Fire Safety Journal, 41, pp. 547-557.

178. Krampf, L., and Haksever, A. (1986), "Possibilities of assessing the temperatures reached by concrete building elements during a fire'" Evaluation and repair of fire damage to concrete, T.Z. Harmathy, ed., ACI/SP92, American Concrete Institute, Detroit, Mich., 115-142.

179. Kumar, R. and Bhattacharjee, B. (1995), "Systematic assessment of extent of damage and residual strength of Fire affected building structures", Proceedings of the National Conference on Civil Engineering. Material and Structures, Jan 19-21, Osmania University Hyderabad, India, pp. 476-487.

180. Kumar Virendra (2012), Fire performance of earthquake damaged reinforced concrete structures. PhD Thesis, Department of Civil Engineering, IIT Roorkee, Roorkee India

181. Kunnath, S.K., Heo, Y., and Mohle, J.F. (2009), "Nonlinear uniaxial material model for reinforcing steel bars", Journal of Structural Engineering, ASCE, Vol. 135(4), pp. 335-343.

182. Kuwahara, T. and Koh, Y. (1995), "Computerized thermal and strength simulation system for concrete structures", ACI Material Journal, V. 92, No.2, pp. 117-125.

183. Lamont, S., Usmani, A.S. and Gillie, M. (2004), "Behaviour of a small composite steel frame structure in a long-cool and a short-hot fire", Fire Safety Journal, V. 39(5), pp. 327–357.

184. Lankard, D. R., Birkimer, D. L. and Fondiest, F. F. (1971), "Effects of moisture content on the structural properties of Portland cement concrete exposed to temperature up to 500 ºF", ACI SP -25 Temperature and Concrete, pp. 59-102.

185. Laskar, A. I., & Talukdar, S. (2008). Rheological behavior of high performance concrete with mineral admixtures and their blending. Construction and Building materials, 22(12), 2345-2354.

186. Laskar AI, Talukdar S (2008). A new mix design method of high-performance concrete, Asian Journal of Civil Engineering, Vol. 9, No. 1, pp 31-39, 2008.

187. Lau, A. and Anson, M. (2006), "Effect of high temperatures on high performance steel fibre reinforced concrete", Cement and Concrete Journal, 36, pp. 1698-1707.

188. Law, M. (1983). Basis for the design of fire protection of building structures. Structural Engineer, 61, 25-33.

189. Lea, F. C. (1920), "The effect of temperature on some of the properties of materials", Engineering London, 110, pp. 293-298.

190. Lea, F. C. and Stradling, R. E. (1922), "The resistance to fire of concrete and reinforced concrete", Engineering London, 114, pp.341-344.pp.380-382.

191. Lee, J.S., Xi, Y., and Willam, K. (2008), "Properties of Concrete after High Temperature Heating and Cooling", J. of Materials, ACI, July-Aug. 105(4), 334-341.

192. Lee, J.S., Xi, Y., and Willam, K. (2009a), "A Multiscale Model for Modulus of Elasticity of Concrete at High Temperatures", *Cement and Concrete Research*, in press.

193. Legeron, F. and Paultre, P. (2003), "Uniaxial confinement model for normal and high strength concrete columns", Journal of Structural Engineering ASCE, 29(2), pp. 241-252.

194. Lennon, T. and Moore, D. (2003), "The natural fire safety concept—full-scale tests at Cardington", Fire Safety Journal V. 38(7), pp. 623–643.

195. Li L. and Purkiss, J. A. (2005), "Stress–strain constitutive equations of concrete material at elevated temperatures", Fire Safety Journal, 40, pp. 669-86.

196. Li, B., Park, R. and Tanaka, H. (1994), "Strength & ductility of reinforced concrete members and frames constructed using high strength concrete", Research Report No. 94-5, University of Canterbury, Christchurch, New Zealand.

197. Li, M., Qian, C. and Sun, W. (2004), "Mechanical properties of high-strength concrete after fire", Cement and Concrete Research, 34, pp. 1001-1005.

198. Lie, T. T. (1992). "Structural fire protection", New York American Society of Civil Engineers.

199. Lie, T. T. and Celikkol, B. (1991), "Method to calculate the fire resistance of circular reinforced concrete columns", ACI Material Journal, V. 88, No. 1, pp.84-91.

200. Lie, T. T. and Chabot, M. (1993), "Evaluation of the fire resistance of compression members using mathematical models", Fire Safety Journal, V.20, pp. 135-149.

201. Lie, T. T. and Irwin, R. J. (1993), "Method to calculate the fire resistance of reinforced concrete columns with rectangular cross section", ACI Structural Journal, V. 9, No. 1, pp. 52-60.

202. Lie, T. T. and J. L. Woolerton (1988). Fire Resistance of Reinforced Concrete Columns – Test Results, National Research Council Canada.

203. Liel, A., Haselton, C., and Deierlein, G. (2011), "Seismic collapse safety of reinforced concrete buildings. II: comparative assessment of nonductile and ductile moment frames." Journal of Structural Engineering 2011 137:4, 492-502

204. Lim, L., Buchanan, A., Moss P. and Franssen, J. M. (2004), "Computer modeling of restrained reinforced concrete slabs in fire conditions", ASCE, Journal of Structural Engineering, Vol. 130, No. 12, pp. 1964-1971.

205. Linse, D., Aschl, H and Stockl, S. (1976), "Strength of concrete under Tri-axial loading and creep at elevated Temperature", Transactions of the International Conference on Structural Mechanics in Reactor Technology, V.H. pp.1-13.

206. Luccioni, B. M., Figueroa, M. I. and Danesi, R. F. (2003), "Thermo-mechanic model for concrete exposed to elevated temperatures", Engineering Structure, 25, pp. 729–742.

207. Magnusson, S. E., & Thelandersson, S. (1970). Temperature-time curves of complete process of fire development. Bulletin of Division of Structural Mechanics and Concrete Construction, Bulletin 16.

208. Malhotra, H. L. (1956), "The effect of on the compressive strength of concrete", Magazine of Concrete Research (London) 8, pp. 85-94.

209. Malhotra, H. L. (1982), “Design of fire-resisting structures”, London, Surrey University Press.

210. Mander, J. B., Priestly, M. J. N. and Park, R. (1988), “Theoretical stress-strain model for confined concrete”, Journal of Structural Engineering ASCE, 114(8), pp. 1804-1826.

211. Mander, J.B., Priestly, M.J.N. and Park, R. (1988), “Observed stress-strain behaviour of confined concrete”, Journal of Structural Engineering ASCE, 114(8), pp. 1827-1849.

212. Mansour, M. Y., & Hsu, T. T. C. (2002). Pinching effect in hysteretic loops of R/C shear elements. ACI Special Publication, 205.

213. Menegotto, M. and Pinto, P.E. (1973), “Method of analysis for cyclically loaded reinforced concrete plane frames including changes in force and bending”, IABSE Symposium on the resistance and ultimate deformability of structures acted on by well-defined repeated loads, Lisbon.

214. Metin, H. (2006), “The effects of high temperature on compressive and flexural strength of ordinary and high performance concrete”, Fire Safety Journal, 41, pp. 155-163.

215. Mohamedbhai, G. T. G. (1982), “Residual strength of reinforced concrete members subjected to elevated temperatures”, Proc.Instn Civ. Engrs., Part 2, V. 73, pp. 407-420.

216. Mohamedbhai, G. T. G. (1986), “Effect of exposure time and rate of heating and cooling on residual strength of heated concrete”, Magazine of Concrete Research, 38(136), pp. 151-158

217. Mondal A, Ghosh S, Reddy GR (2013), Performance-based evaluation of the response reduction factor for ductile RC frames, Engineering Structures 56:1808-1819

218. Monti, G. and Nuti, C. (1992), “Nonlinear cyclic behaviour of reinforcing bars including buckling”, Journal of Structural Engineering, 118(12), pp. 3268-3284.

219. Morita, T., Saito, H., and Kumagai, H. (1992). “Residual mechanical properties of high strength concrete members exposed to high temperature-part 1. Test on material properties”, Summaries of Technical Papers of Annual Meeting, Architectural Institute of Japan, Niigata, Aug.

220. Morley, P. D. and Royles, R. (1979/80), “The influence of high temperature on the bond in reinforced concrete”, Fire Safety Journal, 2, pp. 243 – 255.

221. Mostafaei, H., Sultan, M.A. and Benichou, N. (2009), “Recent developments on structural fire performance engineering-a state-of-the-art report”, National Research Council Canada, Research Report No. IRC-RR-275, 75pp.

222. Mousavi, S., Bagchi, A. and Kodur, V.K.R. (2008), "Review of post-earthquake fire hazard to buildings structures", Canadian Journal of Civil Engineering, Vol. 35, pp.689-698.

223. Mousseau, S. and Pautltre, P. (2008), "Seismic performance of a full-scale reinforced high-performance concrete building, part I: experimental study", Canadian Journal of Civil Engineering, V. 35, pp.832-862.

224. Murty, C. V. R., & Jain, S. K. (2000, January). Beneficial influence of masonry infill walls on seismic performance of RC frame buildings. In *Proceedings of the 12th World Conference on Earthquake Engineering, Auckland, New Zealand, Paper* (No. 1790).

225. Murty, C. V. R., Rai, D. C., Bajpai, K. K., & Jain, S. K. (2003). Effectiveness of reinforcement details in exterior reinforced concrete beam-column joints for earthquake resistance. *ACI structural journal*, *100*(2).

226. Mutairi, N. M. A. and Shaleh, M. S. A. (1997), "Assessment of fire-damaged kuwaiti structures", ASCE, Jourrnal of Materials in Civil Engineering, Vol. 9, No. 1, pp. 7-14.

227. Neves, I. C., Rodrigues, J.P.C. and Loureiro, A.D.P. (1996), "Mechanical properties of reinforcing and prestressing steel after heating", J of Materials in Civil Engineering, ASCE, Vol. 8, No. 4, pp. 189-194.

228. Newman, G.M., Robinson, J.F. and Bailey, C.G. (2000), "Fire safe design: a new approach to multi-story steel-framed buildings", Steel Construction Institute, Berkshire, U.K.

229. Nielsen, C.V., Pearce, C.J., and Bicanic, N. (2004), "Improved phenomenological modeling of transient thermal strains for concrete at high temperature", Computers and Concrete, March, 1(2), 189-209.

230. NIST (2008), "Final report on the collapse of world trade center building 7", National Institute of Standards and Technology, www.nist.govt.

231. Noumowe, A.N., Clastres, P., Debicki, G., and Costaz, J.L. (1996), "Thermal stresses and water vapor pressure of high performance concrete at high temperature", Proceedings, 4th International symposium on utilization of High-strength/High-Performance Concrete, Paris, France.

232. Noumowé; A. Carré; H. Daoud, A. and Toutanji, H. (2006), "High-Strength Self-Compacting Concrete Exposed to Fire Test", ASCE, Journal of Materials in Civil Engineering, Vol. 18, No. 6, pp. 754-758.

233. Panda, K. C., Bhattacharyya, S. K., and Barai, S. V. (2011), “Optimization study of RC T-beams strengthened in shear with side bonded GFRP sheet”, International Journal of Earth Sciences and Engineering (IJEE),4(6):801-804.

234. Papaioannou and Kyriakos (1986), "The Conflagration of two large department stores in the centre of Athens," Fire and Materials, Vol. 10, John Wiley and Sons, Ltd., pp. 171-177.

235. Papia, M., Russo, G. and Zingone, G. (1988), “Instability of longitudinal bars in RC column”, Journal of Structural Engineering, ASCE, Vol. 114, No. 2, pp. 445-461.

236. Park, R. (1988), “State-of-Art Report Ductility Evaluation from Laboratory and Analytical Testing”. Proc of 9th Word Conference of Earthquake Engineering Tokyo-Kyoto, Japan, Vol. III, pp. VIII-605-VIII-616.

237. Park, R. and Paulay, T. (1975), “Reinforced concrete structures”, John Wiley, New York.

238. Park, R. and Sampson, R. A. (1972), “Ductility of reinforced concrete column sections in seismic design”, ACI Journal, American Concrete Institute, 69(9), pp. 543-551.

239. Park, R., Priestly, M. J. N. and Gill, W. D. (1982), “Ductility of square confined concrete columns”, Journal of Structural Division ASCE, 108(4), pp. 929-951.

240. Pautre, P., Eid, R., Langlois, Y. and Levesque, Y. (2010), “Behaviour of steel fibre reinforced high strength concrete columns under uni-axial compression”, Journal of Structural Engineering ASCE, 136(10), pp. 1225-1235.

241. Paya-Marin, M. A., Lim, J. B. P., Chen, J.-F., Lawson, R. M., & Gupta, B. S. (2015). Large scale test of a novel back-pass non-perforated unglazed solar air collector. *Renewable Energy, 83*, 871-880.

242. Peng, G. F. (2000), “Evaluation of fire damage to high performance concrete”, Ph.D. Thesis, Departments of Civil Engineering and Structural Engineering, The Hong Kong Polytechnic University Hong Kong, pp.213.

243. Peng, G. F., Bian, S. H., Guo, Z. Q., Zhao, J., Peng, X. L. and Jiang, Y. C. (2008), “Effect of thermal shock due to rapid cooling on residual mechanical properties of fibre concrete exposed to high temperatures”, Construction and Building Materials 22, pp. 948-955.

244. Peng, G. F., Bian, S. H., Zhao, Z. L., and Yl, Q. X. (2006), “Effect of Cooling Regimes on Mechanical Properties of Fibre-Toughened High-Performance Concrete”, Key Engineering Materials, pp.603-609.

245. Phan, D. T., Lim, J. B. P., Tanyimboh, T. T., Wrzesien, A. M., Sha, W., & Lawson, R. M. (2015). Optimal design of cold-formed steel portal frames for stressed-skin action using genetic algorithm. *Engineering Structures, 93*, 36-49.

246. Phan, L. T. and Carino, N. J. (1998), "Review of mechanical Properties of high strength concrete at elevated temperature", Journal of Materials in Civil Engineering ASCE, 10(1), pp. 58-64.

247. Phan, L. T. and Carino, N. J. (2002), "Effects of test conditions and mixture proportions on behaviour of high-strength concrete exposed to high temperatures", ACI Materials Journal, 99 (1), pp. 54–66.

248. Phan, L.T. (1996), "Fire performance of high-strength concrete: A report of the state-of-the art, Building and Fire Research Laboratory", National Institute of Standards and Technology, NISTIR 5934, Maryland, Dec.

249. Phani Prasad, D. M. S., Sharma, U. K. and Bhargava, P. (2009), "Effect of elevated temperature on the properties of reinforcing steel bar", Journal of the Institution of Engineers (India), 99, pp. 3-6.

250. Pintea, D., Zaharia, R., Stratan, A. and Dubina, D. (2008), "Fire after earthquake", Proc. of the fifth international conference on structures in fire (SiF'08), pp. 324-333.

251. Poon, C. S., Shui, Z. H. and Lam, L. (2004), "Compressive behaviour of fibre reinforced high-performance concrete subjected to elevated temperatures", Cement and Concrete Research, 34, pp. 2215-2222.

252. Purkiss, J. A. and Dougill, J. W. (1973), "Apparatus for compression tests on concrete at high temperatures", Magazine of Concrete Research, 25(83), pp. 102-108.

253. Rafi, M. M., Nadjai, A. and Ali, F. (2008), "Finite element modeling of carbon fiber-reinforced polymer reinforced concrete beams under elevated temperatures", ACI Structural Journal, V. 105, No. 6, pp.701-710.

254. Raju, M. P., Rao, K. S. and Raju, P. S. N. (2007), "Compressive strength of heated high strength concrete", Magazine of Concrete Research, 59(2), pp. 79-85.

255. Ramberg, W. and Osgood, W.R. (1943), "Description of stress-strain curves by three parameters", Technical notes no. 902, National Advisory Committee for Aeronautics, Washington, DC.

256. Raut, N. K. and Kodur, V. K. R. (2011), "Response of high-strength concrete columns under design fire exposure", ASCE, Journal of Structural Engineering, Vol. 137, No. 1, pp. 69-79.

257. Razvi, S. R. and Saatcioglu, M. (1999), "Confinement model for high strength concrete", Journal of Structural Engineering ASCE, 125(3), pp.281-289.

258. Razvi, S.R. and Saatcioglu, M. (1994), "Strength and deformability of confined high strength concrete columns", ACI Structural Journal, 91(6), pp. 678-687.

259. Razvi, S.R. and Saatcioglu, M. (1996), "Tests of high strength concrete under concentric loading", Report No. OCEERC 96-03, Carleton Earthquake Engineering Research Centre, Ottawa, Canada.

260. Richart, F.E., Brandtzaeg, A. and Brown, R.L. (1928), "A study of failure of concrete under combined compressive stresses", Engineering experiment station bulletin no. 185, University of Illinois, Urbana, pp. 104.

261. Rini, D. and Lamont, S. (2008), "Performance based structural fire engineering for modern building design", ASCE, Structures 2008: Crossing Borders.

262. SAA (1990(c)). Fire-resistance tests of elements of structure. AS 1530.4-1990. Standards Association of Australia

263. Saad, M., El-Enein, S. A. A., Hanna, G. B. and Kotkata, M. F. (1996), "Effect of temperature on physical and mechanical properties of concrete containing silica fume", Cement and Concrete Research, 26 (5), pp. 669-675.

264. Saatcioglu, M. and Razvi, S. R. (1992), "Strength and ductility of confined concrete", Journal of Structural Engineering ASCE, 118(6), pp. 1590-1607.

265. Saemann, J. C. and Washa, G. W. (1957), "Variation of mortar and concrete properties with temperature", ACI Journal Proceedings, 54(5), pp. 385-395.

266. Sanad, A.M., Lamont, S., Usmani, A.S. and Rotter, J.M. (2000), "Structural behaviour in fire compartment under different heating regimes-Part-1 (slab thermal gradients)", Fire Safety Journal V.35 (2), pp. 99-116.

267. Sanad, A.M., Rotter, J.M., Usmani, A.S. and O'Connor M.A. (2000), "Composite beams in large buildings under fire-numerical modelling and structural behaviour", Fire Safety Journal V. 35 (3), pp.165-188.

268. Sanjayan, G. and Stocks L. J. (1993), "Spallling of high strength silica fume concrete in fire", ACI Materials Journal, V. 90, No. 2, March–April 1993, pp. 170-173.

269. Sargin, M. (1971), "Stress-strain relationship for concrete and analysis of structural concrete sections", Study No.4, Solid Mech. Div. University of Water Loo On, Canada, pp.167.

270. Scawthorn C., Rourke M.E.T.D., Blackburn F.T., (2006). "The 1906 san Francisco Earthquake and Fire-Enduring Lessons for Fire Protection and Water Supply", Earthquake Spectra, Vol. 22, No. S2, pp. S135-S158.

271. Scawthorn, C., Eidinger, J.M. and Schiff, A.J., (2005), "Fire Following Earthquake", ASCE Publications (Ed.).

272. Schneider U. (1985), "Properties of material at high temperature: Concrete", Germany: Department of Civil Engineering, University of Kassel, Kassel, 131 pp.

273. Schneider, U. & Lebeda, C. (2007), "Baulicher Brandschutz (Structural Fire Protection)", Bauwerk Verlag, Berlin, Germany, 400 pp.

274. Schneider, U. (1985), "Properties of material at high temperatures-concrete", RILEM-Committee 44-PHT, Department of Civil Engineering, University of Kassel.

275. Schneider, U. (1989), "Repairability of fire damaged structures," CIB W14 Rep., Conseil International du Batiment, Kassel, Germany.

276. Schneider, U., and Herbst, H. (2002), "Theoretical considerations about spalling in tunnels at high temperatures", Technical Report, Technical University Vienna, Austria.

277. Sharma U.K, et al (2012), "Full-scale testing of a damaged reinforced concrete frame in fire", Proceedings, Institute of Civil Engineers: Structures & Buildings, V.165, Issue SB7, pp. 335-346.

278. Sharma, U. K., Bhargava, P. and Sheikh, S. A. (2007), "Tie confined fibre reinforced high strength concrete short columns", Magazine of Concrete Research, 59(10), pp. 757-769.

279. Sharma, U. K., Bhargava, P. Singh, S. P. and Kaushik, S. K. (2007), "Confinement reinforcement design for plain and fibre reinforced high strength concrete columns", International Journal of Advanced Concrete Technology, 5(1), pp. 113-127.

280. Sharma, U.K., Zaidi, K.A. and Bhandari, N.M. (2012), "Strength and deformability of heated confined fibrous concrete", Magazine of Concrete Research, Vol. 64, Issue 7 pp. 631-646.

281. Sheikh, S. A. and Toklucu, M. A. (1993), "Reinforced concrete columns confined by circular spirals and hoops", ACI Structural Journal, 90(5), pp. 542-553.

282. Sheikh, S. A. and Uzumeri, S. M. (1980), "Strength and ductility of tied concrete columns", Journal of Structural Division ASCE, 106(5), pp.1079-1102.

283. Sheikh, S. A. and Uzumeri, S. M. (1982), "Analytical model for concrete confinement in tied columns", Proceedings, ASCE, 108, ST12, pp. 2703-2722.

284. Shi, X., Tan, T.H., Tan K.H and Guo, Z. (2004), "Influence of concrete cover on fire resistance of reinforced concrete flexural members", ASCE, Journal of Structural Engineering, Vol. 130, No. 8, pp. 1225-1232.

285. Shirley, S.T., Burg, R. G. and Fiorato, A. E. (1988), "Fire Endurance of High-Strength Concrete Slabs", ACI Material Journal, V. 85, No. 2, pp. 102-108.

286. Sideris, K. K., Manita P. and Chaniotakis, E. (2009), "Performance of thermally damaged fibre reinforced concretes", Construction and Building Materials, 23, pp. 1232-1239.

287. Sidibe, K., Duprat, F., Pinglot, M. and Bourret, B. (2000), "Fire safety of reinforced concrete columns", ACI Structural Journal, V. 97, No. 4, pp. 642-647.

288. Srinivasan S. and Menon, Devdas, "RC rectangular column sections under biaxial eccentric compression – an improved design recommendation", Journal of Structural Engineering, SERC, Vol. 29, No. 4, January-March 2003, pp 205-211

289. Sunder, S. (2008), "Report on the collapse of world trade center building 7, opening statement press briefing-august 21, 2008", National Institute of Standards and Technology, wtc.nist.gov.

290. Suresh, N. (2002), "Flexural Strength of Concrete subjected to sustained elevated temperature", Indian Concrete Institute Journal, India.

291. Suresh, N. (2006), "Studies on compressive strength of concrete subjected to sustained elevated temperature", International Conference on Advances in Concrete Composites Structures (ICACS-2005) Jan 6-8, 2006 at SERC, CSIR Campus, Taramani, Chennai, India

292. Tan, K. H. and Tang, C. Y. (2004), "Interaction formula for reinforced concrete columns in fire conditions", ACI Structural Journal, V. 101, No. 1, pp.19-28.

293. Tan, K. H. and Yao, Y. (2003), "Fire resistance of four-face heated reinforced concrete columns", ASCE, Journal of Structural Engineering, Vol. 129, No. 9, pp. 1220-1229.

294. Tao, J., Yuan, Y. and Taerwe, L. (2010), "Compressive Strength of Self-Compacting Concrete during High-Temperature Exposure", ASCE, Journal of Materials in Civil Engineering, Vol. 22, No. 10, pp. 1005-1011.

295. Taylor, J. (2003), "Post earthquake fire in tall buildings and the New Zealand building code research project report", University of Canterbury, Christchurch, New Zealand.

296. Tenchev, R. & Purnell, P. (2005), "An application of a damage constitutive model to concrete at high temperature and prediction of spalling", Int. J. Solids & Structures, 42, 26, pp. 6550-6565.

297. Terro, M. J. and Hamoush, S. A. (1997), “Effect of confinement on siliceous aggregate concrete subjected to elevated temperatures and cyclic heating”, ACI Materials Journal, 94(2), pp. 83-89.

298. Terro, M. J., (1998), “Numerical Modeling of the Behavior of Concrete Structures in Fire, ACI Structural Journal, V. 95, No. 2, pp. 183-193.

299. Tesfamariam, S.(2010), “Structures in fire and earthquake”, Proceedings of the 9th U.S. National and 10th Canadian Conference on Earthquake Engineering, July 25-29, 2010, Toronto, Ontario, Canada, Paper No 1130.

300. Thomas, P.H. and Heselden, A.J.M. (1972), “Fully-Developed fires in single compartment”–A Co-operative Research Programme of the counseil international du Batiment, CIB Report No. 20, Fire Res. Station, UK, FR Note No. 923.

301. Topcu, I. B. and Ikdag, B. I. (2008), “The effect of cover thickness on rebars exposed to elevated temperatures”, Construction and Building Materials, V. 22, pp. 2053-2058.

302. Topcu, İ.B. and Karakurt, C. (2008), “Properties of reinforced concrete steel bars exposed to high temperatures”, Research Letters in Materials Science, (Article ID 814137), pp. 1-4.

303. Usmani, A. S., Rotter, J. M., Lamont, S., Sanad, A.M. and Gillie, M. (2001), “Fundamental principles of structural behaviour under thermal effects”, Fire Safety Journal. 36, pp. 721-744.

304. Usmani, A.S. (2008), “Research priorities for maintaining structural fire resistance after seismic damage”, The 14th World Conference on Earthquake Engineering, Beijing, China.

305. Vassart, O., Bailey, C.G., Hawes, M., Nadjai, A., Simms, W.I., Zhao, B., Gernay, T. and Franssen, J.-M. (2012), “Large-scale fire test of unprotected cellular beam acting in membrane action”, Structures and Buildings, Vol. 165, Issue SB7, pp.327-334.

306. Vecchio, F. J. (1987), “Nonlinear analysis of reinforced concrete frames subjected to thermal and mechanical loads”, ACI Structural Journal, Vol. 84, No.6, pp. 492-501.

307. Vecchio, F. J. and Sato, J. A. (1990), “Thermal gradient effects in reinforced concrete frame structures”, ACI, Structural Journal, V. 87, No. 3, , pp. 262-275.

308. Wang, H., Zha, X. and Ye, J. (2009), “Fire resistance performance of frp rebar reinforced concrete columns”, International Journal of Concrete Structures and Materials Vol.3, No.2, pp. 111-117.

309. Wang, Y.C. (2000), “An analysis of the global structural behaviour of the Cardington steel-framed building during the two BRE fire tests”, Elsevier, Engineering Structures V. 22 (5), pp. 401–412.

310. Wellington Lifeline Group (2002) “Fire following earthquake: Identifying key issues for New Zealand, Report on a project undertaken for the New Zealand fire service contestable research fund”. Fire Research Report. New Zealand Fire Service Commission, Wellington, NZ.

311. Wetzig, V. (2001), “Destruction mechanisms in concrete material in case of fire, and protection systems”, Proceedings, 4th Int. Conf. on Safety in Road & Rail Tunnels (SIRRT), Madrid, Spain, pp. 281-290.

312. Wikipedia, 1906 San Fracisco Earthquake, Wikipedia The Free Encyclopedia, http://en.wikipedia.org/wiki,Retrieved in 26 January 2009.

313. Wikipedia, 1923 San Great Kanto Earthquake, Wikipedia The Free Encyclopedia, http://en.wikipedia.org/wiki,Retrieved in 23 January 2009.

314. Wikipedia, 1995 Great Hanshin (Kobe) Earthquake, Wikipedia The Free Encyclopedia, http://en.wikipedia.org/wiki,Retrieved in 25 January 2009.

315. Wong, M. B. (2001), “Plastic frame analysis under fire conditions”, ASCE, Journal of Structural Engineering, Vol. 127, No. 3, pp. 290-295.

316. Wu, B., Lam E. S.S., Liu, Q., Chung, W. and Ho, I.F. (2010), “Creep behavior of high-strength concrete with polypropylene fibers at elevated temperatures”, ACI Materials Journal, V. 107, No. 2, pp.176-184.

317. Wu, B., Su, X. P., Li, H. and Yuan, J. (2002), “Effects of high temperature on residual mechanical properties of confined and unconfined high strength concrete”, ACI Material Journal, pp. 399-407.

318. Xiangjun, D., Yining, D. and Tianfeng, W. (2008), “Spalling and mechanical properties of fibre reinforced high-performance concrete subjected to fire”, Journal of Wuhan University of Technology-Mater. Sci. Ed. Oct 2008, pp. 743-749.

319. Xiao, J. and Konig, G. (2004), “Study on concrete at high temperature in China: An overview”, Fire Safety Journal, 39, pp. 89-103.

320. Xiao, J., Xie, M. and Zhang, Ch. (2006), “Residual compressive behaviour of pre heated high performance concrete with blast-furnace slag”, Fire Safety Journal, 41, pp. 91-98.

321. Xiao, J.Z., Li, J. and Huang, Z.F. (2008), “Fire response of high-performance concrete frames and their post-fire seismic performance”, ACI Structural Journal, V. 105, No. 5, pp.531-540.

322. Xua, Y. and Wub, B. (2009), “Fire resistance of reinforced concrete columns with L-, T-, and +-shaped cross-sections”, Fire Safety Journal, V. 44, pp. 869–880.

323. Yan, X., Li, H. and Wong, Y.-L. (2007), “Effect of aggregate on high-strength concrete in fire”, Magazine of Concrete Research, 59, No. 5, June, 323–328.

324. Yao, Y. and Tan, K. H. (2009), “Fire modelling and resistance of RC columns subjected to natural fire”, Magazine of Concrete Research, V. 61, No. 190, pp. 837–847.

325. Youssef, M.A. and Moftah, M. (2007), “General stress-strain relationship for concrete at elevated temperatures”, Engineering Structures, 29, pp. 2618-2634.

326. Yu, C., Huang, Z., Burgess, I. W. and Plank, R. J. (2010), “Development and validation of 3D composite structural elements at elevated temperatures”, Journal of Structural Engineering, Vol. 136, No. 3, pp. 275-541.

327. Yu, J.T., Lu, Z.D., Xie, Q. (2007), “Nonlinear analysis of SRC columns subjected to fire”, Fire Safety Journal, V. 42, pp. 1–10.

328. Yu, X., Huang, Z., Burgess, I. and Plank, R. (2008), “Nonlinear analysis of orthotropic composite slabs in fire”, Engineering Structures, V. 30, pp. 67–80.

329. Zaidi, K.A., Sharma, U.K. and Bhandari, N.M. (2012), “Effect on uni-axial compressive behaviour of confined concrete”, Fire Safety Journal, V. 48, pp. 58-68.

330. Zaidi, S.K.A (2011), “Residual compressive behaviour of confined concrete subjected to elevated temperature”, Ph.D. Thesis, Department of Civil Engineering, Indian Institute of Technology Roorkee, Roorkee, India, 219pp.

331. Zhang, B. (2011), “Effect of moisture evaporation (weight loss) on fracture properties of high performance concrete subjected to high temperatures”, Fire Safety Journal, V. 46, pp. 543-549.

332. Zilli, G. and Fattorini, F. (2002), “Cold-worked stainless-steel bars: a contribution to Eurocode EC 3”, Center for Materials Development- Centro Sviluppo Materiali S.p.A., Rome, Italy: 2002.

333. Zoldners, N. G. (1960), “Effects of high temperature on concrete incorporating different aggregate”, ASTM Proceedings, 60, pp. 1087-1108.

PUBLICATIONS FROM THIS STUDY

Journals

Asif H. Shah, Umesh K. Sharma Praveen Kamath, Pradeep Bhargava, GR Reddy, Tarvinder Singh and Hitesh Lakhani, **Fire Performance of Earthquake-Damaged Reinforced-Concrete Structures**, ***Materials and Structures*** (Published online 27th August, 2015)

Asif H. Shah, Umesh K. Sharma, Praveen Kamath, Pradeep Bhargava, GR Reddy, Tarvinder Singh, **Effect of Ductile Detailing on the Performance of Reinforced Concrete Building Frame under Post Earthquake Fire**. ***Journal of Performance of Constructed Facilities, ASCE*** (Accepted; in production)

Asif H. Shah, Umesh K. Sharma, Pradeep Bhargava, Praveen Kamath GR Reddy, Tarvinder Singh and Hitesh Lakhani, **A Full Scale Fire Test on a Pre Damaged RC Framed Structure**. ***The Indian Concrete Journal****, Jan 2015, Vol. 89, No. 1, pp 17-26.*

Asif H. Shah, Umesh K. Sharma, Pradeep Bhargava, **Fire Resistance and Spalling performance of Confined Concrete Columns**. **Journal of Structural Engineering, ASCE** (Under Review)

Book Chapters

Asif H. Shah, Umesh K. Sharma, Pradeep Bhargava, G. R. Reddy, Tarvinder Singh, Hitesh Lakhani, **A Full Scale Fire Test on a Pre Damaged RC Framed Structure**, *Advances in Structural Engineering*, pp 2259-2274, Springer, India, 2015.

Conferences

Asif H. Shah, Praveen Kamath, Umesh K. Sharma, Pradeep Bhargava , Asif Usmani, GR Reddy, Tarvinder Singh and Hitesh Lakhani, **Influence of Ductility on the Behaviour of RC Frame in Post Earthquake Fire**, *In the Proceedings of SIF'14, Progress on Safety of Structures in Fire, Tongji University, Shanghai, China, 11-13 June 2014*

Asif H. Shah, Umesh K. Sharma, Pradeep Bhargava, GR Reddy, Tarvinder Singh and Hitesh Lakhani, **A Full Scale Fire Test on a Pre Damaged RC Framed Structure**. *Structural Engineering Convention, SEC-14, Indian Institute of Technology Delhi, Delhi, 22-24 December 2014.(Keynote Lecture)*

Asif H. Shah, Umesh K. Sharma, Pradeep Bhargava, GR Reddy, Tarvinder Singh, **Outcomes of a Major Research on Full Scale Testing of RC Frames in Post Earthquake Fire.** *2nd R.N. Raikar International Conference and Banthia- Basheer International Symposium On Advances in Science and Technology of Concrete*. 18-19 December 2015, Mumbai, India (*Keynote Lecture)*

Asif H. Shah, Umesh K. Sharma, Pradeep Bhargava, GR Reddy, Tarvinder Singh, **Effect Of Pre-Damage And Reinforcement Detailing On The Spalling Behaviour Of Reinforced Concrete Building Frame In Post-Earthquake Fire**. *Fire Spalling 2015, IWCS - 4th International Workshop on Concrete Spalling due to Fire Exposure, Leipzig, 08 - 09 October 2015*